

Cover Page



Universiteit Leiden



The handle <http://hdl.handle.net/1887/44707> holds various files of this Leiden University dissertation.

**Author:** Massink, A.

**Title:** Allosteric modulation by sodium ions and amilorides of G protein-coupled receptors : a closer look at the sodium ion site of the adenosine A2a receptor and development of a mass spectrometry ligand binding assay for adenosine A1 and A2a receptors

**Issue Date:** 2016-12-08



# **Allosteric modulation by sodium ions and amilorides of G protein-coupled receptors**

**A closer look at the sodium ion site of  
the adenosine A<sub>2A</sub> receptor**

**and**

**Development of a mass spectrometry  
ligand binding assay for adenosine A<sub>1</sub> and A<sub>2A</sub> receptors**

**Arnault Massink**

The research described in this thesis was performed at the Division of Medicinal Chemistry of the Leiden Academic Centre for Drug Research, Leiden University (Leiden, The Netherlands). The research was financially supported by the Netherlands Organization for Scientific Research - Chemical Sciences (NWO-TOP #714.011.001).

Cover design by Bastiaan van Manen.

Printed by Ipskamp Drukkers (Enschede, The Netherlands).

© Arnault Massink 2016.

All rights reserved. No part of this thesis may be reproduced in any form or by any means without the prior written permission of the holder of copyright.

# **Allosteric modulation by sodium ions and amilorides of G protein-coupled receptors**

**A closer look at the sodium ion site of  
the adenosine A<sub>2A</sub> receptor**

**and**

**Development of a mass spectrometry  
ligand binding assay for adenosine A<sub>1</sub> and A<sub>2A</sub> receptors**

**Proefschrift**

ter verkrijging van  
de graad van Doctor aan de Universiteit Leiden,  
op gezag van Rector Magnificus prof. mr. C.J.J.M. Stolker,  
volgens besluit van het College voor Promoties  
te verdedigen op donderdag 8 december 2016  
klokke 11.15 uur

door

**Arnault Massink**

geboren te Parijs, Frankrijk  
in 1982

Promotor: Prof. dr. A.P. IJzerman

Promotiecommissie: Prof. dr. J.A. Bouwstra  
Prof. dr. M. Danhof  
Dr. J. Carlsson (Universiteit Uppsala, Zweden)  
Prof. dr. M. Smit (Vrije Universiteit Amsterdam, Nederland)  
Prof. dr. B. van de Water  
Prof. dr. T. Hankemeier

## Contents

<b>Chapter 1</b>	General introduction	7
<b>Chapter 2</b>	Allosteric modulation of class A GPCRs by amiloride and its analogues	19
<b>Chapter 3</b>	The role of a sodium ion binding site in the allosteric modulation of the A <sub>2A</sub> adenosine G protein-coupled receptor	47
<b>Chapter 4</b>	Sodium ion binding pocket mutations and adenosine A <sub>2A</sub> receptor function	75
<b>Chapter 5</b>	5'-Substituted amiloride derivatives as allosteric modulators binding in the sodium ion pocket of the adenosine A <sub>2A</sub> receptor	101
<b>Chapter 6</b>	Mass spectrometry-based ligand binding assays on adenosine A <sub>1</sub> and A <sub>2A</sub> receptors	125
<b>Chapter 7</b>	Conclusions and future perspectives	153
	Summary	169
	Samenvatting	173
	List of publications	177
	Curriculum vitae	179
	Acknowledgements	181





# **Chapter 1**

## **General introduction**



From ancient times on mankind has searched for ways to cure diseases. The first written records originate from the Mesopotamians and Egyptians who already had a keen interest in the causes and the healing of diseases.<sup>1,2</sup> In these times healing was strongly tied to religion and superstition, and diseases were mainly ascribed to supernatural powers. Still, the basics of objective and empirical medicine started to emerge, including the description and use of natural products to cure diseases.<sup>3</sup> This mixture of superstition and rationalism in the approach to medicine remained more or less the same until the advent of scientific experimental methods in the 16<sup>th</sup> and 17<sup>th</sup> centuries. The field of pharmacology emerged as late as the 19<sup>th</sup> century, when the concept of chemical structures and their relationship with their pharmacological action became a subject of study.<sup>4</sup> In the following period impressive advancements were made with the formulation of receptor theory and the discovery of numerous receptor types and their endogenous ligands.<sup>5, 6</sup> Today, pharmacology is a very diverse field with elements of molecular biology, genetics, chemistry, and bio-informatics, to name but a few disciplines. Together, these disciplines help to understand why a drug works and give exciting opportunities to develop new drugs.

## **G protein-coupled receptors**

Of the many drug targets currently identified the G protein-coupled receptors (GPCRs) constitute a large fraction. The family of GPCRs encompasses more than 800 different cell membrane-bound receptors,<sup>7</sup> which regulate many different aspects of human physiology, such as vision, homeostasis, and the immune system. This makes it no surprise that they are targeted by 30% to 40% of all drugs on the market.<sup>8</sup> The general role of GPCRs is to relay a diverse collection of extracellular signals, such as photons, hormones, odorants, and neurotransmitters, to the intracellular environment. At the intracellular side GPCRs interface with G proteins that can further transduce the signal. GPCRs share a common structure of seven transmembrane alpha-helices connected by extra- and intra-cellular loops (Figure 1). According to their structural architecture, GPCRs can be subdivided in five different families: rhodopsin-like (class A), secretin-like (class B), glutamate-like (class C), adhesion-like, and frizzled/taste2-like receptors.<sup>7</sup> Of these, the class A rhodopsin-like receptors constitute by far the largest group.

## Allosteric modulation and the sodium ion site

The ligands that can activate GPCRs know a wide variation in both size and chemical structure, from large proteins and peptides to small molecules and ions. The binding sites on GPCRs can be categorized as orthosteric sites, where endogenous ligands bind and activate the receptor, and allosteric sites, where ligand binding can modulate receptor activation (Figure 1). Most drugs target the orthosteric site as antagonists thereby blocking endogenous ligand binding and subsequent activation of the receptor, or as agonists that activate the receptor. Drugs that target the allosteric site may have a less 'blunt' effect, as they enhance or dampen the activation by endogenous ligands.<sup>9-11</sup> This has the advantage that the action is more localized in both time and space, as these allosteric modulators in the most stringent definition only have an effect when the endogenous ligand is present at the orthosteric site.

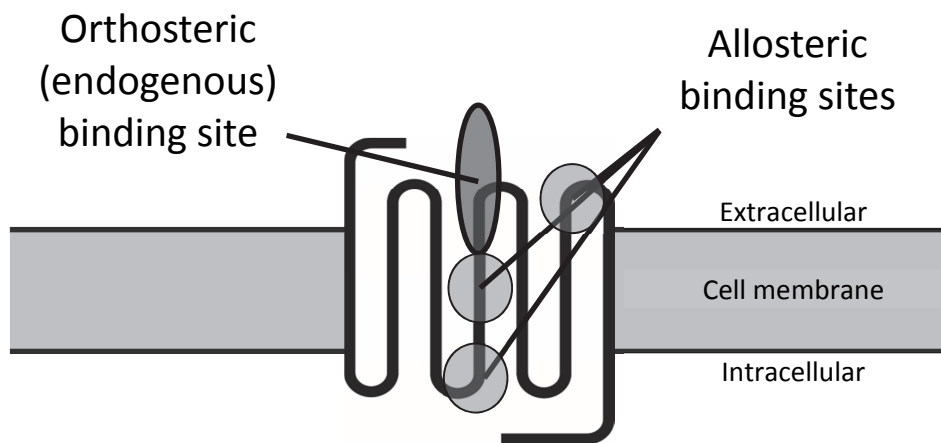


**Figure 1.** Schematic representation of a GPCR embedded in the cell membrane. Seven transmembrane alpha-helices cross the cell membrane, with an extracellular N-terminus, an intracellular C-terminus, and six intra- and extra-cellular loops that connect the transmembrane regions. The orthosteric binding site is represented by an oval and the allosteric binding sites by circles. The middle circle approximates the location of the sodium ion site, in the central region of the receptor just below the orthosteric site. Note that the situation may be different for each GPCR considering the location and the number of binding sites.

The concept of allosteric modulation is a promising one for the discovery of new drugs, and quite a few allosteric modulators have been found for GPCRs.<sup>12</sup> However, the molecular basis of allosteric activity is still largely unknown. The increasing availability of GPCR crystal structures sheds more and more light on the molecular aspects of ligand

binding and GPCR activation.<sup>13-15</sup> Recently, crystal structures have been solved with sufficiently high resolution to be able to spot a sodium ion in an allosteric site of several GPCRs, bound by the highly conserved amino acid Asp<sup>2.50</sup> (Numbering according to Ballesteros and Weinstein<sup>16</sup>).<sup>17-21</sup> Next to these solved crystal structures, sequence alignment indicates that this sodium ion site is very conserved and present in almost all class A GPCRs.<sup>22</sup> This affirmed the results of earlier studies in which sodium ions were described as allosteric modulators of GPCRs.<sup>23</sup>

The small molecule amiloride has been found to be an allosteric modulator for GPCRs as well. Amiloride is used therapeutically as a potassium sparing diuretic by blocking renal epithelial sodium channels (ENaCs).<sup>24</sup> For GPCRs, amilorides have been found to compete with sodium ions for the same allosteric site.<sup>25</sup> The feature of the sodium ion binding site to bind both small ions and small molecules is intriguing. Moreover, sodium ions and amilorides exhibit different allosteric modulation patterns, relative to each other but also between the different GPCRs, as discussed for sodium ions by Katritch et al.<sup>22</sup> and for amilorides in Chapter 2 of this thesis. This makes the sodium ion site an excellent candidate of research to further understand the mechanisms behind allosteric modulation.

## **Adenosine receptors**

The first crystal structure in which a sodium ion binding site was identified was of the adenosine A<sub>2A</sub> receptor.<sup>17</sup> Adenosine receptors belong to the class A rhodopsin-like GPCRs, and as the name suggests adenosine is the endogenous ligand. Caffeine and theophylline are antagonists and have a wide-spread use as a stimulant due to their ability to block adenosine receptors. The group of adenosine receptors encompasses four different subtypes with different structural features and physiological roles, named the adenosine A<sub>1</sub>, A<sub>2A</sub>, A<sub>2B</sub>, and A<sub>3</sub> receptors. These receptors are well-documented by a few decades of research yielding a good understanding of their physiological role and a considerable number of selective agonists and antagonists is available.<sup>26, 27</sup> Adenosine A<sub>2A</sub> receptors couple to G<sub>s</sub> and G<sub>olf</sub> proteins and activation stimulates intracellular cAMP production.<sup>28</sup> Adenosine A<sub>2A</sub> receptors are found in many different tissues, such as the brain striatum, leukocytes, the lung, and the heart. For their wide presence in the body adenosine A<sub>2A</sub> receptors regulate many different physiological processes, amongst which psychiatric

behavior, the sleep-wake cycle, the immune system, myocardial oxygen consumption, and angiogenesis. With these diverse roles the adenosine  $A_{2A}$  receptor attracts substantial clinical interest for the development of drugs. Selective antagonists have been or are currently in clinical trials for treatment of Parkinson's disease and cocaine addiction, and the same is true for selective agonists to replace adenosine as a coronary vasodilator in myocardial perfusion imaging and treatment of sickle cell anemia.<sup>28</sup>

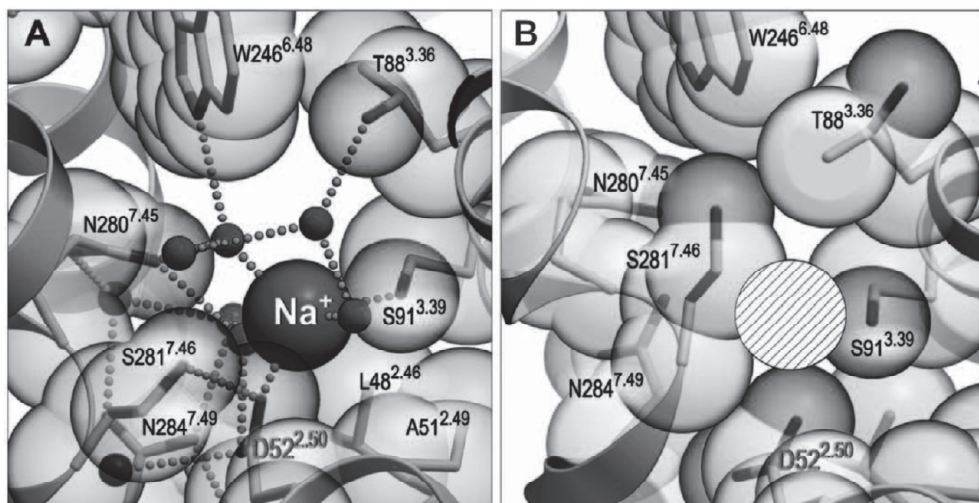


**Figure 2.** The sodium ion site in the crystal structures of the inactive (**A**) and the active state (**B**) of the adenosine  $A_{2A}$  receptor. In **A** the sodium ion is shown as a dark grey sphere, coordinated by D52<sup>2.50</sup> through a salt bridge (dotted lines) and by waters (small solid spheres) and residue S91<sup>3.39</sup> through hydrogen bonds (dotted lines). In **B** the pocket is collapsed leaving no room for the sodium ion to bind (hatched sphere). The receptor backbone is shown as ribbons, residues lining the sodium ion site are shown as sticks, and carbon and oxygen atom spheres are transparent. The crystal structure **A** was co-crystallized with antagonist ZM-241,385 and **B** with agonist UK-432,097.<sup>29</sup> The binding site of these orthosteric ligands is located above residue W246<sup>6.48</sup> and is clipped from this detailed view. From Liu et al.<sup>17</sup> Reprinted with permission from AAAS.

For the adenosine  $A_{2A}$  receptor several crystal structures bound to agonists and antagonists have been solved.<sup>30, 31</sup> The recently solved crystal structure with a bound sodium ion added substantially to our understanding of the molecular mechanism of adenosine  $A_{2A}$  activation.<sup>17</sup> This crystal structure was co-crystallized with the selective antagonist ZM-241,385 and was hence a snapshot of the 'inactive state' of the receptor. Comparison with the 'active state' of the receptor co-crystallized with an agonist made clear that the sodium ion site undergoes substantial changes between the active and the

inactive states of the receptor (Figure 2). The apparent central role of the allosteric sodium ion site in the activation of the adenosine A<sub>2A</sub> receptor urged us to further investigate it in Chapters 3-5 of this thesis.

## Ligand binding assays

To further explain the information derived from crystal structures the 'wet lab' is still indispensable. The field of pharmacology provides a multitude of different experimental setups to probe receptor and ligand characteristics. Most of these methods are dependent on labeled probes, for example radioligands and fluorescent ligands. Radioligand binding is a robust and well-tried method to probe pharmacological properties of ligands,<sup>32</sup> and this method served us well in this thesis. However, the use of radiolabeled ligands is expensive and requires careful handling regarding safety and waste disposal. Therefore new methods to assess ligand binding are being developed, such as fluorescent labeling.<sup>33</sup> Labeling with bulky fluorescent moieties brings however its own risk of changing the pharmacological properties of a ligand. A label-free alternative for ligand binding assays is offered by mass spectrometry (MS).

Advancements in mass spectrometry have made it possible to accurately measure the small quantities of ligand usually found in ligand binding assays. The use of mass spectrometry in ligand binding assays was coined 'mass spectrometry binding' (MS binding) by the group of Wanner. They developed it for several targets, amongst which the dopamine D<sub>2</sub> receptor,<sup>34</sup> the GABA transporter mGAT1,<sup>35</sup> and the serotonin transporter.<sup>36,37</sup> MS binding essentially follows a similar protocol as radioligand binding up to the point of the quantification of bound ligand, except for the use of an unlabeled ligand instead of a radioligand.

In both radioligand and MS binding assays the ligand is allowed to bind to a crude membrane extract of cells expressing the target receptor. Then the reaction mix consisting of the ligand and receptor is filtered over a glass fiber filter, which only retains the membrane with the ligands bound to the receptor, while the unbound ligand is separated. After the filtration step radioligand and MS binding assays diverge. In the radioligand binding assay a scintillation fluid is applied to the filter after which the amount of radioligand can be quantified by scintillation counting. In the MS binding assay the bound ligand is first eluted from the filter by an organic solvent after which the ligand amount in

the solvent is quantified by a mass spectrometer. Before the detection by the mass spectrometer the ligand and remaining membrane content is separated by liquid chromatography (LC). Both the LC method and the MS detection method have to be developed for every ligand specifically, as each ligand has a different molecular mass and a different retention time on an LC column. A ligand for which the LC-MS method is developed is also called a marker ligand, and can be used in the same manner as a radioligand in radioligand binding assays to determine pharmacological binding properties of other, unlabeled ligands.

The types of radioligand binding assays of which equivalents have been applied to MS binding by the group of Wanner are ligand saturation, displacement, association, and dissociation assays. Another type of radioligand binding assay is the competition association assay, in which the kinetic properties of a ligand can be determined without measuring binding of that ligand directly. Instead the ligand of interest competes for binding to the target with a radioligand of which binding can be followed directly. Fitting the resulting association data of the marker ligand to a model describing competition association derives the  $k_{on}$  and  $k_{off}$  for the competing ligand.<sup>38</sup> In this thesis, we describe the development of an MS binding assay for the adenosine A<sub>1</sub> and A<sub>2A</sub> receptors and its validation for the different types of ligand binding assays, including for the first time the competition association assay.



## This thesis

In **Chapter 2** the current knowledge of allosteric modulation of class A GPCRs by amilorides is reviewed. We describe how the allosteric effects of amiloride and its analogues can be very different, depending on the GPCR and the orthosteric ligand in question. In **Chapter 3** we focus on the mechanism of allosteric modulation by sodium ions in the adenosine A<sub>2A</sub> receptor by integrating the results of molecular dynamics, radioligand binding, and thermostability experiments. This approach allowed us to further explore the difference in allosteric modulation by sodium ions and amilorides between agonists and antagonists. In **Chapter 4** we combine molecular dynamics, radioligand binding, and functional assays in a mutagenesis study to investigate the role of the amino acids that form the sodium ion site of the adenosine A<sub>2A</sub> receptor in ligand affinity and receptor signaling. We found that the sodium ion site was not only important for sodium ion and amiloride binding, but also for the overall receptor conformation and signal transduction. In **Chapter 5** we describe the synthesis and biological evaluation of a number of amiloride analogues for the adenosine A<sub>2A</sub> receptor. We found novel potent amiloride analogues that all displace orthosteric ligands, but by different allosteric mechanisms.

In these studies radioligands have been indispensable. Yet, the use of radioactively labeled ligands in the lab has its drawbacks, and hence **Chapter 6** is dedicated to the development of a non-radioactive ligand binding protocol based on mass spectrometry (MS binding) for the adenosine A<sub>2A</sub> receptor and its close homolog the adenosine A<sub>1</sub> receptor. We validated that the MS binding assay works for different types of radioligand binding assays, and in addition we combined it for the first time with the competition association method to determine ligand binding kinetics.

To conclude, we discuss in **Chapter 7** the results of the research presented in this thesis in general together with the further implications for the field of GPCR pharmacology.

## References

1. Retief FP and Cilliers L, *Mesopotamian medicine*. S Afr Med J, 2007. 97(1): p. 27-30.
2. Kwiecinski J, *The dawn of medicine: ancient egypt and Athotis, the king-physician*. Perspect Biol Med, 2013. 56(1): p. 99-104.
3. Eknoyan G, *Beginnings--The kidney and nephrology in ancient mesopotamian culture*. Semin Dial, 2015.
4. Maehle AH, Prüll CR, and Halliwell RF, *The emergence of the drug receptor theory*. Nat Rev Drug Discovery, 2002. 1(8): p. 637-41.
5. Rubin RP, *A brief history of great discoveries in pharmacology: in celebration of the centennial anniversary of the founding of the American Society of Pharmacology and Experimental Therapeutics*. Pharmacol Rev, 2007. 59(4): p. 289-359.
6. Rang HP, *The receptor concept: pharmacology's big idea*. Br J Pharmacol, 2006. 147 Suppl 1: p. S9-16.
7. Fredriksson R, Lagerström MC, Lundin LG, et al., *The G-protein-coupled receptors in the human genome form five main families. Phylogenetic analysis, paralogon groups, and fingerprints*. Mol Pharmacol, 2003. 63(6): p. 1256-72.
8. Rask-Andersen M, Almén MS, and Schiöth HB, *Trends in the exploitation of novel drug targets*. Nat Rev Drug Discovery, 2011. 10(8): p. 579-90.
9. May LT, Leach K, Sexton PM, et al., *Allosteric modulation of G protein-coupled receptors*. Annu Rev Pharmacol Toxicol, 2007. 47: p. 1-51.
10. Göblyös A and IJzerman AP, *Allosteric modulation of adenosine receptors*. Biochim Biophys Acta, 2011. 1808(5): p. 1309-18.
11. Keov P, Sexton PM, and Christopoulos A, *Allosteric modulation of G protein-coupled receptors: a pharmacological perspective*. Neuropharmacology, 2011. 60(1): p. 24-35.
12. Müller CE, Schiedel AC, and Baqi Y, *Allosteric modulators of rhodopsin-like G protein-coupled receptors: opportunities in drug development*. Pharmacol Ther, 2012. 135(3): p. 292-315.
13. Shonberg J, Kling RC, Gmeiner P, et al., *GPCR crystal structures: Medicinal chemistry in the pocket*. Bioorg Med Chem, 2015. 23(14): p. 3880-906.
14. Katritch V, Cherezov V, and Stevens RC, *Structure-function of the G protein-coupled receptor superfamily*. Annu Rev Pharmacol Toxicol, 2013. 53: p. 531-56.
15. Granier S and Kobilka B, *A new era of GPCR structural and chemical biology*. Nat Chem Biol, 2012. 8(8): p. 670-3.
16. Ballesteros JA and Weinstein H, *Integrated methods for the construction of three-dimensional models and computational probing of structure-function relations in G protein-coupled receptors*. Methods Neurosci, 1995. 25: p. 366-428.
17. Liu W, Chun E, Thompson AA, et al., *Structural basis for allosteric regulation of GPCRs by sodium ions*. Science, 2012. 337(6091): p. 232-6.
18. Christopher JA, Brown J, Doré AS, et al., *Biophysical fragment screening of the  $\beta_1$ -adrenergic receptor: identification of high affinity arylpiperazine leads using structure-based drug design*. J Med Chem, 2013. 56(9): p. 3446-55.
19. Miller-Gallacher JL, Nehmé R, Warne T, et al., *The 2.1 Å resolution structure of cyanopindolol-bound  $\beta_1$ -adrenoceptor identifies an intramembrane  $\text{Na}^+$  ion that stabilises the ligand-free receptor*. PLoS ONE, 2014. 9(3): p. e92727.
20. Fenalti G, Giguere PM, Katritch V, et al., *Molecular control of  $\delta$ -opioid receptor signalling*. Nature, 2014. 506(7487): p. 191-6.
21. Zhang C, Srinivasan Y, Arlow DH, et al., *High-resolution crystal structure of human protease-activated receptor 1*. Nature, 2012. 492(7429): p. 387-92.

22. Katritch V, Fenalti G, Abola EE, et al., *Allosteric sodium in class A GPCR signaling*. Trends Biochem Sci, 2014. 39(5): p. 233-44.
23. Horstman DA, Brandon S, Wilson AL, et al., *An aspartate conserved among G-protein receptors confers allosteric regulation of  $\alpha_2$ -adrenergic receptors by sodium*. J Biol Chem, 1990. 265(35): p. 21590-95.
24. Warnock DG, Kusche-Vihrog K, Tarjus A, et al., *Blood pressure and amiloride-sensitive sodium channels in vascular and renal cells*. Nat Rev Nephrol, 2014. 10(3): p. 146-57.
25. Gao ZG and Iljerman AP, *Allosteric modulation of  $A_{2A}$  adenosine receptors by amiloride analogues and sodium ions*. Biochem Pharmacol, 2000. 60(5): p. 669-76.
26. Fredholm BB, Iljerman AP, Jacobson KA, et al., *International Union of Pharmacology. XXV. Nomenclature and classification of adenosine receptors*. Pharmacol Rev, 2001. 53(4): p. 527-52.
27. Fredholm BB, Iljerman AP, Jacobson KA, et al., *International Union of Basic and Clinical Pharmacology. LXXXI. Nomenclature and classification of adenosine receptors — an update*. Pharmacol Rev, 2011. 63(1): p. 1-34.
28. Chen JF, Eltzhig HK, and Fredholm BB, *Adenosine receptors as drug targets — what are the challenges?* Nat Rev Drug Discovery, 2013. 12(4): p. 265-86.
29. Xu F, Wu H, Katritch V, et al., *Structure of an agonist-bound human  $A_{2A}$  adenosine receptor*. Science, 2011. 332(6027): p. 322-7.
30. Bennett KA, Tehan B, Lebon G, et al., *Pharmacology and structure of isolated conformations of the adenosine  $A_{2A}$  receptor define ligand efficacy*. Mol Pharmacol, 2013. 83(5): p. 949-58.
31. Lebon G, Warne T, Edwards PC, et al., *Agonist-bound adenosine  $A_{2A}$  receptor structures reveal common features of GPCR activation*. Nature, 2011. 474(7352): p. 521-25.
32. Hulme EC and Trevethick MA, *Ligand binding assays at equilibrium: validation and interpretation*. Br J Pharmacol, 2010. 161(6): p. 1219-37.
33. Lohse MJ, Nuber S, and Hoffmann C, *Fluorescence/bioluminescence resonance energy transfer techniques to study G-protein-coupled receptor activation and signaling*. Pharmacol Rev, 2012. 64(2): p. 299-336.
34. Niessen KV, Höfner G, and Wanner KT, *Competitive MS binding assays for dopamine  $D_2$  receptors employing spiperone as a native marker*. Chembiochem, 2005. 6(10): p. 1769-75.
35. Zepperitz C, Höfner G, and Wanner KT, *MS-binding assays: kinetic, saturation, and competitive experiments based on quantitation of bound marker as exemplified by the GABA transporter mGAT1*. ChemMedChem, 2006. 1(2): p. 208-17.
36. Hess M, Höfner G, and Wanner KT, *(S)- and (R)-fluoxetine as native markers in mass spectrometry (MS) binding assays addressing the serotonin transporter*. ChemMedChem, 2011. 6(10): p. 1900-8.
37. Grimm SH, Höfner G, and Wanner KT, *MS Binding assays for the three monoamine transporters using the triple reuptake inhibitor (1R,3S)-indatraline as native marker*. ChemMedChem, 2015. 10(6): p. 1027-39.
38. Motulsky HJ and Mahan LC, *The kinetics of competitive radioligand binding predicted by the law of mass action*. Mol Pharmacol, 1984. 25(1): p. 1-9.



# **Chapter 2**

## **Allosteric modulation of class A GPCRs by amiloride and its analogues**

Arnault Massink

Alex Karamychev

Adriaan P. IJzerman

## **Abstract**

The function of G protein-coupled receptors (GPCRs) can be modulated by compounds that bind to other binding sites than the endogenous orthosteric site, called allosteric sites. Recent crystal structures revealed a bound sodium ion in a conserved allosteric site of multiple GPCRs. Amiloride and its analogues have been proposed to bind in this same sodium ion site. This review seeks to recapitulate the current knowledge of allosteric effects by amilorides and its analogues on class A GPCRs. Amilorides are known to modulate adenosine, adrenergic, dopamine, chemokine, muscarinic, serotonin and gonadotropin-releasing hormone receptors. Amiloride analogues with lipophilic substituents are more potent modulators than amiloride for several GPCRs. Some receptors, like adenosine,  $\alpha$ -adrenergic, and dopamine receptors, are strongly modulated by amiloride analogues. In addition, for a few GPCRs more than one binding site for amilorides has been postulated. Interestingly, the allosteric effects by amiloride binding vary considerably between GPCRs, from acting as negative allosteric modulators to in some cases as positive allosteric modulators. Since the sodium ion site is strongly conserved amongst GPCRs it is to be expected that amilorides also bind to GPCRs not yet evaluated for their sensitivity, but with different modulating effects. Investigating this typical amiloride-GPCR interaction further may yield general insight on the allosteric mechanisms of GPCR binding and function.

## Introduction

G protein-coupled receptors (GPCRs) form a family of receptors with approximately 800 members that are responsible for many different physiological functions such as regulation of sleep, vision, blood pressure, CNS activity, taste, and olfaction.<sup>1</sup> This is reflected by the fact that they are targeted by 30% to 40% of therapeutic drugs currently on the market.<sup>2</sup> GPCRs are grouped according to their structural and genomic characteristics in five main groups: rhodopsin-like (class A), secretin-like (class B), glutamate-like (class C), adhesion, and frizzled/taste2, with class A being the largest group.<sup>3,4</sup>

The precise mechanisms of these receptors have been studied for a long time, but due to the complexity of their structures they are not yet fully understood. The recent increase in availability of high resolution GPCR crystal structures allow a better understanding of how GPCRs function.<sup>5, 6</sup> Co-crystallization with orthosteric ligands allows the study of endogenous orthosteric binding sites. However, to study allosteric binding sites co-crystallization with allosteric modulators is necessary, which is a challenge due to their relatively low affinities. Adding high concentrations of sodium ions is a common procedure in the crystallization of GPCRs to stabilize the protein, which makes it possible for them to bind to even low affinity sites. However, sodium ions are relatively small and will need a high resolution (< 2 Å) to be visualized. In recent crystal structures of several GPCRs the resolution was sufficiently high to locate a sodium ion bound in a site which is highly conserved amongst GPCRs.<sup>7</sup> Currently solved crystal structures with a sodium ion bound in its allosteric site are of the human adenosine A<sub>2A</sub> receptor,<sup>8</sup> the β<sub>1</sub>-adrenergic receptor,<sup>9, 10</sup> the human δ-opioid receptor,<sup>11</sup> and the human protease activated receptor 1.<sup>12</sup> The common residues that interact with the sodium ion in these crystal structures, either directly or through water mediated hydrogen bond interactions, are Asp<sup>2.50</sup>, Ser<sup>3.39</sup> Trp<sup>6.48</sup>, Asn<sup>7.45</sup>, and Asn<sup>7.49</sup> (numbering according to Ballesteros-Weinstein<sup>13</sup>). The negatively charged amino acid Asp<sup>2.50</sup> makes a strong salt bridge with the positively charged sodium ion and is essential for its binding in this site, which confirmed previous 'pre-crystal structure' research.<sup>14</sup> It is also the most conserved residue of the sodium ion site amongst GPCRs. The high conservation of the sodium ion pocket amongst GPCRs makes it probable that more crystal structures with sodium ions bound in this site are to be expected.

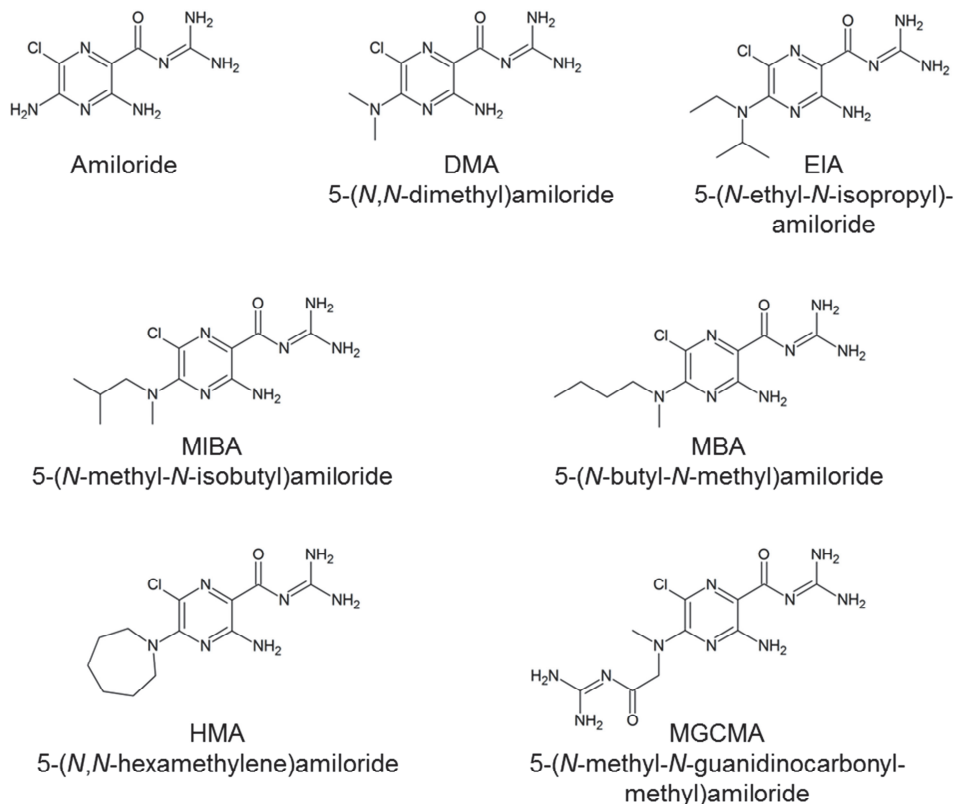


**Figure 1.** Chemical structures of amiloride and its 5'-amino substituted analogues DMA, EIA, MIBA, MBA, HMA, and MGCMA.

Amiloride is primarily known as a potassium sparing diuretic drug, acting through the blockade of renal epithelial sodium channels.<sup>15</sup> Amiloride and its analogues have also been found to bind to the sodium ion site of several GPCRs, modulating orthosteric ligand binding.<sup>16</sup> The negatively charged carboxylate of sodium ion site residue Asp<sup>2.50</sup> interacts with the positively charged guanidinium group present on all amilorides, which makes it important for amiloride binding as discussed in Chapters 3 and 4 of this thesis. The binding of amilorides into the sodium ion site of GPCRs renders these compounds potential pharmacological tools to probe molecular mechanisms of GPCR allosteric modulation. This review summarizes the current knowledge of modulation by amiloride and its analogues on class A GPCRs, which primarily occurs through binding in the sodium ion site. The chemical structures of amiloride and its analogues discussed in this review are depicted in Figures 1 and 2. Effects of the amilorides are represented in Table 1 categorized per GPCR



and orthosteric ligands used. Most of the receptors in Table 1 are discussed in the main text, except for the histamine H<sub>1</sub> and the opioid receptors which have been studied little for amiloride effects.

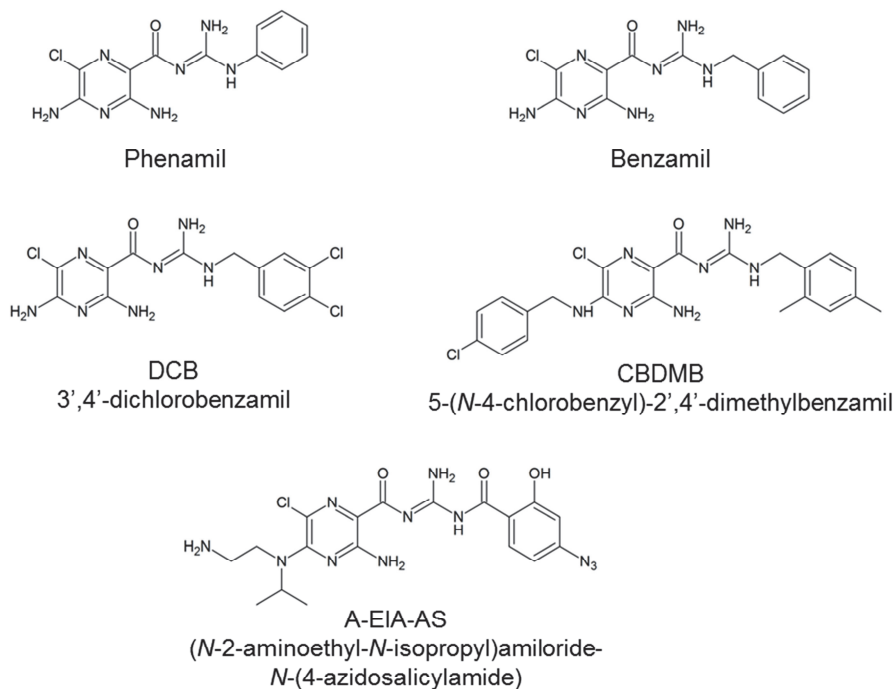


**Figure 2.** Chemical structures of 2-guanidino substituted amiloride analogues phenamil, benzamil, DCB, CBDMB, and A-EIA-AS.

## Adenosine receptors

Adenosine receptors have been studied extensively, and as a result many orthosteric<sup>17</sup> and allosteric<sup>18</sup> ligands have been discovered. Amiloride interactions with adenosine receptors were discovered in the early days of adenosine receptor research.<sup>19</sup> Since the effects of amiloride binding to adenosine receptors appeared to be closely tied to sodium ion interactions, it was necessary to investigate and exclude the involvement of Na<sup>+</sup>/H<sup>+</sup> exchangers (one of the main targets of amiloride) in these interactions.<sup>16</sup> In this study, Garritsen et al. found inhibition of antagonist [<sup>3</sup>H]DPCPX and agonist [<sup>3</sup>H]PIA at the calf adenosine A<sub>1</sub> receptor by amiloride, its 5'-amino substituted analogues 5-(*N,N*-

hexamethylene)amiloride (HMA), 5-(*N*-methyl-*N*-butyl)amiloride (MBA), 5-(*N*-methyl-*N*-guanidinocarbonyl-methyl)amiloride (MCGMA), and 5-(*N*-methyl-*N*-isobutyl)amiloride (MIBA), and its 2-guanidino substituted analogues benzamil, 5-(*N*-4-chlorobenzyl)-2',4'-dimethylbenzamil (CBDMB), 3',4'-dichlorobenzamil (DCB), and phenamil.

Gao and IJzerman found that amiloride analogues benzamil, HMA, MCGMA, MIBA, and phenamil increased the dissociation rate of the antagonist [<sup>3</sup>H]ZM-241,385 at the rat A<sub>2A</sub> receptor, and that they were more potent than amiloride itself (Figure 3).<sup>20</sup> However, the affinity (defined by radioligand displacement in equilibrium) and the allosteric potency (defined by the concentration-dependent effect on the radioligand dissociation rate) did not correlate. This indicated a mixed competitive (i.e., mutually exclusive displacement) and noncompetitive (i.e., amilorides and orthosteric ligands can bind to the receptor at the same time, and amiloride influences the orthosteric ligand's dissociation rate) behavior of amilorides. The amiloride analogues HMA and MIBA, with a lipophilic moiety on the 5'-position, proved to be the most potent compounds in increasing the dissociation rate of the orthosteric ligand, while they had equal affinities to benzamil and phenamil in displacing it. In contrast to the effect of amilorides, sodium ions decreased the dissociation rate of [<sup>3</sup>H]ZM-241,385. Still, sodium ions and HMA appeared to compete for the same allosteric site.

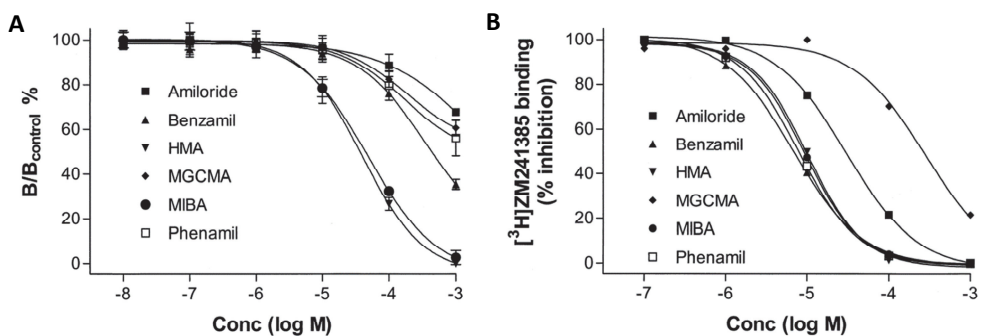


**Figure 3.** Concentration dependence of amiloride and its analogues for increase of [<sup>3</sup>H]ZM-241,385 dissociation (A) and displacement of [<sup>3</sup>H]ZM-241,385 (B) after reaching binding equilibrium at adenosine A<sub>2A</sub> receptors. In A [<sup>3</sup>H]ZM-241,385 was allowed to first reach equilibrium binding at the receptor before the dissociation was induced by addition of an excess of antagonist, in absence and presence of increasing concentrations of amiloride (analogue). The results are expressed as a ratio between the binding of [<sup>3</sup>H]ZM-241,385 after 120 min in presence ('B') and in absence (B<sub>control</sub>) of amiloride (analogue). Reproduced with permission from Gao and IJzerman.<sup>20</sup>

In a study by Gao et al. in 2003 it appeared that agonists and antagonists are differently affected by amilorides on adenosine receptors.<sup>21</sup> Amilorides increased the dissociation rates of antagonists [<sup>3</sup>H]DPCPX at the rat adenosine A<sub>1</sub> and [<sup>3</sup>H]PSB-11 at the human A<sub>3</sub> receptors, just as with [<sup>3</sup>H]ZM-241,385 at the rat A<sub>2A</sub> receptor. However, they did not affect the dissociation rates of agonists [<sup>3</sup>H]R-PIA from the rat A<sub>1</sub> and [<sup>3</sup>H]CGS-21,680 from the rat A<sub>2A</sub> receptors. At the A<sub>2A</sub> receptor amilorides still displaced agonist [<sup>3</sup>H]NECA binding in a mutually exclusive manner, which makes them competitive inhibitors of agonist binding (Chapter 3). Amilorides even decreased the dissociation rate of agonist [<sup>125</sup>I]-AB-MECA at the rat adenosine A<sub>3</sub> receptor, revealing that amilorides can also act as positive allosteric modulators depending on the radiolabeled probe used.<sup>21</sup> Furthermore the amilorides exhibited selectivity for the different adenosine receptor subtypes. Amiloride and 5-(*N,N*-dimethyl)amiloride (DMA) were more potent at the A<sub>1</sub> receptor in accelerating antagonist dissociation, while HMA was the most potent at the A<sub>2A</sub> receptor and to a lesser extent at the A<sub>3</sub> receptor.

Solving the crystal structure of the adenosine A<sub>2A</sub> receptor at a resolution of 1.8 Å provided a sufficiently high resolution to detect for the first time a sodium ion bound in its allosteric binding site.<sup>8</sup> The amino acids interacting with the sodium ion are highly conserved amongst GPCRs which confirmed previous studies in which modulation by sodium ions was tied to the same amino acids for different GPCRs.<sup>7</sup> The most conserved amino acid is a negatively charged aspartic acid (Asp52<sup>2,50</sup>) which interacts directly with the positively charged sodium ion by means of a salt bridge. The positively charged guanidinium moiety of amilorides may also interact in a similar manner with this Asp52<sup>2,50</sup>, and this is confirmed in Chapter 3 of this thesis by a docking study based on the A<sub>2A</sub> crystal structure (Figure 4), and in Chapter 4 by a mutational study in which mutation of this aspartic acid into an alanine decreased the affinity of amiloride and HMA. In the same chapter, the mutation of other amino acids forming the sodium ion site, Trp246<sup>6,48</sup>, Asn280<sup>7,45</sup>, and Asn284<sup>7,49</sup>, into Ala influenced the binding of amiloride and HMA as well. However, mutation of these residues increased the amilorides' affinity, especially in case of Trp246<sup>6,48</sup>. At the adenosine A<sub>3</sub> receptor the mutation of Trp243<sup>6,48</sup> into Ala increased the affinity of HMA as well,<sup>22</sup> and it can be concluded that this residue strongly impedes the binding of amilorides in the sodium ion site of both receptors.

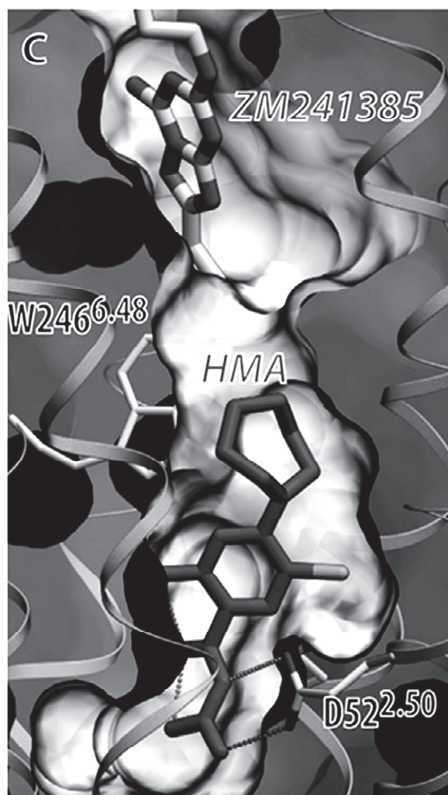


**Figure 4.** Docking of HMA in the sodium ion site. The guanidinium group of HMA has a salt bridge interaction with Asp52<sup>2,50</sup> whereas the 5'-azepane moiety of HMA clashes with Trp246<sup>6,48</sup>. Chapter 3 provides more details about this docking study.

## Adrenergic receptors

One of the first indications that amiloride inhibited the binding of orthosteric ligands at  $\alpha$ - and  $\beta$ -adrenergic receptors was found in 1987 by Howard et al,<sup>23</sup> which was followed by many studies with amiloride and its analogues at adrenergic receptors. At the human  $\alpha_{1A}$ -adrenergic receptor amiloride and its analogues benzamil, DMA, 5-(*N*-ethyl-*N*-isopropyl)-amiloride (EIA), MIBA, and HMA increased the dissociation rate of antagonist [<sup>3</sup>H]prazosin, and the analogues with bulky lipophilic 5'-moieties were more potent in doing so.<sup>24, 25</sup> Amiloride itself was characterized as an allosteric modulator acting at one allosteric site, but all the amiloride analogues appeared to bind to two different allosteric sites. The authors speculated that these allosteric sites could be present on one receptor or were an effect of receptor dimerization, but could not further confirm this. The allosteric

interaction by amilorides was seemingly in contradiction with previous results at rat and mouse  $\alpha_1$ -adrenergic receptors in which amiloride only showed a competitive interaction with antagonist [ $^3$ H]prazosin binding but did not influence its dissociation rate,<sup>23</sup> which may be attributed to the not yet discovered subtypes of  $\alpha_1$ -receptors or the difference in species.

$\alpha_2$ -Adrenergic receptors are allosterically modulated by amilorides as well. At rat, human, bovine, and porcine  $\alpha_{2A}$ -adrenergic receptors amiloride increased the dissociation rate of the antagonists [ $^3$ H]rauwolscine<sup>23, 26</sup> and [ $^3$ H]yohimbine.<sup>27</sup> Amiloride analogues also increased antagonist dissociation at the  $\alpha_{2A}$ -adrenergic receptor, which was found for the amilorides (*N*-2-aminoethyl-*N*-isopropyl)amiloride-*N*-(4-azidosalicylamide) (A-EIA-AS) at the porcine receptor,<sup>28</sup> and DMA, EIA, MIBA, and HMA at the human receptor, in relation to [ $^3$ H]yohimbine, [ $^3$ H]rauwolscine, and [ $^3$ H]RX-821,002 dissociation.<sup>29</sup> It is noteworthy that A-EIA-AS has no affinity for the Na<sup>+</sup>/H<sup>+</sup> exchange protein, making it a GPCR selective amiloride. EIA, HMA, and MIBA were exceptionally strong negative allosteric modulators of antagonist binding, being 50- to 80-fold more potent than amiloride in increasing the dissociation rate of [ $^3$ H]yohimbine, showing that bulky lipophilic moieties at the 5'-position of amiloride increase the allosteric potency at the  $\alpha_{2A}$ -adrenergic receptor considerably. The apparent affinities of these amilorides were not correlating at all with their derived allosteric potencies in this study, cautioning to not confuse these two different pharmacological properties with each other.

In contrast to their effect on antagonists, amiloride, DMA, and HMA decreased the dissociation rate of agonist [ $^3$ H]UK-14,304 at the human  $\alpha_{2A}$ -adrenergic receptor, with HMA having the largest effect.<sup>30</sup> The dissociation slowing effect on agonist binding (2.7-fold slower dissociation by HMA) was considerably smaller though than the dissociation accelerating effect on antagonist binding (140-fold faster dissociation by HMA). Even as they slowed agonist dissociation, amilorides acted as negative allosteric modulators of  $\alpha_{2A}$  receptor agonist activation, since amiloride, DMA, and HMA decreased the potency of norepinephrine and UK-41,304. This paradoxical behavior was in line with previous indications that in addition to their allosteric effects amilorides could displace the orthosteric ligand competitively at the  $\alpha_{2A}$  receptor.<sup>29</sup> Moreover, addition of sodium ions increased the affinity of amiloride in doing so.<sup>23</sup> This led to the conclusion that at  $\alpha_{2A}$ -adrenergic receptors amilorides could bind to two different sites, namely the orthosteric

site and an allosteric sodium ion site. Howard et al. hypothesized that amiloride binding in the orthosteric site was enhanced by binding of a sodium ion in the allosteric site, while amiloride binding in the allosteric site increased the dissociation rate of other orthosteric ligands.<sup>23</sup> In a later study by Leppik et al., variations in the affinity of several amiloride analogues for the antagonist occupied and non-occupied receptor led to two different hypotheses. Either the amilorides could indeed bind to both the allosteric and orthosteric sites, or binding of an antagonist to the orthosteric site modified the conformation of the allosteric binding site in such a way that amiloride affinity decreased.<sup>29</sup>

At the  $\alpha_{2B}$  subtype however, amilorides can both increase and decrease the dissociation rate of antagonists. The 5'-substituted amilorides EIA and MIBA increased the dissociation rate of [<sup>3</sup>H]rauwolscine binding, while the guanidino-substituted amiloride CBDMB decreased it (Figure 5).<sup>31</sup>

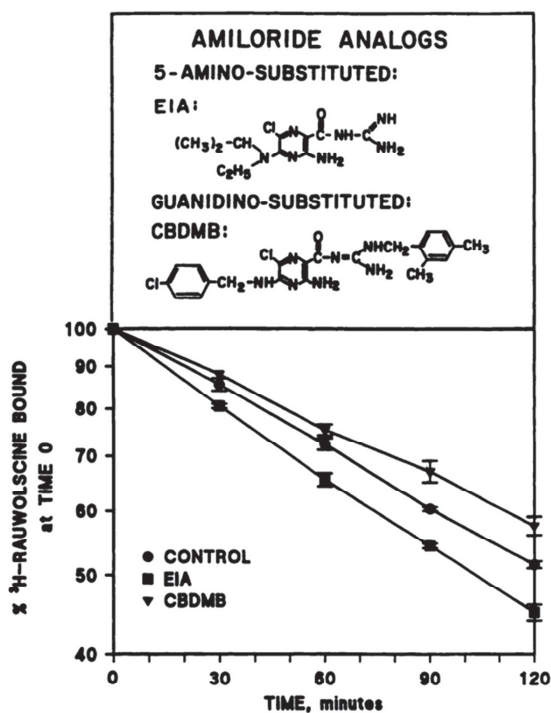


**Figure 5.** Positive and negative allosteric modulation of [<sup>3</sup>H]rauwolscine binding at the  $\alpha_{2B}$ -adrenergic receptor, in presence of 100  $\mu$ M CBDMB and EIA, respectively. CBDMB decreased and EIA increased the dissociation rate of the orthosteric antagonist. Reproduced with permission from Wilson et al.<sup>31</sup>

The interaction of amiloride with the  $\beta$ -adrenergic receptors has only been studied by Howard et al. in 1987. At both the  $\beta_1$ - and  $\beta_2$ -adrenergic receptors amiloride displaced the antagonist [ $^{125}$ I]iodocyanopindolol competitively, since their binding was mutually exclusive.<sup>23</sup> Addition of sodium ions did not compete with amiloride binding, and it was concluded that amiloride did bind to the orthosteric site rather than to an allosteric sodium ion site. Even for the lack of modulation of  $\beta$ -adrenergic receptors by sodium ions and amiloride, a sodium ion site was found in the crystal structure of the  $\beta_1$ -adrenergic receptor.<sup>9</sup> The amino acids forming the sodium ion sites of the  $\beta_1$ -adrenergic and the adenosine A<sub>2A</sub> receptor were the most similar of the solved GPCR crystal structures with such a site.<sup>7</sup> That makes the difference in modulation by sodium ions and amilorides between these receptors remarkable and it is probably due to differences in the overall architecture of the two receptors.

## Chemokine receptors

Amiloride interactions with the chemokine receptor family have only been studied by Zweemer et al. on the chemokine CCR2 receptor.<sup>32</sup> The sodium ion site was the third binding site found on this receptor, next to the more extracellularly located orthosteric and an intracellular allosteric site.<sup>33, 34</sup> Amiloride analogues MIBA and HMA inhibited binding of antagonist [ $^3$ H]INCB3344 binding to the orthosteric site and antagonist [ $^3$ H]CCR2-RA-[R] binding to the intracellular site.<sup>32</sup> Moreover, HMA inhibited binding of the orthosteric agonist [ $^{125}$ I]CCL2. Amiloride, benzamil, MCGMA, and phenamil did however not displace any of these radioligands.

The increased dissociation rates of the orthosteric antagonist [ $^3$ H]INCB3344, the intracellular antagonist [ $^3$ H]CCR2-RA-[R], and the orthosteric agonist [ $^{125}$ I]CCL2 induced by HMA indicated a noncompetitive allosteric interaction. Remarkably, the dissociation rate of the agonist [ $^{125}$ I]CCL2 increased more (9.7-fold) than of the antagonists (1.25- and 1.36-fold) by the presence of HMA. Saturation binding assays revealed that HMA had a mixed competitive/noncompetitive interaction with the orthosteric antagonist [ $^3$ H]INCB3344 (insurmountable binding of HMA indicated by decreased  $B_{\max}$  and competitive interaction indicated by increased  $K_D$ ) while it had a purely noncompetitive interaction with the intracellular antagonist [ $^3$ H]CCR2-RA-[R] (decreased  $B_{\max}$  only).

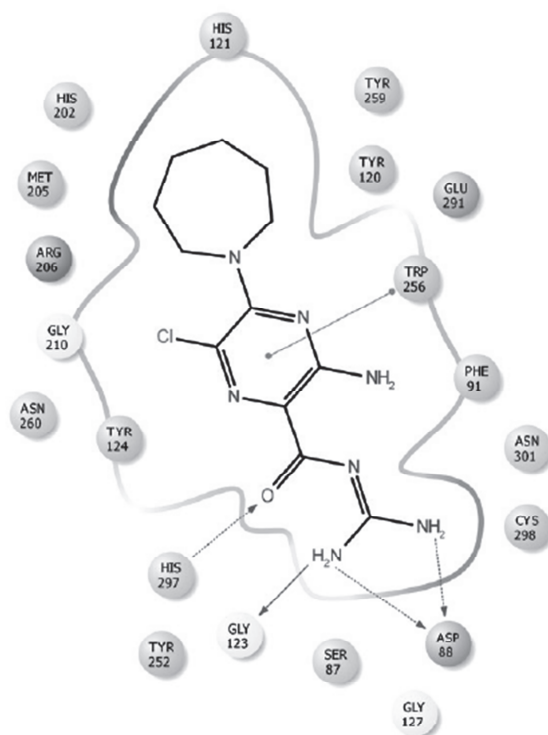


**Figure 6.** Two dimensional interaction map of HMA docking into the sodium ion pocket of a homology model of the CCR2 receptor, demonstrating a salt bridge between the guanidinium group of HMA and Asp88<sup>2,50</sup>,  $\pi$ -stacking between the pyrazine core of HMA and Trp256<sup>6,48</sup>, and a hydrogen bond between the oxygen of HMA and His297<sup>7,45</sup>. The hydrogen bond between Trp256<sup>6,48</sup> and HMA's oxygen was not captured from this angle. Reproduced with permission from Zweemer et al.<sup>32</sup>

The allosteric effect of HMA was diminished by mutation of sodium ion site residues Asp88<sup>2,50</sup> and His297<sup>7,45</sup> into Ala. Mutation of Trp256<sup>6,48</sup> even completely abolished HMA's allosteric effect, which is in contrast to the observed increase of HMA's affinity by the same mutation in adenosine receptors as discussed by Gao et al.<sup>22</sup> and Chapter 4 of this thesis. Indeed, HMA fitted well in the sodium ion site of a homology model of the CCR2 receptor in a docking study, predicting interactions with these three residues (Figure 6). Asp88<sup>2,50</sup> formed a salt bridge with the guanidinium moiety of HMA, Trp256<sup>6,48</sup> formed a hydrogen bond with HMA's oxygen as well as engaging in a  $\pi$ -stacking interaction with its pyrazine core, and His297<sup>7,45</sup> formed a hydrogen bond with the same oxygen of HMA. Amino acid His297<sup>7,45</sup> is different from most class A GPCRs which mostly harbor an Asn at



the same position, but is conserved amongst chemokine receptors, and the binding of HMA in CCR2's sodium ion site indicates that amiloride binding allows for a certain variation in the amino acids that form the sodium ion site.

## Dopamine receptors

The general trend amongst the dopamine receptor subtypes is an increase of the dissociation rate of orthosteric ligands by amiloride and its analogues, as found in a comprehensive study of the effect of amiloride, benzamil, and MIBA.<sup>35</sup> MIBA had the largest effect on the dissociation rates of the antagonists [<sup>3</sup>H]SCH-23,390 at the human D<sub>1</sub> receptor and [<sup>3</sup>H]spiperone at the human D<sub>2(short)</sub>, D<sub>2(long)</sub>, D<sub>3</sub>, and D<sub>4</sub> dopamine receptors. As with other GPCRs the analogues with lipophilic moieties at the 5'-position were more potent than amiloride itself. At the D<sub>1</sub>, D<sub>2(short)</sub>, D<sub>2(long)</sub>, and D<sub>3</sub> dopamine receptors the amilorides displaced the orthosteric antagonist [<sup>3</sup>H]spiperone in both noncompetitive and competitive manners. This may indicate affinity of the amilorides to both the orthosteric and allosteric sites, and moreover a positive homotropic cooperativity was suggested based on a high Hill coefficient, i.e. amilorides binding at the allosteric site modulate the binding of amilorides to the orthosteric site positively.

The results at the D<sub>2</sub> receptor complemented results from other studies, in which similar dissociation rate increasing effects and mixed competitive/noncompetitive behavior were found. Amiloride competed with and increased the dissociation rate of antagonists [<sup>3</sup>H]spiperone and [<sup>125</sup>I]epidepride binding.<sup>36</sup> Amiloride, DMA, benzamil, EIA, MIBA, and HMA did so as well to the antagonist [<sup>3</sup>H]spiperone at both the rat<sup>37</sup> and human<sup>38</sup> D<sub>2</sub> dopamine receptors, and of these amilorides HMA was the most potent amiloride (Figure 7). Agonists are modulated similarly as antagonists by amilorides at the rat D<sub>2</sub> and D<sub>3</sub> dopamine receptors, since amiloride, DMA, and MIBA decreased the potency of the agonist dopamine in inducing receptor activation in functional assays.<sup>35, 39</sup> At the D<sub>4</sub> receptor the allosteric effect of amiloride and its analogues was too small to be measured accurately, but an increase in antagonist [<sup>3</sup>H]spiperone dissociation rate was still detected. As amilorides still inhibited binding of the orthosteric ligand the displacement was more competitive in nature.<sup>35</sup>

The amino acids forming the sodium ion site in the dopamine receptors are conserved compared to the adenosine and adrenergic receptors. Computational and mutagenesis

studies have confirmed the importance of Asp80<sup>2.50</sup>, Ser121<sup>3.39</sup>, Asn419<sup>7.45</sup>, and Asn423<sup>7.49</sup> for the allosteric effects by sodium ions.<sup>40-42</sup> At the D<sub>4</sub> dopamine receptor mutation of Asp80<sup>2.50</sup> into Asn decreased MIBA affinity,<sup>43</sup> indicating that amilorides bind in the sodium ion site as well. It may be assumed that amilorides also bind in the sodium ion site of the other dopamine receptors, but this has not been confirmed yet.

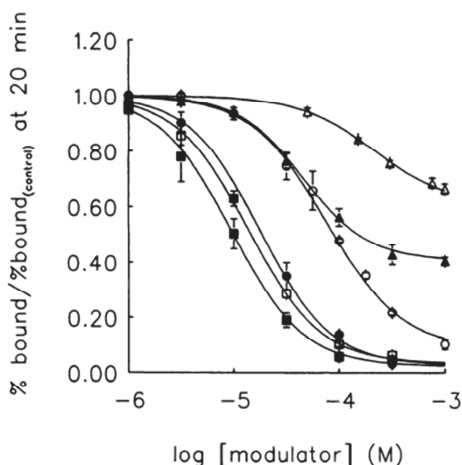


**Figure 7.** Concentration dependent dissociation modulation by amiloride and its analogues of [<sup>3</sup>H]spiperone at the dopamine D<sub>2</sub> receptor after 20 minutes. (Δ-amiloride, ▲-benzamil, ○-DMA, ●-EIA, ◻-MIBA, ■-HMA). Amiloride modulates dissociation the least, while HMA and MIBA are the most effective modulators of dissociation. Reproduced with permission from Hoare and Strange (1996).<sup>38</sup>

## Gonadotropin-releasing hormone receptor

The gonadotropin-releasing hormone (GnRH) receptor, also known as luteinizing hormone-releasing hormone receptor, is targeted by various drugs on the market for treatment of sex-hormone-dependent diseases such as breast or prostate cancer.<sup>44, 45</sup> These drugs are mostly peptidic agonists and antagonists that need to be administered by subcutaneous or intramuscular injections. The development of small molecule ligands that may replace these peptidic ligands is therefore desirable.<sup>46</sup> Earlier results had indicated allosteric modulation of GnRH stimulated luteinizing hormone release by sodium ions and amilorides.<sup>47</sup> In that light, the allosteric effects of amilorides on the GnRH receptor were investigated by Heitman et al.<sup>48</sup> Amiloride, benzamil, MCGMA, and phenamil had a

negligible effect on displacement of the peptide agonist [<sup>125</sup>I]triptorelin at the GnRH receptor. However, DCB, MIBA, and HMA increased the dissociation rate of [<sup>125</sup>I]triptorelin, with HMA having the strongest effect. In a luciferase assay, HMA acted as a purely insurmountable noncompetitive allosteric modulator as it only decreased the efficacy ( $E_{\max}$ ) of GnRH receptor activation by triptorelin and the endogenous ligand GnRH. Furthermore, it was demonstrated that the GnRH receptor harbors a second allosteric site next to the sodium ion site, since HMA did not compete with FD-1, an allosteric modulator with a distinct chemical structure, for the same allosteric site.

### **Muscarinic receptors**

Amiloride effects have been found on muscarinic receptors in rat tissue preparations. Benzamil and HMA inhibited [<sup>3</sup>H]pirenzepine binding at the muscarinic M<sub>1</sub> and [<sup>3</sup>H]N-methylscopolamine binding at the muscarinic M<sub>2</sub> and M<sub>3</sub> receptors.<sup>16</sup> In rat trachea amiloride inhibited muscarinic M<sub>3</sub> receptor mediated smooth muscle contraction<sup>49</sup> by the endogenous agonist acetylcholine, by an insurmountable noncompetitive interaction as its efficacy ( $E_{\max}$ ) was reduced.<sup>50</sup> In rat parotid acini, which express the muscarinic M<sub>3</sub> receptor,<sup>51</sup> amiloride inhibited binding of the muscarinic receptor antagonist [<sup>3</sup>H]N-methylscopolamine in a competitive manner.<sup>52</sup> In the recent relatively low resolution crystal structures of the muscarinic M<sub>2</sub> and M<sub>3</sub> receptors sodium ion binding was not detected,<sup>53-55</sup> but the amino acids making up the sodium ion site are perfectly conserved compared to adenosine and adrenergic receptors,<sup>7</sup> making amiloride binding to this site likely.

### **Serotonin receptors**

Amiloride and analogues have been found to inhibit orthosteric ligand binding to serotonin receptors. Benzamil inhibited agonist [<sup>3</sup>H]8-OH-DPAT binding at the rat 5-HT<sub>1A</sub> receptor.<sup>16</sup> Amiloride and EIA inhibited agonist [<sup>3</sup>H]5-carboxamidotryptamine binding at the human 5-HT<sub>1B</sub> receptor.<sup>56</sup> In functional assays at the same receptor, amiloride inhibited receptor activation by agonist sumatriptan in a competitive manner, while EIA had intrinsic antagonistic activity as it inhibited forskolin-stimulated cAMP formation, albeit with a 15-fold higher EC<sub>50</sub> value (200 μM) compared to its K<sub>i</sub> in inhibiting [<sup>3</sup>H]5-carboxamidotryptamine binding (13 μM).<sup>56</sup> Endogenous agonist [<sup>3</sup>H]serotonin binding was inhibited by HMA at the rat 5-HT<sub>1C</sub> receptor and by benzamil and HMA at the rat 5-HT<sub>2</sub>

receptor.<sup>16</sup> Crystal structures of the agonist bound 5-HT<sub>1B</sub> receptor<sup>57</sup> and the 5-HT<sub>2B</sub> receptor,<sup>58</sup> again at relatively low resolution, did not reveal a bound sodium ion, but the well conserved amino acids of the sodium ion site compared to the other class A GPCRs<sup>7</sup> makes binding of amiloride in the same location likely.

## Concluding remarks

This review summarizes the current knowledge of the allosteric effects of amiloride and its analogues on GPCRs. Allosteric effects of amilorides have been found on adenosine receptors,  $\alpha$ -adrenergic receptors, the CCR2 chemokine receptor, dopaminergic receptors, the gonadotropin-releasing hormone receptor, the histamine H<sub>1</sub> receptor, muscarinic receptors, opioid receptors, and serotonin receptors.

Amiloride and its analogues seem to follow a few general 'rules' in their activity on these receptors. The propensity of amilorides to bind to the well conserved sodium ion site amongst GPCRs may explain these common behaviors. For most receptors, amiloride analogues with bulky lipophilic moieties on the 5'-position have greater affinity and potency than the unsubstituted parent compound. This has not been explained fully, but it is clear that in most GPCRs there is a hydrophobic pocket above the sodium ion site that can accommodate these lipophilic moieties. Most receptors allow substitution on the guanidinium group as well, with a good affinity in displacing orthosteric ligands, but with less or no effect on the dissociation of orthosteric ligands.

Another general 'rule' is the importance of Asp<sup>2.50</sup> for amiloride binding, just as for sodium ions. In the docking studies performed, the binding mode of amiloride and HMA was predicted in the sodium ion site of the adenosine A<sub>2A</sub> receptor crystal structure and a CCR2 chemokine receptor homology model. The positively charged guanidinium group has a strong salt bridge interaction with Asp<sup>2.50</sup>, underlining the great importance of this residue for amiloride binding as found before in mutagenesis studies. Trp<sup>6.48</sup> interacts with amilorides as well, in some cases hampering and in other cases accommodating amiloride binding. These interactions of amilorides with the amino acids of the sodium ion site are of interest since these have been shown to be important in receptor functionality, with Asp<sup>2.50</sup> and Trp<sup>6.48</sup> as most noticeable examples. Mutation of Asp<sup>2.50</sup> silences receptor activation in many GPCRs.<sup>59</sup> Trp<sup>6.48</sup> is noteworthy as a 'toggle switch' between the active

and inactive states of GPCRs,<sup>60, 61</sup> and in docking studies of the adenosine A<sub>2A</sub> receptor amiloride and HMA seem to toggle it into its inactive rotamer (Chapter 3).

In contrast with these general 'rules', differences in the affinities, potencies, and modulatory behaviors of amilorides are quite diverse, even between receptors where the sodium ion site constitutes of exactly the same amino acids (i.e. adenosine, adrenergic, dopamine, and muscarinic receptors). To appreciate these differences it is important to discern between the different properties by which the allosteric effect of amilorides on orthosteric ligand binding may be described. In Table 1 we collected values for the different amilorides, of their affinity in displacing orthosteric ligands (IC<sub>50</sub> or K<sub>i</sub>), their effect on dissociation of orthosteric ligand ( $k_{\text{off}}/k_{\text{off}(\text{control})}$ ), and their potency for these dissociation effects (EC<sub>50</sub>). This information also helps to understand whether the interaction of a particular amiloride with an orthosteric ligand is competitive or noncompetitive. If an amiloride inhibits orthosteric ligand binding, but does not affect its dissociation rate, the binding is mutually exclusive and the interaction is defined as competitive. If the dissociation rate is changed though, both the orthosteric ligand and amiloride can bind to the receptor at the same time and the interaction is deemed noncompetitive. Another way to confirm a noncompetitive interaction is by showing insurmountability of the inhibiting effect in radioligand saturation (B<sub>max</sub> decrease) or functional assays (E<sub>max</sub> decrease), as discussed for the chemokine CCR2, muscarinic M<sub>3</sub>, and gonadotropin-releasing hormone receptor. However, these assays have been conducted far less than dissociation assays in amiloride research so we did not include them in Table 1.

In some cases, amilorides behave only as purely competitive inhibitors, while in other cases they behave as noncompetitive negative modulators, and a mixed behavior has also been observed. For some receptors the cause for mixed competitive/noncompetitive behavior was explained by a tendency of amilorides to bind both orthosteric and allosteric sites, but also in these cases the observed effect may be caused by binding in the sodium ion site only, where the competitive 'fraction' of the allosteric effect is caused by either an overlap of binding with the orthosteric site or a conformational change of the receptor by amiloride binding. The latter option is quite likely from the structural evidence provided by the recently elucidated crystal structures.

At some of the discussed receptors the modulatory effect by amilorides is probe-dependent, which has been described in other cases of allosteric modulation as well.<sup>62,63</sup> Amilorides act as positive allosteric modulators for agonist binding and as negative modulators for antagonists at the  $\alpha_{2A}$ -adrenergic and adenosine  $A_3$  receptors. At the  $\alpha_{2B}$ -adrenergic receptor different amilorides even exhibit both positive and negative modulatory effects. Some of the differences in affinity and modulatory effect may be caused by differences in the sodium ion site itself, but the substantial conservation of the sodium ion site residues amongst GPCRs makes it more likely that these differences are caused by variations in structural conformations elsewhere in the receptor.

Clinical application of amilorides targeting GPCRs is unlikely, due to their micromolar range affinities and lack of selectivity. However, it may be feasible to synthesize amiloride analogues with variations on the 5'-position to improve their affinity and selectivity for GPCRs. The possibility to use amilorides as tools to understand GPCR pharmacology is of greater interest though. For some of the amiloride-modulated receptors it has been confirmed that amilorides bind in the allosteric sodium ion site, and for the other receptors this is very likely. Indeed, allosteric modulation by sodium ions and amilorides often go together, and the investigation of confirmed sodium ion-modulated GPCRs that have not yet been researched for amiloride effects may be worthwhile. The sodium ion pocket region is important in the overall receptor activation of GPCRs, since mutation of sodium ion site residues has been shown to affect receptor functionality. With the ongoing expansion of the crystal structure pool of GPCRs, further study and knowledge of the mechanisms of amiloride modulation will help in understanding and appreciating the allosteric mechanism in GPCR functioning.

**Table 1.** Modulation of G protein-coupled receptors by amiloride and amiloride analogues. The given values reflect i) inhibitory potency or affinity for ligand displacement in radioligand binding assays or inhibition of ligand-induced receptor activation in functional assays, ii) modulatory potency of their effect on radioligand dissociation, and iii) fold change of dissociation rates of orthosteric ligands. References are in numbered superscript.

Receptor	Orthosteric ligand antagonist; agonist	Amiloride (analogue)	Inhibitory potency or affinity <sup>a</sup> - Displacement of orthosteric ligand by amiloride (analogue) in IC <sub>50</sub> or K <sub>i</sub> ± S.E.M. (μM)	Modulatory potency - Concentration- effect on dissociation of orthosteric ligand by amiloride (analogue) in EC <sub>50</sub> ± S.E.M. (μM)	Effect on dissociation of orthosteric ligand by 100 μM <sup>c</sup> amiloride (analogue) in k <sub>off</sub> / k <sub>off(control)</sub> >1, Increase <1, Decrease	
Adenosine A <sub>1</sub>	[ <sup>3</sup> H]DPCPX	Amiloride	2.0 ± 0.2 <sup>B19</sup>	-	1.5 <sup>Rd21</sup>	
			197 ± 23 <sup>R21</sup>			
		Benzamil	0.65 ± 0.04 <sup>B19</sup>	-	-	
		CBDMB	1.2 ± 0.1 <sup>B19</sup>	-	-	
		DCB	1.6 ± 0.1 <sup>B19</sup>	-	-	
		DMA	8 ± 2 <sup>R21</sup>	-	1.9 <sup>R21</sup>	
		HMA	0.41 ± 0.03 <sup>B19</sup>	-	1.7 <sup>R21</sup>	
			22 ± 4 <sup>R21</sup>			
		MBA	0.070 ± 0.004 <sup>B19</sup>	-	-	
		MGCMA	22 ± 1 <sup>B19</sup>	-	-	
		MIBA	0.16 ± 0.01 <sup>B19</sup>	-	-	
	13 ± 1 <sup>R21</sup>					
	Phenamil	1.5 ± 0.1 <sup>B19</sup>	-	-		
	[ <sup>3</sup> H]PIA	Amiloride	2.4 ± 0.1 <sup>B19</sup>	-	No effect <sup>Rd21</sup>	
			Benzamil	0.85 ± 0.03 <sup>B19</sup>	-	-
			CBDMB	4.0 ± 0.4 <sup>B19</sup>	-	-
			DCB	2.7 ± 0.2 <sup>B19</sup>	-	-
			DMA	-	-	No effect <sup>R21</sup>
			HMA	0.50 ± 0.03 <sup>B19</sup>	-	No effect <sup>R21</sup>
MBA			0.09 ± 0.01 <sup>B19</sup>	-	-	
MGCMA			16 ± 1 <sup>B19</sup>	-	-	
MIBA			0.20 ± 0.01 <sup>B19</sup>	-	-	
Phenamil	2.3 ± 0.1 <sup>B19</sup>	-	-			

Adenosine A <sub>2A</sub>	<sup>[3]H</sup> ZM-241,385	Amiloride	9.7 ± 1.1 <sup>R20</sup>	-	1.2 <sup>Rd20</sup>
		Benzamil	2.2 ± 0.3 <sup>R20</sup>	-	2.4 <sup>Rd20</sup>
		HMA	3.3 ± 0.5 <sup>R20</sup>	-	12 <sup>Rd20</sup>
		MGCMA	89 ± 13 <sup>R20</sup>	-	1.2 <sup>Rd20</sup>
		MIBA	3.0 ± 0.2 <sup>R20</sup>	-	5.7 <sup>Rd20</sup>
		Phenamyl	2.6 ± 0.4 <sup>R20</sup>	-	1.9 <sup>Rd20</sup>
	<sup>[3]H</sup> CGS-21,680	Amiloride	-	-	No effect <sup>Rd21</sup>
		DMA	-	-	No effect <sup>R21</sup>
		HMA	-	-	No effect <sup>R21</sup>
Adenosine A <sub>3</sub>	<sup>[3]H</sup> PSB-11	Amiloride	82 ± 7 <sup>H21</sup>	-	No effect <sup>Hd21</sup>
		DMA	13 ± 2 <sup>H21</sup>	-	1.3 <sup>H21</sup>
		HMA	6 ± 1 <sup>H21</sup>	-	2.3 <sup>H21</sup>
		MIBA	8 ± 1 <sup>H21</sup>	-	1.6 <sup>H21</sup>
	<sup>[125]I</sup> I-AB-MECA	Amiloride	>100 <sup>R21</sup>	-	No effect <sup>Hd21</sup>
		DMA	20 ± 3 <sup>R21</sup>	-	0.80 <sup>H21</sup>
		HMA	7 ± 1 <sup>R21</sup>	-	0.53 <sup>H21</sup>
		MIBA	7 ± 2 <sup>R21</sup>	-	0.59 <sup>H21</sup>
α <sub>1A</sub> <sup>-</sup> Adrenergic	<sup>[3]H</sup> Prazosin	Amiloride	11 ± 2 <sup>H24</sup>	-	1.2 <sup>H24</sup>
		Benzamil	0.8 ± 0.1 <sup>H24</sup>	-	1.7 <sup>H24</sup>
		DMA	0.82 ± 0.03 <sup>H24</sup>	-	1.5 <sup>H24</sup>
		EIA	2.7 ± 0.3 <sup>H24</sup>	-	2.2 <sup>H24</sup>
		HMA	1.1 ± 0.2 <sup>H24</sup>	-	5.5 <sup>H24</sup>
		MIBA	0.49 ± 0.07 <sup>H24</sup>	-	2.4 <sup>H24</sup>
α <sub>2A</sub> <sup>-</sup> Adrenergic	<sup>[3]H</sup> Yohimbine	Amiloride	30 ± 2 <sup>H29</sup>	-	2.0 <sup>He29</sup>
		A-EIA-AS	-	40 <sup>P28</sup>	> 1 <sup>P28</sup>
		Benzamil	3.5 ± 0.7 <sup>H29</sup>	-	No effect <sup>He29</sup>
		DMA	3.6 ± 0.1 <sup>H29</sup>	-	5.3 <sup>He29</sup>
	<sup>[3]H</sup> Rauwolscine		-	-	6.3 <sup>He29</sup>
	<sup>[3]H</sup> RX-821,002	DMA	-	-	7.1 <sup>He29</sup>
	<sup>[3]H</sup> Yohimbine	EIA	1.7 ± 0.2 <sup>H29</sup>	50 <sup>P28</sup>	> 1 <sup>P28</sup> 155 <sup>He29</sup>
		HMA	0.21 ± 0.00 <sup>H29</sup>	-	138 <sup>He29</sup>
		<sup>[3]H</sup> Rauwolscine	-	-	57 <sup>He29</sup>
	<sup>[3]H</sup> Yohimbine	MIBA	0.56 ± 0.01 <sup>H29</sup>	-	101 <sup>He29</sup>
	<sup>[3]H</sup> UK-14,304	Amiloride	25 ± 0.2 <sup>H30</sup>	-	0.67 <sup>He30</sup>
		DMA	3.2 ± 0.2 <sup>H30</sup>	-	0.77 <sup>He30</sup>
		HMA	0.18 ± 0.02 <sup>H30</sup>	-	0.37 <sup>He30</sup>



$\alpha_{2B}$ - Adrenergic	$[^3\text{H}]$ Rauwolscine	CBDMB	-	-	$< 1^{R31}$	
		EIA	-	-	$> 1^{R31}$	
		MIBA	-	-	$> 1^{R31}$	
$\beta_1$ - Adrenergic	$[^{125}\text{I}]$ Iodocyano- pindolol	Amiloride	$83 \pm 14^{R23}$	-	-	
$\beta_2$ - Adrenergic	$[^{125}\text{I}]$ Iodocyano- pindolol	Amiloride	$60^{R23}$	-	-	
CCR2	$[^3\text{H}]$ INCB3344	Amiloride	No effect <sup>Hf32</sup>	-	-	
		Benzamil	No effect <sup>Hf32</sup>	-	-	
		HMA	$79^{H32}$	-	$1.25^{H32}$	
		MCGMA	No effect <sup>Hf32</sup>	-	-	
		MIBA	$158^{H32}$	-	-	
		Phenamil	No effect <sup>Hf32</sup>	-	-	
	$[^3\text{H}]$ CCR2- RA-[R] <sup>g</sup>	Amiloride	No effect <sup>Hf32</sup>	-	-	
		Benzamil	No effect <sup>Hf32</sup>	-	-	
		HMA	$79^{H32}$	-	$1.36^{H32}$	
		MCGMA	No effect <sup>Hf32</sup>	-	-	
		MIBA	$126^{H32}$	-	-	
		Phenamil	No effect <sup>Hf32</sup>	-	-	
		$[^{125}\text{I}]$ CCL2	HMA	-	-	$9.7^{H32}$
Dopamine D <sub>1</sub>	$[^3\text{H}]$ SCH-23,390	Amiloride	$49 \pm 1^{H35}$	$>1000^{H35}$	-	
		Benzamil	$1.6 \pm 0.5^{H35}$	$74 \pm 8^{H35}$	-	
		MIBA	$4.4 \pm 0.2^{H35}$	$13 \pm 1^{H35}$	$26^{He35}$	
Dopamine D <sub>2</sub>	$[^{125}\text{I}]$ Epidepride	Amiloride	-	-	$2.5^{Ri36}$	
			$390 \pm 4^{H35}$	$215 \pm 35^{R38}$	$1.5^{Ri36}$	
	$[^3\text{H}]$ Spiperone		-	$100 \pm 10^{H35}$	$2.7^{Rj38}$	
	Benzamil	$25 \pm 2^{H35}$	$46 \pm 4^{R38}$	$4.8^{Rk38}$		
		-	$29 \pm 7^{H35}$			
	DMA	-	$76 \pm 8^{R38}$	$8.4^{Rk38}$		
	EIA	-	$20 \pm 5^{R38}$	$18^{Ri38}$		
	HMA	-	$10 \pm 2^{R38}$	$16^{Ri38}$		
	MIBA	$6.6 \pm 0.4^{H35}$	$14 \pm 1^{R38}$	$14^{Ri38}$		
			$2.1 \pm 0.2^{H35}$	$88^{He35}$		
	Dopamine	Dopamine	Amiloride	$29^{Rm39}$	-	-
			DMA	$1.4^{Rm39}$	-	-
			MIBA	$0.9^{Rm39}$	-	-
$0.6 \pm 0.2^{Hn35}$				-	-	

Dopamine D <sub>3</sub>	<sup>[3H]</sup> Spiperone	Amiloride	120 ± 7 <sup>H35</sup>	43 ± 3 <sup>H35</sup>	-
		Benzamil	16 ± 1 <sup>H35</sup>	15 ± 2 <sup>H35</sup>	-
		MIBA	1.7 ± 0.1 <sup>H35</sup>	0.29 ± 0.14 <sup>H35</sup>	18 <sup>He35</sup>
	<i>Dopamine</i>	MIBA	1.8 <sup>R039</sup>	-	-
Dopamine D <sub>4</sub>	<sup>[3H]</sup> Spiperone	Amiloride	280 ± 30 <sup>H35</sup>	420 ± 4 <sup>H35</sup>	-
		Benzamil	6.1 ± 0.4 <sup>H35</sup>	28 ± 2 <sup>H35</sup>	-
		MIBA	1.3 ± 0.2 <sup>H35</sup>	22 ± 5 <sup>H35</sup>	> 1 <sup>He35</sup>
GnRH	<sup>[125I]</sup> Triptorelin	Amiloride	> 100 <sup>H48</sup>	-	-
		Benzamil	> 100 <sup>H48</sup>	-	-
		DCB	30 ± 3 <sup>H48</sup>	-	1.7 <sup>H48</sup>
		MIBA	39 ± 7 <sup>H48</sup>	-	2.1 <sup>H48</sup>
		HMA	29 ± 3 <sup>H48</sup>	49 ± 7 <sup>H48</sup>	2.5 <sup>H48</sup>
		MCGMA	> 100 <sup>H48</sup>	-	-
		Phenamyl	> 100 <sup>H48</sup>	-	-
Histamine H <sub>1</sub>	<sup>[3H]</sup> Mepyramine	Amiloride	> 10 <sup>R16</sup>	-	-
		Benzamil	3.2 ± 0.2 <sup>R16</sup>	-	-
		HMA	5.6 ± 1.2 <sup>R16</sup>	-	-
Muscarinic M <sub>1</sub>	<sup>[3H]</sup> Pirenzepine	Amiloride	> 10 <sup>R16</sup>	-	-
		Benzamil	2.9 ± 0.7 <sup>R16</sup>	-	-
		HMA	3.6 ± 1.0 <sup>R16</sup>	-	-
Muscarinic M <sub>2</sub>	<sup>[3H]</sup> N-methyl-scopolamine	Amiloride	> 10 <sup>R16</sup>	-	-
		Benzamil	5.8 ± 1.1 <sup>R16</sup>	-	-
		HMA	2.9 ± 0.5 <sup>R16</sup>	-	-
Muscarinic M <sub>3</sub>	<sup>[3H]</sup> N-methyl-scopolamine	Amiloride	50 <sup>R52</sup>	-	-
		Benzamil	2.8 ± 0.5 <sup>R16</sup>	-	-
		HMA	4.7 ± 0.8 <sup>R16</sup>	-	-
	<i>Acetylcholine</i>	Amiloride	478 <sup>Rq50</sup>	-	-
δ-Opioid	<sup>[3H]</sup> DADLE	Amiloride	> 10 <sup>R16</sup>	-	-
		Benzamil	> 10 <sup>R16</sup>	-	-
		HMA	1.0 ± 0.2 <sup>R16</sup>	-	-
κ-Opioid	<sup>[3H]</sup> Ethyl-ketazocine	Amiloride	> 10 <sup>R16</sup>	-	-
		Benzamil	> 10 <sup>R16</sup>	-	-
		HMA	3.9 ± 0.6 <sup>R16</sup>	-	-
μ-Opioid	<sup>[3H]</sup> Naloxone	Amiloride	> 10 <sup>R16</sup>	-	-
		Benzamil	1.1 ± 0.4 <sup>R16</sup>	-	-
		HMA	0.06 ± 0.02 <sup>R16</sup>	-	-

Serotonin 5-HT <sub>1A</sub>	<sup>3</sup> H]8-OH-DPAT	Amiloride	> 10 <sup>R16</sup>	-	-
		Benzamil	1.9 ± 0.3 <sup>R16</sup>	-	-
		HMA	> 10 <sup>R16</sup>	-	-
Serotonin 5-HT <sub>1B</sub>	<sup>3</sup> H]5-Carboxa- midotryptamine	Amiloride	20 <sup>H56</sup>	-	-
		Sumatriptan	35 <sup>H56</sup>	-	-
	<sup>3</sup> H]Serotonin	Benzamil	> 10 <sup>R16</sup>	-	-
	<sup>3</sup> H]5-Carboxa- midotryptamine	EIA	13 <sup>H56</sup>	-	-
	<sup>3</sup> H]Serotonin	HMA	>10 <sup>R16</sup>	-	-
Serotonin 5-HT <sub>1C</sub>	<sup>3</sup> H]Serotonin	Amiloride	>10 <sup>R16</sup>	-	-
		Benzamil	>10 <sup>R16</sup>	-	-
		HMA	6.7 ± 1.2 <sup>R16</sup>	-	-
Serotonin 5-HT <sub>1D</sub>	<sup>3</sup> H]Serotonin	Amiloride	> 10 <sup>R16</sup>	-	-
		Benzamil	> 10 <sup>R16</sup>	-	-
		HMA	> 10 <sup>R16</sup>	-	-
Serotonin 5-HT <sub>2</sub>	<sup>3</sup> H]Serotonin	Amiloride	> 10 <sup>R16</sup>	-	-
		Benzamil	1.4 ± 0.1 <sup>R16</sup>	-	-
		HMA	0.40 ± 0.06 <sup>R16</sup>	-	-

-: Not determined.

a: IC<sub>50</sub> values determined with concentrations of orthosteric radioligands around their K<sub>D</sub>.

B: Bovine receptor.

c: In presence of 100 μM amiloride (analogue) except when stated otherwise.

d: In presence of 1 mM amiloride (analogue).

e: Calculated for the amiloride (analogue) occupied receptor.

f: No displacement of orthosteric ligand by 100 μM amiloride (analogue).

g: [<sup>3</sup>H]CCR2-RA-[R] is an 'intracellular antagonist' as it binds to the second intracellular site of the chemokine CCR2 receptor.

H: Human receptor.

i: In presence of 500 μM amiloride (analogue).

j: In presence of 3.16 mM amiloride (analogue).

k: In presence of 1 mM amiloride (analogue).

l: In presence of 316 μM amiloride (analogue).

m: Inhibition by amiloride (analogue) of dopamine-stimulated increase in extracellular acidification rate in cells expressing the dopamine D<sub>2</sub> receptor.

n: Inhibition by MIBA of dopamine-stimulated [<sup>35</sup>S]GTPγS binding to dopamine D<sub>2</sub> receptors.

o: Inhibition by MIBA of dopamine-stimulated increase in extracellular acidification rate in cells expressing the dopamine D<sub>3</sub> receptor.

P: Porcine receptor.

q: Modulation by amiloride of acetylcholine-induced contractions of rat tracheal smooth muscle, which expresses the muscarinic M<sub>3</sub> receptor.

R: Rat receptor.

s: Inhibition by amiloride of the sumatriptan-induced reduction of cAMP formation stimulated by forskolin in cells expressing the Serotonin 5-HT<sub>1B</sub> receptor.

## References

1. Rosenbaum DM, Rasmussen SGF, and Kobilka BK, *The structure and function of G-protein-coupled receptors*. *Nature*, 2009. 459(7245): p. 356-63.
2. Rask-Andersen M, Almén MS, and Schiöth HB, *Trends in the exploitation of novel drug targets*. *Nat Rev Drug Discovery*, 2011. 10(8): p. 579-90.
3. Foord SM, Bonner TI, Neubig RR, et al., *International Union of Pharmacology. XLVI. G protein-coupled receptor list*. *Pharmacol Rev*, 2005. 57(2): p. 279-88.
4. Fredriksson R, Lagerström MC, Lundin LG, et al., *The G-protein-coupled receptors in the human genome form five main families. Phylogenetic analysis, paralogon groups, and fingerprints*. *Mol Pharmacol*, 2003. 63(6): p. 1256-72.
5. Shonberg J, Kling RC, Gmeiner P, et al., *GPCR crystal structures: Medicinal chemistry in the pocket*. *Bioorg Med Chem*, 2015. 23(14): p. 3880-906.
6. Katritch V, Cherezov V, and Stevens RC, *Structure-function of the G protein-coupled receptor superfamily*. *Annu Rev Pharmacol Toxicol*, 2013. 53: p. 531-56.
7. Katritch V, Fenalti G, Abola EE, et al., *Allosteric sodium in class A GPCR signaling*. *Trends Biochem Sci*, 2014. 39(5): p. 233-44.
8. Liu W, Chun E, Thompson AA, et al., *Structural basis for allosteric regulation of GPCRs by sodium ions*. *Science*, 2012. 337(6091): p. 232-36.
9. Miller-Gallacher JL, Nehmé R, Warne T, et al., *The 2.1 Å resolution structure of cyanopindolol-bound  $\beta_1$ -adrenoceptor identifies an intramembrane  $\text{Na}^+$  ion that stabilises the ligand-free receptor*. *PLoS ONE*, 2014. 9(3): p. e92727.
10. Christopher JA, Brown J, Doré AS, et al., *Biophysical fragment screening of the  $\beta_1$ -adrenergic receptor: identification of high affinity arylpiperazine leads using structure-based drug design*. *J Med Chem*, 2013. 56(9): p. 3446-55.
11. Fenalti G, Giguere PM, Katritch V, et al., *Molecular control of  $\delta$ -opioid receptor signalling*. *Nature*, 2014. 506(7487): p. 191-6.
12. Zhang C, Srinivasan Y, Arlow DH, et al., *High-resolution crystal structure of human protease-activated receptor 1*. *Nature*, 2012. 492(7429): p. 387-92.
13. Ballesteros JA and Weinstein H, *Integrated methods for the construction of three-dimensional models and computational probing of structure-function relations in G protein-coupled receptors*. *Methods Neurosci*, 1995. 25: p. 366-428.
14. Horstman DA, Brandon S, Wilson AL, et al., *An aspartate conserved among G-protein receptors confers allosteric regulation of  $\alpha_2$ -adrenergic receptors by sodium*. *J Biol Chem*, 1990. 265(35): p. 21590-5.
15. Warnock DG, Kusche-Vihrog K, Tarjus A, et al., *Blood pressure and amiloride-sensitive sodium channels in vascular and renal cells*. *Nat Rev Nephrol*, 2014. 10(3): p. 146-57.
16. Garritsen A, Ilzerman AP, Tulp MTM, et al., *Receptor binding profiles of amiloride analogues provide no evidence for a link between receptors and the  $\text{Na}^+/\text{H}^+$  exchanger, but indicate a common structure on receptor proteins*. *J Recept Res*, 1991. 11(6): p. 891-907.
17. Fredholm BB, Ilzerman AP, Jacobson KA, et al., *International Union of Basic and Clinical Pharmacology. LXXXI. Nomenclature and classification of adenosine receptors — an update*. *Pharmacol Rev*, 2011. 63(1): p. 1-34.
18. Göblyös A and Ilzerman AP, *Allosteric modulation of adenosine receptors*. *Biochim Biophys Acta*, 2011. 1808(5): p. 1309-18.
19. Garritsen A, Ilzerman AP, Beukers MW, et al., *Interaction of amiloride and its analogues with adenosine  $A_1$  receptors in calf brain*. *Biochem Pharmacol*, 1990. 40(4): p. 827-34.
20. Gao ZG and Ilzerman AP, *Allosteric modulation of  $A_{2A}$  adenosine receptors by amiloride analogues and sodium ions*. *Biochem Pharmacol*, 2000. 60(5): p. 669-76.

21. Gao ZG, Melman N, Erdmann A, et al., *Differential allosteric modulation by amiloride analogues of agonist and antagonist binding at A<sub>1</sub> and A<sub>3</sub> adenosine receptors*. *Biochem Pharmacol*, 2003. 65(4): p. 525-34.
22. Gao ZG, Kim SK, Gross AS, et al., *Identification of essential residues involved in the allosteric modulation of the human A<sub>3</sub> adenosine receptor*. *Mol Pharmacol*, 2003. 63(5): p. 1021-31.
23. Howard MJ, Hughes RJ, Motulsky HJ, et al., *Interactions of amiloride with  $\alpha$ - and  $\beta$ -adrenergic receptors: amiloride reveals an allosteric site on  $\alpha_2$ -adrenergic receptors*. *Mol Pharmacol*, 1987. 32(1): p. 53-8.
24. Leppik RA, Mynett A, Lazareno S, et al., *Allosteric interactions between the antagonist prazosin and amiloride analogs at the human  $\alpha_{1A}$ -adrenergic receptor*. *Mol Pharmacol*, 2000. 57(3): p. 436-45.
25. Ciolek J, Maïga A, Marcon E, et al., *Pharmacological characterization of zinc and copper interaction with the human  $\alpha_{1A}$ -adrenoceptor*. *Eur J Pharmacol*, 2011. 655(1-3): p. 1-8.
26. Jagadeesh G, Cragoe EJ, Jr., and Deth RC, *Modulation of bovine aortic alpha-2 receptors by Na<sup>+</sup>, 5'-guanylylimidodiphosphate, amiloride and ethylisopropylamiloride: evidence for receptor G-protein precoupling*. *J Pharmacol Exp Ther*, 1990. 252(3): p. 1184-96.
27. Nunnari JM, Repaske MG, Brandon S, et al., *Regulation of porcine brain  $\alpha_2$ -adrenergic receptors by Na<sup>+</sup>, H<sup>+</sup> and inhibitors of Na<sup>+</sup>/H<sup>+</sup> exchange*. *J Biol Chem*, 1987. 262(25): p. 12387-92.
28. Wilson AL, Womble SW, Prakash C, et al., *Novel amiloride analog allosterically modulates the  $\alpha_2$ -adrenergic receptor but does not inhibit Na<sup>+</sup>/H<sup>+</sup> exchange*. *Mol Pharmacol*, 1992. 42(2): p. 175-9.
29. Leppik RA, Lazareno S, Mynett A, et al., *Characterization of the allosteric interactions between antagonists and amiloride analogues at the human  $\alpha_{2A}$ -adrenergic receptor*. *Mol Pharmacol*, 1998. 53(5): p. 916-25.
30. Leppik RA and Birdsall NJM, *Agonist binding and function at the human  $\alpha_{2A}$ -adrenoceptor: allosteric modulation by amilorides*. *Mol Pharmacol*, 2000. 58(5): p. 1091-9.
31. Wilson AL, Seibert K, Brandon S, et al., *Monovalent cation and amiloride analog modulation of adrenergic ligand binding to the unglycosylated  $\alpha_{2B}$ -adrenergic receptor subtype*. *Mol Pharmacol*, 1991. 39(4): p. 481-6.
32. Zweemer AJM, Hammerl DM, Massink A, et al., *Allosteric modulation of the chemokine receptor CCR2 by amiloride analogues and sodium ions. The ins and outs of ligand binding to CCR2*. Doctoral thesis, Leiden Univ Repos, 2014. 29763: p. 98-119.
33. Zweemer AJM, Nederpelt I, Vrieling H, et al., *Multiple binding sites for small-molecule antagonists at the CC chemokine receptor 2*. *Mol Pharmacol*, 2013. 84(4): p. 551-61.
34. Zweemer AJM, Bunnik J, Veenhuizen M, et al., *Discovery and mapping of an intracellular antagonist binding site at the chemokine receptor CCR2*. *Mol Pharmacol*, 2014. 86(4): p. 358-68.
35. Hoare SRJ, Coldwell MC, Armstrong D, et al., *Regulation of human D<sub>1</sub>, D<sub>2(long)</sub>, D<sub>2(short)</sub>, D<sub>3</sub> and D<sub>4</sub> dopamine receptors by amiloride and amiloride analogues*. *Br J Pharmacol*, 2000. 130(5): p. 1045-59.
36. Neve KA, *Regulation of dopamine D2 receptors by sodium and pH*. *Mol Pharmacol*, 1991. 39(4): p. 570-8.
37. Hoare SRJ and Strange PG, *Allosteric regulation of the rat D<sub>2</sub> dopamine receptor*. *Biochem Soc Trans*, 1995. 23(1): p. 92S.
38. Hoare SRJ and Strange PG, *Regulation of D<sub>2</sub> dopamine receptors by amiloride and amiloride analogs*. *Mol Pharmacol*, 1996. 50(5): p. 1295-308.
39. Chio CL, Lajiness ME, and Huff RM, *Activation of heterologously expressed D<sub>3</sub> dopamine receptors: comparison with D<sub>2</sub> dopamine receptors*. *Mol Pharmacol*, 1994. 45(1): p. 51-60.

40. Neve KI, Cumbay MG, Thompson KR, et al., *Modeling and mutational analysis of a putative sodium-binding pocket on the dopamine D<sub>2</sub> Receptor*. *Mol Pharmacol*, 2001. 60(2): p. 373-81.
41. Michino M, Free RB, Doyle TB, et al., *Structural basis for Na<sup>+</sup>-sensitivity in dopamine D<sub>2</sub> and D<sub>3</sub> receptors*. *Chem Commun (Camb)*, 2015. 51(41): p. 8618-21.
42. Selent J, Sanz F, Pastor M, et al., *Induced effects of sodium ions on dopaminergic G-protein coupled receptors*. *PLoS Comput Biol*, 2010. 6(8): p. e1000884.
43. Schetz JA and Sibley DR, *The binding-site crevice of the D<sub>4</sub> dopamine receptor is coupled to three distinct sites of allosteric modulation*. *J Pharmacol Exp Ther*, 2001. 296(2): p. 359-63.
44. Conn PM and Crowley WF, Jr., *Gonadotropin-releasing hormone and its analogs*. *Annu Rev Med*, 1994. 45: p. 391-405.
45. Kiesel LA, Rody A, Greb RR, et al., *Clinical use of GnRH analogues*. *Clin Endocrinol (Oxf)*, 2002. 56(6): p. 677-87.
46. Armer RE and Smelt KH, *Non-peptidic GnRH receptor antagonists*. *Curr Med Chem*, 2004. 11(22): p. 3017-28.
47. McArdle CA, Cragoe EJ, Jr., and Poch A, *Na<sup>+</sup> dependence of gonadotropin-releasing hormone action: characterization of the Na<sup>+</sup>/H<sup>+</sup> antiport in pituitary gonadotropes*. *Endocrinology*, 1991. 128(2): p. 771-8.
48. Heitman LH, Ye K, Oosterom J, et al., *Amiloride derivatives and a nonpeptidic antagonist bind at two distinct allosteric sites in the human gonadotropin-releasing hormone receptor*. *Mol Pharmacol*, 2008. 73(6): p. 1808-15.
49. Eglén RM, *Overview of muscarinic receptor subtypes*, in *Handb Exp Pharmacol*. 2012, Springer Berlin Heidelberg. p. 3-28.
50. Santacana GE and Silva WI, *Differential antagonism by amiloride and pirenzepine of the muscarinic receptors of rat tracheal smooth muscle*. *Bol Asoc Med P R*, 1990. 82(9): p. 403-6.
51. Proctor GB, *Muscarinic receptors and salivary secretion*. *J Appl Physiol* (1985), 2006. 100(4): p. 1103-4.
52. Dehaye JP and Verhasselt V, *Interaction of amiloride with rat parotid muscarinic and alpha-adrenergic receptors*. *Gen Pharmacol*, 1995. 26(1): p. 155-9.
53. Haga K, Kruse AC, Asada H, et al., *Structure of the human M<sub>2</sub> muscarinic acetylcholine receptor bound to an antagonist*. *Nature*, 2012. 482(7386): p. 547-51.
54. Kruse AC, Ring AM, Manglik A, et al., *Activation and allosteric modulation of a muscarinic acetylcholine receptor*. *Nature*, 2013. 504(7478): p. 101-6.
55. Kruse AC, Hu J, Pan AC, et al., *Structure and dynamics of the M<sub>3</sub> muscarinic acetylcholine receptor*. *Nature*, 2012. 482(7386): p. 552-6.
56. Pauwels PJ, *Competitive and silent antagonism of recombinant 5-HT<sub>1B</sub> receptors by amiloride*. *Gen Pharmacol*, 1997. 29(5): p. 749-51.
57. Wang C, Jiang Y, Ma J, et al., *Structural basis for molecular recognition at serotonin receptors*. *Science*, 2013. 340(6132): p. 610-4.
58. Wacker D, Wang C, Katritch V, et al., *Structural features for functional selectivity at serotonin receptors*. *Science*, 2013. 340(6132): p. 615-9.
59. Parker MS, Wong YY, and Parker SL, *An ion-responsive motif in the second transmembrane segment of rhodopsin-like receptors*. *Amino Acids*, 2008. 35(1): p. 1-15.
60. Schwartz TW, Frimurer TM, Holst B, et al., *Molecular mechanism of 7TM receptor activation-a global toggle switch model*. *Annu Rev Pharmacol Toxicol*, 2006. 46: p. 481-519.
61. Nygaard R, Frimurer TM, Holst B, et al., *Ligand binding and micro-switches in 7TM receptor structures*. *Trends Pharmacol Sci*, 2009. 30(5): p. 249-59.

62. Kenakin T, *New concepts in drug discovery: collateral efficacy and permissive antagonism*. Nat Rev Drug Discovery, 2005. 4(11): p. 919-27.
63. Keov P, Sexton PM, and Christopoulos A, *Allosteric modulation of G protein-coupled receptors: a pharmacological perspective*. Neuropharmacology, 2011. 60(1): p. 24-35.





# Chapter 3

## The role of a sodium ion binding site in the allosteric modulation of the A<sub>2A</sub> adenosine G protein-coupled receptor

Hugo Gutiérrez-de-Terán\*

Arnault Massink\*

David Rodríguez

Wei Liu

Gye Won Han

Jeremiah S. Joseph

Ilia Katritch

Laura H. Heitman

Lizi Xia

Adriaan P. IJzerman

Vadim Cherezov

Vsevolod Katritch

Raymond C. Stevens

*\*These authors contributed equally*

*Structure, 2013, 21(12): 2175-85*

## **Abstract**

The function of G protein-coupled receptors (GPCRs) can be modulated by a number of endogenous allosteric molecules. In this study, we used molecular dynamics, radioligand binding and thermostability experiments to elucidate the role of the recently discovered sodium ion binding site in the allosteric modulation of the human A<sub>2A</sub> adenosine receptor, conserved among class A GPCRs. While the binding of antagonists and sodium ions to the receptor was noncompetitive in nature, the binding of agonists and sodium ions appears to require mutually exclusive conformational states of the receptor. Amiloride analogs can also bind to the sodium binding pocket, showing distinct patterns of agonist and antagonist modulation. These findings suggest that physiological concentrations of sodium ions affect functionally relevant conformational states of GPCRs, and can help to design novel synthetic allosteric modulators or bitopic ligands exploiting the sodium ion binding pocket.

## Introduction

Cellular responses to a wide variety of extracellular signals are mediated by the superfamily of seven transmembrane helical receptors coupled to intracellular G proteins (G protein-coupled receptors, GPCRs). It is now well recognized that many GPCRs function as “allosteric machines” with the orthosteric binding pocket representing just one of the many sites for possible signal modulation and pharmacological intervention. Thus, molecules targeting other (allosteric) sites can modulate binding of native orthosteric ligands and shift the delicate equilibrium between active and inactive states of GPCRs.<sup>1</sup> Potential therapeutic advantages include a gain in target selectivity, the “ceiling effect”, and preservation of the spatiotemporal profile of intercellular signaling.<sup>2-5</sup> Some endogenous chemical entities, such as ions or lipids, have also been demonstrated to act as allosteric modulators of GPCRs,<sup>1, 6, 7</sup> but the structural basis and functional importance of these interactions are not well understood.

Recent advances in protein engineering and membrane protein crystallography<sup>8-10</sup> have led to the elucidation of a growing number of experimental GPCR structures,<sup>11</sup> contributing to the alluring perspective of structure-based drug design,<sup>12</sup> and the deciphering of molecular mechanisms underlying conformational equilibrium.<sup>13</sup> Several receptors, including one of the best-characterized GPCRs, the A<sub>2A</sub> adenosine receptor (A<sub>2A</sub>AR), have been crystallized in inactive<sup>14-17</sup> and active-like<sup>18, 19</sup> conformations. The conformational changes associated with A<sub>2A</sub>AR activation mirrored similar structural changes observed in other receptors, namely the β<sub>2</sub>-adrenergic receptor (β<sub>2</sub>AR)<sup>20</sup> and rhodopsin.<sup>21</sup> Recently, the 1.8 Å resolution structure of inactive A<sub>2A</sub>AR in complex with ZM-241,385 revealed the presence of a sodium ion bound to the core of the transmembrane (TM) bundle,<sup>22</sup> coordinated by Asp<sup>2,50</sup> and other side chains highly conserved in class A GPCRs<sup>23</sup> and by a cluster of structural water molecules.<sup>24, 25</sup> The allosteric effect of sodium ions has been described previously in A<sub>2A</sub> and A<sub>1</sub> adenosine receptors,<sup>6, 26</sup> as well as in GPCRs from other subfamilies such as dopamine D<sub>2</sub>,<sup>7, 27</sup> opioid,<sup>28, 29</sup> or α-adrenergic receptors,<sup>30, 31</sup> among others. Similarly, the positively charged, synthetic small molecule amiloride and its analogs have been found to be allosteric modulators of agonist and antagonist binding of a number of GPCRs (Chapter 2), including A<sub>2A</sub>AR, and were shown to compete with sodium ions for the same binding site.<sup>6</sup> Moreover, mutation of Asp<sup>2,50</sup> to either asparagine or alanine has been shown to reduce or abrogate the allosteric effects of

sodium ions or amiloride in many GPCRs.<sup>7, 32-34</sup> While the 1.8 Å structure of A<sub>2A</sub>AR provides a static picture of sodium interactions with the receptor, the dynamic nature of the sodium ion-water cluster, its effect on binding of orthosteric agonists and antagonists, and its functional role are poorly understood. Molecular dynamics (MD) studies, supported by biochemical and biophysical experiments, provide a molecular framework for the allosteric effects of sodium and amilorides, which can ultimately aid in the discovery of new compounds targeting this site.<sup>4</sup>

## Material and methods

### Computational simulations

The standard amino acid sequence numbering for the human A<sub>2A</sub>AR is used in the text, with the Ballesteros and Weinstein residue numbering for GPCRs<sup>35</sup> shown in superscript if the residue belongs to a transmembrane helix. The inactive structure of the A<sub>2A</sub>AR in complex with ZM-241,385 and a sodium ion (PDB code 4E1Y),<sup>22</sup> was refined in order to model the missing loops and add protons as detailed in the supplemental information, prior to MD simulations. When the sodium ion was not considered, manual replacement with a water molecule, also maintaining the surrounding water molecules, was followed by energy minimization to fully optimize the H-bond network in the allosteric site. In the simulations with amiloride, the initial conformation of the A<sub>2A</sub>AR-amiloride complex was used as proposed previously by flexible docking.<sup>22</sup> The starting coordinates of the antagonist caffeine were obtained by superimposing the A<sub>2A</sub>AR-caffeine complex (PDB code 3RFM)<sup>14</sup> with the A<sub>2A</sub>AR structure described above using PyMOL (The PyMOL Molecular Graphics System version 1.4, Schrödinger). The MD simulations of the active-like conformation were performed starting from the A<sub>2A</sub>AR in complex with the stabilizing agonist UK-432,097 (PDB code 3QAK).<sup>19</sup> The starting coordinates of the sodium ion and coordinating water molecules were transposed from the inactive structure by structural superimposition with 4E1Y. Finally, the A<sub>2A</sub>AR in complex with the agonist NECA was obtained by "morphing" the A<sub>2A</sub>AR-ZM-241,385 structure (PDB code 4E1Y) to the active-state A<sub>2A</sub>AR-UK-432,097 conformation (PDB code 3QAK), and subsequent reconstruction of the intracellular loop 3 as detailed in the supplemental experimental procedures. Note that the available crystal structure of NECA in complex with thermostabilized A<sub>2A</sub>AR (PDB code 2YDV),<sup>18</sup> was not suitable for this analysis because of a highly distorted conformation

of the allosteric site, which includes a deformed helix VII backbone due to a cis-Proline in the NPxxY motif.

**Table 1.** Setup of the different MD simulations reported in this work.

	<b>Receptor Conformation</b>	<b>Ligand</b>	<b>Allosteric Modulator</b>	<b>Replicas, length</b>
<b>MDS1<sup>a</sup></b>	Inactive	ZM-241,385	Na <sup>+</sup>	3x100 ns
<b>MDS1-b<sup>a</sup></b>	Inactive	ZM-241,385	Na <sup>+</sup>	3x100 ns
<b>MDS2</b>	Inactive	---	Na <sup>+</sup>	3x100 ns
<b>MDS3</b>	Inactive	ZM-241,385	---	3x100 ns
<b>MDS4</b>	Inactive	---	---	3x100 ns
<b>MDS5</b>	Active	UK-432,097	Na <sup>+</sup>	3x40 ns
<b>MDS6</b>	Active	NECA	Na <sup>+</sup>	3x40 ns
<b>MDS7</b>	Active	---	Na <sup>+</sup>	3x40 ns
<b>MDS8</b>	Inactive	ZM-241,385	Amiloride	3x100 ns
<b>MDS9</b>	Inactive	Caffeine	Amiloride	3x40 ns
<b>MDS10</b>	Inactive	Caffeine	---	3x40 ns
<b>MDS11</b>	Inactive	ZM-241,385	HMA	3x100 ns
<b>MDS12</b>	Inactive	Caffeine	HMA	3x40 ns

*a*: MDS1-b corresponds to the same system as MDS1, but considering the physiological saline concentration of 150mM.

Membrane insertion and all MD simulations were performed with the GROMACS software,<sup>36</sup> using our original protocol for the MD simulations of GPCRs<sup>37</sup> as adapted in the PyMemDyn program.<sup>38</sup> The final systems, consisting of approximately 50,000 atoms (~74% belong to solvent molecules, ~15% to lipids and ~11% to protein and ligand atoms), were energy minimized and equilibrated for a total of 5 ns, with specific details provided in the supplemental experimental procedures. The production phase of unrestrained MD simulations followed for 100 ns simulation time (shorter production times were considered in certain cases, see Table 1 and explanation in main text). MD simulations were performed under the OPLSAA force field,<sup>39</sup> with ligand parameters obtained with Macromodel,<sup>40</sup> lipid parameters adapted from Berger<sup>41</sup> together with the use of the half- $\epsilon$  double-pairlist method<sup>42</sup> and the SPC water model.<sup>43</sup> The periodic boundary conditions (PBC) were implemented with hexagonal prism-shaped boxes in the isobaric NPT ensemble, using a Nose-Hoover thermostat<sup>44</sup> with a target temperature of 310 K using.

Electrostatic interactions beyond a cutoff of 12 Å were estimated with the particle mesh Ewald (PME) method. All MD analyses were conducted with several GROMACS and VMD<sup>45</sup> utilities. Molecular superimpositions, trajectory visualizations and molecular images were performed with PyMOL.

### **Cell growth and transfection**

HEK293T cells were grown in culture medium consisting of Dulbecco's modified Eagle's medium (DMEM) supplemented with 10% newborn calf serum (NCS), 50 µg/ml streptomycin and 50 IU/ml penicillin at 37 °C and 7% CO<sub>2</sub>. Cells were subcultured twice a week at a ratio of 1:15 on 10 cm ø plates. Cells were transfected with the wild-type A<sub>2A</sub>AR-plasmid (pcDNA3.1, 1 µg) using the calcium phosphate precipitation method.<sup>46</sup>

### **Membrane preparation**

Cells were detached from plates 48 h after transfection by scraping them into 5 ml phosphate buffered saline (PBS), collected and centrifuged at 700 ×g (3000 rpm) for 5 min. Pellets derived from 50 plates (10 cm ø) were pooled and resuspended in 40 ml of ice-cold assay buffer (50 mM Tris-HCl supplemented with 5 mM MgCl<sub>2</sub>, pH 7.4). An Ultra-Turrax was used to homogenize the cell suspension. Membranes and the cytosolic fraction were separated by centrifugation at 100,000 ×g (31,000 rpm) in a Beckman Optima LE-80K ultracentrifuge at 4 °C for 20 min. The pellet was resuspended in 20 ml of Tris buffer and the homogenization and centrifugation step was repeated. Assay buffer (10 ml) was used to resuspend the pellet and adenosine deaminase (ADA) was added (0.8 IU/ml) to break down endogenous adenosine. Membranes were stored in 250 µl aliquots at -80 °C. Membrane protein concentrations were measured using the BCA (bicinchoninic acid) method.<sup>47</sup>

### **Competition and saturation binding assays using HEK293T cell membranes**

For competition binding experiments with [<sup>3</sup>H]ZM-241,385 (46.6 Ci/mmol, ARC Inc, St. Louis, MO, USA), between 6 and 8 µg of membranes was used to ensure that total binding was less than 10% of the total radioactivity added to prevent radioligand depletion. For [<sup>3</sup>H]NECA (16.3 Ci/mmol, Perkin Elmer, Groningen, The Netherlands) competition binding experiments between 18 and 25 µg of membranes were used for the experiments. Membrane aliquots were incubated in a total volume of 100 µl of assay buffer at 25 °C for 2 h. Radioligand displacement experiments were performed using five concentrations of

competing ligand (NaCl, amiloride or HMA (5-[N,N-hexamethylene]amiloride), all from Sigma Aldrich, Zwijndrecht, The Netherlands). [<sup>3</sup>H]ZM-241,385 and [<sup>3</sup>H]NECA were used at concentrations of ~ 4.0 nM and 15-20 nM, respectively. Nonspecific binding was determined in the presence of 100 μM CGS21680 (Ascent Scientific, Bristol, UK, for experiments with [<sup>3</sup>H]ZM-241,385) or 10 μM ZM-241,385 (Ascent Scientific, Bristol, UK, for experiments with [<sup>3</sup>H]NECA) and represented less than 15% of the total binding. For saturation experiments, total binding was determined at increasing concentrations of [<sup>3</sup>H]ZM-241,385 (0.10-45 nM), in the absence or presence of ZM-241,385 (10 nM), NaCl (30 or 100 mM), amiloride (30 μM), or HMA (3 μM). In addition, unlabeled NECA (Ascent Scientific, Bristol, UK) was spiked with 25% [<sup>3</sup>H]NECA resulting in final concentrations of 8.0 to 400 nM, in the absence or presence of ZM-241,385 (10 nM), NaCl (30 or 100 mM), amiloride (30 μM), or HMA (4 μM). Nonspecific binding was determined at three concentrations of radioligand and analyzed by linear regression. Incubations were terminated by rapid vacuum filtration to separate the bound and free radioligand through 96-well GF/B filter plates using a Filtermate-harvester (PerkinElmer Life Sciences). Filters were subsequently washed three times with ice-cold assay buffer. The filter-bound radioactivity was determined by scintillation spectrometry using the PE 1450 Microbeta Wallac Trilux scintillation counter (PerkinElmer Life Sciences).

### **Thermostability assays**

The A<sub>2A</sub>AR-BRIL-ΔC receptor construct was purified from *Spodoptera frugiperda* (Sf9) insect cells in the apo form as described previously,<sup>22</sup> except that KCl was used throughout purification instead of NaCl. N-(4-[7-diethylamino-4-methyl-3-coumarinyl]phenyl)-maleimide (CPM) dye (Invitrogen) was dissolved in DMSO (Sigma) at 4 mg/ml and stored at -80 °C. Before use, the CPM stock solution was thawed and diluted 1:40 in dye dilution buffer (10 mM HEPES pH 7.50, 10% glycerol, 0.05% dodecyl maltoside (DDM) (Anatrace)). The thermal denaturation assay was performed with a total volume of 200 μl per sample in a quartz fluorimeter cuvette (Starna Cells, Inc., Atascadero, CA) and an apparent relative T<sub>m</sub> was obtained.<sup>48</sup> Receptor (4 μg) was diluted in assay buffer (10 mM HEPES pH 7.5, 0.05% DDM, 0.01% cholesterol hemisuccinate (CHS) (Sigma)) with and without different concentrations and combinations of NaCl, amiloride, and ZM-241,385 to a final volume of 200 μl. 5 μl of the diluted dye was added to the protein-containing assay solution and incubated for 30 min at 4 °C. The mixed solutions were transferred into cuvettes and

fluorescence data were collected by a Cary Eclipse spectrofluorometer (Varian, USA) with a temperature ramping rate of 2 °C/min. The excitation wavelength was 387 nm and the emission wavelength was 463 nm. All assays were performed over a temperature range starting from 20 °C to 90 °C.

### **Data analysis**

The radioligand binding and thermostability data were processed with Prism 5 (GraphPad Software, San Diego, CA, USA). Statistical significance was assessed with a Student's t-test.

## **Results**

### **Molecular dynamics studies**

A series of MD simulations were designed to evaluate the functional role of the sodium ion in the A<sub>2A</sub>AR, as summarized in Table 1. Three MD replicates of 40-100 ns length each were run for each setup, in order to increase the statistics of the sampling, with a total simulation time exceeding 2.8 μs. The effect of the sodium ion on the conformational equilibrium of the receptor was examined considering both the inactive and active-like conformation of the A<sub>2A</sub>AR (simulations MDS1-MDS7). The influence of the orthosteric ligands in this process was examined by comparing the MD simulations with and without the antagonist ZM-241,385 (MDS1 and MDS2) or the agonists UK-432,097 and NECA (MDS5 through MDS7). In addition, the allosteric effect of amiloride and its derivative HMA in the antagonist-bound conformation was examined in MDS8 through MDS12, with two distinct chemotypes of antagonists (i.e., ZM-241,385 and caffeine).

### **The sodium binding site in the A<sub>2A</sub>AR inactive conformation**

In the high resolution crystal structure of inactive A<sub>2A</sub>AR,<sup>22</sup> the sodium ion is directly coordinated by Asp52<sup>2,50</sup> and Ser91<sup>3,39</sup> (first shell residues) and three structured water molecules (Figure 1A). Water molecules also bridge interactions with residues in the second (Trp246<sup>6,48</sup> and Asn280<sup>7,45</sup>), and the third shells (Thr88<sup>3,36</sup> and Ser281<sup>7,46</sup>). Overall, the sodium ion/water binding pocket is formed by 15 out of the 34 amino acids that are conserved in the majority of non-olfactory class A GPCRs<sup>23</sup> and their conformation is similar in most GPCRs crystallized in the inactive state (Figure 1B-D).



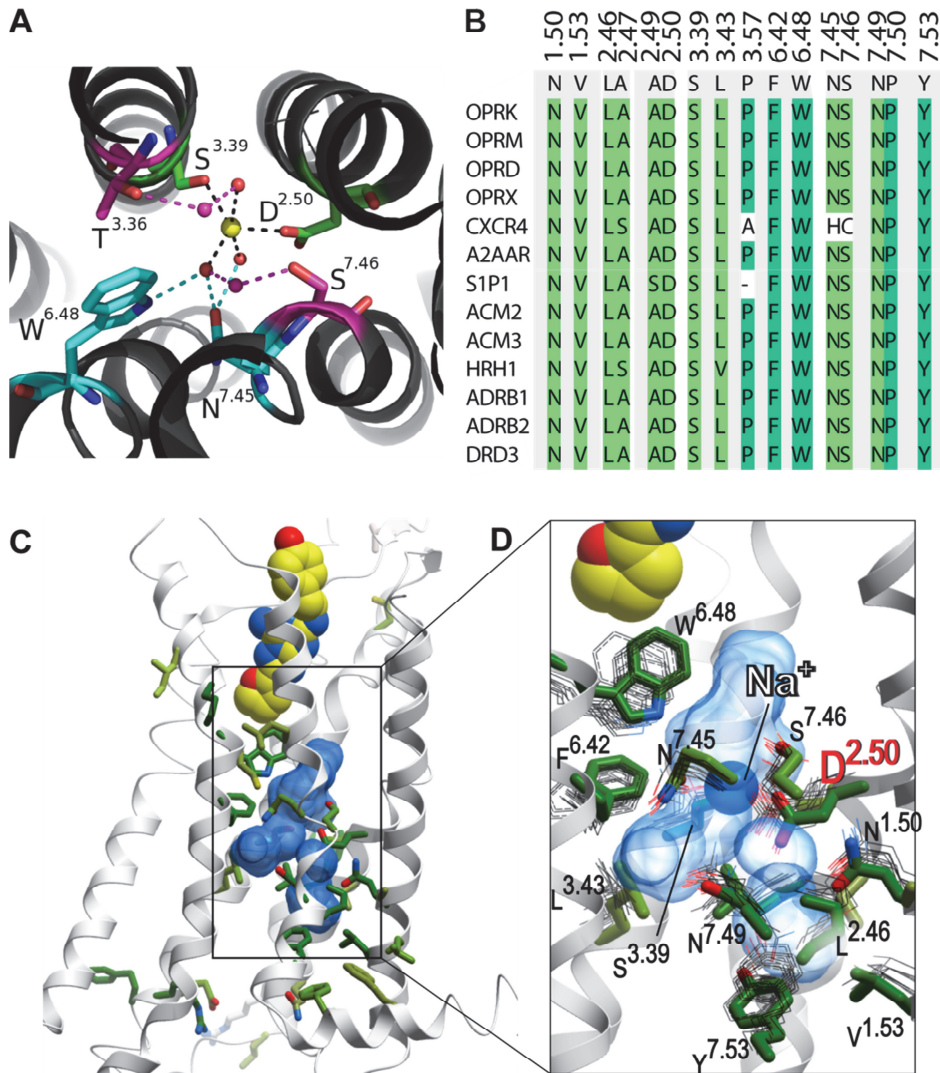


**Figure 1.** Structure and conservation of the central sodium ion-binding allosteric pocket in Class A GPCRs. **A)** The sodium ion distorted octahedral coordination as in the A<sub>2A</sub>AR crystal structure: The first shell is occupied by two conserved polar residues (green) and three water molecules, which contact with a second shell of residues (cyan), or with a second layer of water molecules connecting with the third shell of residues (magenta). **B)** Sequence conservation of the 15 residues lining the binding pocket among inactive GPCR crystal structures. **C)** Structure of the A<sub>2A</sub>AR complex with ZM-241,385, showing residues with higher than 50% conservation in all Class A receptors as sticks with green carbons. **D)** A close-up of the central allosteric pocket (transparent blue surface), showing the side chains located within 5 Å from the ten waters of the sodium ion-water cluster (green sticks: A<sub>2A</sub>AR; gray thin lines: the corresponding side chains of the overlaid GPCR crystal structures listed in B. See also supplemental Figure S1.

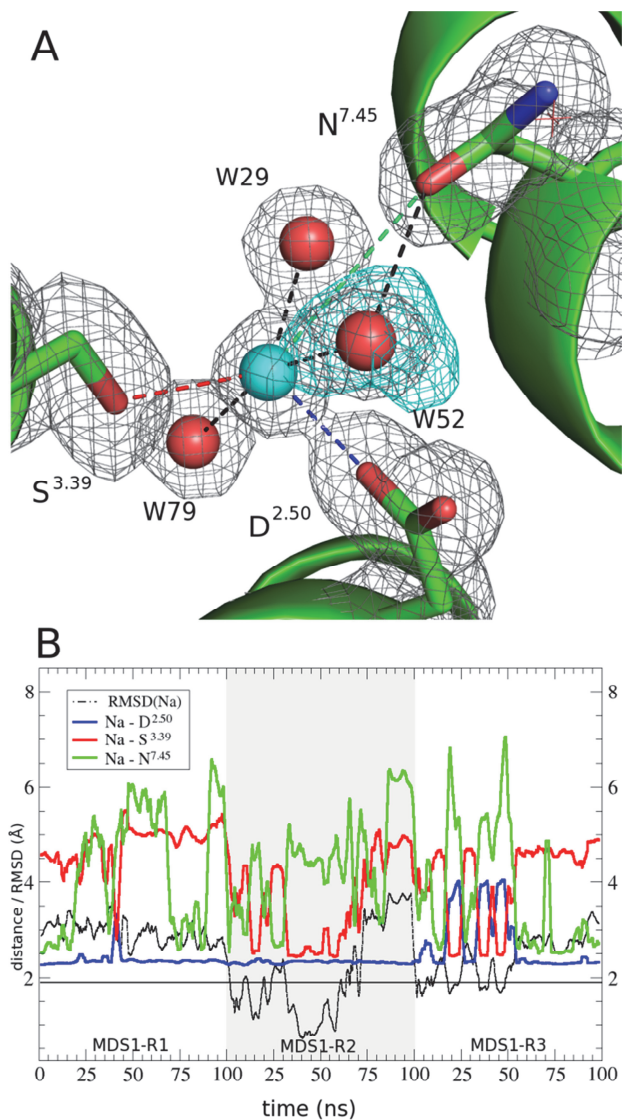


**Figure 2.** The two coordination states of the sodium ion as observed in MD simulations **A)** Volumetric density map (isosurface contoured at  $0.3 \text{ \AA}^{-3}$  value, blue) corresponding to the sodium ion occupancy as calculated from simulations MDS1 (see Table 1). The starting crystal structure is displayed, together with the electron density (contoured at  $1 \sigma$  level, black). **B)** The time-evolution of the distances between the sodium ion and Asp<sup>2.50</sup> (blue), Ser<sup>3.39</sup> (red) and Asn<sup>7.45</sup> (green), shown for the 3 independent replicates (R1-R3) of MDS1. The corresponding distances are denoted as dashed lines in **A** with the same color code, and are the source of the data in Table S1. The RMSD of the ion with respect to its crystallographic position is indicated with a black line, while the horizontal bar at  $1.8 \text{ \AA}$  (the resolution of the parent crystal structure) denotes the limit for the crystallographic coordination state (position c1). See also Table S1 and Figure S2.

Analysis of the sodium ion's mobility and its coordination state reveals a high level of stability for the ion when bound to the receptor's inactive conformation. The dominant charge-charge interaction with Asp52<sup>2,50</sup> is clearly maintained along the simulation runs in the different MD trajectories, while the side chain oxygen atoms of Ser91<sup>3,39</sup> and Asn280<sup>7,45</sup> alternate direct interactions with the ion (Figure 2). More precisely, the ion fluctuates between a coordination state as seen in the crystal structure, which we will refer to as position c1, and a second state that we will refer to as position c2. This fluctuation involves an exchange between the sodium ion and the water molecule W52, initially linked to the OD1 of Asn280<sup>7,45</sup>, as shown in Figure 2A by the overlay of the electron density of the crystal structure with the volumetric density map calculated from the MD simulations. In position c2, the ion is still coordinated by Asp52<sup>2,50</sup> (OD1), while it is the OD1 of Asn280<sup>7,45</sup> (occasionally replaced by a new water molecule) that participates in the first coordination shell, which is completed with three other water molecules. The radial distribution function indicates the average sodium-oxygen distance is 2.4 Å, with the first coordination shell predominantly formed by 4 or 5 oxygen atoms (see supplemental Figure S2), in agreement with the geometric analysis of sodium ion binding sites found in the Protein Data Bank (PDB).<sup>49</sup> The consistent observation of these two dominant coordination modes suggests a possibility of fast exchange between the sodium ion and the water molecule, supported by the significantly shorter distance (2.2 Å) observed in the crystal structure for the Na<sup>+</sup>-O(W52) pair. Interestingly, this fast exchange occurs regardless of the presence of the antagonist ZM-241,385 in the orthosteric binding site (Table S1). In the setup MDS1b, we evaluated the effects of a physiological saline concentration in the simulations, and observed no difference in results (see supplemental Figure S2 and Table S1). Moreover, none of the sodium ions from the extracellular solvent could cross the narrow channel into the allosteric pocket during 100 ns simulations, suggesting that exchange of sodium ions in A<sub>2A</sub>AR may occur on a longer time scale.

To investigate a possible effect of the sodium ion on the stability of the inactive conformation of the receptor, the MD simulations described above (MDS1 and MDS2) were compared with the corresponding simulations of the inactive A<sub>2A</sub>AR in the absence of the ion (MDS3 and MDS4). The most pronounced difference in local conformational dynamics was located in the region of the sodium ion: the highly conserved residue Trp246<sup>6,48</sup> in the second sphere of solvation experienced a rotameric transition from

the initial *g+* rotamer to the *trans* (*t*) conformation, observed in two out of three independent simulations of the *apo* receptor without sodium ion (MDS4, see Figure 3). This rotameric change appears connected to a rotation of residue Asn280<sup>7,45</sup> from the initial *g-* rotamer to either *trans* or *g+* (Figure 3A and C). In contrast, rotamer changes in Trp246<sup>6,48</sup> and to a lesser extent Asn280<sup>7,45</sup> were not observed when the sodium ion was bound to the allosteric site (MDS2), suggesting that the sodium ion contributes to a stabilization of these two residues (Figure 3A and B). Similarly, the furyl moiety of the antagonist ZM-241,385 stabilized the *g+* rotamer of Trp246<sup>6,48</sup> through Van der Waals interactions (simulations MDS1 and MDS3). Consequently, no movements in this microenvironment occurred with ZM-241,385 bound, regardless of the presence of the sodium ion.

### **The sodium ion binding site in the A<sub>2A</sub>AR active-like conformation**

Analysis of the agonist-bound structures of A<sub>2A</sub>AR<sup>18,19</sup> indicates that the activation-related changes in helix VII partially collapse the sodium ion pocket, making it incompatible with ion binding.<sup>22</sup> In order to further evaluate this effect, the sodium ion-water cluster was simulated in the context of the active-like conformation of A<sub>2A</sub>AR with agonists UK-432,097 (MDS5) or NECA (MDS6), or without any agonist (MDS7, see Table 1). The simulations show that in the active-like state the receptor cannot bind the sodium ion, as evidenced by two alternative events that occur in the early stages of production runs. In the first event, (observed in 1 out of 3 replicas in MDS5, in 2 out of 3 replicas in MDS6, and in all 3 replicas in MDS7) the ion escaped from the proposed binding site. In the alternative event, observed in the remaining simulations, the ion remained in the allosteric binding site, but a conformational change of helix VII occurred, resembling the inactive-like conformation of helix VII observed in all antagonist-bound A<sub>2A</sub>AR structures. In particular, the region between His278<sup>7,43</sup> and Asn284<sup>7,49</sup> undergoes an outward movement driving helix VII apart from helix III and expanding the pocket cavity (Figure 4). In the MDS5 and MDS6 simulations, this rearrangement was also accompanied by a loss of contact between His278<sup>7,43</sup> and the O2' of the ribose moiety of the agonist, suggesting that sodium ion binding destabilizes activation-related movements and agonist binding. Note that all conformational events described here occurred within the first 5-10 ns of the simulation, justifying that a total simulation time of 40 ns was sufficient to properly sample the sodium binding site in the active-like system. These findings indicate that the

binding of sodium ions and agonists each require a different conformational state of the receptor and, therefore, are mutually exclusive.

A	MDS2	MDS4
% $\chi_1$ -W <sup>6.48</sup> g(+) rotamer	96.8%	38.5%
% $\chi_2$ -N <sup>7.45</sup> g(-) rotamer	53.3%	1.0%
Average # water @3Å of D <sup>2.50</sup>	2.7	3.6

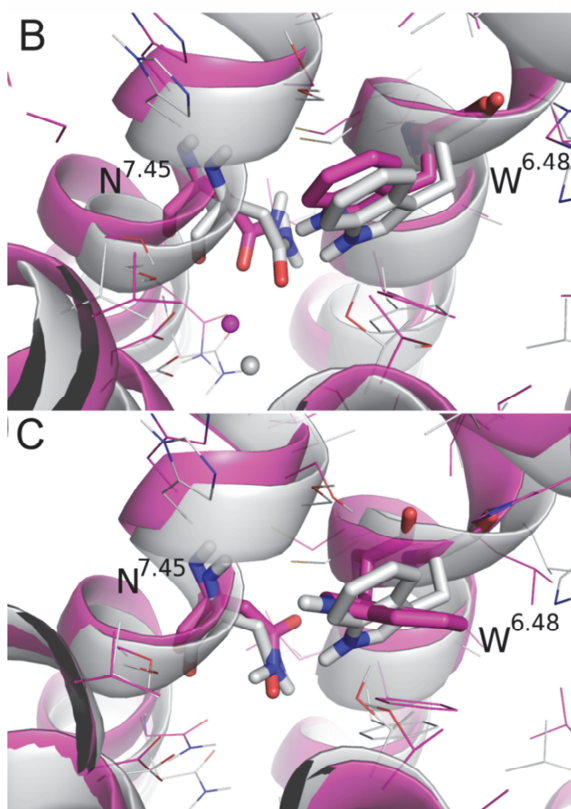


**Figure 3.** Rotameric transitions of Trp<sup>6.48</sup> and Asn<sup>7.45</sup> in the *apo* simulations of the inactive A<sub>2A</sub>AR. **A)** Populations of the initial conformational states in the simulations with (MDS2) and without (MDS4) the sodium ion, and the number of waters in the ion binding site (each data is an average of the 3 MD replicas). Note that Trp<sup>6.48</sup> only finds the trans conformation when not in the initial g(+) conformation, while Asn<sup>7.45</sup> is more flexible and can be found in either trans, g(+) or the initial g(-) conformations. **B)** and **C)** Representative snapshot (magenta) of the conformation of these two residues in MDS2 (**B**) and MDS4 (**C**), with the reference crystal structure overlaid in light gray.

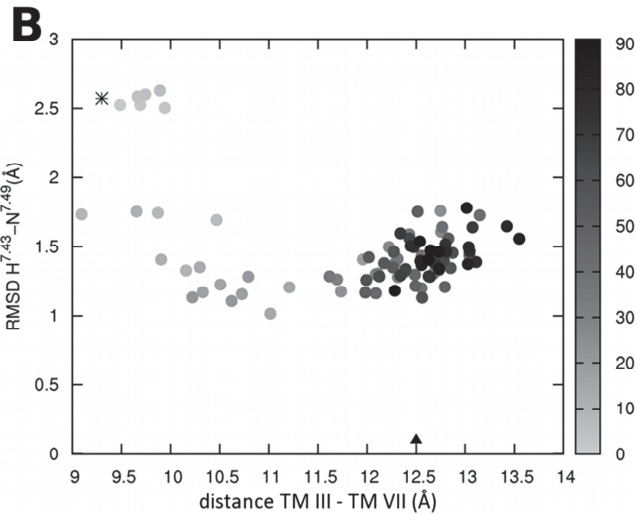
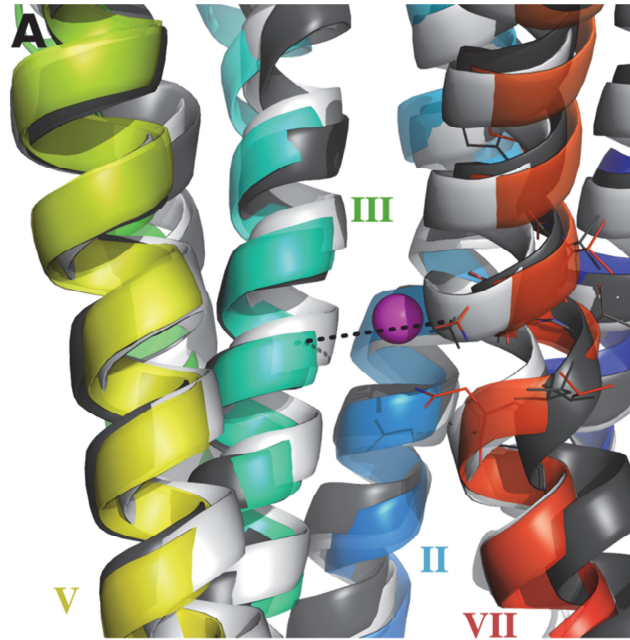


**Figure 4.** The movement of helix VII in order to accommodate the sodium ion. **A)** Starting (light grey) and ending (rainbow, with helix VII colored orange) conformations of the agonist-bound  $A_{2A}$ AR in the presence of sodium ion (MDS5), with the inactive crystal structure denoted in anthracite. **B)** The distance between helices III and VII (X axis, C $\alpha$  of residues Ile<sup>3.40</sup> and Asn<sup>7.45</sup> as indicated by a dashed line in **A**) is plotted against the backbone RMSD of the motif His<sup>7.43</sup>-Asn<sup>7.49</sup>, (Y axis), using as a reference the inactive conformation of  $A_{2A}$ AR. Each dot is a snapshot extracted every 0.5 ns, with the time evolution depicted by the shading code (light grey  $\rightarrow$  black). Active and inactive conformations are indicated with an asterisk and a triangle, respectively.

### Amiloride and HMA as A<sub>2A</sub>AR allosteric modulators

Amiloride and its derivatives are known to be nonspecific GPCR modulators.<sup>50</sup> A binding mode of amiloride and its bulkier analog HMA to the A<sub>2A</sub>AR was determined by flexible side chain docking where the charged guanidinium group of amiloride interacted with Asp52<sup>2,50,22</sup>. An additional hydrogen bond was also predicted between amiloride and the Trp246<sup>6,48</sup> side chain (see Figure 5A), which is shifted ~1.5 Å towards the orthosteric pocket as a result of induced fit. This tight binding of amilorides is clearly not compatible with the collapsed allosteric pocket observed in the active-like conformation of the A<sub>2A</sub>AR, in an even more pronounced way than in the case of sodium ions. Therefore, we explored this docking hypothesis with a series of MD simulations of the inactive A<sub>2A</sub>AR in the presence of different orthosteric antagonists, i.e. the ternary complexes A<sub>2A</sub>AR-ZM-241,385-amiloride (MDS8) and A<sub>2A</sub>AR-caffeine-amiloride (MDS9). The effect of amiloride on the binding of antagonists turned out to be complex and varied between the different antagonist chemotypes tested. Figure 5D shows a comparison of the RMSF (root mean square fluctuation) of compound ZM-241,385 with no allosteric modulator present (MDS3), and with either sodium ion (MDS1), amiloride (MDS8) or HMA (MDS11) present in the proposed allosteric site. A significant increase in the mobility of ZM-241,385 ( $p < 0.05$ ) was observed in the presence of both amilorides. This effect is likely due to the influence of the side chain of Trp246<sup>6,48</sup>, which is the only residue that interacts with ZM-241,385 and amilorides simultaneously (in particular with the 5'-azepane substituent of HMA, see Figure 5C), leading to the hypothesis that this highly conserved residue acts as an important link between the two sites. Consequently, binding of antagonists that do not directly interact with Trp246<sup>6,48</sup>, for example, caffeine,<sup>14</sup> should be less affected by the presence of amiloride in the allosteric site (Figure 5B). Indeed, we found no statistically significant difference for the mobility of caffeine as a function of the presence of amilorides (Figure 5D). Due to the high mobility of caffeine, which is small in size, has few receptor contacts, and displays low affinity, the simulation time in this particular system was limited to 40 ns time scale.

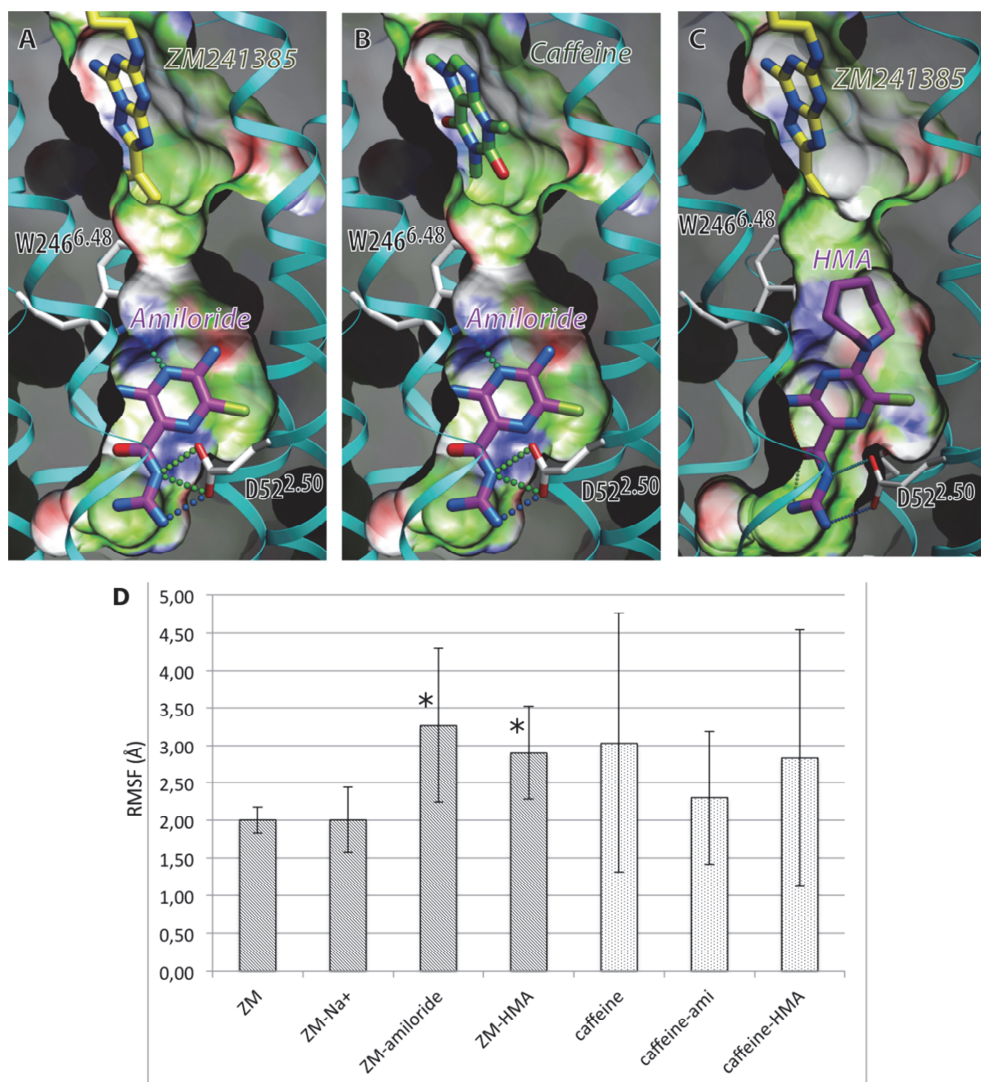


**Figure 5.** Impact of amiloride and HMA on binding of antagonists. **A)** Amiloride docking (magenta carbons) induces a shifted position of Trp246<sup>6.48</sup> side chain, revealing potential steric clashes with the orthosteric ligand ZM-241,385 (yellow carbons, superimposed from the crystal structure with PDB code 4EIY). **B)** Same conformation of the amiloride-bound A<sub>2A</sub>AR, with the caffeine pose (green carbons) superimposed from the crystal structure of A<sub>2A</sub>AR/caffeine complex (PDB code 3RFM). **C)** Flexible docking of HMA (magenta carbons) is predicted to further shift Trp246<sup>6.48</sup> and interfere with ZM-241,385 binding. **D)** Mobility of antagonists in presence or absence of amiloride, HMA and the sodium ion in the allosteric pocket, calculated as RMSF from the MD simulations (dark shaded bars for ZM-241,385; light shaded bars for caffeine). Error bars indicate the standard deviation estimated from three MD replicas (n=3); ami=amiloride; ZM= ZM-241,385. Significantly different from the control simulation (absence of any allosteric ligand) in a Student's t-test with \*p < 0.05.



## Biochemical studies

Radioligand binding experiments were performed to examine the effects of sodium ions and amiloride derivatives on antagonist, [ $^3\text{H}$ ]ZM-241,385, and agonist, [ $^3\text{H}$ ]NECA, binding to the  $A_{2A}\text{AR}$ . In order to experimentally assess the dependence of ligand binding on the presence of a sodium ion in the allosteric site, we performed equilibrium displacement studies with increasing concentrations of NaCl (Figure 6A). These experiments show a full displacement of [ $^3\text{H}$ ]NECA by sodium ions, with an  $\text{IC}_{50}$  value of  $49 \pm 7$  mM (Table S2 and Figure 6A). In contrast, there is an enhancement of antagonist [ $^3\text{H}$ ]ZM-241,385 binding, especially at higher sodium ion concentrations. All these results correlate with the MD conclusions that the sodium ion selectively stabilizes the antagonist-bound receptor state.

Saturation binding experiments performed with [ $^3\text{H}$ ]NECA also show that the presence of NaCl significantly reduces [ $^3\text{H}$ ]NECA binding to the  $A_{2A}\text{AR}$  (Table 2 and Figure S3). Interestingly, this reduction in agonist binding was due to an increase of the  $K_D$  value while the radioligand's  $B_{\text{max}}$  value remained at a control level, within experimental error. This profile of pharmacological parameters usually implies a competitive interaction between the two ligands. However, in this case the binding sites of the two ligands are not overlapping, therefore the observed “mutually exclusive binding” suggests that the sodium ion-bound conformation of  $A_{2A}\text{AR}$  is not compatible with agonist binding, and vice-versa. In contrast, no significant effect of sodium ions was observed on the binding of the antagonist radioligand [ $^3\text{H}$ ]ZM-241,385 to the  $A_{2A}\text{AR}$  (Table 2).

We also characterized the influence of amiloride and HMA on radioligand binding to the  $A_{2A}\text{AR}$ . The two compounds inhibited the binding of both agonist and antagonist radioligands in displacement assays, albeit with different potencies (Figure 6B and 6C and Table S2). HMA proved to be more active than amiloride in both cases, and displayed the highest potency ( $2.4 \mu\text{M}$ ) with the agonist [ $^3\text{H}$ ]NECA as the radiolabel. Radioligand saturation experiments were performed in the presence of the amiloride analogs, revealing distinct differences between the two radioligands (Table 2 and Figure S3). The interaction between amiloride and [ $^3\text{H}$ ]ZM-241,385 was noncompetitive in nature as the radioligand's  $B_{\text{max}}$  value was significantly reduced with little effect on the  $K_D$  value, whereas unlabeled ZM-241,385, serving as a control orthosteric ligand, showed all traits of a competitive ligand. In this experimental setup, HMA behaved somewhat in between ZM-241,385 and amiloride, showing a small but significant shift in  $K_D$  and a nonsignificant

change in  $B_{\max}$  value. Similar experiments with the radiolabeled agonist [ $^3\text{H}$ ]NECA produced a very different outcome. While unlabeled ZM-241,385 appeared competitive with [ $^3\text{H}$ ]NECA, as expected for two orthosterically binding compounds, the same was true for the interaction between the amilorides and [ $^3\text{H}$ ]NECA. Hardly any effect was observed on NECA's  $B_{\max}$  value, whereas all  $K_D$  values were significantly increased, which we attribute to the mechanism of “mutually exclusive binding” discussed above for the case of agonist and sodium ion binding.

**Table 2.** Saturation of [ $^3\text{H}$ ]ZM-241,385 and NECA spiked with 25% [ $^3\text{H}$ ]NECA binding to human  $A_{2A}$ ARs transiently expressed in HEK293T cell membranes in the absence and presence of ZM-241,385, NaCl, amiloride, and HMA. See associated experiments in Figure S3.

	$[^3\text{H}]ZM-241,385$		$[^3\text{H}]NECA$	
	$K_D$ (nM)	$B_{\max}^a$ (%)	$K_D$ (nM)	$B_{\max}^a$ (%)
<b>Control</b>	1.3 ± 0.4	100 ± 10	84 ± 11	100 ± 2
<b>+ 10 nM ZM</b>	8.3 ± 2.2**	85 ± 7	123 ± 9*	95 ± 3
<b>+ 30 mM NaCl</b>	1.2 ± 0.3	120 ± 11	213 ± 10***	106 ± 4
<b>+ 100 mM NaCl</b>	0.8 ± 0.1	87 ± 3	471 ± 53***	114 ± 9
<b>+ 30 μM Amiloride</b>	1.9 ± 0.8	61 ± 4*	290 ± 52**	119 ± 13
<b>+ 3 or 4 μM HMA<sup>b</sup></b>	4.1 ± 0.9*	78 ± 9	246 ± 2***	110 ± 1*

*a*: % of  $B_{\max}$  of control (= 100%)

*b*: 3 μM HMA for [ $^3\text{H}$ ]ZM-241,385 and 4 μM HMA for [ $^3\text{H}$ ]NECA

Significantly different from control in a Student's t-test with \*  $p < 0.05$ , \*\*  $p < 0.01$ , or \*\*\*  $p < 0.001$ . Values are means ± SEM of 2-5 separate assays performed in duplicate.

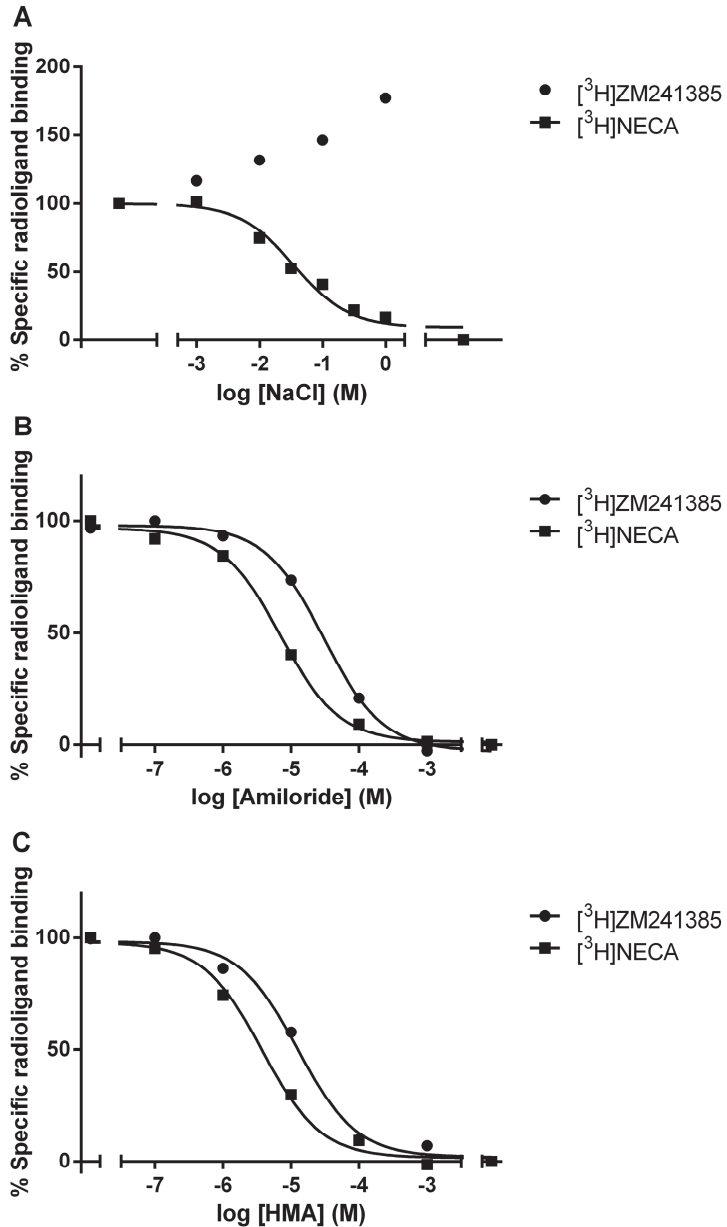


**Figure 6.** Equilibrium displacement of  $[^3\text{H}]$ ZM-241,385 and  $[^3\text{H}]$ NECA by allosteric modulators. NaCl (**A**), amiloride (**B**), and HMA (**C**). Representative graphs from one experiment performed in duplicate on  $\text{hA}_{2\text{A}}$ ARs transiently expressed in HEK293T cell membranes. Associated  $\text{IC}_{50}$  values listed in Table S2.

## Biophysical studies

The effects of sodium ions, orthosteric ligands and amiloride analogs on A<sub>2A</sub>AR stability were analyzed with a series of thermal stability assays.<sup>48</sup> Increasing sodium ion concentrations induced a significant increase in the thermostability of the unliganded A<sub>2A</sub>AR-BRIL complex, as shown in Figure 7A. A two-phase response was observed, with a modest increase in thermostability from 52 to 57 °C at sodium ion concentrations below the physiological concentration of 150 mM, and a further more substantial increase to 65 °C upon addition of higher concentrations up to 500 mM NaCl.

In order to evaluate the effects of allosteric modulators on various receptor-ligand complexes, we measured the thermal stability of the A<sub>2A</sub>AR-BRIL construct in the presence or absence of sodium ions and/or amiloride, and their combinations with the orthosteric ligands caffeine (antagonist), ZM-241,385 (antagonist), or UK-432,097 (full agonist) (Figure 7B). Sodium ions and amiloride each increased A<sub>2A</sub>AR thermostability by 5-6 °C, but their effect when combined was non-additive, corroborating the suggested competition of these two charged molecules for the same binding site. In contrast, the addition of caffeine in the presence of saturating concentrations of amiloride or sodium ions caused a further 6 °C increase in the thermostability of the complex, suggesting an additive stabilizing effect of the orthosteric caffeine and allosteric ligands. Also, while we observed an additive effect of sodium ions and ZM-241,385, amiloride did not contribute to the stability of A<sub>2A</sub>AR in saturating concentrations of ZM-241,385, in agreement with unfavorable indirect interactions between amiloride and ZM-241,385. Finally, neither sodium ions nor amiloride had a stabilizing effect on the A<sub>2A</sub>AR saturated with UK-432,097, likely because this agonist precluded binding of these allosteric modulators.

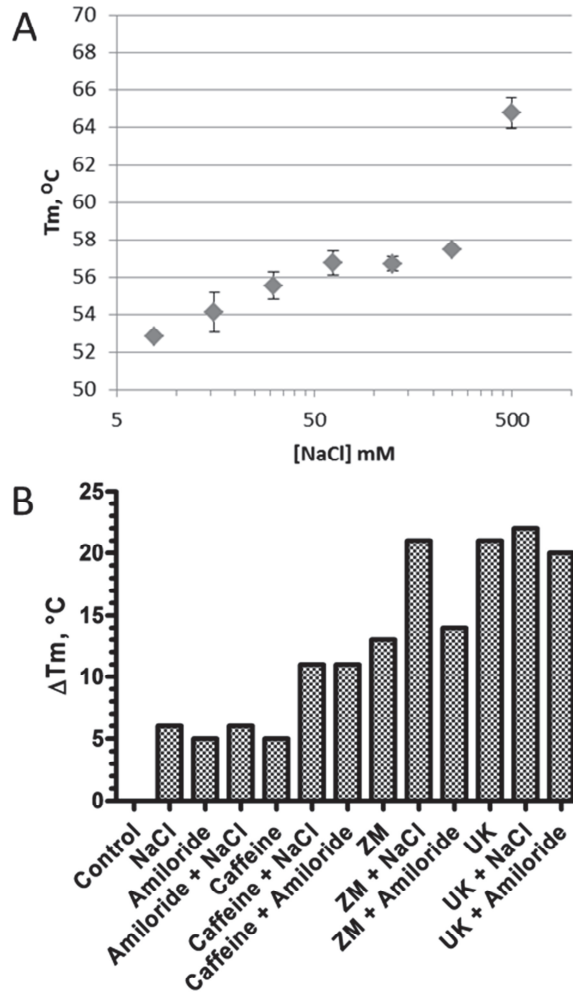


**Figure 7.** Effect of allosteric binders on  $A_{2A}AR$  thermostability measured by CPM assays. **A)** Effect of titration of NaCl on  $A_{2A}AR$  thermostability, mean  $\pm$  SEM shown for measurements performed in triplicate. **B)** Effect of NaCl (150 mM), amiloride (100  $\mu$ M), caffeine (500  $\mu$ M), ZM-241,385 (50  $\mu$ M), UK-432,097 (50  $\mu$ M) and combinations thereof on  $A_{2A}AR$  thermostability.

## Discussion

The 1.8 Å resolution structure of A<sub>2A</sub>AR in complex with the antagonist ZM-241,385 revealed a highly conserved sodium ion binding site<sup>22</sup> and provided an excellent opportunity to examine the molecular mechanism of the allosteric modulation of sodium ions in this receptor. Our MD simulations suggest that the electron density assigned to the water molecule closest to sodium ion in the crystal structure (W52) could correspond to a second resonance position of the ion, which would involve direct interaction with another conserved residue, Asn280<sup>7,45</sup> (Figure 2). Although we could not find a clear evidence of such dynamic rearrangements in the A<sub>2A</sub>AR crystal structure, this may reflect the “frozen” state of the sodium ion-water cluster at the low temperatures (~100K) used in cryo-crystallography. While further crystallographic studies at room temperature may help to validate such subtle effects experimentally,<sup>51</sup> the thermal fluctuations explored by the MD simulations under physiological conditions are particularly suited to explore this phenomenon.<sup>52</sup> The potential dynamic nature of the sodium ion and water network in the allosteric pocket could partially explain why the ion was not observed previously in lower resolution GPCR structures. A closer look at this region in two recently published, antagonist-bound GPCR structures, i.e. carvedilol-β<sub>1</sub>-adrenergic receptor<sup>53</sup> and βFNA-μ opioid receptor,<sup>54</sup> reveals that they are indeed compatible with the presence of a sodium ion (Figure S1). More recently, a similar configuration of the sodium ion/water network was also identified in other ligand complexes of the β<sub>1</sub>-adrenergic receptor.<sup>55</sup>

The communication between the highly conserved class A GPCR residues Asp<sup>2,50</sup>, Trp<sup>6,48</sup>, and to a lesser extent Asn<sup>7,45</sup>, had been suggested to occur through a cluster of water molecules.<sup>24</sup> The current MD results strongly support the preference of the sodium ion for the inactive conformation of this micro-environment, at least in the A<sub>2A</sub>AR, suggesting that it contributes to its stabilization. The increased dynamic flexibility of Trp246<sup>6,48</sup> and Asn280<sup>7,45</sup> in the absence of the sodium ion (Figure 3) is consistent with previous MD simulations of the A<sub>2A</sub>AR,<sup>37</sup> and agrees well with similar MD simulations in the dopamine D<sub>2</sub> receptor with explicit consideration of a sodium ion.<sup>27</sup> The conformational flexibility of Trp<sup>6,48</sup> has been associated with the initial steps of the activation mechanism of GPCRs,<sup>56, 57</sup> probably by facilitating the higher order conformational changes observed in helix VI between inactive and active states. Conversely, the presence of the sodium ion and coordinating water molecules in this

pocket hampers an activation-related inward movement of helix VII towards helix III,<sup>18, 19</sup> as indicated by MD simulations. Instead, we observed an “inactivation” movement of helix VII in the agonist-bound conformation (Figure 4) that led to the loss of key agonist-receptor interactions, suggesting that the simultaneous binding of the allosteric ion and the orthosteric agonist to the same receptor molecule is unlikely. Such a structural mechanism explains the negative allosteric effect of sodium ions on agonist binding to the A<sub>2A</sub>AR observed here (Figure 6A and Table 2) and in earlier studies.<sup>6, 22</sup>

In radioligand binding experiments performed with both agonist and antagonist radioligands, sodium ions differentially affected radioligand binding to the A<sub>2A</sub>AR, providing further insights into its allosteric effect: they induced an increase in [<sup>3</sup>H]ZM-241,385 binding, but abrogated [<sup>3</sup>H]NECA binding in a concentration-dependent manner with an IC<sub>50</sub> value of approximately 50 mM (Figure 6A). This potency is in the same range of sodium ion concentrations that cause an increase in receptor thermostability (Figure 7), indicating that sodium ion binding could mediate both effects. Moreover, this IC<sub>50</sub> corresponds to about one third of the extracellular physiological concentration of sodium ions. This suggests that about 75% of the A<sub>2A</sub>ARs that are present in the body are in a sodium ion occupied state, provided that there is unrestricted access to the sodium binding site from the outside of the cell, as recently proposed for the dopamine D<sub>2</sub> receptor.<sup>27</sup> Thus, it is likely that sodium is significantly involved in modulating the physiological state of the A<sub>2A</sub>AR and possibly other class A GPCRs.

Interestingly, saturation binding experiments (Table 2) demonstrate that the presence of sodium ions (30 and 100 mM) reduces [<sup>3</sup>H]NECA affinity (K<sub>D</sub>) rather than its B<sub>max</sub> value, while no affinity reduction was observed for [<sup>3</sup>H]ZM-241,385. This fact, together with the observed increase of [<sup>3</sup>H]ZM-241,385 binding at high sodium ion concentrations (Figure 6A), is in good agreement with an earlier study where the slight affinity increase of this radioligand at even higher sodium concentrations (1 M)<sup>58</sup> was due to a decrease in its dissociation rate.<sup>6</sup> The structural information and the computational results provided in this study suggest that binding of agonists and sodium ions can be considered as “mutually exclusive”.<sup>59</sup> This mechanism is further supported by thermal stability assays, showing that antagonists ZM-241,385 and caffeine display additive stabilizing effects with sodium ions, whereas the agonist UK-432,097 stabilizes the receptor but shows no additive effect when any allosteric ligand is added (Figure 7B).

Similar to sodium ions, the diuretic drug amiloride is an allosteric modulator of several GPCRs (Chapter 2), including such diverse subfamilies as adenosine, aminergic and gonadotropin-releasing hormone receptors.<sup>6, 60-64</sup> The present study in the human A<sub>2A</sub>AR shows that both amiloride and its derivative HMA negatively modulate agonist binding (Table 2), with HMA being more potent than amiloride in radioligand displacement studies (Figure 6) as previously suggested by kinetic studies in the rat A<sub>2A</sub>AR.<sup>6</sup> The saturation studies with [<sup>3</sup>H]ZM-241,385 as the radioligand (Table 2) also point to a noncompetitive interaction between amiloride and the antagonist binding site. Moreover, the additive increase in A<sub>2A</sub>AR thermostability in the presence of both amiloride and the orthosteric antagonist caffeine (Figure 7B) suggests that both allosteric and orthosteric ligands can bind simultaneously. These findings are in concert with docking and MD simulations (Figure 5), which suggest that amiloride and HMA bind in the allosteric sodium pocket, with the charged guanidinium group anchored by the carboxyl of Asp<sup>2.50</sup>. Although the proposed amiloride binding does not directly overlap with the orthosteric ligand binding site, our simulations indicate that amiloride derivatives can impact orthosteric ligand binding indirectly, primarily via modulation of Trp246<sup>6.48</sup> conformation. This explains a more pronounced negative allosteric effect of HMA, which has extensive steric interactions with the Trp246<sup>6.48</sup> side chain. Overall, the distinct allosteric effects of amilorides are probably the result of a delicate balance between an improved stability of the inactive conformation and an indirect (noncompetitive) interference with the orthosteric site for antagonists.

In summary, a combination of biochemical and thermal stability data with MD simulations, based on both inactive and the active-like crystal structures of the A<sub>2A</sub>AR, provided valuable mechanistic insights into the role of the allosteric sodium ion in the conformational equilibrium of the receptor. Our findings suggest that the binding of either the sodium ion or amilorides to the allosteric pocket selectively stabilizes the inactive conformation of the receptor, and this allosteric effect is responsible for the observed reduction in orthosteric agonist binding. Comprehensive experimental and theoretical analyses of A<sub>2A</sub>AR in simultaneous complex with both allosteric modulators and orthosteric ligands also explain, on a molecular basis, the distinct interaction profiles observed between allosteric amiloride derivatives and different orthosteric antagonists. These observations pave the way for better understanding of GPCR allosteric control,



which may be used in the design of novel allosteric modulators to more precisely tune receptor function.

## Supplemental information

Supplemental information includes supplemental experimental procedures, Figures S1-S3, and Tables S1 and S2, and can be found with this article online at [dx.doi.org/10.1016/j.str.2013.09.020](https://doi.org/10.1016/j.str.2013.09.020)

## Acknowledgements

This work was supported by NIGMS PSI:Biological grant U54 GM094618 (R.C.S., V.K., V.C.). H.G.T. acknowledges the Spanish Ministry of Education for the mobility program (JC2011-0387) and financial support from the Spanish National Plan for R+D (SAF2011-30104). L.H.H., A.P.IJ. and A.M. thank the Dutch Research Council (NWO) for financial support (NWO-TOP #714.011.001 and NWO-Veni #11188).

## References

1. Christopoulos A, *Allosteric binding sites on cell-surface receptors: novel targets for drug discovery*. Nat Rev Drug Discov, 2002. 1(3): p. 198-210.
2. Conn PJ, Christopoulos A, and Lindsley CW, *Allosteric modulators of GPCRs: a novel approach for the treatment of CNS disorders*. Nat Rev Drug Discov, 2009. 8(1): p. 41-54.
3. Gao ZG and Jacobson KA, *Keynote review: allosterism in membrane receptors*. Drug Discov Today, 2006. 11(5-6): p. 191-202.
4. Göblyös A and Ilzerman AP, *Allosteric modulation of adenosine receptors*. Biochim Biophys Acta, 2011. 1808(5): p. 1309-18.
5. Jacobson KA, Gao ZG, Göblyös A, et al., *Allosteric modulation of purine and pyrimidine receptors*. Adv Pharmacol, 2011. 61: p. 187-220.
6. Gao ZG and Ilzerman AP, *Allosteric modulation of A<sub>2A</sub> adenosine receptors by amiloride analogues and sodium ions*. Biochem Pharmacol, 2000. 60(5): p. 669-76.
7. Neve KA, Cumbay MG, Thompson KR, et al., *Modeling and mutational analysis of a putative sodium-binding pocket on the dopamine D<sub>2</sub> receptor*. Mol Pharmacol, 2001. 60(2): p. 373-81.
8. Rosenbaum DM, Cherezov V, Hanson MA, et al., *GPCR engineering yields high-resolution structural insights into  $\beta_2$ -adrenergic receptor function*. Science, 2007. 318(5854): p. 1266-73.
9. Cherezov V, *Lipidic cubic phase technologies for membrane protein structural studies*. Curr Opin Struct Biol, 2011. 21(4): p. 559-66.
10. Tate CG and Schertler GF, *Engineering G protein-coupled receptors to facilitate their structure determination*. Curr Opin Struct Biol, 2009. 19(4): p. 386-95.
11. Katritch V, Cherezov V, and Stevens RC, *Structure-function of the G protein-coupled receptor superfamily*. Annu Rev Pharmacol Toxicol, 2013. 53: p. 531-56.
12. Congreve M, Langmead CJ, Mason JS, et al., *Progress in structure based drug design for G protein-coupled receptors*. J Med Chem, 2011. 54(13): p. 4283-311.

13. Dror RO, Arlow DH, Borhani DW, et al., *Identification of two distinct inactive conformations of the  $\beta_2$ -adrenergic receptor reconciles structural and biochemical observations*. Proc Natl Acad Sci USA, 2009. 106(12): p. 4689-94.
14. Dore AS, Robertson N, Errey JC, et al., *Structure of the adenosine  $A_{2A}$  receptor in complex with ZM241385 and the xanthines XAC and caffeine*. Structure, 2011. 19(9): p. 1283-93.
15. Jaakola VP, Griffith MT, Hanson MA, et al., *The 2.6 Ångstrom crystal structure of a human  $A_{2A}$  adenosine receptor bound to an antagonist*. Science, 2008. 322(5905): p. 1211-7.
16. Congreve M, Andrews SP, Dore AS, et al., *Discovery of 1,2,4-triazine derivatives as adenosine  $A_{2A}$  antagonists using structure based drug design*. J Med Chem, 2012. 55(5): p. 1898-903.
17. Hino T, Arakawa T, Iwanari H, et al., *G-protein-coupled receptor inactivation by an allosteric inverse-agonist antibody*. Nature, 2012. 482(7384): p. 237-40.
18. Lebon G, Warne T, Edwards PC, et al., *Agonist-bound adenosine  $A_{2A}$  receptor structures reveal common features of GPCR activation*. Nature, 2011. 474(7352): p. 521-5.
19. Xu F, Wu H, Katritch V, et al., *Structure of an agonist-bound human  $A_{2A}$  adenosine receptor*. Science, 2011. 332(6027): p. 322-7.
20. Rasmussen SG, DeVree BT, Zou Y, et al., *Crystal structure of the  $\beta_2$  adrenergic receptor- $G_s$  protein complex*. Nature, 2011. 477(7366): p. 549-55.
21. Park JH, Scheerer P, Hofmann KP, et al., *Crystal structure of the ligand-free G-protein-coupled receptor *opsin**. Nature, 2008. 454(7201): p. 183-7.
22. Liu W, Chun E, Thompson A, et al., *Structural basis for allosteric regulation of GPCRs by sodium ions*. Science, 2012. 337: p. 232-6.
23. Mirzadegan T, Benko G, Filipek S, et al., *Sequence analyses of G-protein-coupled receptors: Similarities to rhodopsin*. Biochemistry, 2003. 42(10): p. 2759-67.
24. Pardo L, Deupi X, Dölker N, et al., *The role of internal water molecules in the structure and function of the rhodopsin family of G protein-coupled receptors*. Chembiochem, 2007. 8(1): p. 19-24.
25. Angel TE, Chance MR, and Palczewski K, *Conserved waters mediate structural and functional activation of family A (rhodopsin-like) G protein-coupled receptors*. Proc Natl Acad Sci USA, 2009. 106(21): p. 8555-60.
26. Barbhuiya H, McClain R, Ilzerman A, et al., *Site-directed mutagenesis of the human  $A_1$  adenosine receptor: influences of acidic and hydroxy residues in the first four transmembrane domains on ligand binding*. Mol Pharmacol, 1996. 50(6): p. 1635-42.
27. Selent J, Sanz F, Pastor M, et al., *Induced effects of sodium ions on dopaminergic G-protein coupled receptors*. PLoS Comput Biol, 2010. 6(8): p. e1000884.
28. Pert CB, Pasternak G, and Snyder SH, *Opiate agonists and antagonists discriminated by receptor binding in brain*. Science, 1973. 182(4119): p. 1359-61.
29. Snyder SH and Pasternak GW, *Historical review: Opioid receptors*. Trends Pharmacol Sci, 2003. 24(4): p. 198-205.
30. Tsai BS and Lefkowitz RJ, *Agonist-specific effects of monovalent and divalent cations on adenylate cyclase-coupled  $\alpha$  adrenergic receptors in rabbit platelets*. Mol Pharmacol, 1978. 14(4): p. 540-8.
31. Horstman DA, Brandon S, Wilson AL, et al., *An aspartate conserved among G-protein receptors confers allosteric regulation of  $\alpha_2$ -adrenergic receptors by sodium*. J Biol Chem, 1990. 265(35): p. 21590-5.
32. Proulx CD, Holleran BJ, Boucard AA, et al., *Mutational analysis of the conserved Asp2.50 and ERY motif reveals signaling bias of the urotensin II receptor*. Mol Pharmacol, 2008. 74(3): p. 552-61.

33. Gao ZG, Kim SK, Gross AS, et al., *Identification of essential residues involved in the allosteric modulation of the human A<sub>3</sub> adenosine receptor*. *Mol Pharmacol*, 2003. 63(5): p. 1021-31.
34. Nie J and Lewis DL, *Structural domains of the CB<sub>1</sub> cannabinoid receptor that contribute to constitutive activity and G-protein sequestration*. *J Neurosci*, 2001. 21(22): p. 8758-64.
35. Ballesteros JA and Weinstein H, *Integrated methods for the construction of three dimensional models and computational probing of structure-function relations in G-protein coupled receptors*, in *Methods Neurosci*. 1995, Academic Press: San Diego. p. 366-428.
36. Hess B, Kutzner C, Van der Spoel D, et al., *GROMACS 4: Algorithms for highly efficient, load-balanced, and scalable molecular simulation*. *J Chem Theory Comput*, 2008. 4(3): p. 435-47.
37. Rodríguez D, Piñeiro A, and Gutiérrez-de-Terán H, *Molecular dynamics simulations reveal insights into key structural elements of adenosine receptors*. *Biochemistry*, 2011. 50(19): p. 4194-08.
38. Gutiérrez-de-Terán H, Bello X, and Rodríguez D, *Characterization of the dynamic events of GPCRs by automated computational simulations*. *Biochem Soc Trans*, 2013. 41(1): p. 205-12.
39. Kaminski GA, Friesner RA, Tirado-Rives J, et al., *Evaluation and reparametrization of the OPLS-AA force field for proteins via comparison with accurate quantum chemical calculations on peptides*. *J Phys Chem B*, 2001. 105(28): p. 6474-87.
40. Schrödinger LLC, *Macromodel, version 9.7*. 2009: New York, NY.
41. Berger O, Edholm O, and Jähnig F, *Molecular dynamics simulations of a fluid bilayer of dipalmitoylphosphatidylcholine at full hydration, constant pressure, and constant temperature*. *Biophys J*, 1997. 72(5): p. 2002-13.
42. Chakrabarti N, Neale C, Payandeh J, et al., *An iris-like mechanism of pore dilation in the CorA magnesium transport system*. *Biophys J*, 2010. 98(5): p. 784-92.
43. Berendsen HJC, Postma JPM, Van Gunsteren WF, et al., *Interaction models for water in relation to protein hydration*, in *Intermolecular Forces*, 1981, Dordrecht: D. Reidel Publishing Company. p. 331-42.
44. Nose S and Klein ML, *Constant pressure molecular-dynamics for molecular-systems*. *Mol Phys*, 1983. 50(5): p. 1055-76.
45. Humphrey W, Dalke A, and Schulten K, *VMD - Visual molecular dynamics*. *J Mol Graphics*, 1996. 14: p. 33-8.
46. Sambrook J and Fritsch EF, *Molecular Cloning: A Laboratory Manual*. 2nd ed. 1989, Cold Spring Harbor, NY: Cold Spring Harbor Laboratory.
47. Smith PK, Krohn RI, Hermanson GT, et al., *Measurement of protein using bicinchoninic acid*. *Anal Biochem*, 1985. 150(1): p. 76-85.
48. Alexandrov AI, Mileni M, Chien EY, et al., *Microscale fluorescent thermal stability assay for membrane proteins*. *Structure*, 2008. 16(3): p. 351-9.
49. Harding MM, *Small revisions to predicted distances around metal sites in proteins*. *Acta Crystallogr D*, 2006. 62: p. 678-82.
50. Garritsen A, IJzerman AP, Tulp MTM, et al., *Receptor binding profiles of amiloride analogues provide no evidence for a link between receptors and the Na<sup>+</sup>/H<sup>+</sup> exchanger, but indicate a common structure on receptor proteins*. *J Recept Res*, 1991. 11(6): p. 891-907.
51. Fraser JS, Van den Bedem H, Samelson AJ, et al., *Assessing protein conformational ensembles using room-temperature X-ray crystallography*. *Proc Natl Acad Sci USA*, 2011. 108(39): p. 16247-52.
52. Ulmschneider MB, Bagnieris C, McCusker EC, et al., *Molecular dynamics of ion transport through the open conformation of a bacterial voltage-gated sodium channel*. *Proc Natl Acad Sci USA*, 2013. 110(16): p. 6364-9.

53. Warne T, Edwards PC, Leslie AG, et al., *Crystal structures of a stabilized  $\beta_1$ -adrenoceptor bound to the biased agonists bucindolol and carvedilol*. *Structure*, 2012. 20(5): p. 841-9.
54. Manglik A, Kruse AC, Kobilka TS, et al., *Crystal structure of the  $\mu$ -opioid receptor bound to a morphinan antagonist*. *Nature*, 2012. 485(7398): p. 321-6.
55. Christopher JA, Brown J, Dore AS, et al., *Biophysical fragment screening of the  $\beta_1$ -adrenergic receptor: identification of high affinity arylpiperazine leads using structure-based drug design*. *J Med Chem*, 2013. 56(9): p. 3446-55.
56. Schwartz TW, Frimurer TM, Holst B, et al., *Molecular mechanism of 7TM receptor activation—a global toggle switch model*. *Annu Rev Pharmacol Toxicol*, 2006. 46: p. 481-519.
57. Shi L and Javitch JA, *The binding site of aminergic G protein-coupled receptors: the transmembrane segments and second extracellular loop*. *Annu Rev Pharmacol Toxicol*, 2002. 42: p. 437-67.
58. Gao ZG, Jiang Q, Jacobson KA, et al., *Site-directed mutagenesis studies of human  $A_{2A}$  adenosine receptors: involvement of Glu<sup>13</sup> and His<sup>278</sup> in ligand binding and sodium modulation*. *Biochem Pharmacol*, 2000. 60(5): p. 661-8.
59. Neubig RR, Spedding M, Kenakin T, et al., *International Union of Pharmacology Committee on Receptor Nomenclature and Drug Classification. XXXVIII. Update on terms and symbols in quantitative pharmacology*. *Pharmacol Rev*, 2003. 55(4): p. 597-606.
60. Heitman LH, Ye K, Oosterom J, et al., *Amiloride derivatives and a nonpeptidic antagonist bind at two distinct allosteric sites in the human gonadotropin-releasing hormone receptor*. *Mol Pharmacol*, 2008. 73(6): p. 1808-15.
61. Gao ZG, Melman N, Erdmann A, et al., *Differential allosteric modulation by amiloride analogues of agonist and antagonist binding at  $A_1$  and  $A_3$  adenosine receptors*. *Biochem Pharmacol*, 2003. 65(4): p. 525-34.
62. Hoare SR, Coldwell MC, Armstrong D, et al., *Regulation of human  $D_1$ ,  $D_{2(long)}$ ,  $D_{2(short)}$ ,  $D_3$  and  $D_4$  dopamine receptors by amiloride and amiloride analogues*. *Br J Pharmacol*, 2000. 130(5): p. 1045-59.
63. Pauwels PJ, *Competitive and silent antagonism of recombinant 5-HT<sub>1B</sub> receptors by amiloride*. *Gen Pharmacol*, 1997. 29(5): p. 749-51.
64. Howard MJ, Hughes RJ, Motulsky HJ, et al., *Interactions of amiloride with  $\alpha$ - and  $\beta$ -adrenergic receptors: amiloride reveals an allosteric site on  $\alpha_2$ -adrenergic receptors*. *Mol Pharmacol*, 1987. 32(1): p. 53-8.

# Chapter 4

## Sodium ion binding pocket mutations and adenosine A<sub>2A</sub> receptor function

Arnault Massink\*

Hugo Gutiérrez-de-Terán\*

Eelke B. Lenselink

Natalia V. Ortiz Zacarías

Lizi Xia

Laura H. Heitman

Vsevolod Katritch

Raymond C. Stevens

Adriaan P. IJzerman

*\*These authors contributed equally*

*Molecular Pharmacology, 2015, 87(2): 305-13*

## Abstract

Recently a sodium ion binding pocket in a high resolution structure of the human adenosine A<sub>2A</sub> receptor was identified. In the present study we explored this binding site through site-directed mutagenesis and molecular dynamics simulations. Amino acids in the pocket were mutated to alanine, and their influence on agonist and antagonist affinity, allosterism by sodium ions and amilorides, and receptor functionality was explored. Mutation of the polar residues in the sodium ion pocket was shown to either abrogate (D52A<sup>2.50</sup> and N284A<sup>7.49</sup>) or reduce (S91A<sup>3.39</sup>, W246A<sup>6.48</sup>, and N280A<sup>7.45</sup>) the negative allosteric effect of sodium ions on agonist binding. Mutations D52A<sup>2.50</sup> and N284A<sup>7.49</sup> completely abolished receptor signaling, while mutations S91A<sup>3.39</sup> and N280A<sup>7.45</sup> elevated basal activity and mutations S91A<sup>3.39</sup>, W246A<sup>6.48</sup>, and N280A<sup>7.45</sup> decreased agonist-stimulated receptor signaling. In molecular dynamics simulations D52A<sup>2.50</sup> directly affected the mobility of sodium ions, which readily migrated to another pocket formed by Glu13<sup>1.39</sup> and His278<sup>7.43</sup>. The D52A<sup>2.50</sup> mutation also decreased the potency of amiloride with respect to ligand displacement, but did not change orthosteric ligand affinity. In contrast, W246A<sup>6.48</sup> increased some of the allosteric effects of sodium ions and amiloride, while orthosteric ligand binding was decreased. These new findings suggest that the sodium ion in the allosteric binding pocket not only impacts ligand affinity, but also plays a vital role in receptor signaling. Because the sodium ion binding pocket is highly conserved in other class A GPCRs, our findings may have a general relevance for these receptors and may guide the design of novel synthetic allosteric modulators or bitopic ligands.

## Introduction

G protein-coupled receptors (GPCRs) are seven transmembrane helical proteins, which regulate a multitude of physiological processes, and therefore are targeted by 30-40% of the drugs currently on the market.<sup>1</sup> GPCR crystal structures are becoming increasingly available, which considerably contributes to our understanding of both drug-receptor interactions and receptor activation mechanisms.<sup>2</sup> Still, much remains to be discovered and therefore the new crystal structure repertoire of GPCRs is continuously analyzed by biochemical, computational and pharmacological studies.

One of the most widely explored GPCRs is the human adenosine  $A_{2A}$  receptor ( $hA_{2A}AR$ ), a drug target related to Parkinson's disease, cardiovascular diseases, and inflammatory disorders.<sup>3</sup> Recently, a high resolution crystal structure of the inactive  $hA_{2A}AR$  in complex with antagonist ZM-241,385 identified the precise location of a sodium ion in the region around the conserved Asp52<sup>2,50,4</sup>, as previously hypothesized for other GPCRs<sup>5,6</sup> (numbering in superscript according to Ballesteros and Weinstein).<sup>7</sup> Residues Ser91<sup>3,39</sup>, Trp246<sup>6,48</sup>, Asn280<sup>7,45</sup>, and Asn284<sup>7,49</sup>, together with a network of structural water molecules, completed the coordination of the ion in the  $hA_{2A}AR$ . The fact that this site changes its conformation dramatically between inactive and active-like structures of the  $hA_{2A}AR$ ,<sup>4,8</sup> inspired us to further explore the nature of this allosteric binding site.

In Chapter 3 we used a combination of molecular dynamics (MD) simulations, biophysical and biochemical experiments to conclude that sodium ions selectively stabilize the inactive conformation of the wild-type receptor, and that a physiological concentration was sufficient to achieve this effect. This mechanism was further corroborated with radioligand binding data, indicative of a competitive interaction between the sodium ion in this allosteric pocket and an agonist in the orthosteric pocket. Further, we proposed in Chapter 3 that the diuretic drug amiloride and analogs compete for the same site, and exert an allosteric control on the  $hA_{2A}AR$  quite similar to that of sodium ions, albeit with pharmacological differences in modulation of orthosteric ligand binding.

In the present study we mutated residues in the first and second coordination shell around the sodium ion, to define the role of individual amino acids in allosteric modulation by sodium ions, amiloride and its derivative HMA. This enabled us to analyze

the effects of these manipulations on orthosteric ligand binding and receptor activation, employing a combination of biochemical and computational techniques.

## **Materials and methods**

### **Cell growth and transfection**

HEK293 cells were grown in culture medium consisting of Dulbecco's modified Eagle's medium (DMEM) supplemented with 10% newborn calf serum (NCS), 50 µg/ml streptomycin and 50 IU/ml penicillin at 37 °C and 7% CO<sub>2</sub>. Cells were subcultured twice a week at a ratio of 1:20 on 10 cm ø plates. Single point mutations were introduced in the wild-type hA<sub>2A</sub>AR-plasmid DNA (FLAG-tag at N-terminus, in pcDNA3.1) by BaseClear (Leiden, The Netherlands). Cells were transfected with the indicated plasmids (1 µg each) using the calcium phosphate precipitation method.<sup>9</sup> All experiments were performed 48 h after transfection. HEK293 cells stably expressing the wild-type A<sub>2A</sub>AR receptor (A<sub>2A</sub>AR-WT) were grown in the same medium as the other HEK293 cells but with the addition of G-418 (200 µg/ml).

### **Enzyme-linked immunosorbent assay**

Twenty-four hours after transfection, cells were brought into 96-well poly-D-lysine-coated plates at a density of 10<sup>5</sup> cells per well. After an additional 24 h, the monolayers were washed with phosphate-buffered saline (PBS) and fixed for 10 minutes with 3.7% formaldehyde. Subsequently, cells were washed two times with PBS and cell-surface receptors were labeled with mouse anti-FLAG (M2) primary antibody (Sigma, 1:1000) in culture medium for 30 min at 37 °C. The cells were then washed once with DMEM supplemented with 25 mM HEPES and then incubated for another 30 min at 37 °C in culture medium supplemented with horseradish peroxidase-conjugated anti-mouse IgG produced in goat (Brunschwig, Amsterdam, The Netherlands; 1:5000) as the secondary antibody. The cells were washed twice with PBS. Finally, the cells were incubated with 3,3',5,5'-tetramethylbenzidine (TMB) for 5 min in the dark at room temperature. The reaction was stopped with 1 M H<sub>3</sub>PO<sub>4</sub> and after 5 min the absorbance was read at 450 nm using a VICTOR 2 plate reader (PerkinElmer Life Sciences, Groningen, The Netherlands).



### Radioligand binding assays

[<sup>3</sup>H]ZM-241,385 (50 Ci/mmol) and [<sup>3</sup>H]NECA (17 Ci/mmol) were obtained from ARC Inc. (St. Louis, MO, USA) and PerkinElmer (Groningen, The Netherlands), respectively. ZM-241,385 was obtained from Ascent Scientific (Bristol, UK). Amiloride and HMA were obtained from Sigma Aldrich (Zwijndrecht, The Netherlands). All other materials were purchased from commercial sources and were of the highest available purity.

HEK293 cells were grown and transfected as described above. Membranes were prepared as follows. Cells were detached from plates 48 h after transfection by scraping them into 5 ml PBS, collected and centrifuged at 700 ×g (3000 rpm) for 5 min. Pellets derived from 20 plates (10 cm ø) were pooled and resuspended in 16 ml of ice-cold assay buffer (50 mM Tris-HCl, pH 7.4). An Ultra-Turrax was used to homogenize the cell suspension. Membranes and the cytosolic fraction were separated by centrifugation at 100,000 ×g (31,000 rpm) in a Beckman Optima LE-80K ultracentrifuge (Woerden, The Netherlands) at 4 °C for 20 min. The pellet was resuspended in 8 ml of Tris buffer and the homogenization and centrifugation step was repeated. Assay buffer (4 ml) was used to resuspend the pellet and adenosine deaminase (ADA) was added (0.8 IU/ml) to break down endogenous adenosine. Membranes were stored in 250 µl aliquots at -80 °C. Membrane protein concentrations were measured using the BCA (bicinchoninic acid) method.<sup>10</sup>

For competition binding experiments with [<sup>3</sup>H]ZM-241,385 membranes with transiently expressed A<sub>2A</sub>AR-WT (7 µg of total protein), A<sub>2A</sub>AR-D52A<sup>2.50</sup> (5 µg), A<sub>2A</sub>AR-S91A<sup>3.39</sup> (1 µg), A<sub>2A</sub>AR-W246A<sup>6.48</sup> (2 µg), A<sub>2A</sub>AR-N280A<sup>7.45</sup> (1.5 µg), A<sub>2A</sub>AR-N284A<sup>7.49</sup> (1 µg) were used; we added different protein amounts to ensure that total binding to the membrane preparations was less than 10% of the total radioactivity added in order to prevent radioligand depletion. For [<sup>3</sup>H]NECA competition binding experiments 30 µg, 15 µg, 10 µg, 45 µg, 50 µg, 10 µg of expressed A<sub>2A</sub>AR-WT, D52A<sup>2.50</sup>, S91A<sup>3.39</sup>, W246A<sup>6.48</sup>, N280A<sup>7.45</sup>, N284A<sup>7.49</sup> receptors were used, respectively. Membrane aliquots were incubated in a total volume of 100 µl of assay buffer at 25 °C for 2 h. For homologous competition curves, radioligand displacement experiments were performed in the presence of nine concentrations of NECA (0.1 nM – 100 µM) and ZM-241,385 (0.01 nM – 10 µM). For concentration-effect curves, radioligand displacement experiments were performed in the presence of six concentrations of NaCl (10 µM – 1 M) and five

concentrations of amiloride (100 nM – 1 mM) and HMA (10 nM – 1 mM). [<sup>3</sup>H]ZM-241,385 and [<sup>3</sup>H]NECA were used at concentrations of 2.5 nM and 20 nM, respectively. Nonspecific binding was determined in the presence of 10 μM ZM-241,385 ([<sup>3</sup>H]NECA) or 100 μM NECA ([<sup>3</sup>H]ZM-241,385) and represented less than 10% of the total binding. Incubations were terminated by rapid vacuum filtration to separate the bound from free radioligand through 96-well GF/B filter plates using a Filtermate-harvester (PerkinElmer Life Sciences). Filters were subsequently washed three times with ice-cold assay buffer. The filter-bound radioactivity was determined by scintillation spectrometry using a PE 1450 Microbeta Wallac Trilux scintillation counter (PerkinElmer Life Sciences).

### **Functional cAMP assays**

HEK293 cells were grown and transfected as described above. Experiments were performed 48 h after transfection. The amount of cAMP produced was determined with the LANCE cAMP 384 kit (PerkinElmer). In short, 5000 cells per well were pre-incubated for 30 min at 37°C and subsequently incubated for one hour at room temperature with a range of CGS-21680 concentrations (0.1 nM – 10 μM), one concentration of ZM-241,385 (10 μM), or without addition of ligand. cAMP generation was performed in the medium containing cilostamide (50 μM), rolipram (50 μM) and ADA (0.8 IU·ml<sup>-1</sup>). The incubation was stopped by adding detection mix and antibody solution, according to the instructions of the manufacturer. The generated fluorescence intensity was quantified on an EnVision® Multilabel Reader (PerkinElmer). cAMP production by 10 μM CGS-21680 on the parental HEK293 cell line represented less than 5% of cAMP production generated in cells expressing the hA<sub>2A</sub>AR receptor.

### **Molecular dynamics simulations**

Molecular dynamics (MD) simulations of wild-type and mutant forms of the A<sub>2A</sub> receptor were performed following the computational protocol in Chapter 3. Briefly, the inactive structure of the A<sub>2A</sub>AR in complex with ZM-241,385 and a sodium ion (PDB code 4EIY)<sup>4</sup> was used as a basis for our simulations, after a refinement process that consisted in modeling the missing ICL3 segment and proton addition, assessing the protonation state of titratable residues (i.e. all charged) and histidine residues, which were protonated on Nδ except for His155<sup>ECL2</sup> (protonated on Nε) and His264<sup>ECL3</sup> (positively charged). The sodium ion and coordinating water molecules were explicitly considered except in the simulations

with amiloride or HMA, which occupied the allosteric sodium ion site. Further details are summarized in Chapter 3. Building the mutant variants of the A<sub>2A</sub> receptor explored in this work was achieved by means of the “protein mutation tool” in Maestro.<sup>11</sup>

MD simulations were performed with GROMACS software,<sup>12</sup> using our original protocol for the MD simulations of GPCRs.<sup>13</sup> Our PyMemDyn program was used for membrane insertion, soaking with bulk water and inserting the resulting system, consisting of approximately 50,000 atoms (~74% belong to solvent molecules, ~15% to lipids and ~11% to protein and ligand atoms), into a hexagonal prism-shaped box, which was then energy-minimized and carefully equilibrated in the framework of periodic boundary conditions (PBC) for 5 ns.<sup>14</sup> Three replicate production simulations (i.e., changing the initial velocities of the system) were followed for 100 ns simulation time each, thus accounting for a total of 300 ns MD sampling of each system. The OPLSAA force field was adopted throughout the simulations,<sup>15</sup> with ligand parameters obtained from Macromodel,<sup>16</sup> and lipid parameters adapted from Berger<sup>17</sup> together with the use of the half- $\epsilon$  double-pairlist method<sup>18</sup> and the SPC water model.<sup>19</sup> A Nose-Hoover thermostat<sup>20</sup> with a target temperature of 310 K was used. Electrostatic interactions beyond a cutoff of 12 Å were estimated with the particle mesh Ewald (PME) method. All MD analyses were conducted with several GROMACS and VMD<sup>21</sup> utilities. Molecular superimpositions, trajectory visualizations and molecular images were performed with PyMOL.<sup>22</sup>

## Results

### Design of mutations in the sodium ion binding pocket

We mutated the residues important for the sodium ion coordination (Figure 1) to alanine, i.e. D52A<sup>2,50</sup>, S91A<sup>3,39</sup>, W246A<sup>6,48</sup>, N280A<sup>7,45</sup>, and N284A<sup>7,49</sup>. This approach thus yielded a total of five mutant receptors, which were studied further and compared to the wild-type receptor with respect to their expression levels and pharmacology.

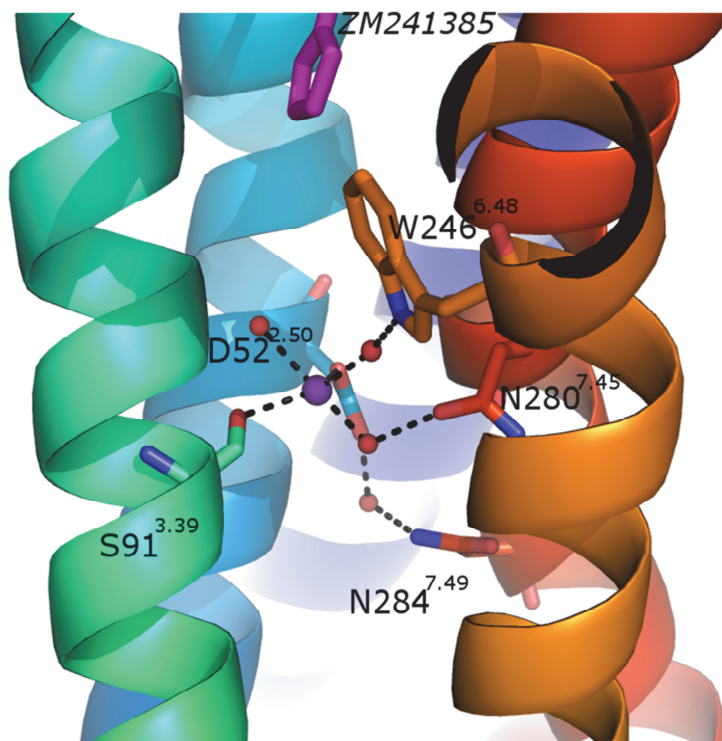


**Figure 1.** Residues in or close to the sodium ion binding site that we subjected to an alanine scan in the hA<sub>2A</sub>AR, mapped on the crystal structure of the hA<sub>2A</sub>AR in the inactive ZM-241,385 and sodium ion bound conformation (PDB 4E1Y)<sup>4</sup>. Residues Asp52<sup>2,50</sup>, Ser91<sup>3,39</sup>, Trp246<sup>6,48</sup>, Asn280<sup>7,45</sup>, and Asn284<sup>7,49</sup> (represented by sticks, of which red and blue sticks are oxygen and nitrogen atoms, respectively) coordinate the sodium ion (purple sphere). Numbering of the residues follows the Ballesteros-Weinstein system for comparison of positions between GPCRs.<sup>7</sup> Water molecules interacting with the sodium ion are represented by red spheres; hydrogen bonds are represented by black dotted lines; receptor backbone is represented by ribbons. Purple stick structure on top represents (part of) co-crystallized ZM-241,385.

### Cell surface receptor expression of mutated receptors

ELISA was performed on HEK293 cells transiently expressing FLAG-tagged wild-type and mutant hA<sub>2A</sub>AR (Figure 2). Wild-type and mutant receptors were expressed efficiently at similar levels.

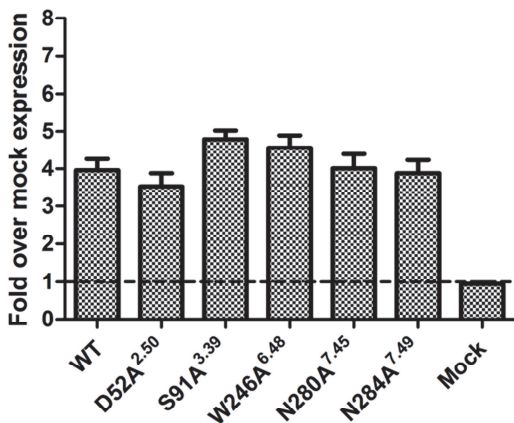


**Figure 2.** Receptor expression levels on the cell surface of HEK293 cells transiently transfected with wild-type hA<sub>2A</sub>AR or D52A<sup>2.50</sup>, S91A<sup>3.39</sup>, W246A<sup>6.48</sup>, N280A<sup>7.45</sup>, or N284A<sup>7.49</sup> single point mutated hA<sub>2A</sub>AR, represented as fold-over-mock transfected HEK293T cells. The figure represents data combined from at least two separate experiments performed in quadruplicate.

### Homologous competition assays

First we analyzed the effect of mutation of these residues on the affinity of radioligands [<sup>3</sup>H]NECA (agonist) and [<sup>3</sup>H]ZM-241,385 (antagonist) in the absence of NaCl (Table 1). The affinity of [<sup>3</sup>H]NECA and [<sup>3</sup>H]ZM-241,385 for the wild-type hA<sub>2A</sub>AR was 81 nM and 4.6 nM, respectively. D52A<sup>2.50</sup> showed the same affinity as the wild-type receptor for both radioligands (77 nM and 3.5 nM, respectively). The other mutations caused some decrease in affinity for both radioligands, with a more pronounced effect on the agonist. An approximately 3-fold decrease of [<sup>3</sup>H]NECA affinity was observed for receptors with mutations S91A<sup>3.39</sup> and N284A<sup>7.49</sup>, while [<sup>3</sup>H]ZM-241,385's affinity did not change significantly by these mutations. Radioligand agonist affinity decreased approximately 9-fold on N280A<sup>7.45</sup>, while a 1.8-fold decrease was observed for the antagonist. The W246A<sup>6.48</sup> mutation affected affinities most, i.e. a 24-fold decrease in [<sup>3</sup>H]NECA affinity and a 5-fold decrease in [<sup>3</sup>H]ZM-241,385 affinity.

**Table 1.** Homologous competition displacement studies yielding  $K_D$  values (nM) for [ $^3$ H]NECA and [ $^3$ H]ZM-241,385 binding to wild-type human  $A_{2A}$ AR and single point mutants D52A<sup>2.50</sup>, S91A<sup>3.39</sup>, W246A<sup>6.48</sup>, N280A<sup>7.45</sup>, and N284A<sup>7.49</sup>, transiently expressed on HEK293 cell membranes.

	[ $^3$ H]NECA		[ $^3$ H]ZM-241,385	
	$K_D$ (nM)	Change <sup>a</sup>	$K_D$ (nM)	Change <sup>a</sup>
<b>Wild-type</b>	81 ± 5	1.0	4.6 ± 0.5	1.0
<b>D52A</b> <sup>2.50</sup>	77 ± 8	1.0	3.5 ± 0.5	0.75
<b>S91A</b> <sup>3.39</sup>	258 ± 24***	3.2	7.0 ± 0.2	1.5
<b>W246A</b> <sup>6.48</sup>	1942 ± 124***	24	23.2 ± 4.3***	5.0
<b>N280A</b> <sup>7.45</sup>	752 ± 147***	9.3	8.4 ± 1.3*	1.8
<b>N284A</b> <sup>7.49</sup>	237 ± 27***	2.9	7.0 ± 0.7	1.5

a: Change in fold over wild-type.

Significantly different from wild-type with \*  $p < 0.05$  or \*\*\*  $p < 0.001$  (one-way ANOVA with Dunnett's post test performed on corresponding  $pK_D$  values).

Values are means ± SEM of at least three separate assays performed in duplicate.

### Concentration-effect curves in radioligand displacement studies

Displacement curves of [ $^3$ H]ZM-241,385 and [ $^3$ H]NECA binding were recorded with different concentrations of NaCl, amiloride, and its more lipophilic derivative HMA for the wild-type and mutant receptors (Figure 3). Whenever possible,  $IC_{50}$  values were derived for the inhibitory modulation of agonist [ $^3$ H]NECA and antagonist [ $^3$ H]ZM-241,385 binding by NaCl, amiloride, and HMA (Tables 2 and 3). NaCl inhibited [ $^3$ H]NECA binding to the wild-type receptor with an  $IC_{50}$  value of  $44 \pm 6$  mM. At the highest concentration tested (1 M) NaCl had modest effects with  $59 \pm 3$  %,  $89 \pm 2$  %, and  $52 \pm 11$  % of [ $^3$ H]NECA binding remaining on mutants S91A<sup>3.39</sup>, N280<sup>7.45</sup>, and W246A<sup>6.48</sup>, respectively (Figure 3A). [ $^3$ H]NECA binding was not inhibited by NaCl on mutant N284A<sup>7.49</sup> (Figure 3A). Increasing concentrations of NaCl showed a tendency to enhance [ $^3$ H]ZM-241,385 binding to the wild-type receptor as well as to the mutants tested, with W246A<sup>6.48</sup> showing the biggest enhancement (Figure 3B). At the highest concentration of NaCl (1 M), [ $^3$ H]NECA agonist binding was also enhanced in the mutant receptor D52A<sup>2.50</sup> ( $172 \pm 9$  %), which suggests that at such extreme concentrations NaCl can exert allosteric effects that are different from the specific effect of sodium ion binding at Asp52<sup>2.50</sup>.

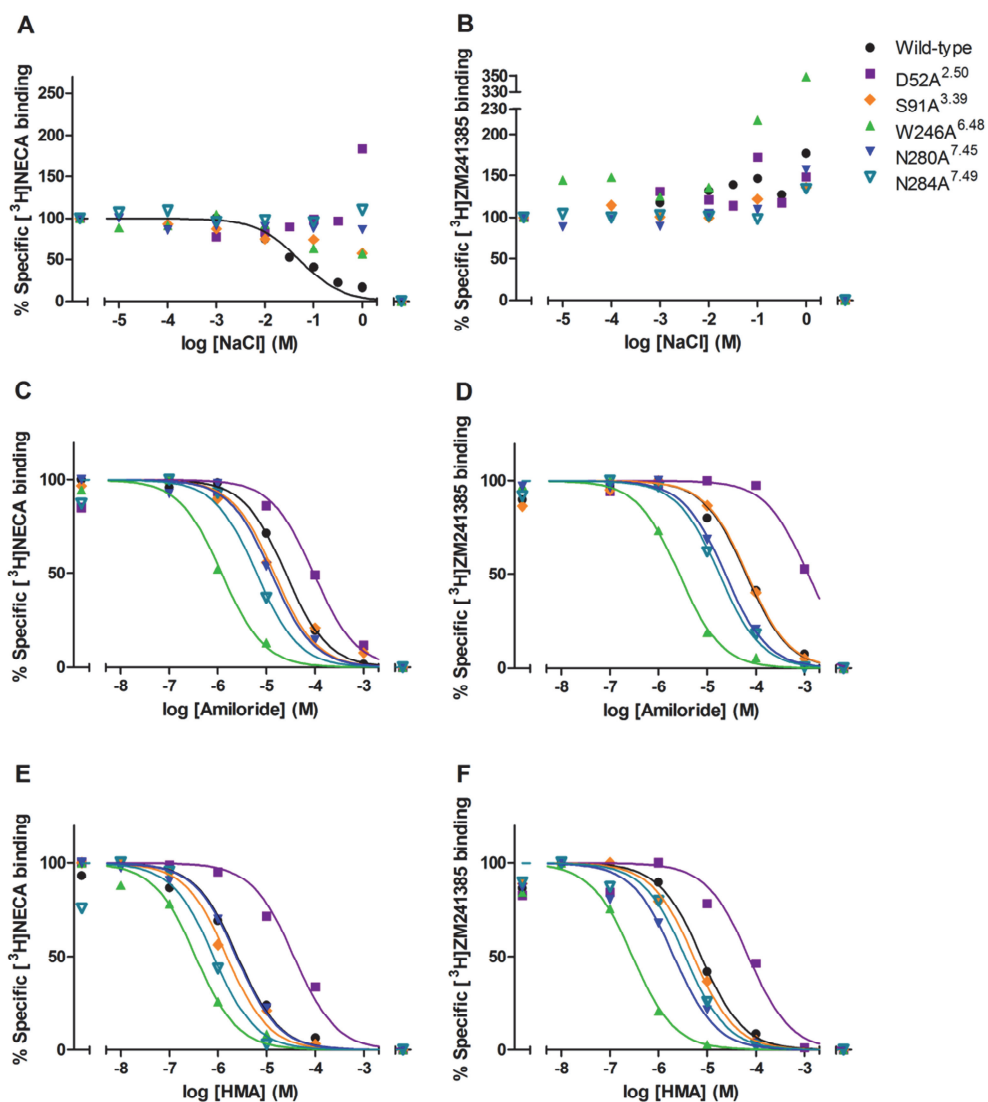


**Figure 3.** Displacement/enhancement of specific [<sup>3</sup>H]NECA (A, C, E) and [<sup>3</sup>H]ZM-241,385 (B, D, F) binding by NaCl (A, B), amiloride (C, D), and HMA (E, F) on wild-type human A<sub>2A</sub>AR and point mutants D52A<sup>2.50</sup>, S91A<sup>3.39</sup>, W246A<sup>6.48</sup>, N280A<sup>7.45</sup>, and N284A<sup>7.49</sup> transiently expressed on HEK293T cell membranes. Representative graphs from one experiment performed in duplicate are shown.

**Table 2.** Displacement of specific [<sup>3</sup>H]NECA binding by amiloride and HMA from wild-type human A<sub>2A</sub>AR and point mutants D52A<sup>2.50</sup>, S91A<sup>3.39</sup>, W246A<sup>6.48</sup>, N280A<sup>7.45</sup>, N284A<sup>7.49</sup> transiently expressed on HEK293 cell membranes.

	[ <sup>3</sup> H]NECA			
	Amiloride		HMA	
	IC <sub>50</sub> (μM)	Change <sup>a</sup>	IC <sub>50</sub> (μM)	Change <sup>a</sup>
<b>Wild-type</b>	16 ± 3	1.0	2.5 ± 0.4	1.0
<b>D52A<sup>2.50</sup></b>	175 ± 75***	11	35 ± 9***	14
<b>S91A<sup>3.39</sup></b>	13 ± 1.8	0.81	2.3 ± 0.6	0.92
<b>W246A<sup>6.48</sup></b>	2.7 ± 0.9***	0.17	0.43 ± 0.05***	0.17
<b>N280A<sup>7.45</sup></b>	10 ± 2	0.63	2.4 ± 0.6	1.0
<b>N284A<sup>7.49</sup></b>	5.9 ± 1.4	0.37	1.0 ± 0.3*	0.40

*a*: Change in fold over wild-type.

Significantly different from wild-type with \* *p* < 0.05 or \*\*\* *p* < 0.001 (one-way ANOVA with Dunnett's post test performed on corresponding pIC<sub>50</sub> values).

Values are means ± SEM of at least three separate assays performed in duplicate.

Amiloride and HMA were capable of displacing [<sup>3</sup>H]NECA and [<sup>3</sup>H]ZM-241,385 binding on the point mutant receptors (Figures 3C-F), although with different IC<sub>50</sub> values with respect to the wild-type receptor (Tables 2 and 3). D52A<sup>2.50</sup> was particularly insensitive to amilorides: the inhibitory potency of amiloride and HMA on [<sup>3</sup>H]NECA binding was decreased by 11- and 14-fold and on [<sup>3</sup>H]ZM-241,385 binding by 17- and 18-fold, respectively. Conversely, W246A<sup>6.48</sup> showed an increased inhibitory potency of amiloride and HMA, both on [<sup>3</sup>H]NECA (6-fold for both amilorides) and on [<sup>3</sup>H]ZM-241,385 (24- and 25-fold, respectively) binding. For N280A<sup>7.45</sup> we observed a smaller but also significant increase (3.6-fold) of the negative modulation of [<sup>3</sup>H]ZM-241,385 binding by HMA, and for N284A<sup>7.49</sup> a similar increase (2.6-fold) of the modulation of both [<sup>3</sup>H]NECA and [<sup>3</sup>H]ZM-241,385 binding by HMA. For N284A<sup>7.49</sup> the potency of amiloride increased significantly only in case of [<sup>3</sup>H]ZM-241,385 displacement. Mutant S91A<sup>3.39</sup> exhibited similar potencies as the wild-type receptor for displacement of both radioligands by amiloride and HMA (Tables 2 and 3). These observations suggest that while polar interactions with W246A<sup>6.48</sup>, N280A<sup>7.45</sup> and N284A<sup>7.49</sup> are important for binding of the sodium ion and coordinating water molecules, the interactions of amilorides with these three side chains are somewhat suboptimal.



**Table 3.** Displacement of specific [<sup>3</sup>H]ZM-241,385 binding by amiloride and HMA from wild-type human A<sub>2A</sub>AR and point mutants D52A<sup>2.50</sup>, S91A<sup>3.39</sup>, W246A<sup>6.48</sup>, N280A<sup>7.45</sup>, N284A<sup>7.49</sup> transiently expressed on HEK293 cell membranes.

	[ <sup>3</sup> H]ZM-241,385			
	Amiloride		HMA	
	IC <sub>50</sub> (μM)	Change <sup>a</sup>	IC <sub>50</sub> (μM)	Change <sup>a</sup>
<b>Wild-type</b>	63 ± 16	1.0	8.9 ± 1.5	1.0
<b>D52A<sup>2.50</sup></b>	1065 ± 274***	17	164 ± 47***	18
<b>S91A<sup>3.39</sup></b>	82 ± 8	1.3	8.2 ± 0.5	0.92
<b>W246A<sup>6.48</sup></b>	2.6 ± 0.4***	0.04	0.36 ± 0.06***	0.04
<b>N280A<sup>7.45</sup></b>	20 ± 4	0.32	2.5 ± 0.6**	0.28
<b>N284A<sup>7.49</sup></b>	16 ± 4*	0.25	3.3 ± 0.8*	0.37

a: Change in fold over wild-type.

Significantly different from wild-type with \*  $p < 0.05$ , \*\*  $p < 0.01$ , or \*\*\*  $p < 0.001$  (one-way ANOVA with Dunnett's post test performed on corresponding pIC<sub>50</sub> values).

Values are means ± SEM of at least three separate assays performed in duplicate.

### Concentration-effect curves for cAMP production

Functional assays were performed to further characterize the effect of the single point mutations on hA<sub>2A</sub>AR signaling. As an agonist CGS-21680 was used to activate the receptor, yielding an increase in cAMP production through G<sub>s</sub> protein activation (Figure 4 and Table 4). The use of the selective agonist CGS-21680 for the hA<sub>2A</sub>AR rather than the nonselective NECA ensured that no endogenously expressed hA<sub>2B</sub>AR was activated in the HEK293 cells. The absence of activation by 10 μM CGS-21680 in the untransfected parental cell line confirmed that indeed no endogenously expressed receptor was activated in this experimental setup. Mutations of the residues involved in the sodium ion binding site affected basal activity and efficacy of cAMP signaling by the hA<sub>2A</sub>AR. D52A<sup>2.50</sup> and N284A<sup>7.49</sup> mutants showed neither basal activity nor any activation by CGS-21680. In all other cases, the mutant receptor showed a dramatically decreased receptor signaling response to CGS-21680 binding ( $E_{max} - E_{basal}$ ), ranging from only 27 % to 46 % of the wild-type response. The basal activity significantly increased over wild-type in mutation S91A<sup>3.39</sup>. The N280A<sup>7.45</sup> mutant also showed a tendency to increased basal activity but this was not significantly different from wild-type. This constitutive activity was inhibited by addition of 10 μM ZM-241,385, confirming that the elevated basal cAMP production in the transiently transfected cells was caused by these mutant receptors (supplemental Figure

S1). CGS-21680 activated both the wild-type and mutant N280A<sup>7.45</sup> hA<sub>2A</sub>AR with an EC<sub>50</sub> value of 17 nM. The potency of CGS-21680 was somewhat decreased on mutant W246A<sup>6.48</sup> (~5-fold). In the case of S91A<sup>3.39</sup> the difference between basal and maximum activity was judged too small to derive an accurate EC<sub>50</sub> value.

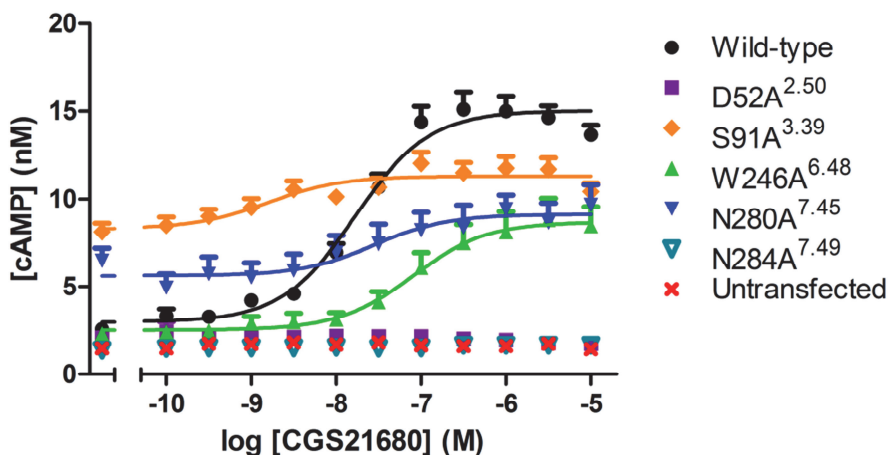


**Figure 4.** Full concentration-effect curves of hA<sub>2A</sub>AR selective agonist CGS-21680 induced stimulation of cAMP production by HEK293T cells stably expressing wild-type, transiently expressing D52A<sup>2.50</sup>, S91A<sup>3.39</sup>, W246A<sup>6.48</sup>, N280A<sup>7.45</sup>, or N284A<sup>7.49</sup> hA<sub>2A</sub>AR, or by untransfected parental HEK293T cells. Graphs represent mean ± SEM from at least three separate experiments performed in triplicate.

### Molecular dynamics simulations

The dynamic behaviors of the wild-type receptor and the receptors with mutated residues important for sodium ion coordination D52A<sup>2.50</sup>, S91A<sup>3.39</sup>, W246A<sup>6.48</sup>, N280A<sup>7.45</sup>, and N284A<sup>7.49</sup>, were simulated with either only antagonist ZM-241,385 present or with both ZM-241,385 in the orthosteric pocket and the sodium ion in its allosteric binding site (Supplemental Table S1). In addition, the wild-type receptor and mutated receptors D52A<sup>2.50</sup> and W246A<sup>6.48</sup> were simulated with ZM-241,385 in the orthosteric pocket and amiloride or HMA in the sodium ion binding site. Analysis of the root mean squared deviation (RMSD) revealed equilibrated trajectories typically after 20-30 ns with an average value of 1.8 Å in all simulations, and analysis of the root mean squared fluctuation (RMSF) confirmed no major conformational changes in the receptor due to any of the mutations.

**Table 4.** Agonist activation of wild-type and mutant adenosine A<sub>2A</sub> receptor. cAMP production by HEK293T cells stably expressing wild-type or transiently transfected with D52A<sup>2.50</sup>, S91A<sup>3.39</sup>, W246A<sup>6.48</sup>, N280A<sup>7.45</sup>, or N284A<sup>7.49</sup> hA<sub>2A</sub>AR, was measured in presence of increasing concentrations of CGS-21680.

	CGS-21680		
	pEC <sub>50</sub> (EC <sub>50</sub> <sup>a</sup> )	Change <sup>b</sup>	% Response <sup>c</sup>
<b>Wild-type</b>	7.8 ± 0.0 (17)	1.0	100 ± 14
<b>D52A</b> <sup>2.50</sup>	N.D. <sup>d</sup>	N.D. <sup>d</sup>	-2 ± 1***
<b>S91A</b> <sup>3.39</sup>	N.D. <sup>e</sup>	N.D. <sup>e</sup>	27 ± 11***
<b>W246A</b> <sup>6.48</sup>	7.1 ± 0.0*** (86)	5.1	46 ± 13**
<b>N280A</b> <sup>7.45</sup>	7.8 ± 0.1 (17)	1.0	29 ± 12***
<b>N284A</b> <sup>7.49</sup>	N.D. <sup>d</sup>	N.D. <sup>d</sup>	2 ± 2***

a: EC<sub>50</sub> (nM) in parentheses.

b: Change in fold over wild-type.

c: % Signaling response of receptor to CGS-21680 (E<sub>max</sub> - E<sub>basal</sub>) in % of wild-type response.

d: No stimulation of cAMP was observed with 10 μM CGS-21680.

e: Basal activity was too high to determine an accurate EC<sub>50</sub> value.

Significantly different from wild-type with \*\* *p* < 0.01 or \*\*\* *p* < 0.001 (one-way ANOVA with Dunnett's post test).

pEC<sub>50</sub> and % response values are means ± SEM of at least three separate assays performed in triplicate.

The effect of each single point mutation on the sodium ion mobility and coordination was assessed (Table 5). During the simulation in the wild-type model conducted in Chapter 3 the sodium ion alternated between two resonance positions, in which the sodium ion had a direct interaction with either Ser91<sup>3.39</sup> (22% occurrence of direct interaction during the simulations) or Asn280<sup>7.45</sup> (29%), while maintaining a continuous direct interaction with Asp52<sup>2.50</sup> (90%). In mutation D52A<sup>2.50</sup> however, sodium ion mobility increased by 5-fold and almost no direct interactions with residues Ser91<sup>3.39</sup> (1%) and Asn280<sup>7.49</sup> (0%) occurred. In the first 10 ns of the simulation with the D52A<sup>2.50</sup> mutant receptor, the sodium ion migrated from its starting position in the sodium ion binding site near Ala52<sup>2.50</sup> to a vestibular pocket formed by residues Glu13<sup>1.39</sup> and His278<sup>7.43</sup>, where the sodium ion remained stable for the remaining 90 ns of the simulation (Figure 5). In contrast, mutants S91A<sup>3.39</sup>, W246A<sup>6.48</sup>, N280A<sup>7.45</sup> or N284A<sup>7.49</sup> did not show major deviations as compared to the wild-type situation with regards to either the ion mobility or the average number of oxygen atoms coordinating it (Supplemental Table S2),<sup>23</sup> due to the replacement of the mutated side chain by an additional water molecule. However, the occurrence of direct

interactions with the three coordinating residues appeared lowered to some extent, indicative of a non-optimal ion coordination by these mutants. This was true in particular for the interaction with Asp52<sup>2.50</sup> (51-76%, see Table 5).

Mobility and interactions with the receptor of amiloride and HMA, as docked in the sodium ion binding site, were assessed in simulations of the wild-type receptor and mutant receptors D52A<sup>2.50</sup> and W246A<sup>6.48</sup> (Figure 6). In these relatively short MD runs amiloride was equally stable in the proposed binding site upon both mutations, with an RMSF value of approx. 2 Å. The mobility of the amiloride derivative HMA was increased 3-fold by mutation D52A<sup>2.50</sup>, and in one out of three simulations it left the putative binding pocket following the same pathway as depicted in Figure 5B. Mutation W246A<sup>6.48</sup>, on the contrary, did not affect HMA stability in the same way. However, it is worth noting that specific contacts changed for the two ligands with both mutants. In the wild-type receptor, both ligands achieved an average number of 4 simultaneous hydrogen bonds, mainly with residues Asp52<sup>2.50</sup> and Trp246<sup>6.48</sup> (Supplemental Figure S2 and Chapter 3). For amiloride, the number of hydrogen bonds dropped to approx. 2 in the two mutants examined, as well as for HMA with mutant W246A<sup>6.48</sup>, while mutation D52A<sup>2.50</sup> had a more dramatic effect on HMA with only one hydrogen bond left on average (Supplemental Figure S2). Note that in this analysis, interactions between amino (amilorides) and carbonyl (Asp52<sup>2.50</sup>) groups were approximated as hydrogen bonds, instead of the stronger salt bridge interactions that occur in reality, the loss of which is expected to have a large effect on the affinities of amilorides. This analysis did not reveal stable hydrogen bonds of amilorides with either of the asparagines close by (Asn280<sup>7.45</sup> and Asn284<sup>7.49</sup>).

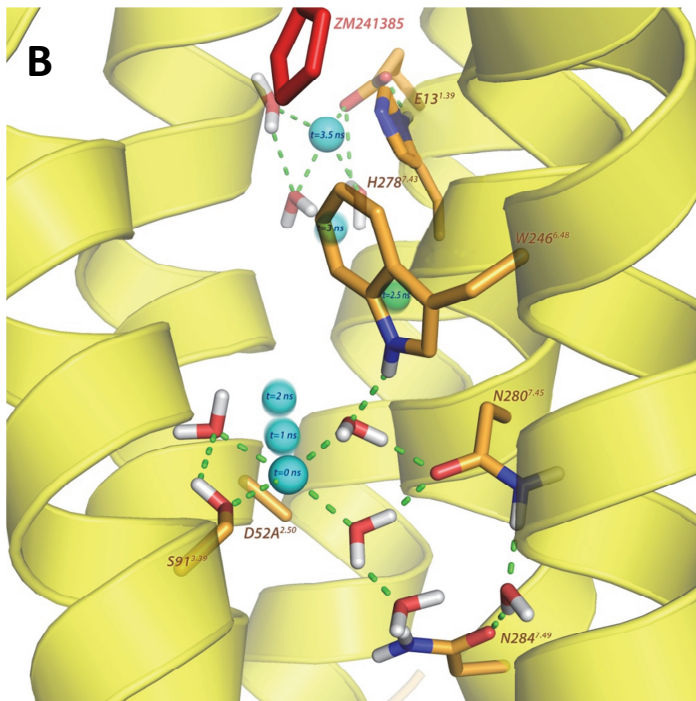
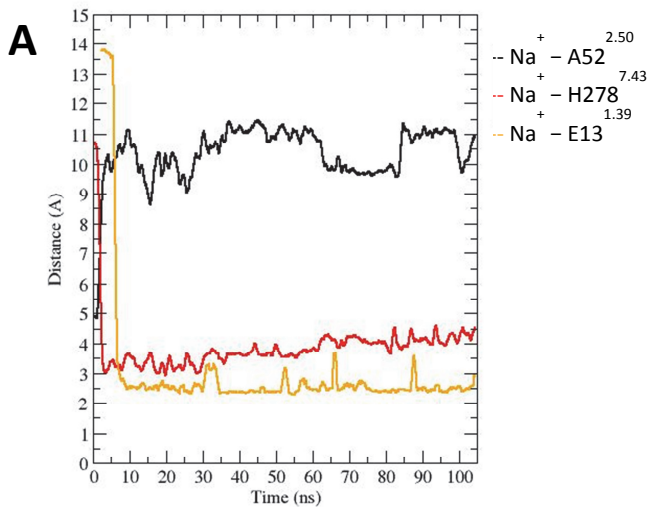


**Figure 5. A)** Average distance in Å of sodium ion from Glu13<sup>1.39</sup> (Oε), Ala52<sup>2.50</sup> (Cα), and His278<sup>7.43</sup> (Nδ) as a function of the simulation time for the D52A<sup>2.50</sup> mutant. Graphs represent means from three independent simulations. **B)** 3D representation of the migration pathway of the sodium ion (cyan sphere, with labels indicating the occupancy at averaged MD simulation windows) from its putative binding site towards the vestibular pocket formed by Glu13<sup>1.39</sup> and His278<sup>7.43</sup>. The residues and water molecules interacting with the sodium ion are represented in sticks, and hydrogen bonds represented by green dotted lines.

**Table 5.** Mobility of the sodium ion in root mean squared fluctuation (RMSF) in wild-type and mutant receptor, and the occurrence in % of direct interactions with the different residues coordinating the ion in the crystal structure along the simulation time.

	<b>Na<sup>+</sup> mobility</b>	<b>Na<sup>+</sup> interactions</b>		
	<i>RMSF in Å</i>	<i>% occurrence with indicated residues</i>		
		<b>Asp52<sup>2.50</sup></b>	<b>Ser91<sup>3.39</sup></b>	<b>Asn280<sup>7.45</sup></b>
<b>Wild-type</b>	2.5 ± 0.3	89.6 ± 7.8	22.3 ± 10.3	28.7 ± 5.4
<b>D52A<sup>2.50</sup></b>	11.2 ± 0.3*	-	1.1 ± 0.2*	0.0 ± 0.0*
<b>S91A<sup>3.39</sup></b>	1.8 ± 0.2	75.6 ± 5.9	-	25.5 ± 2.9
<b>W246A<sup>6.48</sup></b>	2.5 ± 0.3	51.1 ± 7.9*	17.1 ± 6.2	10.0 ± 4.3*
<b>N280A<sup>7.45</sup></b>	2.6 ± 0.2	67.1 ± 0.7*	12.4 ± 3.1	-
<b>N284A<sup>7.49</sup></b>	2.6 ± 0.1	75.5 ± 7.3	3.8 ± 1.5*	25.6 ± 17.9

RMSF values are means ± SEM of three separate 100 ns simulations.

% interaction occurrence values are means ± SEM of three separate 100 ns simulations.

Significantly different from control with \*  $p < 0.05$  (Student's t-test).

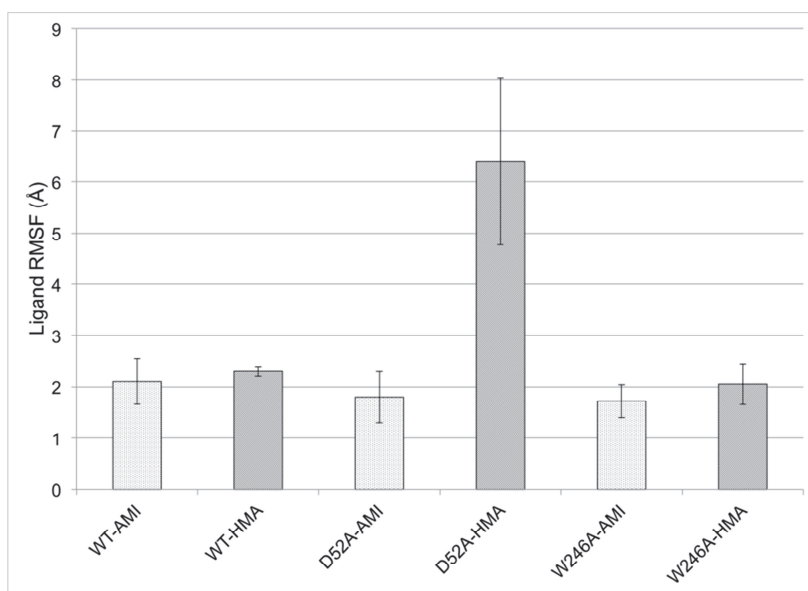


**Figure 6.** Root mean squared fluctuation (RMSF, Y axis, in Ångstrom) of amiloride (AMI, dotted bars) or HMA (gray bars) indicating their mobility in the wild-type (WT) or mutant forms D52A<sup>2.50</sup> and W246A<sup>6.48</sup>. The figures represent data (± SD) combined from three independent simulations of 100 ns.

## Discussion

The sodium ion binding site appears conserved amongst class A GPCRs.<sup>24</sup> Subsequent to the hA<sub>2A</sub>AR the crystal structures of the human protease-activated receptor 1,<sup>25</sup> the  $\beta_1$ -adrenergic receptor,<sup>26, 27</sup> and the human  $\delta$ -opioid receptor<sup>28</sup> further confirmed the common role of this site in the inactive conformation of GPCRs. A sequence comparison of the sodium ion binding site between more distant class A GPCRs shows that individual amino acids may differ, but collectively they apparently maintain the properties to coordinate a sodium ion.

These observations made us examine the residues involved in the hA<sub>2A</sub>AR sodium ion binding site in more detail, through a combined approach of mutational and computational studies. Most importantly, we learned that all mutations in the sodium ion binding pocket impact A<sub>2A</sub> receptor signaling significantly, including both constitutive and agonist-stimulated activity. Although all mutant data in the present study is novel, we have shown a number of similar findings on the wild-type receptor before (Chapter 3 and Lane et al.),<sup>29</sup> indicative of the robustness of the assay system. We will discuss our findings in the light of available mutation data in literature, by examining the mutated amino acids individually. For the search we made use of data available in the GPCRDB.<sup>30</sup>

**Asp<sup>2.50</sup>**. The pronounced effects of mutation of the conserved Asp<sup>2.50</sup> are in agreement with previous studies. Mutation of Asp<sup>2.50</sup> abolished the effect of NaCl on agonist binding in studies on a multitude of GPCRs, for example in the  $\alpha_2$ -adrenergic receptor,<sup>31</sup> dopamine D<sub>2</sub>,<sup>32</sup> adenosine A<sub>1</sub>,<sup>33</sup> adenosine A<sub>3</sub>,<sup>34</sup> and  $\delta$ -opioid receptors.<sup>28</sup> In MD simulations of the wild-type hA<sub>2A</sub>AR Asp52<sup>2.50</sup> dominated coordination of the sodium ion (Chapter 3). Mutation of Asp<sup>2.50</sup> is known to silence signaling in many GPCRs.<sup>5</sup> The migration of the sodium ion to Glu13<sup>1.39</sup> and His278<sup>7.43</sup> agrees with the involvement of these amino acids in sodium ion allostereism observed previously by Gao et al.<sup>35</sup> From a reversed perspective, this simulation could envisage a pathway for the entrance of the sodium ion, which should occur from the extracellular side according to the physiological gradient,<sup>6, 36</sup> and where residue Glu13<sup>1.39</sup>, conserved in all adenosine receptors, could stabilize such a pathway. The enhancement of agonist binding to the D52A<sup>2.50</sup> mutant at high (1 M) concentrations of NaCl suggests that binding of the ion to alternative sites may produce further allosteric effects, different from the effects on wild-type Asp52<sup>2.50</sup>.

The affinities of amiloride and HMA were 10 – 20-fold decreased on the Asp52<sup>2,50</sup> mutant receptor (Tables 2 and 3), strongly suggesting that the positively charged guanidinium moiety of the compounds interacts with the negatively charged aspartic acid. A more modest, 4-fold, decrease in affinity for an amiloride derivative has been reported for the D<sub>4</sub> dopamine receptor by mutation D<sup>2,50</sup>N.<sup>37</sup> In adenosine A<sub>3</sub> and α<sub>2</sub>-adrenergic receptors affinities of amiloride and its derivatives were largely undisturbed by mutation D<sup>2,50</sup>N,<sup>31, 34</sup> suggesting that the more drastic mutation to Ala in the current study more precisely revealed the importance of this residue for amiloride binding.

**Trp<sup>6,48</sup>.** It appeared that sodium ions and agonist NECA can bind simultaneously to the W246A<sup>6,48</sup> receptor (Figure 3A), in contrast with the *wild-type* receptor where NECA and sodium ion binding are mutually exclusive (Chapter 3). Conversely, mutant W246A<sup>6,48</sup> augmented the positive effect of sodium ions on antagonist ZM-241,385 binding (Figure 3B). It seems that Trp246<sup>6,48</sup> may clash with both agonists and antagonists in the orthosteric pocket, as the absence of this residue has a positive effect on binding of both agonists and antagonists in presence of the sodium ion. Trp<sup>6,48</sup>, conserved in many GPCRs, has long been suggested to act as a “toggle switch” in receptor activation,<sup>38</sup> but has never been studied in the context of allosteric modulation by sodium ions. It has been mutated to both Phe and Ala in the human adenosine A<sub>3</sub> receptor, being the closest homolog to the A<sub>2A</sub> receptor.<sup>34, 39</sup> Interestingly, agonist binding was hardly affected by these mutations, whereas antagonists showed a modest decrease in affinity. Receptor activation, however, was largely impeded, seemingly more than our current findings on the A<sub>2A</sub> receptor (see e.g. Figure 4).

Remarkably, the affinities for amiloride and HMA were strongly increased on this mutant (Tables 2 and 3), suggesting that the wild-type tryptophan creates a substantial steric strain for the binding of amilorides. In the adenosine A<sub>3</sub> receptor the W<sup>6,48</sup>A mutation increased HMA potency on agonist binding as well.<sup>34</sup> The mobility of amiloride and HMA was unaffected by the W246A<sup>6,48</sup> mutation (Figure 6), which indicates that the weakened polar interactions (Supplemental Figure S2) are compensated by the absence of steric strain with Trp246<sup>6,48</sup> in this mutant. The collision of the bulkier azepane group of HMA with Trp246<sup>6,48</sup> in the wild-type receptor may result in a loosened interaction with the receptor, which explains HMA's increased mobility by mutation D52A<sup>2,50</sup> compared to



amiloride. In Chapter 3, the more substantial steric clash of HMA with Trp246<sup>6,48</sup> compared to amiloride had been observed as well.

**Ser<sup>3,39</sup>, Asn<sup>7,45</sup>, and Asn<sup>7,49</sup>**. In the wild-type receptor the sodium ion alternates direct interactions with Ser91<sup>3,39</sup> and Asn280<sup>7,45</sup> in two distinct resonance positions, as predicted in MD simulations (Table 5 and Chapter 3), while maintaining contact with Asp52<sup>2,50</sup>. This is in agreement with the observation that sodium ion modulation of agonist binding is not completely abolished in mutant receptors S91A<sup>3,39</sup> and N280A<sup>7,45</sup> (Figure 3A), and that the two remaining residues in mutants S91A<sup>3,39</sup> and N280A<sup>7,45</sup> (Asp52<sup>2,50</sup>, and Asn280<sup>7,45</sup> or Ser91<sup>3,39</sup>, respectively) still interact directly with the sodium ion, although less than in the wild-type receptor (Table 5). Jiang et al. had found that the same S91A mutation did not affect orthosteric ligand binding very much,<sup>40</sup> even less so than the slight decrease in affinity in our experiments (Table 1). In the adenosine A<sub>1</sub> receptor however, orthosteric ligand binding could not be detected for this mutation, maybe due to lack of expression.<sup>33</sup>

In mutant N284A<sup>7,49</sup> sodium ion modulation of agonist binding was completely abolished (Figure 3A). In the antagonist-bound inactive conformation of the receptor, Asn284<sup>7,49</sup> might improve sodium ion coordination through stabilization of the side chain of Asp52<sup>2,50</sup>, explaining the disruption of sodium ion binding by mutation N284A<sup>7,49</sup>. The same role of Asn<sup>7,49</sup> in stabilization of Asp<sup>2,50</sup> was proposed previously in e.g., the histamine H<sub>1</sub> and thyrotropin receptors.<sup>41, 42</sup> At the same time, in the agonist-bound structure of the A<sub>2A</sub>AR residues Asn280<sup>7,45</sup> and Asn284<sup>7,49</sup> form a hydrogen bond, possibly stabilizing the collapsed state of the pocket that excludes sodium ion binding.<sup>8, 43</sup> Consequently, mutations N280A<sup>7,45</sup> and N284A<sup>7,49</sup> might facilitate the formation of the uncollapsed state of the sodium ion pocket and shift the receptor away from the active state, even when the sodium ion is not present in its binding site. Our results support this hypothesis, as mutation of either residue decreases agonist affinity drastically, while antagonist affinity is only slightly decreased (Table 1), sodium ions inhibit agonist binding only weakly (N280A<sup>7,45</sup>) or not at all (N284A<sup>7,49</sup>, Figure 3A). In the adenosine A<sub>1</sub> receptor mutation N<sup>7,49</sup>C increased antagonist binding slightly, which could point to a similar mechanism.<sup>44</sup> Moreover, mutation N284A<sup>7,49</sup> abolished agonist activation completely (Table 4). Correspondingly, Asn284<sup>7,49</sup> is part of the highly conserved NPXXY motif, involved in GPCR activation.<sup>38, 45</sup>

Mutants N280A<sup>7.45</sup> and N284A<sup>7.49</sup> generally affected the potencies of amilorides in a positive way, in particular for HMA (Figures 3E, F and Tables 2, 3). According to the binding mode proposed in Chapter 3, the nitrogen atoms in the amide moiety of both asparagines lie close to the guanidinium group of both amilorides coordinated by Asp52<sup>2.50</sup>, yet they only make sporadic H-bond contacts (Supplemental Figure S2). Thus alanine substitutions might indeed facilitate binding of amilorides by avoiding unfavorable polar interactions (Asn280<sup>7.45</sup>) or by allowing more conformational freedom to Asp52<sup>2.50</sup> (Asn284<sup>7.49</sup>), accommodating in particular the bulky HMA and enhancing its binding.

The MD simulations showed only minor effects on the capacity of mutants S91A<sup>3.39</sup>, W246A<sup>6.48</sup>, N280A<sup>7.45</sup>, and N284A<sup>7.49</sup> to bind the sodium ion in the inactive conformation of the receptor. This seems in contrast to the greatly reduced sensitivity of these mutants to physiological concentrations of NaCl (Figure 3A). In addition to the explanations discussed above, an alternative explanation arises from the observation that each of these four side chain annihilations creates additional room for an extra water molecule, thus fulfilling the coordination number of the ion (Supplemental Table S2). This might allow that, in contrast to the wild-type receptor, the mutants also bind the sodium ion in an active receptor conformation, resulting in the observed loss of modulatory effect on agonist binding.

In conclusion, our results show the importance of the sodium ion binding site in orthosteric ligand binding and receptor activity. Mutation D52A<sup>2.50</sup> caused an immediate displacement of the sodium ion to a distant pocket in MD simulations, in agreement with the loss of the modulatory effect in our molecular pharmacology experiments. The effects of the other mutations were varied, but they significantly affected sodium ion modulation of agonist binding and modulation by amilorides of both agonist and antagonist binding. In addition, all mutations influenced receptor activation, particularly by affecting the levels of constitutive and agonist-stimulated activity, emphasizing the importance of the sodium ion binding pocket for the receptor's active conformation(s). These findings imply that because of allostery by sodium ions and amilorides, the sodium ion binding pocket is a prominent player in receptor functionality and ligand affinity. Our study also opens the door to the design of novel synthetic allosteric modulators or bitopic ligands connecting the sodium ion binding site and the orthosteric binding pocket.

## Supplemental information

Supplemental information includes Figures S1 and S2, and Tables S1 and S2, and can be found with this article online at [dx.doi.org/10.1124/mol.114.095737](https://doi.org/10.1124/mol.114.095737)

## Acknowledgments

This work was supported by the Netherlands Organization for Scientific Research - Chemical Sciences (Grant 714.011.001), the Swedish Research Council (Grant 521-2014-2118), the Swedish strategic research program eSSENCE, and the Swedish National Infrastructure for Computing.

## References

1. Rask-Andersen M, Almén MS, and Schiöth HB, *Trends in the exploitation of novel drug targets*. Nat Rev Drug Discovery, 2011. 10(8): p. 579-90.
2. Katritch V, Cherezov V, and Stevens RC, *Structure-function of the G protein-coupled receptor superfamily*. Annu Rev Pharmacol Toxicol, 2013. 53: p. 531-56.
3. Chen JF, Eltzschig HK, and Fredholm BB, *Adenosine receptors as drug targets — what are the challenges?* Nat Rev Drug Discovery, 2013. 12(4): p. 265-86.
4. Liu W, Chun E, Thompson AA, et al., *Structural basis for allosteric regulation of GPCRs by sodium ions*. Science, 2012. 337(6091): p. 232-36.
5. Parker MS, Wong YY, and Parker SL, *An ion-responsive motif in the second transmembrane segment of rhodopsin-like receptors*. Amino Acids, 2008. 35(1): p. 1-15.
6. Selent J, Sanz F, Pastor M, et al., *Induced effects of sodium ions on dopaminergic G-protein coupled receptors*. PLoS Comput Biol, 2010. 6(8): p. e1000884.
7. Ballesteros JA and Weinstein H, *Integrated methods for the construction of three-dimensional models and computational probing of structure-function relations in G protein-coupled receptors*, in *Methods Neurosci*. 1995, Academic Press: San Diego. p. 366-428.
8. Xu F, Wu H, Katritch V, et al., *Structure of an agonist-bound human A<sub>2A</sub> adenosine receptor*. Science, 2011. 332(6027): p. 322-7.
9. Sambrook J, Fritsch EF, and Maniatis T, *Molecular Cloning: A Laboratory Manual*. 2nd ed. 1989, New York: Cold Spring Harbor Laboratory Press.
10. Smith PK, Krohn RI, Hermanson GT, et al., *Measurement of protein using bicinchoninic acid*. Anal Biochem, 1985. 150(1): p. 76-85.
11. Schrödinger LLC, *Maestro, version 9.3*. 2012: New York.
12. Hess B, Kutzner C, van der Spoel D, et al., *GROMACS 4: algorithms for highly efficient, load-balanced, and scalable molecular simulation*. J Chem Theory Comput, 2008. 4(3): p. 435-47.
13. Rodríguez D, Piñeiro A, and Gutiérrez-de-Terán H, *Molecular dynamics simulations reveal insights into key structural elements of adenosine receptors*. Biochemistry, 2011. 50(19): p. 4194-208.
14. Gutiérrez-de-Terán H, Bello X, and Rodriguez D, *Characterization of the dynamic events of GPCRs by automated computational simulations*. Biochem Soc Trans, 2013. 41(1): p. 205-12.

15. Kaminski GA, Friesner RA, Tirado-Rives J, et al., *Evaluation and reparametrization of the OPLS-AA force field for proteins via comparison with accurate quantum chemical calculations on peptides*. J Phys Chem B, 2001. 105(28): p. 6474-87.
16. Schrödinger LLC, *Macromodel, version 9.7*. 2009: New York.
17. Berger O, Edholm O, and Jähnig F, *Molecular dynamics simulations of a fluid bilayer of dipalmitoylphosphatidylcholine at full hydration, constant pressure, and constant temperature*. Biophys J, 1997. 72(5): p. 2002-13.
18. Chakrabarti N, Neale C, Payandeh J, et al., *An iris-like mechanism of pore dilation in the CorA magnesium transport system*. Biophys J, 2010. 98(5): p. 784-92.
19. Berendsen HJC, Postma JPM, Van Gunsteren WF, et al., *Interaction models for water in relation to protein hydration*, in *Intermolecular Forces*, B. Pullman, Editor. 1981, D. Reidel Publishing Company: Dordrecht. p. 331-42.
20. Nose S and Klein ML, *Constant pressure molecular dynamics for molecular systems*. Mol Phys, 1983. 50(5): p. 1055-76.
21. Humphrey W, Dalke A, and Schulten K, *VMD - visual molecular dynamics*. J Mol Graph, 1996. 14(1): p. 33-8.
22. Schrödinger LLC, *The PyMOL Molecular Graphics System, version 1.5.0.4*. New York.
23. Harding MM, *Small revisions to predicted distances around metal sites in proteins*. Acta Crystallogr D Biol Crystallogr, 2006. 62(Pt 6): p. 678-82.
24. Katritch V, Fenalti G, Abola EE, et al., *Allosteric sodium in class A GPCR signaling*. Trends Biochem Sci, 2014. 39(5): p. 233-44.
25. Zhang C, Srinivasan Y, Arlow DH, et al., *High-resolution crystal structure of human protease-activated receptor 1*. Nature, 2012. 492(7429): p. 387-92.
26. Christopher JA, Brown J, Doré AS, et al., *Biophysical fragment screening of the  $\beta_1$ -adrenergic receptor: identification of high affinity arylpiperazine leads using structure-based drug design*. J Med Chem, 2013. 56(9): p. 3446-55.
27. Müller-Gallacher JL, Nehmé R, Warne T, et al., *The 2.1 Å resolution structure of cyanopindolol-bound  $\beta_1$ -adrenoceptor identifies an intramembrane  $\text{Na}^+$  ion that stabilises the ligand-free receptor*. PLoS ONE, 2014. 9(3): p. e92727.
28. Fenalti G, Giguere PM, Katritch V, et al., *Molecular control of  $\delta$ -opioid receptor signalling*. Nature, 2014. 506(7487): p. 191-6.
29. Lane JR, Klein Herenbrink C, Van Westen GJP, et al., *A novel nonribose agonist, LUF5834, engages residues that are distinct from those of adenosine-like ligands to activate the adenosine  $A_{2A}$  receptor*. Mol Pharmacol, 2012. 81(3): p. 475-87.
30. Isberg V, Vroiling B, Van der Kant R, et al., *GPCRDB: an information system for G protein-coupled receptors*. Nucleic Acids Res, 2014. 42(Database issue): p. D422-5.
31. Horstman DA, Brandon S, Wilson AL, et al., *An aspartate conserved among G-protein receptors confers allosteric regulation of  $\alpha_2$ -adrenergic receptors by sodium*. J Biol Chem, 1990. 265(35): p. 21590-5.
32. Neve KA, Cox BA, Henningsen RA, et al., *Pivotal role for aspartate-80 in the regulation of dopamine  $D_2$  receptor affinity for drugs and inhibition of adenylyl cyclase*. Mol Pharmacol, 1991. 39(6): p. 733-9.
33. Barbhaiya H, McClain R, IJzerman AP, et al., *Site-directed mutagenesis of the human  $A_1$  adenosine receptor: influences of acidic and hydroxy residues in the first four transmembrane domains on ligand binding*. Mol Pharmacol, 1996. 50(6): p. 1635-42.
34. Gao ZG, Kim SK, Gross AS, et al., *Identification of essential residues involved in the allosteric modulation of the human  $A_3$  adenosine receptor*. Mol Pharmacol, 2003. 63(5): p. 1021-31.

35. Gao ZG, Jiang Q, Jacobson KA, et al., *Site-directed mutagenesis studies of human A<sub>2A</sub> adenosine receptors: involvement of Glu<sup>13</sup> and His<sup>278</sup> in ligand binding and sodium modulation*. *Biochem Pharmacol*, 2000. 60(5): p. 661-8.
36. Shang Y, LeRouzic V, Schneider S, et al., *Mechanistic insights into the allosteric modulation of opioid receptors by sodium ions*. *Biochemistry*, 2014. 53(31): p. 5140-49.
37. Schetz JA and Sibley DR, *The binding-site crevice of the D<sub>4</sub> dopamine receptor is coupled to three distinct sites of allosteric modulation*. *J Pharmacol Exp Ther*, 2001. 296(2): p. 359-63.
38. Nygaard R, Frimurer TM, Holst B, et al., *Ligand binding and micro-switches in 7TM receptor structures*. *Trends Pharmacol Sci*, 2009. 30(5): p. 249-59.
39. Gao ZG, Chen A, Barak D, et al., *Identification by site-directed mutagenesis of residues involved in ligand recognition and activation of the human A<sub>3</sub> adenosine receptor*. *J Biol Chem*, 2002. 277(21): p. 19056-63.
40. Jiang Q, Van Rhee AM, Kim J, et al., *Hydrophilic side chains in the third and seventh transmembrane helical domains of human A<sub>2A</sub> adenosine receptors are required for ligand recognition*. *Mol Pharmacol*, 1996. 50(3): p. 512-21.
41. Urizar E, Claeysen S, Deupí X, et al., *An activation switch in the rhodopsin family of G protein-coupled receptors: the thyrotropin receptor*. *J Biol Chem*, 2005. 280(17): p. 17135-41.
42. Bakker RA, Jongejan A, Sansuk K, et al., *Constitutively active mutants of the histamine H<sub>1</sub> receptor suggest a conserved hydrophobic asparagine-cage that constrains the activation of class A G protein-coupled receptors*. *Mol Pharmacol*, 2008. 73(1): p. 94-103.
43. Lebon G, Warne T, Edwards PC, et al., *Agonist-bound adenosine A<sub>2A</sub> receptor structures reveal common features of GPCR activation*. *Nature*, 2011. 474(7352): p. 521-25.
44. Dawson ES and Wells JN, *Determination of amino acid residues that are accessible from the ligand binding crevice in the seventh transmembrane-spanning region of the human A<sub>1</sub> adenosine receptor*. *Mol Pharmacol*, 2001. 59(5): p. 1187-95.
45. Rosenbaum DM, Rasmussen SGF, and Kobilka BK, *The structure and function of G-protein-coupled receptors*. *Nature*, 2009. 459(7245): p. 356-63.



# Chapter 5

## **5'-Substituted amiloride derivatives as allosteric modulators binding in the sodium ion pocket of the adenosine A<sub>2A</sub> receptor**

Arnault Massink

Julien Louvel

Ilze Adlere

Corine van Veen

Berend J. H. Huisman

Gabrielle S. Dijksteel

Dong Guo

Eelke B. Lenselink

Benjamin J. Buckley

Hayden Matthews

Marie Ranson

Michael Kelso

Adriaan P. IJzerman

*Journal of Medicinal Chemistry*, 2016, 59(10): 4769-77

## Abstract

The sodium ion site is an allosteric site conserved among many G protein-coupled receptors (GPCRs). Amiloride **1** and 5-(*N,N*-hexamethylene)amiloride **2** (HMA) supposedly bind in this sodium ion site and can influence orthosteric ligand binding. The availability of a high resolution X-ray crystal structure of the human adenosine A<sub>2A</sub> receptor (hA<sub>2A</sub>AR), in which the allosteric sodium ion site was elucidated, makes it an appropriate model receptor for investigating the allosteric site. In this study, we report the synthesis and evaluation of novel 5'-substituted amiloride derivatives as hA<sub>2A</sub>AR allosteric antagonists. The potency of the amiloride derivatives was assessed by their ability to displace orthosteric radioligand [<sup>3</sup>H]4-(2-((7-amino-2-(furan-2-yl)-[1,2,4]triazolo[1,5-*σ*]-[1,3,5]triazin-5-yl)amino)ethyl)phenol ([<sup>3</sup>H]ZM-241,385) from both the wild-type and sodium ion site W246A mutant hA<sub>2A</sub>AR. 4-Ethoxyphenethyl-substituted amiloride **12I** was found to be more potent than both amiloride and HMA, and the shift in potency between the wild-type and mutated receptor confirmed its likely binding to the sodium ion site.



## Introduction

G protein-coupled receptors (GPCRs) are proteins that consist of seven transmembrane helices and reside in cell membranes. They are able to transfer a multitude of signals, conducted by carriers such as light, hormones, and small molecules, from the extracellular environment to the interior of the cell. The superfamily is predicted to contain approximately 800 different receptors, of which a considerable number are yet to be characterized.<sup>1</sup> Approximately 30% to 40% of drugs currently on the market target GPCRs, underlining their importance in physiology and medicine.<sup>2</sup> Most of these drugs are orthosteric ligands that target endogenous ligand-binding sites of GPCRs. However, GPCRs also contain allosteric binding sites, and ligands that bind to these can influence endogenous GPCR signaling. The use of allosteric ligands as drugs has several potential advantages, such as a more specific drug effect in time and location, due to their ability to modulate orthosteric ligand responses.<sup>3,4</sup>

The sodium ion binding site is an allosteric site that is well-conserved among GPCRs. The first X-ray crystal structure of a GPCR containing an allosterically bound sodium ion was of the human adenosine A<sub>2A</sub> receptor (hA<sub>2A</sub>AR),<sup>5</sup> which was followed by several other GPCR structures with a sodium ion.<sup>6-9</sup> At physiological concentrations of sodium ions, approximately 80% of hA<sub>2A</sub>ARs are occupied by the cation, which reduces orthosteric agonist binding (Chapter 3). Mutation of amino acids that make up the sodium ion site changes the activation characteristics of the hA<sub>2A</sub>AR, highlighting the importance of the site for receptor function (Chapter 4).

Amiloride **1** and its derivative 5-(*N,N*-hexamethylene)amiloride **2** (HMA) are known to bind to the sodium ion site of several GPCRs,<sup>10-13</sup> including adenosine receptors.<sup>14, 15</sup> Amiloride and HMA act on other targets as well, such as the enzyme urokinase-type plasminogen activator (uPA).<sup>16, 17</sup> Furthermore, amiloride is used clinically as a potassium-sparing diuretic drug, where its action arises predominantly through blockade of renal epithelial sodium channels (ENaCs).<sup>18</sup> The positively charged guanidinium moiety of amiloride and HMA may explain their propensity to bind to negatively charged target sites and their pharmacological promiscuity more generally. Nevertheless, their affinity for the sodium ion site of GPCRs makes amiloride and its derivatives potentially useful pharmacological tools for probing molecular mechanisms of GPCR activation and regulation, as demonstrated in Chapter 4. The increased affinity of HMA compared to that

of amiloride for the sodium ion site of the hA<sub>2A</sub>AR<sup>14</sup> suggests that there is potential to further elaborate the amiloride core at its 5' position, possibly yielding derivatives with higher potency.

In a study by Matthews et al., several new amiloride derivatives with substituents at the 5' position were found to be active against uPA.<sup>16</sup> In our current study, we tested a selection of these for their activity at the hA<sub>2A</sub>AR by measuring their ability to displace orthosteric radioligand [<sup>3</sup>H]4-(2-((7-amino-2-(furan-2-yl)-[1,2,4]triazolo[1,5-*a*]-[1,3,5]triazin-5-yl)amino)ethyl)phenol ([<sup>3</sup>H]ZM-241,385).<sup>19</sup> After identifying the most potent derivatives, we designed and synthesized novel 5'-substituted amiloride analogues and evaluated their hA<sub>2A</sub>AR activity. From these analogues, compounds were identified that were equipotent or more potent than reference compound HMA.

Compounds were also evaluated using an hA<sub>2A</sub>AR mutant, where the Trp246<sup>6,48</sup> 'toggle switch'<sup>20</sup> (numbering in superscript according to Ballesteros and Weinstein)<sup>21</sup> was replaced by Ala. This tryptophan forms part of the sodium ion pocket, and mutation to alanine has been shown to significantly increase the potency of amiloride and HMA (Chapter 4), making the W246A<sup>6,48</sup> mutant receptor a useful tool for assessing the binding of ligands in the sodium ion pocket. Finally, the most potent derivative was docked into the sodium ion site of the hA<sub>2A</sub>AR crystal structure (PDB: 4E1Y).<sup>5</sup> Comparisons of the binding of compounds to the wild-type and W246A<sup>6,48</sup> mutant receptors and docking of the most potent derivatives into the hA<sub>2A</sub>AR structure provided insights into the molecular interactions occurring between the amiloride derivatives and the sodium ion site.

## Materials and methods

### Materials

[<sup>3</sup>H]ZM-241,385 (50 Ci/mmol) was obtained from ARC Inc. (St. Louis, MO, USA). ZM-241,385<sup>22</sup> was obtained from Ascent Scientific (Bristol, UK). NECA, amiloride, HMA, and bovine serum albumin (BSA) were obtained from Sigma Aldrich (Zwijndrecht, The Netherlands). Adenosine deaminase (ADA) was purchased from Boehringer Mannheim (Mannheim, Germany). Bicinchoninic acid (BCA) and BCA protein assay reagent were obtained from Pierce Chemical Company (Rockford, IL, USA). HEK293 cells stably expressing the hA<sub>2A</sub>AR (HEK293-hA<sub>2A</sub>AR) were a gift from Dr. J. Wang (Biogen/IDEC,

Cambridge, MA, USA). All other chemicals were of analytical grade and obtained from standard commercial sources.

### Chemistry

2-(4-(Allyloxy)phenyl)ethan-1-amine Hydrochloride (20). To a suspension of  $\text{LiAlH}_4$  (41 mmol) in dry THF (20 mL) at 0 °C was added nitro-styrene **19** (2.54 g, 12.4 mmol) slowly. The mixture was stirred at 0 °C for 1 h and then heated at reflux for 2 h. The reaction was cooled to 0 °C and water (6 mL) was added. The mixture was diluted with THF (10 mL) and filtered. The filtrate was extracted with EtOAc/ $\text{H}_2\text{O}$ , and the organic layer was washed with water and dried using  $\text{MgSO}_4$ . The volatiles were removed in vacuo to afford the free amine; HCl (1 M in EtOAc, 5 mL) was added and then evaporated, yielding **20** (1.65 g, 78%) as its HCl salt.  $^1\text{H}$  NMR (400 MHz,  $\text{CD}_3\text{OD}$ ) 7.19 (d,  $J = 8.3$  Hz, 2H), 6.92 (d,  $J = 8.3$  Hz, 2H), 6.11–5.99 (m, 1H), 5.39 ( $\delta$ ,  $J = 17.3$  Hz, 1H), 5.24 (d,  $J = 10.6$  Hz, 1H), 4.53 (d,  $J = 4.7$  Hz, 2H), 3.13 (t,  $J = 7.6$  Hz, 2H), 2.89 (t,  $J = 7.6$  Hz, 2H).

General Procedure for the Synthesis of Compounds 12a-12p. To a solution of **21** (0.3 mmol) and corresponding amine or amine hydrochloride (0.3 mmol) in dry *N,N*-dimethylformamide (DMF) (5 mL) was added DiPEA (0.75 mmol in the case of the free amine or 1.05 mmol in the case of the amine hydrochloride) at room temperature. The resulting reaction mixture was stirred at 100 °C for 1-2 h. Upon reaction completion (TLC), the reaction mixture was cooled to room temperature, poured into ice-water and extracted with AcOEt/ $\text{H}_2\text{O}$ . The organic layer was dried over  $\text{MgSO}_4$  and, after concentration in vacuum, yielded the desired free base of the final compound with a purity of at least 95%. The free base was dissolved in 6 mL of 1 N HCl/AcOEt solution, stirred at room temperature for 2 h, and evaporated to dryness to give the hydrochloride salt of the desired product as a powder (compounds **12a-f**, **h-k**, **n**, and **p**).

The other compounds were further purified by preparative HPLC (using the free base), which was performed on a Shimadzu HPLC-ultraviolet (UV) system with a diode array detector using a Gemini 5  $\mu\text{m}$  C18 110A column (100  $\times$  10 mm, 5  $\mu\text{m}$ ) and a linear gradient from 1 to 99% mobile phase B. Mobile phase A consisted of  $\text{H}_2\text{O}$ , and mobile phase B consisted of  $\text{CH}_3\text{CN}/1\%$  TFA in  $\text{H}_2\text{O}$ . The flow rate was 5 mL/min. The TFA salt of the desired product was obtained as a yellow powder (compounds **12g**, **l-m**, and **o**).

3-Amino-N-carbamimidoyl-6-chloro-5-((2,3-dihydro-1H-inden-2-yl)amino)pyrazine-2-carboxamide Hydrochloride (12a). Yield = 67%. <sup>1</sup>H NMR (400 MHz, DMSO-d<sub>6</sub>): δ 10.64 (s, 1H), 8.61 (br s, 2H), 8.44 (br s, 2H), 8.02 (d, *J* = 7.2 Hz, 1H), 7.58 (br s, 2H), 7.23–7.14 (m, 4H), 4.87–4.77 (X part of ABX system, sextet, *J* = 8.0 Hz, 1H), 3.62 (A part of ABX system, dd, *J* = 16.0, 7.6 Hz, 2H), 3.06 (B part of ABX system, dd, *J* = 15.6, 8.0 Hz, 2H). ESI-MS *m/z*: 346.13 [M+H]<sup>+</sup>; *t<sub>R</sub>* = 7.38 min.

## Biology

HEK293 cells were grown in culture medium consisting of Dulbecco's modified Eagle's medium (DMEM) supplemented with 10% newborn calf serum (NCS), 50 µg/ml streptomycin and 50 IU/ml penicillin at 37 °C and 7% CO<sub>2</sub>. Cells were subcultured twice a week at a ratio of 1:20 on 10 cm ø plates. A point mutation corresponding to W246A<sup>6,48</sup> was introduced into the wild-type hA<sub>2A</sub>AR-plasmid DNA (FLAG-tag at the N-terminus, in pcDNA3.1) by BaseClear (Leiden, The Netherlands). Cells were transfected with 1 µg per plate of the resulting plasmid using the calcium phosphate precipitation method.<sup>23</sup> HEK293 cells stably expressing the wild-type receptor were grown in the same medium but with the addition of G-418 (200 µg/ml).

Membranes were prepared as follows. HEK293 cells were detached from plates 48 h after transfection (cells transiently expressing hA<sub>2A</sub>AR-W246A<sup>6,48</sup>) or from confluent plates (cells stably expressing hA<sub>2A</sub>AR-WT) by scraping them into 5 ml PBS, collected and centrifuged at 700 g (3000 rpm) for 5 min. Pellets derived from 20 plates were pooled and resuspended in 16 ml of ice-cold assay buffer (50 mM Tris-HCl, pH 7.4). An Ultra-Turrax was used to homogenize the cell suspension. Membranes and the cytosolic fraction were separated by centrifugation at 100000 g (31000 rpm) in a Beckman Optima LE-80K ultracentrifuge at 4 °C for 20 min. The pellet was resuspended in 8 ml of Tris buffer, and the homogenization and centrifugation steps were repeated. Assay buffer (4 ml) was used to resuspend the pellet, and adenosine deaminase (ADA) was added (0.8 IU/ml) to break down endogenous adenosine. Membranes were stored in 250 µL aliquots at -80 °C. Membrane protein concentrations were measured using the BCA method.<sup>24</sup>

For [<sup>3</sup>H]ZM-241,385 displacement binding experiments membranes with stably expressed hA<sub>2A</sub>AR-WT (15 µg of total protein) or with transiently expressed hA<sub>2A</sub>AR-W246A<sup>6,48</sup> (4 µg) were used. These protein amounts ensured that total binding to the membrane preparations was less than 10% of the total radioactivity added in order to

prevent radioligand depletion. Membrane aliquots were incubated in a total volume of 100  $\mu\text{l}$  of assay buffer at 25 °C for 2 h. [ $^3\text{H}$ ]ZM-241,385 was used at a concentration of 2.5 nM. Total binding was determined in the presence of [ $^3\text{H}$ ]ZM-241,385 without addition of other compounds. Nonspecific binding was determined in the presence of 100  $\mu\text{M}$  NECA ( $\text{hA}_{2\text{A}}\text{AR-WT}$ ) or 10  $\mu\text{M}$  ZM-241,385 ( $\text{hA}_{2\text{A}}\text{AR-W246A}^{6,48}$ ) and represented less than 10% of the total binding. For single-point assays, radioligand displacement experiments were performed in the presence or absence of 10  $\mu\text{M}$  amiloride **1**, HMA **2**, or compounds **3-18**. For concentration-effect curves, radioligand displacement experiments were performed in the absence or presence of increasing concentrations of HMA **2** or **12h, i, k, or l**. For radioligand dissociation experiments, membrane preparations were first allowed to reach binding equilibrium with [ $^3\text{H}$ ]ZM-241,385 for 1 h at 4 °C. Dissociation was started by addition of 100  $\mu\text{M}$  NECA with or without 100  $\mu\text{M}$  HMA **2** or **12h, i, k, or l** ( $\text{hA}_{2\text{A}}\text{AR-WT}$ ), or addition of 10  $\mu\text{M}$  ZM-241,385 with or without 10  $\mu\text{M}$  HMA **2** or **12h, i, k, or l** ( $\text{hA}_{2\text{A}}\text{AR-W246A}^{6,48}$ ) at each time point. The time points were distributed over 180 min ( $\text{hA}_{2\text{A}}\text{AR-WT}$ ) or 30 min ( $\text{hA}_{2\text{A}}\text{AR-W246A}^{6,48}$ ). Incubations were terminated by rapid vacuum filtration to separate the bound radioligand from free radioligand through 96-well GF/B filter plates using a Filtermate-harvester (PerkinElmer Life Sciences). Filters were subsequently washed three times with ice-cold assay buffer. The filter-bound radioactivity was determined by scintillation spectrometry using a PE 1450 Microbeta Wallac Trilux scintillation counter (PerkinElmer Life Sciences).

The radioligand binding data was analyzed with GraphPad Prism 5.0 (GraphPad Software Inc., San Diego, CA, USA). The displacement curves were fitted to a one-state site binding model, and the dissociation curves were fitted to a one-phase dissociation model. A one-way ANOVA with Dunnett's post hoc test was performed to test for significant differences.

### Computational receptor modeling

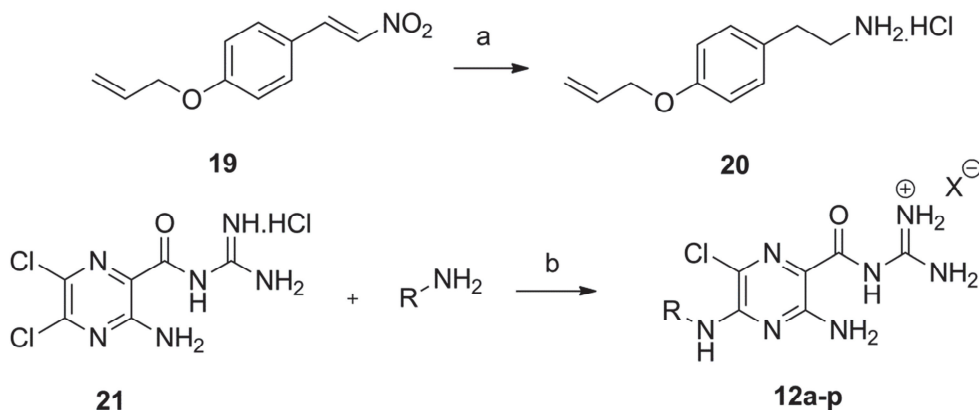
All structure-based studies were performed in the Schrödinger suite.<sup>25</sup> The inactive structure of the  $\text{A}_{2\text{A}}\text{AR}$  in complex with ZM-241,385 and a sodium ion (PDB: 4E1Y)<sup>5</sup> was used as the basis for docking. Docking of **12h, i, k, and l** was based on the docking pose of HMA described in Chapter 3. To allow for side chain rearrangements, we used core-constrained docking (with the guanidinium moiety as the core) with a decreased van der Waals (vdW) sphere (0.5 instead of 0.8). The vdW sphere was decreased to allow for an

induced fit in the sodium pocket. Subsequently, we optimized this pose using an exhaustive hierarchical optimization procedure available in Prime,<sup>26</sup> which has been used previously to model induced fit effects.<sup>27</sup> Figures were rendered using PyMol.<sup>28</sup>

## Results

### Chemistry

The synthesis of compounds **3–18** has been described previously.<sup>16</sup> New compounds **12a-p** were synthesized in a similar manner, through addition of the appropriate phenethylamine onto the amiloride core **21** in the presence of base (Scheme 1). The compounds were obtained as hydrochloride or trifluoroacetate salts depending on the purification method employed. Amine hydrochloride salt **20**, which has not been previously described, was synthesized by reducing nitrostyrene **19**<sup>29</sup> with LiAlH<sub>4</sub> followed by treatment with HCl.<sup>30</sup>



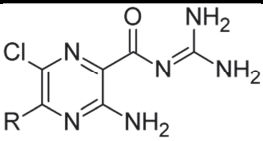
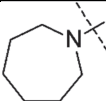
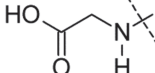
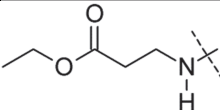
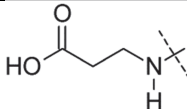
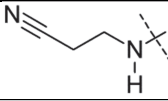
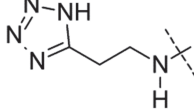
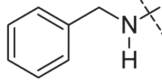
**Scheme 1. Synthesis of phenethyl amiloride derivatives 12a-p.** Reagents and conditions: a) i. LiAlH<sub>4</sub>, THF, 0 °C to 76 °C, 2 h, ii. HCl, 78%; b) i. DiPEA, DMF, 100 °C, ii. HCl (X<sup>-</sup> = Cl<sup>-</sup>) or prep HPLC purification (X<sup>-</sup> = CF<sub>3</sub>CO<sub>2</sub><sup>-</sup>), 1–75%.

## Biology and structure-activity relationships

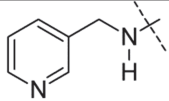
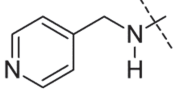
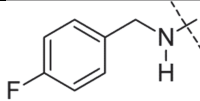
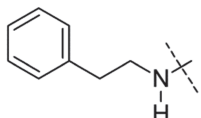
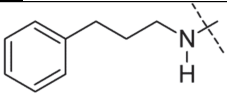
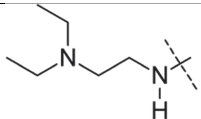
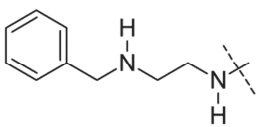
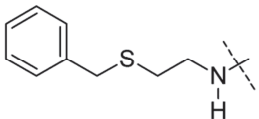
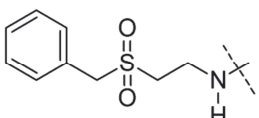
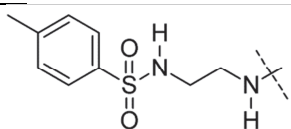
Single point displacement assays were performed in which [<sup>3</sup>H]ZM-241,385 binding to the hA<sub>2A</sub>AR was displaced by 10 μM of compounds **1–18** (Table 1) and **12a–p** (Table 2). Reference compounds amiloride **1** and HMA **2** displaced [<sup>3</sup>H]ZM-241,385 binding from the wild-type receptor by 29 % and 70 %, respectively, and from the W246A<sup>6.48</sup> mutant receptor by 89 % and 98 %. Of amiloride derivatives **3–18**, compounds **3–5**, **7**, **8**, **10**, **11**, and **14–18** displaced less [<sup>3</sup>H]ZM-241,385 than amiloride at both the wild-type and W246A<sup>6.48</sup> receptors. Carboxylate derivatives **3** and **5**, and tetrazole **7** showed no or marginal displacement of [<sup>3</sup>H]ZM-241,385 from both receptors. Carboxylate ester **4** and diethylamino-ethyl derivative **14** showed negligible displacement of [<sup>3</sup>H]ZM-241,385 binding from the wild-type receptor, but they displaced approximately one-half of [<sup>3</sup>H]ZM-241,385 binding from the W246A<sup>6.48</sup> mutant. Nitrile derivative **6** displaced slightly more [<sup>3</sup>H]ZM-241,385 binding from the wild-type receptor (35%) than amiloride, but it displaced less than amiloride at the W246A<sup>6.48</sup> receptor (83%). Benzylic derivatives **8–11** did not or marginally displaced [<sup>3</sup>H]ZM-241,385 binding from the wild-type receptor, except for 3-pyridyl derivative **9**, which performed similarly to amiloride. However, compounds **8**, **9**, and **11** were able to displace [<sup>3</sup>H]ZM-241,385 binding from the mutant receptor by approximately 80% (benzyl **8**) and 50% (3-pyridyl **9** and 4-fluorobenzyl **11**). 4-Pyridyl derivative **10** showed minor radioligand displacement at the mutated receptor.

Extension of the carbon chain to phenylethyl derivative **12** yielded the largest decrease in orthosteric [<sup>3</sup>H]ZM-241,385 binding to both the wild-type (46%) and W246A<sup>6.48</sup> mutant (99%) receptors. Further extension of the carbon chain to phenylpropyl derivative **13** produced slightly lower reductions in [<sup>3</sup>H]ZM-241,385 binding to the wild-type (40%) and mutant (91%) receptors relative to that with **12**. Increased linker sizes and inclusion of heteroatoms (compounds **15–18**) marginally displaced [<sup>3</sup>H]ZM-241,385 binding from the wild-type receptor. However, these compounds were able to displace [<sup>3</sup>H]ZM-241,385 binding from the W246A<sup>6.48</sup> mutant receptor by approximately 80% (sulfone **17**), 65% (sulfide **16** and sulfonamide **18**), and 35% (amine **15**).

**Table 1. hA<sub>2A</sub>AR binding of amiloride derivatives.** % [<sup>3</sup>H]ZM-241,385 binding to the hA<sub>2A</sub>AR-WT and -W246A<sup>6,48</sup> in the presence of 10 μM amiloride **1**, HMA **2**, or amiloride derivatives **3-18**. The concentration of [<sup>3</sup>H]ZM-241,385 was 2.5 nM. 100 % [<sup>3</sup>H]ZM-241,385 binding was determined in the absence of any amiloride, while 0 % binding was determined as nonspecific binding of [<sup>3</sup>H]ZM-241,385 assessed in the presence of 100 μM NECA (WT) or 10 μM ZM-241,385 (W246A<sup>6,48</sup>). Values are means ± standard error of mean (SEM) of at least three independent assays performed in duplicate.

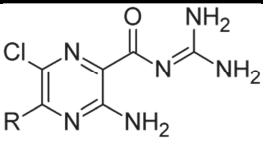
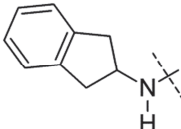
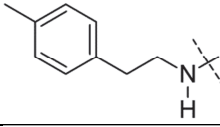
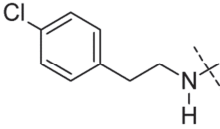
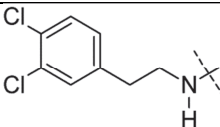
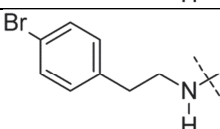
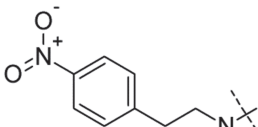
			
Compound	R	% [ <sup>3</sup> H]ZM-241,385 binding ± SEM to hA <sub>2A</sub> AR in the presence of 10 μM compound	
		WT	W246A <sup>6,48</sup>
Amiloride <b>1</b>	NH <sub>2</sub>	71 ± 2	11 ± 1
HMA <b>2</b>		30 ± 2	1.8 ± 0.3
<b>3</b>		88 ± 1	111 ± 9
<b>4</b>		87 ± 7	48 ± 10
<b>5</b>		96 ± 3	70 ± 9
<b>6</b>		65 ± 3	17 ± 3
<b>7</b>		99 ± 4	101 ± 2
<b>8</b>		77 ± 4	21 ± 4



9		$71 \pm 3$	$46 \pm 3$
10		$87 \pm 4$	$73 \pm 4$
11		$96 \pm 6$	$48 \pm 5$
12		$54 \pm 3$	$1.1 \pm 0.4$
13		$60 \pm 2$	$9.0 \pm 1.9$
14		$85 \pm 3$	$53 \pm 7$
15		$90 \pm 3$	$65 \pm 8$
16		$84 \pm 3$	$35 \pm 2$
17		$82 \pm 4$	$18 \pm 2$
18		$85 \pm 3$	$32 \pm 5$

After observing increased potency with phenylethyl derivative **12**, we synthesized and tested compounds **12a-p** carrying different substituents on the phenyl moiety (Table 2). Compounds **12a**, **12c-g**, and **12n-p** displaced less [<sup>3</sup>H]ZM-241,385 binding than **12** from both the wild-type and W246A<sup>6,48</sup> mutant hA<sub>2A</sub>AR. These derivatives performed similarly to amiloride at the wild-type receptor, whereas they performed better at the mutated receptor, with close to 100% radioligand displacement, with the exception of 4-chlorophenethyl derivative **12c** and 3,4-dichlorophenethyl derivative **12d**, which caused minor displacement of [<sup>3</sup>H]ZM-241,385 binding from the wild-type receptor (8% and 18%, respectively) and the lowest, although significant, displacement from the mutated receptor (68% and 89%, respectively) of the phenethyl derivatives. Compared to parent **12**, 2-(*p*-tolyl)ethyl derivative **12b** displaced similar amounts of radioligand from the wild-type and W246A<sup>6,48</sup> receptors. 4-Bromo **12e**, 4-nitro **12f**, and 4-hydroxy **12g** substituted phenethyl derivatives showed lower activity than **12** at both the wild-type and mutant receptors. Ether substituted phenethyl derivatives **12h-m** displaced more radioligand than **12** from the wild-type receptor, and reached close to 100% radioligand displacement at the W246A<sup>6,48</sup> receptor. 4-Methoxyphenethyl derivative **12h** displaced 69% of radioligand binding from the wild-type receptor, thus performing similarly to HMA, whereas changing the methoxy position to give 3-methoxyphenethyl derivative **12i** resulted in less radioligand displacement (59%). Addition of a second methoxy group, as in 3,4-dimethoxyphenethyl derivative **12j**, decreased radioligand displacement from the wild-type receptor even more (49%). Dioxolyl derivative **12k** increased radioligand displacement from the wild-type receptor (65%), bringing its effect close to that of HMA. Elongation of **12h** by a methyl group resulting in 4-ethoxyphenethyl derivative **12l** yielded the most effective amiloride derivative of this series, reducing [<sup>3</sup>H]ZM-241,385 binding from the wild-type receptor by 73%. Further elongation of the ethoxy substituent to give 4-(allyloxy)phenethyl derivative **12m** decreased radioligand displacement again, whereas the even bulkier ether substituted phenethyl derivatives **12n-p** displaced less radioligand than **12**.

**Table 2. hA<sub>2A</sub>AR binding of amiloride phenethyl substituted derivatives.** % [<sup>3</sup>H]ZM-241,385 binding to the hA<sub>2A</sub>AR-WT and -W246A<sup>6,48</sup> in the presence of 10 μM amiloride derivatives **12a-p**. The concentration of [<sup>3</sup>H]ZM-241,385 was 2.5 nM. 100 % [<sup>3</sup>H]ZM-241,385 binding was determined in the absence of any amiloride, while 0 % binding was determined as nonspecific binding of [<sup>3</sup>H]ZM-241,385 assessed in the presence of 100 μM NECA (WT) or 10 μM ZM-241,385 (W246A<sup>6,48</sup>). Values are means ± standard error of mean (SEM) of at least three independent assays performed in duplicate.

			
Compound	R	% [ <sup>3</sup> H]ZM-241,385 binding ± SEM to hA <sub>2A</sub> AR in the presence of 10 μM compound	
		WT	W246A <sup>6,48</sup>
<b>12a</b>		68 ± 3	6.6 ± 0.3
<b>12b</b>		50 ± 3	2.1 ± 0.2
<b>12c</b>		92 ± 2	32 ± 1
<b>12d</b>		82 ± 1	11 ± 1
<b>12e</b>		67 ± 4	4.8 ± 1.0
<b>12f</b>		68 ± 2	5.8 ± 0.5

<b>12g</b>		$72 \pm 2$	$9.5 \pm 0.8$
<b>12h</b>		$31 \pm 1$	$-0.4 \pm 0.1$
<b>12i</b>		$41 \pm 2$	$5.4 \pm 1.0$
<b>12j</b>		$51 \pm 2$	$1.8 \pm 0.5$
<b>12k</b>		$35 \pm 2$	$1.0 \pm 0.6$
<b>12l</b>		$27 \pm 1$	$3.5 \pm 0.2$
<b>12m</b>		$43 \pm 2$	$2.2 \pm 0.6$
<b>12n</b>		$66 \pm 2$	$3.4 \pm 0.8$
<b>12o</b>		$75 \pm 2$	$4.0 \pm 0.3$
<b>12p</b>		$63 \pm 2$	$5.2 \pm 0.3$

The binding of the four most potent phenethyl derivatives, **12h**, **i**, **k**, and **l**, was characterized further by establishing their IC<sub>50</sub> values in full curve assays for both receptors (Table 3). 4-Ethoxyphenethyl derivative **12l** had the highest potency at displacing [<sup>3</sup>H]ZM-241,385 binding from the wild-type hA<sub>2A</sub>AR, showing an IC<sub>50</sub> value of 3.4 μM, which was lower than HMA (5.1 μM, Table 3). 4-Methoxyphenethyl derivative **12h** and dioxolyl derivative **12k** showed similar potencies compared to that of HMA, whereas 3-methoxyphenethyl derivative **12i** showed lower potency (8.1 μM) for radioligand displacement from the wild-type hA<sub>2A</sub>AR. For the W246A<sup>6,48</sup> mutant hA<sub>2A</sub>AR, compounds **12h**, **k**, and **l** showed increased potencies compared to that of HMA, whereas **12i** showed similar potency. The fold change in potency for W246A<sup>6,48</sup> compared to the wild-type receptor was 19-fold for HMA, approximately 35-fold for methoxyphenethyl derivatives **12h** and **i**, and approximately 80-fold for the dioxolyl **12k** and 4-ethoxyphenethyl **12l** derivatives.

**Table 3. hA<sub>2A</sub>AR affinities of selected amiloride derivatives.** IC<sub>50</sub> values for the displacement of [<sup>3</sup>H]ZM-241,385 binding to the hA<sub>2A</sub>AR-WT and -W246A<sup>6,48</sup> by HMA **2** and phenethyl amiloride derivatives **12h**, **i**, **k**, and **l**. The concentration used of [<sup>3</sup>H]ZM-241,385 was 2.5 nM. Nonspecific binding was determined in the presence of 100 μM NECA (WT) or 10 μM ZM-241,385 (W246A<sup>6,48</sup>). Values are means ± SEM of at least three independent assays performed in duplicate.

	<b>[<sup>3</sup>H]ZM-241,385 displacement from hA<sub>2A</sub>AR</b>		
	<b>WT</b>	<b>W246A<sup>6,48</sup></b>	
	<b>IC<sub>50</sub> ± SEM (μM)</b>	<b>IC<sub>50</sub> ± SEM (μM)</b>	<b>Fold change to WT<sup>a</sup></b>
<b>HMA 2</b>	5.1 ± 0.2	0.27 ± 0.04	19
<b>12h</b>	4.4 ± 0.4	0.12 ± 0.01**	37
<b>12i</b>	8.1 ± 0.9*	0.25 ± 0.05	32
<b>12k</b>	5.6 ± 0.8	0.07 ± 0.01***	80
<b>12l</b>	3.4 ± 0.6*	0.05 ± 0.00***	76

<sup>a</sup> Change in fold IC<sub>50</sub> of wild-type over W246A<sup>6,48</sup>.

One-way ANOVA with Dunnett's post hoc test performed against HMA on log IC<sub>50</sub> values, with \* p < 0.05, \*\* p < 0.01, and \*\*\* p < 0.001.

The effect of saturating concentrations of HMA and compounds **12h**, **i**, **k**, and **l** on the dissociation characteristics (residence time) of [<sup>3</sup>H]ZM-241,385 from the wild-type and W246A<sup>6.48</sup> hA<sub>2A</sub>AR was examined next (Table 4 and Figure 1). HMA had the largest effect on the dissociation velocity of [<sup>3</sup>H]ZM-241,385 from the wild-type hA<sub>2A</sub>AR, producing a 2.2-fold decrease in its residence time (1/k<sub>off</sub>). Methoxyphenethyl derivatives **12h** and **i**, and 4-ethoxyphenethyl derivative **12l** decreased residence time by approximately 1.5-fold. In the case of dioxolyl derivative **12k**, the effect on the residence time was lost at the wild-type receptor. At the W246A<sup>6.48</sup> hA<sub>2A</sub>AR, HMA, **12h**, and **12l** showed similar effects as those at the wild-type receptor, producing 1.9-, 1.3-, and 2.1-fold decreases in residence time, respectively. In contrast, the effect of 3-methoxyphenethyl derivative **12i** and dioxolyl derivative **12k** increased significantly at the W246A<sup>6.48</sup> mutant receptor, where 3.4- and 2.3-fold decreases in residence time of [<sup>3</sup>H]ZM-241,385, respectively, were observed.

**Table 4. Effect of amiloride derivatives on residence time of [<sup>3</sup>H]ZM-241,385.** Residence times of [<sup>3</sup>H]ZM-241,385 dissociating from hA<sub>2A</sub>AR-WT and -W246A<sup>6.48</sup> in the absence (control) or presence of 100 μM (WT) or 10 μM (W246A<sup>6.48</sup>), i.e. saturating concentrations, of HMA **2** or amiloride derivatives **12h**, **i**, **k**, or **l**. The concentration of [<sup>3</sup>H]ZM-241,385 was 2.5 nM. Nonspecific binding was determined in the presence of 100 μM NECA (WT) or 10 μM ZM-241,385 (W246A<sup>6.48</sup>). Values are means ± SEM of at least three independent assays performed in duplicate.

	<b>[<sup>3</sup>H]ZM-241,385 dissociation from hA<sub>2A</sub>AR</b>	
	<b>Residence time (min)</b>	
	<b>WT</b>	<b>W246A<sup>6.48</sup></b>
Control	61 ± 4	2.8 ± 0.4
+ HMA <b>2</b>	28 ± 2***	1.4 ± 0.2**
+ <b>12h</b>	44 ± 3**	2.0 ± 0.5
+ <b>12i</b>	42 ± 5*	0.8 ± 0.3**
+ <b>12k</b>	61 ± 5	1.2 ± 0.5*
+ <b>12l</b>	40 ± 1**	1.3 ± 0.3*

One-way ANOVA with Dunnett's post hoc test against control, with \* p < 0.05, \*\* p < 0.01, and \*\*\* p < 0.001.

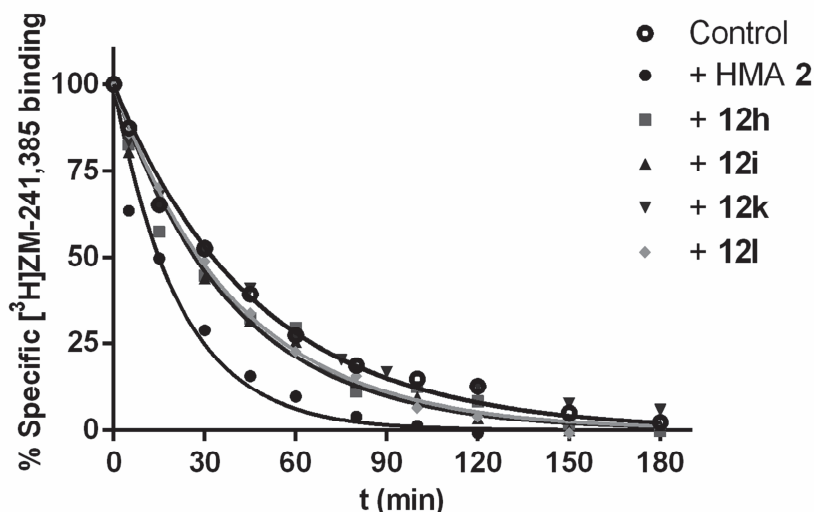


**Figure 1.** [ $^3\text{H}$ ]ZM-241,385 dissociation from the  $\text{hA}_{2\text{A}}\text{AR-WT}$  in absence (control) or presence of 100  $\mu\text{M}$  of HMA **2** or amiloride derivatives **12h**, **i**, **k**, or **l**. After allowing [ $^3\text{H}$ ]ZM-241,385 to bind to its target, the dissociation was induced by addition of 100  $\mu\text{M}$  NECA together with 100  $\mu\text{M}$  of the respective compounds. Graph shows mean values of one representative dissociation experiment performed in duplicate.

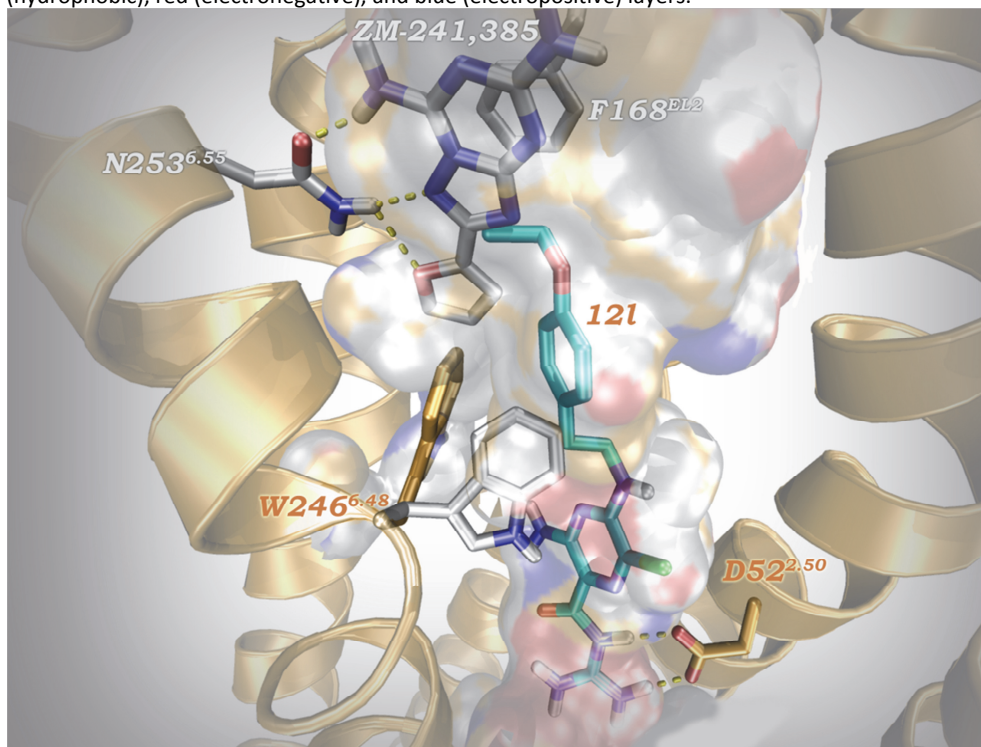
### Docking study

The most potent amiloride derivatives, **12h**, **i**, **k**, and **l** were docked into the sodium ion binding site of the  $\text{hA}_{2\text{A}}\text{AR}$  X-ray cocrystal structure bearing orthosteric ligand ZM-241,385 (Figures 2 and S1-S3, PDB: 4E1Y).<sup>5</sup> The cores of these amiloride derivatives were predicted to adopt binding poses similar to those of amiloride and HMA observed in Chapter 3 (Figure S1). The hydrogen bonding and salt bridge interactions with Asp52<sup>2,50</sup> and Thr88<sup>3,36</sup> were predicted similarly for the novel derivatives and HMA. Furthermore, **12h**, **i**, **k**, and **l** were predicted to occupy Trp246<sup>6,48</sup> position, forcing it to adopt a different rotameric position, as was observed previously for amiloride and HMA in Chapter 3.

However, the interactions with Trp246<sup>6,48</sup> were predicted to be different for each amiloride derivative. Whereas for HMA no  $\pi$ - $\pi$  stacking was predicted,  $\pi$ - $\pi$  stacking was predicted between Trp246<sup>6,48</sup> and the phenyl group of **12h**, **i**, and **k**, and a second  $\pi$ - $\pi$  stacking interaction was predicted with the pyrazine core of **12i**. Furthermore, the phenethyl moieties of the novel derivatives were predicted to intrude a hydrophobic pocket not reached by the azepane moiety of HMA. Compared to HMA, the phenethyl

substitutions were predicted to be in a 4 Å range of three to four additional hydrophobic residues, specifically Phe168<sup>EL2</sup>, Met177<sup>5.38</sup>, Leu249<sup>6.51</sup> (**12h**, **i**, **k**, and **l**), and Ile274<sup>7.39</sup> (**12i** and **l**) (Figures S1 and S2). In addition, the dioxolyl and ethoxy substituents of compounds **12k** and **l** were predicted to be in the vicinity of Asn253<sup>6.55</sup> (Figure S2). Residues Phe168<sup>EL2</sup>, Met177<sup>5.38</sup>, Leu249<sup>6.51</sup>, Asn253<sup>6.55</sup>, and Ile274<sup>7.39</sup> are part of the orthosteric binding site, and their predicted vicinity to these residues indicates that **12h**, **i**, **k**, and **l** can intrude the orthosteric site and displace orthosteric ligand ZM-241,385 in a direct, competitive manner.

**Figure 2.** Docking of compound **12l** into the sodium ion binding site of wild-type hA<sub>2A</sub>AR (PDB: 4EIY).<sup>5</sup> Compound **12l** is represented by cyan colored sticks, and ZM-241,385 in the orthosteric site is represented by grey sticks. Trp246<sup>6.48</sup> is represented by transparent white sticks (crystal structure position) and yellow sticks (proposed rotamer with **12l** docked in the sodium ion site). Oxygen and nitrogen atoms are represented in red and blue, respectively. The local protein backbone is represented by yellow ribbons, and relevant binding site confinements are indicated by white-grey (hydrophobic), red (electronegative), and blue (electropositive) layers.





## Discussion

Amiloride and HMA act as allosteric modulators of several GPCRs,<sup>10</sup> including  $\alpha_2$  adrenergic receptors,<sup>11</sup> dopamine receptors,<sup>12</sup> and the gonadotropin-releasing hormone receptor.<sup>13</sup> Allosteric effects of both compounds have been extensively explored for adenosine receptors. Gao et al. demonstrated that HMA and a few other 5'-substituted amiloride derivatives increase the dissociation rate of antagonists from the adenosine A<sub>1</sub> and A<sub>3</sub> receptors, whereas amiloride itself was effective only at the adenosine A<sub>1</sub> receptor.<sup>15</sup> At the hA<sub>2A</sub>AR, amiloride and its derivatives exhibited similar effects, where dissociation of radiolabeled antagonist [<sup>3</sup>H]ZM-241,385 increases in their presence.<sup>14</sup> Amilorides supposedly bind in the sodium ion binding site of GPCRs. This has been visualized in Chapter 3 by docking amiloride and HMA into the high resolution X-ray crystal structure of the hA<sub>2A</sub>AR.<sup>5</sup> Like sodium ions, the positively charged guanidinium moiety of amiloride and HMA made strong interactions with the carboxylate of Asp52<sup>2,50</sup>. Furthermore, the presence of amiloride or HMA forced Trp246<sup>6,48</sup> to rotate away from its most stable position. This proposed binding mode was confirmed in the mutation study in Chapter 4, where the effects of amiloride and HMA were largely diminished by mutation D52A<sup>2,50</sup> but were increased by mutation W246A<sup>6,48</sup>. The strong increase in potency of HMA compared to that of amiloride against the hA<sub>2A</sub>AR provided the impetus to investigate whether different substituents at the 5' position of amiloride might yield more potent amiloride derivatives. In the current study, a selection of 5'-substituted amilorides was tested for binding to the wild-type and W246A<sup>6,48</sup> mutant hA<sub>2A</sub>AR (Table 1).

Carboxylate derivatives **3** and **5** and tetrazole **7** showed minimal or no displacement of [<sup>3</sup>H]ZM-241,385 binding from either receptor. Apparently, amiloride derivatives carrying a negative charge on an extended 5'-substituent do not bind in the sodium ion pocket. Indeed, 5' substituents are predicted to enter a hydrophobic pocket, as suggested by the proposed binding modes of HMA and **12h**, **i**, **k**, and **l** (Figures S1 and S2). Most of the other amilorides were more or less active at the W246A<sup>6,48</sup> mutant hA<sub>2A</sub>AR, indicating at least some affinity of these compounds for the sodium ion site. The most potent derivative at both the wild-type and mutant hA<sub>2A</sub>ARs in the preliminary series was phenethyl derivative **12**. This derivative was the starting point for the synthesis of novel derivatives **12a-p** carrying substituents on the phenyl moiety (Table 2). The four most potent derivatives to emerge for the wild-type receptor were **12h**, **i**, **k**, and **l**, of which 4-ethoxyphenethyl

derivative **12l** proved to be more potent than HMA (Table 3). Differences in potency shifts between the wild-type and W246A<sup>6,48</sup> mutant hA<sub>2A</sub>AR ranged from 19-fold for HMA to 80-fold for **12k**. Together with the predicted binding modes, in which Trp246<sup>6,48</sup> is forced to rotate away from its most stable position, as observed previously for amiloride and HMA in Chapter 3 (Figures 2 and S3), these potency shifts support the binding of these ligands in the sodium ion site. The bulkiest compounds, dioxolyl derivative **12k** and 4-ethoxyphenethyl derivative **12l**, benefited the most from the absence of the bulky tryptophan residue, which suggests increased steric clash between Trp246<sup>6,48</sup> and bulkier 5' substituents.

Trp246<sup>6,48</sup> separates the sodium ion binding pocket from the orthosteric binding pocket, which are adjacent.<sup>5</sup> The proposed binding modes in the docking study predicted that the elongated phenethyl substituents of the amiloride derivatives are in close proximity to at least four amino acids that make up the orthosteric pocket (Figures 2 and S1-S3), which makes it likely that they protrude into the orthosteric pocket and enter in a direct competition with orthosteric ligands. This would change the allosteric mechanism of these amiloride derivatives from a noncompetitive to a more competitive nature. To investigate whether this was the case, the four most potent phenethyl-amiloride derivatives, **12h**, **i**, **k**, and **l**, were tested for their influence on the dissociation characteristics of the orthosteric ligand [<sup>3</sup>H]ZM-241,385 from the wild-type hA<sub>2A</sub>AR (Table 4). The noncompetitive allosteric effect of HMA was evident as it decreased the residence time of [<sup>3</sup>H]ZM-241,385 significantly at the wild-type receptor, which is in agreement with previous studies (Gao et al.<sup>14</sup> and Chapter 3). Compounds **12h**, **i**, and **l** were more competitive in nature, as illustrated by their smaller effects on the dissociation characteristics of the orthosteric ligand. Interestingly, compound **12k** did not influence the dissociation of [<sup>3</sup>H]ZM-241,385 at all, which suggests that the displacement of the orthosteric ligand by **12k** is entirely due to direct competition between the two ligands.

The position of Trp246<sup>6,48</sup> at the interface of the orthosteric and allosteric sites of the hA<sub>2A</sub>AR suggests that this amino acid influences the nature of the allosteric mechanism of amilorides. Indeed compounds **12i** and **k** showed quite different effects on the dissociation of [<sup>3</sup>H]ZM-241,385 from the W246A<sup>6,48</sup> mutant compared to the wild-type receptor. These two compounds became noncompetitive allosteric modulators in the absence of the bulky tryptophan side chain, as their effect on the dissociation

characteristics of [<sup>3</sup>H]ZM-241,385 increased significantly. For **12k**, the effect was remarkable, showing no effect at the wild-type receptor while producing a 2.3-fold decrease in the residence time of [<sup>3</sup>H]ZM-241,385 at the mutated receptor. This suggests that the presence of Trp246<sup>6,48</sup> ‘guides’ the methoxy and dioxolyl substituents on the phenethyl moieties of **12i** and **k** toward the orthosteric site, inducing their competitive effect.

## Conclusions

We demonstrated that it is possible to extend amiloride with substituents at the 5' position to produce amiloride derivatives with similar or even higher potencies than HMA at the wild-type hA<sub>2A</sub>AR. Similar to amiloride and HMA, all novel amiloride derivatives showed significantly higher potencies at the W246A<sup>6,48</sup> mutant hA<sub>2A</sub>AR, implying that Trp246<sup>6,48</sup> hinders the binding of these amiloride derivatives. HMA showed the largest allosteric effect on [<sup>3</sup>H]ZM-241,385 dissociation, whereas the most potent novel amilorides showed reduced or no effects on this dissociation process. This indicates that these novel amilorides engage in a more direct competition with the orthosteric ligand, and it can be hypothesized that they do so by intrusion into the orthosteric pocket. The striking differences in effect on the dissociation of [<sup>3</sup>H]ZM-241,385 between the wild-type and W246A<sup>6,48</sup> hA<sub>2A</sub>ARs imply that Trp246<sup>6,48</sup> influences the nature of the allosteric interaction by amilorides. The well-conserved sodium ion pocket and the effects of amilorides and HMA shared among a multitude of GPCRs suggest a general mechanism of their interaction with the superfamily of GPCRs.

## Supplemental information

Supplemental information includes full experimental procedures for synthesis of compounds **12a-p**, including NMR and HPLC data, 2D interaction maps of docking of HMA **2** and **12h, i, k, and l** (Figures S1 and S2), 3D representation of docking of **12h, i, k, and l** (Figure S3), and SMILES strings and binding and inhibition data for **1-18** and **12a-p** in (CSV). It can be found with this article online at [dx.doi.org/10.1021/acs.jmedchem.6b00142](https://dx.doi.org/10.1021/acs.jmedchem.6b00142)

## Acknowledgments

This work was supported by a TOP grant from the Netherlands Organization for Scientific Research - Chemical Sciences (Grant 714.011.001) and partially supported (fellowship grant for Ilze Adlere) by the EC 7th Framework Programme (Grant REGPOT-CT-2013-316149-InnovaBalt).

## References

1. Lagerström MC and Schiöth HB, *Structural diversity of G protein-coupled receptors and significance for drug discovery*. Nat Rev Drug Discovery, 2008. 7(4): p. 339-357.
2. Rask-Andersen M, Almén MS, and Schiöth HB, *Trends in the exploitation of novel drug targets*. Nat Rev Drug Discovery, 2011. 10(8): p. 579-590.
3. Göblyös A and Ilzerman AP, *Allosteric modulation of adenosine receptors*. Biochim Biophys Acta, Biomembr, 2011. 1808(5): p. 1309-1318.
4. May LT, Leach K, Sexton PM, et al., *Allosteric modulation of G protein-coupled receptors*. Annu Rev Pharmacol Toxicol, 2007. 47: p. 1-51.
5. Liu W, Chun E, Thompson AA, et al., *Structural basis for allosteric regulation of GPCRs by sodium ions*. Science, 2012. 337(6091): p. 232-236.
6. Zhang C, Srinivasan Y, Arlow DH, et al., *High-resolution crystal structure of human protease-activated receptor 1*. Nature, 2012. 492(7429): p. 387-392.
7. Christopher JA, Brown J, Doré AS, et al., *Biophysical fragment screening of the  $\beta_1$ -adrenergic receptor: identification of high affinity arylpiperazine leads using structure-based drug design*. J Med Chem, 2013. 56(9): p. 3446-3455.
8. Miller-Gallacher JL, Nehmé R, Warne T, et al., *The 2.1 Å resolution structure of cyanopindolol-bound  $\beta_1$ -adrenoceptor identifies an intramembrane  $\text{Na}^+$  ion that stabilises the ligand-free receptor*. PLoS ONE, 2014. 9(3): p. e92727.
9. Fenalti G, Giguere PM, Katritch V, et al., *Molecular control of  $\delta$ -opioid receptor signalling*. Nature, 2014. 506(7487): p. 191-196.
10. Garritsen A, Ilzerman AP, Tulp MTM, et al., *Receptor binding profiles of amiloride analogues provide no evidence for a link between receptors and the  $\text{Na}^+/\text{H}^+$  exchanger, but indicate a common structure on receptor proteins*. J Recept Res, 1991. 11(6): p. 891-907.
11. Howard MJ, Hughes RJ, Motulsky HJ, et al., *Interactions of amiloride with  $\alpha$ - and  $\beta$ -adrenergic receptors: amiloride reveals an allosteric site on  $\alpha_2$ -adrenergic receptors*. Mol Pharmacol, 1987. 32(1): p. 53-58.

12. Hoare SRJ, Coldwell MC, Armstrong D, et al., *Regulation of human D<sub>1</sub>, d<sub>2(long)</sub>, d<sub>2(short)</sub>, D<sub>3</sub> and D<sub>4</sub> dopamine receptors by amiloride and amiloride analogues*. *Br J Pharmacol*, 2000. 130(5): p. 1045-1059.
13. Heitman LH, Ye K, Oosterom J, et al., *Amiloride derivatives and a nonpeptidic antagonist bind at two distinct allosteric sites in the human gonadotropin-releasing hormone receptor*. *Mol Pharmacol*, 2008. 73(6): p. 1808-1815.
14. Gao ZG and IJzerman AP, *Allosteric modulation of A<sub>2A</sub> adenosine receptors by amiloride analogues and sodium ions*. *Biochem Pharmacol (Amsterdam, Neth)*, 2000. 60(5): p. 669-676.
15. Gao ZG, Melman N, Erdmann A, et al., *Differential allosteric modulation by amiloride analogues of agonist and antagonist binding at A<sub>1</sub> and A<sub>3</sub> adenosine receptors*. *Biochem Pharmacol (Amsterdam, Neth)*, 2003. 65(4): p. 525-534.
16. Matthews H, Ranson M, Tyndall JDA, et al., *Synthesis and preliminary evaluation of amiloride analogs as inhibitors of the urokinase-type plasminogen activator (uPA)*. *Bioorg Med Chem Lett*, 2011. 21(22): p. 6760-6766.
17. Matthews H, Ranson M, and Kelso MJ, *Anti-tumour/metastasis effects of the potassium-sparing diuretic amiloride: an orally active anti-cancer drug waiting for its call-of-duty?* *Int J Cancer*, 2011. 129(9): p. 2051-2061.
18. Warnock DG, Kusche-Vihrog K, Tarjus A, et al., *Blood pressure and amiloride-sensitive sodium channels in vascular and renal cells*. *Nat Rev Nephrol*, 2014. 10(3): p. 146-157.
19. Alexander SPH and Millns PJ, *[<sup>3</sup>H]ZM241385 - an antagonist radioligand for adenosine A<sub>2A</sub> receptors in rat brain*. *Eur J Pharmacol*, 2001. 411(3): p. 205-210.
20. Nygaard R, Frimurer TM, Holst B, et al., *Ligand binding and micro-switches in 7TM receptor structures*. *Trends Pharmacol Sci*, 2009. 30(5): p. 249-259.
21. Ballesteros JA and Weinstein H, *Integrated methods for the construction of three-dimensional models and computational probing of structure-function relations in G protein-coupled receptors*. *Methods Neurosci*, 1995. 25: p. 366-428.
22. Poucher SM, Keddie JR, Singh P, et al., *The in vitro pharmacology of ZM 241385, a potent, non-xanthine A<sub>2a</sub> selective adenosine receptor antagonist*. *Br J Pharmacol*, 1995. 115(6): p. 1096-1102.
23. Green MR and Sambrook J, *Molecular cloning: a laboratory manual*. 2012, Cold Spring Harbor Laboratory Press: New York. p. 1150-1159.
24. Smith PK, Krohn RI, Hermanson GT, et al., *Measurement of protein using bicinchoninic acid*. *Anal Biochem*, 1985. 150(1): p. 76-85.
25. Schrödinger LLC, *Small-Molecule Drug Discovery Suite 2014-3: Glide, version 6.4*. 2014: New York.
26. Schrödinger LLC, *Schrödinger Release 2014-3: Prime, version 3.7*. 2014.
27. Borrelli KW, Cossins B, and Guallar V, *Exploring hierarchical refinement techniques for induced fit docking with protein and ligand flexibility*. *J Comput Chem*, 2010. 31(6): p. 1224-1235.
28. Schrödinger LLC, *The PyMOL Molecular Graphics System, version 1.5.0.4*. New York.
29. Montagnier L, Bisagni E, Bourzat JD, et al., *Cytotoxicity and antitumor activity of β-nitrostyrenes*. *Chim Ther*, 1971. 6: p. 186-191.
30. Qian W, Lu W, Sun H, et al., *Design, synthesis, and pharmacological evaluation of novel tetrahydroprotoberberine derivatives: selective inhibitors of dopamine D<sub>1</sub> receptor*. *Bioorg Med Chem*, 2012. 20(15): p. 4862-4871.



# Chapter 6

## Mass spectrometry-based ligand binding assays on adenosine A<sub>1</sub> and A<sub>2A</sub> receptors

Arnault Massink

Mira Holzheimer

Anna Hölscher

Julien Louvel

Dong Guo

Gerwin Spijksma

Thomas Hankemeier

Adriaan P. IJzerman

*Purinergic Signalling*, 2015, 11(4): 581-94

## Abstract

Conventional methods to measure ligand-receptor binding parameters typically require radiolabeled ligands as probes. Despite the robustness of radioligand binding assays, they carry inherent disadvantages in terms of safety precautions, expensive synthesis, special lab requirements, and waste disposal. Mass spectrometry (MS) is a method that can selectively detect ligands without the need of a label. The sensitivity of MS equipment increases progressively, and currently it is possible to detect the low ligand quantities that are usually found in ligand binding assays. We developed a label-free MS ligand binding (MS binding) assay on the adenosine  $A_1$  and  $A_{2A}$  receptors ( $A_1$ AR and  $A_{2A}$ AR), which are well-characterized members of the class A G protein-coupled receptor (GPCR) family. Radioligand binding assays for both receptors are well established, and ample data is available to compare and evaluate the performance of an MS binding assay. 1,3-Dipropyl-8-cyclopentyl-xanthine (DPCPX) and 4-{2-((7-amino-2-(furan-2-yl)-[1,2,4]triazolo[1,5-*a*]-[1,3,5]triazin-5-yl)amino)ethyl)phenol (ZM-241,385) are high-affinity ligands selective for the  $A_1$ AR and  $A_{2A}$ AR, respectively. To proof the feasibility of MS binding on the  $A_1$ AR and  $A_{2A}$ AR we first developed an MS detection method for unlabeled DPCPX and ZM-241,385. To serve as internal standards, both compounds were also deuterium-labeled. Subsequently, we investigated whether the two unlabeled compounds could substitute for their radiolabeled counterparts as marker ligands in binding experiments, including saturation, displacement, dissociation, and competition association assays. Furthermore, we investigated the accuracy of these assays if the use of internal standards was excluded. The results demonstrate the feasibility of the MS binding assay, even in the absence of a deuterium-labeled internal standard, and provide great promise for the further development of label-free assays based on MS for other GPCRs.



## Introduction

Conventional methods to measure ligand-receptor binding parameters typically require labeled probes such as radiolabeled<sup>1</sup> or fluorescently labeled ligands.<sup>2</sup> Despite the robustness of radioligand binding assays, they carry inherent disadvantages in terms of safety precautions, expensive synthesis, special lab requirements, and waste disposal. Alternatively, the addition of fluorescent moieties holds a substantial risk of affecting the pharmacological properties of a ligand; moreover, in many instances it is also required to engineer the receptor protein, in particular for fluorescence resonance energy transfer assays.<sup>3</sup>

The development of the mass spectrometry (MS) binding assay by the group of Wanner permits to measure binding of an unlabeled ligand to its target.<sup>4</sup> Instead of the radiolabeled ligand in radioligand binding assays, an unlabeled marker ligand is employed in MS binding assays. The amount of marker ligand bound to the target receptor is detected by mass spectrometry. As the mass of the molecule itself is detected, a label is not necessary. However, the marker ligand still has to fulfill the same requirements as radioligands: high affinity and selectivity for the target, and low nonspecific binding.<sup>5</sup> Therefore, it is practical to choose a ligand for MS binding applications that has already been validated as a good radioligand. This also ensures a straightforward validation of an MS binding assay by comparing it to existing radioligand binding assays.

In this study, we developed an MS binding assay for the adenosine A<sub>1</sub> (hA<sub>1</sub>AR) and adenosine A<sub>2A</sub> receptors (hA<sub>2A</sub>AR). The particular robustness and abundance of published results of radioligand binding assays on the hA<sub>1</sub>AR and hA<sub>2A</sub>AR make these receptors good candidates for development of an MS binding assay.<sup>6</sup> The adenosine receptors are members of the class A of G protein-coupled receptors (GPCRs). Both receptors are important in physiology. The hA<sub>1</sub>AR has been related to sleep regulation, epilepsy, and asthma. The hA<sub>2A</sub>AR is implicated in neurodegeneration, inflammatory diseases, and cancer pathogenesis. Both receptors are involved in cardiovascular physiology.<sup>6, 7</sup> As marker ligands for the MS binding assay, we chose 1,3-dipropyl-8-cyclopentyl-xanthine (DPCPX) for the hA<sub>1</sub>AR and 4-(2-((7-amino-2-(furan-2-yl)-[1,2,4]triazolo[1,5-*a*]-[1,3,5]triazin-5-yl)amino)ethyl)phenol (ZM-241,385) for the hA<sub>2A</sub>AR. These ligands are well-established radioligands for their respective targets and hence a logical choice to serve as marker ligands in MS binding assays.<sup>8, 9</sup>

The development of liquid chromatography-MS (LC-MS) detection methods for nonlabeled DPCPX and ZM-241,385 as marker ligands involved the following steps. Firstly, deuterated isotopologues of the marker ligands were synthesized to serve as internal standards for increased accuracy of the MS detection. In MS detection methods, it is common to add a fixed amount of an internal standard to each sample to compensate for ion suppression, sample evaporation, and instrumental drift.<sup>10</sup> Technically, the use of deuterium-labeled internal standards makes the MS binding assay a labeled assay, even if the marker ligand that binds to the target is unlabeled itself. Therefore, we also investigated whether the results of the MS binding assays were accurate in the absence of an internal standard. Secondly, a fast LC method was developed to separate the marker ligands from cell membrane contents in the sample. The duration of the LC separation is the limiting step for the throughput of the method so this is preferably fast, i.e., within one minute. Thirdly, for MS detection, a triple quadrupole MS (TQMS) was employed, which has the required sensitivity to measure typical bound ligand quantities of ligand binding assays, in the pM range. In a TQMS, the parent ions with the mass of the molecule of interest are filtered by the first quadrupole, which are then fragmented in the second quadrupole. The fragmentation results in daughter ions that are analyzed by the third quadrupole. This setup ensures a high selectivity and sensitivity for the detection of a molecule of interest.<sup>11</sup>

After establishing the LC-MS methods for detection of the marker ligands, the MS binding assays were performed with and without deuterium-labeled internal standard, and analogous to radioligand binding assays. Saturation, association, and dissociation assays were performed to determine the affinity and kinetic rates of the marker ligands DPCPX for the hA<sub>1</sub>AR and ZM-241,385 for the hA<sub>2A</sub>AR. Then displacement and competition association assays were performed to determine the affinity and kinetic rates of ligands competing with the marker ligands. The ensuing results were compared to and validated with reference radioligand binding data.

## Materials and methods

### Materials

Adenosine deaminase (ADA) was purchased from Boehringer Mannheim (Mannheim, Germany). DPCPX, 5'-*N*- ethylcarboxamidoadenosine (NECA), and bovine serum albumin (BSA) were purchased from Sigma (St. Louis, MO, USA). ZM-241,385 was purchased from Ascent Scientific (Bristol, UK). *N*<sup>6</sup>-Cyclopentyladenosine (CPA) was purchased from Abcam Biochemicals (Cambridge, UK). 6-(2,2-Diphenylethylamino)-9-((2*R*,3*R*,4*S*,5*S*)-5-(ethylcarbonyl)-3,4-dihydroxytetrahydrofuran-2-yl)-*N*-(2-(3-(1-(pyridin-2-yl)piperidin-4-yl)ureido)ethyl)-9*H*-purine-2-carboxamide (UK-432,097) was obtained as a gift through Pfizer's Compound Transfer Program. 3-(3-Hydroxypropyl)-7-methyl-1-propargyl-8-(*m*-methoxystryryl)xanthine (MSX-2)<sup>12</sup> was a gift from Prof. C. E. Müller (Bonn University, Germany). 8-Cyclopentyltheophylline (8-CPT) was purchased from Research Biochemicals Inc. (Natick, MA, USA). 8-Cyclopentyl-3-(3-((4-(fluorosulfonylbenzoyl)oxy)propyl)-1-propylxanthine (FSCPX)<sup>13</sup> and *N*<sup>5</sup>-(2-(4-(2,4-difluorophenyl)piperazin-1-yl)ethyl)-2-(furan-2-yl)-[1,2,4]triazolo[1,5-*a*][1,3,5]triazine-5,7-diamine (LUF6632)<sup>14</sup> were synthesized in-house. Bicinchoninic acid (BCA) and BCA protein assay reagent were obtained from Pierce Chemical Company (Rockford, IL, USA). CHO cells stably expressing the hA<sub>1</sub>AR (CHO-hA<sub>1</sub>AR) were a gift from Prof. S. Hill (University of Nottingham, UK). HEK293 cells stably expressing the hA<sub>2A</sub>AR (HEK293-hA<sub>2A</sub>AR) were a gift from Dr. J. Wang (Biogen/IDEC, Cambridge, MA, USA). All other chemicals were of analytical grade and obtained from standard commercial sources.

### General synthesis procedures

Demineralised water is simply referred to as H<sub>2</sub>O, as was used in all cases unless stated otherwise. <sup>1</sup>H and <sup>13</sup>C NMR spectra were recorded on a Bruker AV 400 liquid spectrometer (<sup>1</sup>H NMR, 400 MHz; <sup>13</sup>C NMR, 100 MHz) at ambient temperature. Chemical shifts are reported in parts per million (ppm), are designated by  $\delta$  and are downfield to the internal standard tetramethylsilane (TMS) in CDCl<sub>3</sub>. Coupling constants are reported in Hertz and are designated as *J*. Analytical purity of the final compounds was determined by high pressure liquid chromatography (HPLC) with a Phenomenex Gemini 3- $\mu$ m C18 110A column (50 x 4.6 mm, 3  $\mu$ m), measuring UV absorbance at 254 nm. Sample preparation and HPLC method were - unless stated otherwise - as follows: 0.3-0.8 mg of

compound was dissolved in 1 ml of a 1:1:1 mixture of CH<sub>3</sub>CN/H<sub>2</sub>O/tBuOH and eluted from the column within 15 min, with a three-component system of H<sub>2</sub>O/CH<sub>3</sub>CN/1% TFA in H<sub>2</sub>O, decreasing polarity of the solvent mixture in time from 80:10:10 to 0:90:10. All compounds showed a single peak at the designated retention time and were at least 95% pure. The synthesized compounds were identified by LC-MS analysis using a Thermo Finnigan Surveyor-LCQ Advantage Max LC-MS system and a Gemini C18 Phenomenex column (50 × 4.6 mm, 3 μm). The sample preparation was the same as for HPLC analysis. The elution method was set up as follows: 1–4 min isocratic system of H<sub>2</sub>O/CH<sub>3</sub>CN/1% TFA in H<sub>2</sub>O, 80:10:10, from the 4<sup>th</sup> min, a gradient was applied from 80:10:10 to 0:90:10 within 9 min, followed by 1 min of equilibration at 0:90:10 and 1 min at 80:10:10. Thin-layer chromatography (TLC) was routinely performed to monitor the progress of reactions, using aluminum-coated Merck silica gel F254 plates. Purification by column chromatography was achieved by use of Grace Davison Davisil silica column material (LC60A 30-200 μm). Solutions were concentrated using a Heidolph laborota W8 2000 efficient rotary evaporation apparatus and by a high vacuum on a Binder APT line Vacuum Drying Oven.

### **Preparation of 8-cyclopentyl-1,3-bis(propyl-2,3-d<sub>2</sub>)-3,9-dihydro-1H-purine-2,6-dione **2** ([<sup>2</sup>H<sub>4</sub>] DPCPX)**

Synthesis steps to arrive to compound **1** (SI Scheme 3) were performed as previously described.<sup>15-17</sup> 1,3-Diallyl-8-cyclopentyl-3,9-dihydro-1H-purine-2,6-dione **1** (1 mmol, 300 mg) and NaBD<sub>4</sub> (4 mmol, 167 mg) were placed in a flask. The flask was flame-dried under vacuum to remove traces of water and then purged with N<sub>2</sub> gas. Dry THF (10 ml) was added. RhCl(PPh<sub>3</sub>)<sub>3</sub> was placed in another flame-dried flask under N<sub>2</sub>-atmosphere and suspended in dry THF (1 ml). The flask containing **1** was heated to 60 °C and the reaction was started upon addition of the catalyst suspension, followed by D<sub>2</sub>O (2 mmol, 0.04 ml). The mixture was stirred at 60 °C for 19 h. The reaction mixture was then poured into EtOAc and washed with brine (3x). The organic layer was dried over MgSO<sub>4</sub> and concentrated. The crude product was purified by column chromatography (PET/EtOAc 5/1 → 4/1 → 3/2). The product **2** was obtained as white solid (46%, 0.46 mmol, 141 mg). <sup>1</sup>H NMR (400 MHz, CDCl<sub>3</sub>): δ 11.92 (br s, 1H), 4.11 – 4.06 (m, 2H), 4.03 – 3.97 (m, 2H), 3.30 – 3.21 (m, 1H), 2.18 – 2.11 (m, 2H), 1.98 – 1.68 (m, 8H), 0.99 – 0.94 (m, 4H) ppm. MS:

[M+H]<sup>+</sup> calculated 309.22, found 309.20. HPLC purity 97% (*t*<sub>R</sub> 9.587 min, mobile phase 15-65% MeCN/H<sub>2</sub>O + TFA).

**Preparation of 4-(2-((7-amino-2-(furan-2-yl)-1,3a-dihydro-[1,2,4]triazolo[1,5-*a*][1,3,5]triazin-5-yl)amino)ethyl)phen-2,3,5,6-d<sub>4</sub>-ol 5 ([<sup>2</sup>H<sub>4</sub>] ZM-241,385)**

Synthesis steps to arrive to compounds **3** and **4** (SI Scheme 4) were performed as previously described.<sup>18-20</sup> [<sup>2</sup>H<sub>4</sub>]Tyramine **4** (0.37 mmol, 53 mg) was suspended in 4 ml MeCN, and Et<sub>3</sub>N (0.14 ml) and 2-(furan-2-yl)-5-(methylsulfonyl)-1,3a-dihydro-[1,2,4]triazolo[1,5-*a*][1,3,5]triazin-7-amine **3** (0.34 mmol, 95 mg) were added. The mixture was stirred for 3 h at 70 °C under microwave irradiation. The solvent was evaporated, and the crude material was adsorbed onto Silica and purified by column chromatography (EtOAc/MeOH 99/1) and subsequent PTLC (EtOAc/MeOH 99.5/0.5) to give the product **5** as an off-white solid (45%, 0.15 mmol, 52 mg). <sup>1</sup>H NMR (400 MHz, DMSO-*d*<sub>6</sub>): δ 9.17 (s, 1H), 8.13 (br s, 2H), 7.86 (s, 1H), 7.53 – 7.52 and 7.50 – 7.42 (m, 1H, rotamers), 7.05 (d, *J* = 3.2, 1H), 6.67 (m, 1H), 3.43 – 3.40 (m, 2H), 2.74 – 2.71 (m, 2H) ppm. MS: [M+H]<sup>+</sup> calculated 342.16, found 342.7. HPLC purity 95% (*t*<sub>R</sub> 6.408 min, mobile phase 10-90 % MeCN/H<sub>2</sub>O + TFA).

**Cell culture**

CHO-hA<sub>1</sub>AR cells were grown in Ham's F12 medium containing 10% normal adult bovine serum, 100 µg/ml streptomycin, 100 IU/ml penicillin, and 400 µg/ml G418, at 37 °C in 5% CO<sub>2</sub>. HEK293-hA<sub>2A</sub>AR cells were grown in Dulbecco's modified Eagle's medium (DMEM) supplemented with 10% newborn calf serum, 50 µg/ml streptomycin, 50 IU/ml penicillin, and 200 µg/ml G418, at 37 °C and 7% CO<sub>2</sub>. Cells were subcultured twice a week on 10 cm ø plates at a ratio of 1:20 for CHO hA<sub>1</sub>R cells and 1:8 for HEK293 hA<sub>2A</sub>AR cells.

**Membrane preparation**

CHO-hA<sub>1</sub>AR and HEK293-hA<sub>2A</sub>AR cells were grown as described above. Membranes were prepared as follows. Cells were detached from plates grown to confluency by scraping them into 5 ml PBS, collected and centrifuged at 700 g (3000 rpm) for 5 min. Pellets derived from 20 plates (10 cm ø) were pooled and resuspended in 16 ml of ice-cold assay buffer (50 mM Tris-HCl, 5 mM MgCl<sub>2</sub>, pH 7.4). An Ultra-Turrax was used to homogenize the cell suspension. Membranes and the cytosolic fraction were separated by centrifugation at 100000 g (31000 rpm) in a Beckman Optima LE-80K ultracentrifuge at 4

°C for 20 min. The pellet was resuspended in 8 ml of Tris buffer and the homogenization and centrifugation step was repeated. Assay buffer (4 ml) was used to resuspend the pellet, and adenosine deaminase (ADA) was added (0.8 IU/ml) to break down endogenous adenosine. Membranes were stored in 250 µl aliquots at -80 °C. Membrane protein concentrations were measured using the BCA (bicinchoninic acid) method.<sup>21</sup>

### **Radioligand binding assays**

The reference radioligand binding data were published before by our lab or were acquired as described before.<sup>22,23</sup>

### **Membrane harvesting procedure MS binding assays**

100 µl membrane aliquots containing 5 µg (CHO-hA<sub>1</sub>AR) or 22 µg (HEK293-hA<sub>2A</sub>AR) of protein in assay buffer were harvested by rapid vacuum filtration through 1 µm glass fiber AcroPrep Advance 96 filter plates (Pall Corporation, Ann Arbor, MI, USA) using an extraction plate manifold (Waters, Milford, MA, USA) and a 12-channel electronic pipette (Gilson, Middleton, WI, USA). Filters were subsequently washed three times with ice-cold assay buffer and dried for 1 h at 55 °C. It was essential that the filter plates were completely dry before continuing with ligand elution as described below in 'Sample elution'.

### **MS binding saturation assays**

Membrane aliquots containing 5 µg (CHO-hA<sub>1</sub>AR) or 22 µg (HEK293-hA<sub>2A</sub>AR) of protein were incubated in a total volume of 100 µl of assay buffer at 25 °C for 1 h (hA<sub>1</sub>AR) or at 4 °C for 3 h (hA<sub>2A</sub>AR). Total binding was determined at increasing concentrations of marker ligand DPCPX (0.08 - 40 nM on hA<sub>1</sub>AR) or marker ligand ZM-241,385 (0.05 - 15 nM on hA<sub>2A</sub>AR). Dilutions were prepared with a HP D300 Digital Dispenser (Tecan Group, Männerdorf, Swiss) from DMSO stocks. Nonspecific binding in presence of 100 µM CPA (hA<sub>1</sub>AR) or 100 µM NECA (hA<sub>2A</sub>AR) was determined at three concentrations of marker ligand and analyzed by linear regression. Incubations were terminated and samples were harvested as described under 'Membrane harvesting procedure MS binding assays'.

### **MS binding displacement assays**

Ligand displacement experiments were performed using nine concentrations of competing ligand. For the hA<sub>1</sub>AR the competing ligands used were CPA, 8-CPT, ZM-241,385, and NECA, while for the hA<sub>2A</sub>AR they were UK-432,097, MSX-2, DPCPX, and NECA. As marker

ligand DPCPX was used for the hA<sub>1</sub>AR at a concentration of 6 nM, and ZM-241,385 for the hA<sub>2A</sub>AR at a concentration of 3 nM. Nonspecific binding was determined in the presence of 100 μM CPA for the hA<sub>1</sub>AR and 100 μM NECA for the hA<sub>2A</sub>AR. Incubations were terminated as described under 'Membrane harvesting procedure MS binding assays'.

#### **MS binding association assays**

Membrane aliquots containing 5 μg / 100 μl (CHO-hA<sub>1</sub>AR) or 22 μg / 100 μl (HEK293-hA<sub>2A</sub>AR) of protein were incubated in a total volume of 2400 μl of assay buffer at 25 °C with 6 nM DPCPX for hA<sub>1</sub>AR or at 4 °C with 3 nM ZM-241,385 for hA<sub>2A</sub>AR. At each time point, 100 μl from the reaction mix was harvested as described under 'Membrane harvesting procedure MS binding assays' to determine the amount of marker ligand bound to the receptor. Nonspecific binding was determined as described under 'MS binding displacement assays'.

#### **MS binding dissociation assays**

Membrane aliquots containing 5 μg / 100 μl (CHO-hA<sub>1</sub>AR) or 22 μg / 100 μl (HEK293-hA<sub>2A</sub>AR) of protein were incubated in a total volume of 2400 μl of assay buffer at 25 °C with 6 nM DPCPX (hA<sub>1</sub>AR) or at 4 °C with 3 nM ZM-241,385 (hA<sub>2A</sub>AR). The reaction mixes were allowed to reach equilibrium for 1 h before starting the dissociation by adding 100 μM CPA (hA<sub>1</sub>AR) or NECA (hA<sub>2A</sub>AR). At each time point, 100 μl from the reaction mix was harvested as described under 'Membrane harvesting procedure MS binding assays' to determine the amount of marker ligand still bound to the receptor. Nonspecific binding was determined as described under 'MS binding displacement assays'.

#### **MS binding competition association assays**

Membrane aliquots containing 5 μg / 100 μl (CHO-hA<sub>1</sub>AR) or 22 μg / 100 μl (HEK293-hA<sub>2A</sub>AR) of protein were incubated in a total volume of 2400 μl of assay buffer at 25 °C with 6 nM DPCPX in the absence or presence of 250 nM 8-CPT or 250 nM FSCPX (hA<sub>1</sub>AR) or at 4 °C with 3 nM ZM-241,385 in the absence or presence of 90 nM MSX-2 or 15 nM LUF6632 (hA<sub>2A</sub>AR). At each time point, 100 μl from the reaction mix was harvested as described under 'Membrane harvesting procedure MS binding assays' to determine the amount of marker ligand bound to the receptor. Nonspecific binding was determined as described under 'MS binding displacement assays'.

### Sample elution

The ligand was eluted from the ligand-receptor complex on the dried filter plates over which MS binding samples were harvested. 100 µl eluent (50 % methanol, 50 % ammonium formate buffer [final concentration 5 mM] at pH 7, spiked with 2 nM [<sup>2</sup>H]DPCPX or [<sup>2</sup>H]ZM-241,385 as internal standard, all HPLC grade) was applied to the filter plates which were then centrifuged 1 min at 800 g (2000 rpm) in a 5810 plate centrifuge (Eppendorf, Hamburg, Germany), while filter eluates were collected in 1.1 ml polystyrene deep 96-wells plates (BrandTech Scientific, Essex, CT, USA). This procedure was performed twice resulting in a total of 200 µl eluate for each sample. For standard curve samples, the same procedure was followed but for the presence of increasing concentrations (1 – 100 pM) of DPCPX or ZM-241,385 in the eluent. After elution, 96-deep-well plates were sealed with rapid easy pierce film (Nacalai, San Diego, CA, USA) and stored at -20 °C before LC-MS-MS quantification.

### LC-MS-MS quantification

All solvents used were of LC-MS grade or better. The LC-ESI-MS-MS setup consisted of a Nexera X2 UHPLC (Shimadzu, Kyoto, Japan; degassing unit: 20A3R, autosampler: 30AC, column oven: 30AD) and a LCM-8050 triple quadrupole mass spectrometer (Shimadzu, Kyoto, Japan) with an electrospray ionization source (ESI) in positive mode. Chromatographic separation was performed on an Acquity UPLC BEH C18 column (1 x 50 mm, 1.7 µm; Waters, Milford, MA, USA) with a VanGuard precolumn of the same type (2.1 x 5 mm). The column oven was set at 40 °C. Mobile phases consisted of acetonitrile, methanol, ammonium formate buffer (final concentration 5 mM) at pH 7, all of LC-MS grade or better, in respective volume fractions of 5:5:90 (solvent A) and 45:45:10 (solvent B). An isocratic mobile phase flow of 0.2 ml/min was applied consisting of solvents A:B (10:90 for the DPCPX and 35:65 for the ZM-241,385 quantification methods), which resulted in column pressures of 400 bar and 500 bar, respectively. The sample eluate injection volume was 20 µl and run time was 1 min. Source and fragmentation parameters were acquired by the Shimadzu optimization for method function (Table 1). For each ligand, the parent and four daughter ions were detected by multiple reaction monitoring (MRM) in positive mode. Additional MS settings were as follows: ESI interface temperature 300 °C; DL temperature 250 °C; heat block temperature 400 °C; ion spray voltage 4 kV; heating and drying gas flows 10 L/min; nebulizing gas flow 3 L/min.



**Table 1.** Mass of detected parent and daughter ions. Parent ions were fragmented to daughter ions with different optimal collision energies for each daughter ion.

	Parent ion	Daughter ion	Collision energy (V)
<b>DPCPX</b>	305.00	178.15	35
		204.10	36
		221.15	27
		263.10	23
<b>[<sup>2</sup>H]DPCPX</b>	309.00	178.10	36
		204.05	35
		221.05	29
		265.00	23
<b>ZM-241,385</b>	338.10	77.05	55
		121.05	29
		176.10	30
		218.10	24
<b>[<sup>2</sup>H]ZM-241,385</b>	342.10	80.05	65
		125.10	30
		176.05	32
		218.05	26

### Data analysis

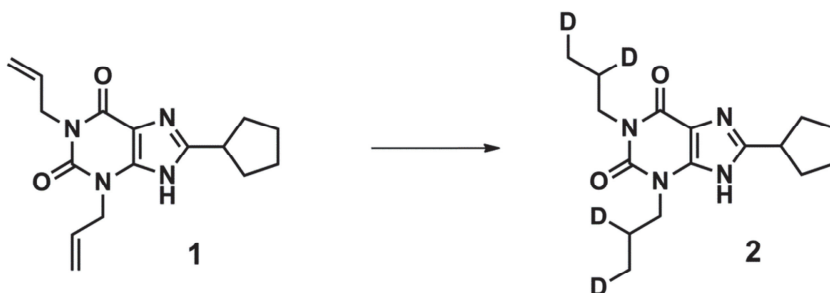
Shimadzu LabSolutions software (Shimadzu, Kyoto, Japan) was used to analyze resulting chromatogram peaks. The peak area of the total ion count (TIC) of the daughter ions was calculated at the expected retention times, resulting in marker and internal standard peak area. To compensate for eluent evaporation and signal suppression by matrix effects from the membrane sample, marker peak area was divided by internal standard peak area (M/IS). Lower limit of quantitation (LLOQ) values of each marker ligand were defined as the lowest concentration in membrane matrix where signal to noise ratio was higher than 5, the standard deviation within and between runs in hexaplicate was lower than 20% (and for all higher concentrations lower than 15%), and calculation of concentration by a function derived from  $1/x^2$  linear regression deviated from nominal values less than 20%. M/IS values were converted to concentration of marker ligand in pM using the function established by  $1/x^2$  linear regression on the 10 – 100 pM standard curve results. The resulting MS binding data was then analyzed with GraphPad Prism 5.0 (GraphPad

Software Inc., San Diego, CA, USA). Marker ligand displacement curves were fitted to one- and two-state site binding models.  $k_{\text{on}}$  and  $k_{\text{off}}$  values of the marker ligands DPCPX and ZM-241,385 were derived by fitting one-phase association and dissociation models. Association and dissociation rates for the competing ligands were calculated by fitting the data to the competition association model using 'kinetics of competitive binding'.<sup>24</sup> Log-transformed  $K_i$ ,  $K_D$ ,  $k_{\text{on}}$ , and  $k_{\text{off}}$  values from MS binding and radioligand binding assays were plotted, and a linear regression analysis was applied. A similar correlation plot was prepared with values from MS binding assays based on solely marker peak area values instead of M/IS.

## Results

### Synthesis of [<sup>2</sup>H<sub>4</sub>]DPCPX **2**

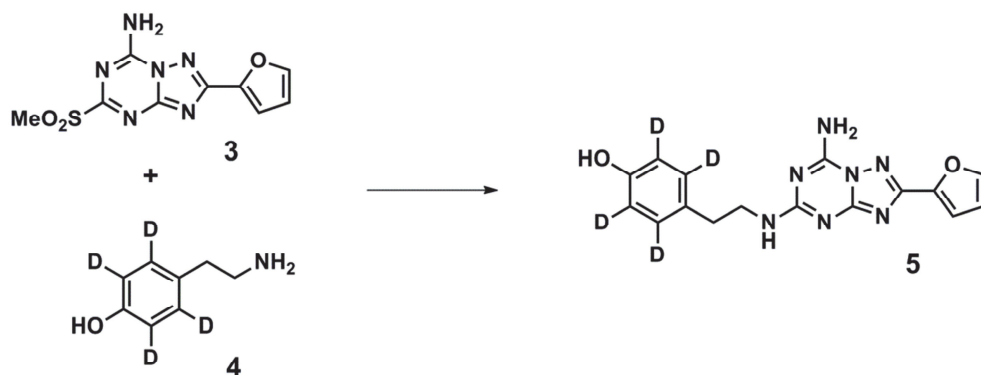
[<sup>2</sup>H<sub>4</sub>]DPCPX **2** was prepared according to the synthetic route shown in Scheme 1 and SI Scheme 3 and was adopted from previously described syntheses of nondeuterated DPCPX.<sup>15-17</sup> After the synthesis steps to arrive at compound **1** (SI Scheme 3), the allylic double bonds of the DPCPX precursor **1** were reductively deuterated in the presence of Wilkinson's catalyst with NaBD<sub>4</sub> as a deuterium source generating deuterium gas *in situ* upon addition of D<sub>2</sub>O.<sup>25</sup> The mass spectrum showed a mass range for the (M+H<sup>+</sup>) species from 305.20 ([<sup>2</sup>H<sub>0</sub>] isotopologue) to 313.27 ([<sup>2</sup>H<sub>8</sub>] isotopologue) in a Gaussian distribution with the desired [<sup>2</sup>H<sub>4</sub>]DPCPX **2** as most abundant isotopologue generating the main mass peak at 309.33.



**Scheme 1.** Synthesis of [<sup>2</sup>H<sub>4</sub>]DPCPX **2**. Reagents and conditions: Rh(PPh<sub>3</sub>)<sub>3</sub>Cl, NaBD<sub>4</sub>, D<sub>2</sub>O, dry THF, 60 °C, 3.5 h.

### Synthesis of [<sup>2</sup>H<sub>4</sub>]ZM-241,385 5

[<sup>2</sup>H<sub>4</sub>]ZM-241,385 5 was prepared according to the synthetic route shown in Scheme 2 and SI Scheme 4 and was adopted from previously described syntheses of nondeuterated ZM-241,385.<sup>18-20</sup> After the synthesis steps to arrive at compounds 3 and 4 (SI Scheme 4), reaction of the [<sup>2</sup>H<sub>4</sub>]tyramine 4 with methylsulfone compound 3 yielded the final product [<sup>2</sup>H<sub>4</sub>]ZM-241,385 5.<sup>18</sup> MS analysis showed a mass of 342.7 (M+H<sup>+</sup>) and confirmed the incorporation of four deuterium atoms in the final product.



**Scheme 2.** Synthesis of [<sup>2</sup>H<sub>4</sub>]ZM-241,385 5. Reagents and conditions: Et<sub>3</sub>N, MeCN, MW, 70 °C, 3 h.

### LC-MS results of DPCPX, [<sup>2</sup>H]DPCPX, ZM-241,385, and [<sup>2</sup>H]ZM-241,385

Standard curves were made for the quantitation of DPCPX and ZM-241,385 concentrations in biological membrane matrix by LC-MS (Figure 1). Membrane samples without addition of ligand were filtered, and the applied eluent contained increasing concentrations of DPCPX and ZM-241,385, in addition to 2 nM of their deuterated counterparts. This method ensured standard curves in presence of the same biological matrix as for the quantitated MS binding samples. The LLOQ values derived from the standard curves were 20 pM for DPCPX and 40 pM for ZM-241,385 and were below nonspecific binding concentrations found in MS binding assays for DPCPX (31 pM) and ZM-241,385 (42 pM). The linear regression equations to calculate marker ligand concentrations from the M/IS values derived from the standard curves were  $y = 0.00341x + 0.117$  with  $R^2 = 0.988$  for DPCPX and  $y = 0.00130x + 0.0225$  with  $R^2 = 0.987$  for ZM-241,385.

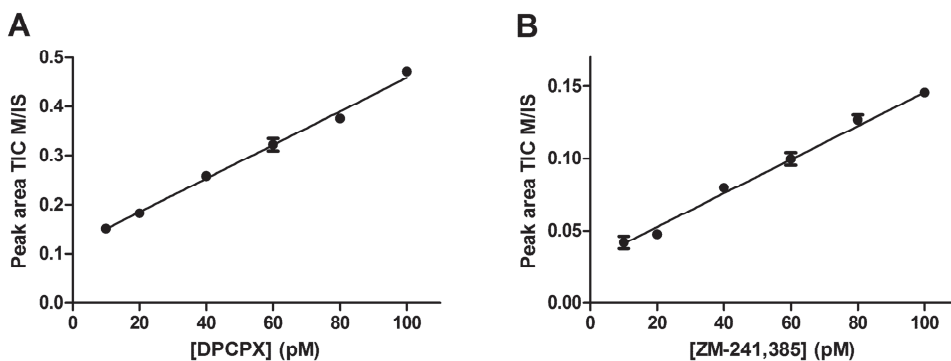


**Figure 1.** Standard curve of increasing concentrations of marker ligands **A)** DPCPX with 2 nM [ $^2\text{H}$ ]DPCPX and **B)** ZM-241,385 with 2 nM [ $^2\text{H}$ ]ZM-241,385 in matrix membrane samples. On the X-axis is plotted the concentration of marker ligand. On the Y-axis is plotted the marker area TIC divided by IS area TIC (M/IS). Data shown is the average of M/IS values  $\pm$  SEM from four runs in hexuplicate.

### Binding assays

DPCPX and ZM-241,385 were used as marker ligands for the MS binding assays. These marker ligands are also available as well-established tritium-labeled radioligands with high affinity for respectively the  $\text{hA}_1\text{AR}$  and  $\text{hA}_{2A}\text{AR}$ , which made it possible to validate the MS binding assays. For the displacement assays, the competing ligands on the  $\text{hA}_1\text{AR}$  were CPA (selective agonist), 8-CPT (selective antagonist), ZM-241,385 ( $\text{hA}_{2A}\text{AR}$ -selective antagonist), and NECA (nonselective agonist), and on the  $\text{hA}_{2A}\text{AR}$  they were UK-432,097 (selective agonist), MSX-2 (selective antagonist), DPCPX ( $\text{hA}_1\text{AR}$ -selective antagonist), and NECA. For the competition association assays, the competing ligands on the  $\text{hA}_1\text{AR}$  were 8-CPT (fast dissociation) and FSCPX (irreversibly binding to  $\text{hA}_1\text{AR}$  resulting in an apparent slow dissociation), and on the  $\text{hA}_{2A}\text{AR}$  they were MSX-2 (fast dissociation) and LUF6632 (slow dissociation). Marker ligand concentrations that were found in the eluates of the MS binding assays ranged from 31 pM to 242 pM for DPCPX and 42 pM to 289 pM for ZM-241,385 (Figure 2). The MS binding data in Figures 3-6 and Tables 2-6 is based on data with deuterium-labeled internal standard compensation of the marker ligand peak area (M/IS), except when stated otherwise in Tables 5 and 6. In Figure 7 both M/IS-based and marker peak area-based (without internal standard compensation and thus completely unlabeled) data are compared with radioligand binding data.

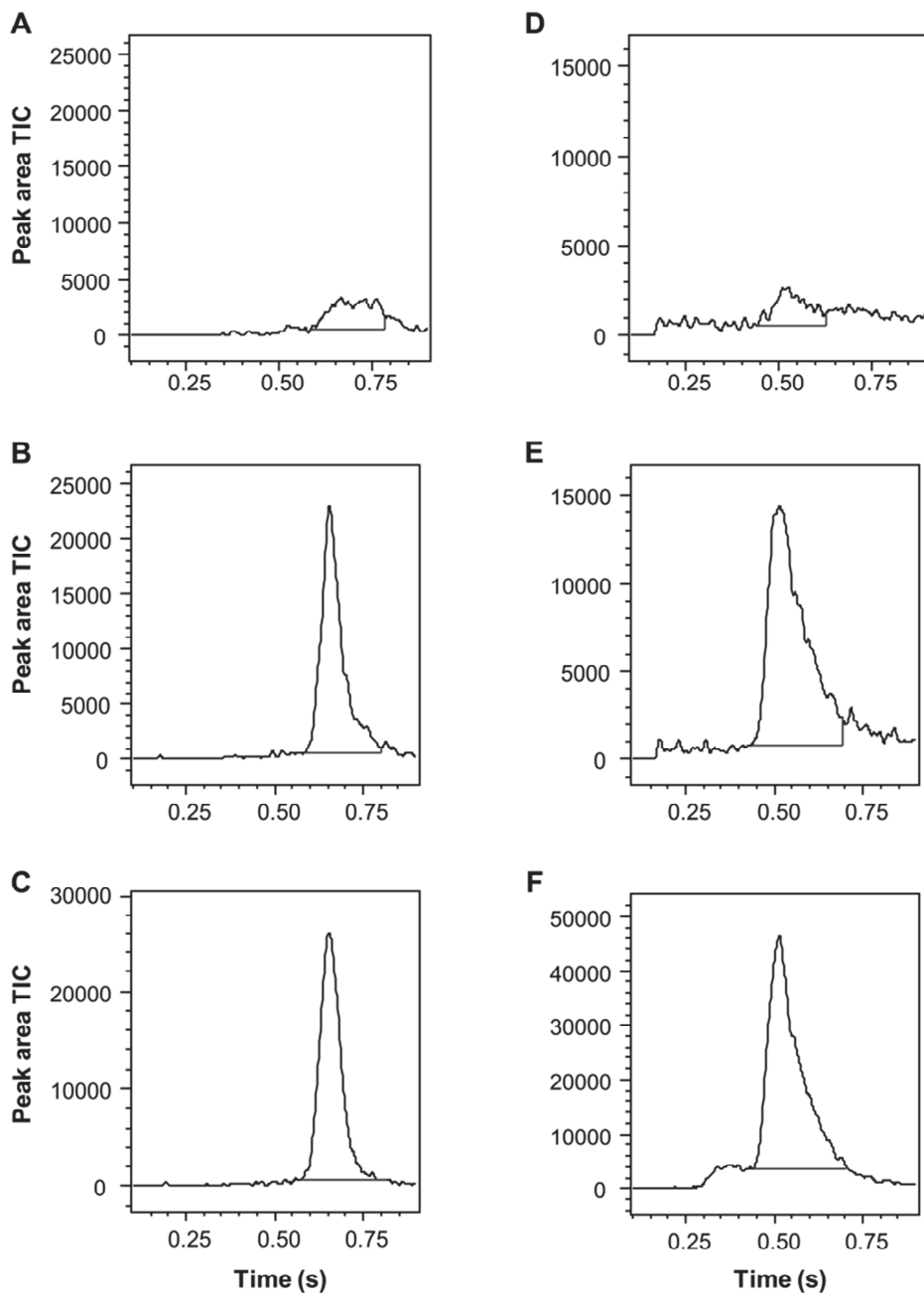


**Figure 2.** Typical chromatograms of **A)** nonspecific binding of DPCPX (31  $\mu$ M), **B)** total binding of DPCPX (242  $\mu$ M), and **C)** [ $^2$ H]DPCPX (2 nM) in eluate containing hA<sub>1</sub>AR membrane matrix, and of **D)** nonspecific binding of ZM-241,385 (42  $\mu$ M), **E)** total binding of ZM-241,385 (289  $\mu$ M), and **F)** [ $^2$ H]ZM-241,385 (2 nM) in eluate containing hA<sub>2A</sub>AR membrane matrix. The straight lines below the peaks delineate area of peak integration.

For the validation of MS binding assays, radioligand binding data that was published previously by our group was used. In the case that no in-house radioligand binding data was available, the concerning assays were performed following previously established protocols.<sup>22, 23</sup> Radioligand binding data for the marker ligands DPCPX and ZM-241,385 on their respective targets from saturation, association, and dissociation assays was published previously (Table 2). Displacement and competition association radioligand binding data of the competing ligands NECA (displacement on hA<sub>1</sub>AR and hA<sub>2A</sub>AR), UK-432,097 (displacement on hA<sub>2A</sub>AR), FSCPX (competition association on hA<sub>1</sub>AR), and LUF6632 (competition association on hA<sub>2A</sub>AR) was available as well from previous publications (Tables 3 - 6). Newly acquired radioligand binding data was from radioligand displacement assays with CPA, 8-CPT, and ZM-241,385 on the hA<sub>1</sub>AR; radioligand displacement assays with MSX-2 and DPCPX on the hA<sub>2A</sub>AR; and radioligand competition association assays with 8-CPT on the hA<sub>1</sub>AR and with MSX-2 on the hA<sub>2A</sub>AR.

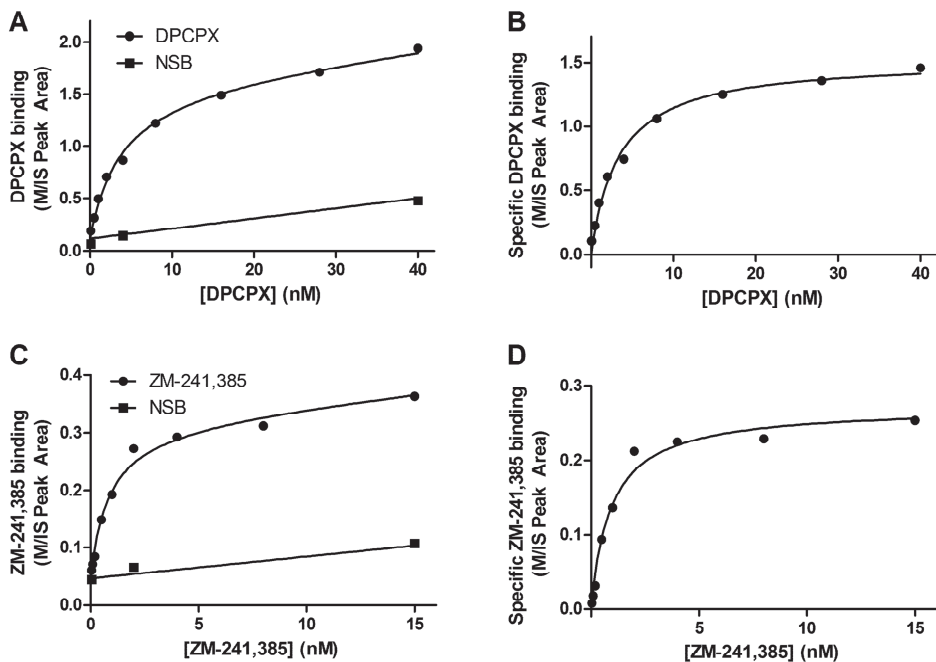


**Figure 3.** Saturation of DPCPX binding to hA<sub>1</sub>AR (A, B) and ZM-241,385 binding to hA<sub>2A</sub>AR (C, D). Increasing concentrations of marker ligands were incubated with the respective membranes. Data shown without (A, C) and with (B, D) nonspecific binding values subtracted. Graphs show mean values of one representative MS binding saturation experiment performed in duplicate.

**Table 2.** Affinity and  $B_{\max}$  values of DPCPX for the  $hA_1AR$  and ZM-241,385 for the  $hA_{2A}AR$  as determined in MS binding and radioligand binding saturation assays. Values are mean  $K_D$  in nM  $\pm$  SEM and mean  $B_{\max}$  in pmol/mg protein  $\pm$  SEM of at least three independent experiments performed in duplicate.

	$K_D \pm$ SEM (nM)		$B_{\max}$ (pmol/mg protein)	
	MS binding	Radioligand binding	MS binding	Radioligand binding
<b>DPCPX on <math>hA_1AR</math></b>	$3.43 \pm 0.02$	$2.5 \pm 0.1^a$	$17.3 \pm 0.3$	$14 \pm 1^a$
<b>ZM-241,385 on <math>hA_{2A}AR</math></b>	$1.03 \pm 0.07$	$0.60 \pm 0.07^b$	$2.3 \pm 0.3$	$1.9 \pm 0.4^b$

*a:* D. Guo, J Biomol Screen, 2013.<sup>26</sup>

*b:* D. Guo, Br J Pharmacol, 2012.<sup>23</sup>

MS binding saturation of the marker ligands DPCPX and ZM-241,385 to the  $hA_1AR$  and  $hA_{2A}AR$ , respectively, fitted a one-site saturation binding model (Figure 3). DPCPX had an affinity of  $3.43 \pm 0.02$  nM and a  $B_{\max}$  of  $17.3 \pm 0.3$  pmol/mg protein for the  $hA_1AR$  which was well in accordance with the previously found data from radioligand binding assays of  $2.5 \pm 0.1$  nM and  $14 \pm 1$  pmol/mg protein, respectively (Table 2). The same was true for ZM-241,385 with an MS binding affinity of  $1.03 \pm 0.07$  nM and  $B_{\max}$  of  $2.3 \pm 0.3$  pmol/mg protein for the  $hA_{2A}AR$ , compared to a radioligand binding affinity of  $0.60 \pm 0.07$  nM and  $B_{\max}$  of  $1.9 \pm 0.4$  pmol/mg protein.

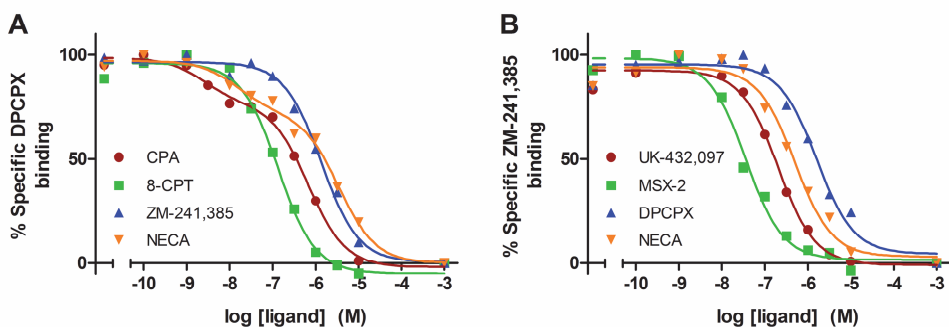


**Figure 4.** Displacement of DPCPX binding to  $hA_1AR$  by CPA, 8-CPT, ZM-241,385, or NECA (A), and of ZM-241,385 binding to  $hA_{2A}AR$  by UK-432,097, MSX-2, DPCPX, or NECA (B). Nonspecific binding is plotted at -3 on the x-axis. Graphs show mean values of one representative MS binding displacement experiment performed in duplicate.

**Table 3.** Affinity ( $K_i$  values) of CPA, 8-CPT, ZM-241,385, and NECA as determined in MS binding and radioligand binding displacement assays on  $hA_1AR$ . The displacement curves of CPA and NECA fitted to a two-state site binding model, which yielded high and low binding affinities for the receptor. Values are mean  $K_i$  in  $nM \pm SEM$  of at least three independent experiments performed in duplicate.

	$K_i \pm SEM$ (nM)	
	MS binding	Radioligand binding
<b>CPA</b>	139 $\pm$ 32	175 $\pm$ 13
<b>CPA-High</b>	1.2 $\pm$ 0.4	1.0 $\pm$ 0.5
<b>CPA-Low</b>	256 $\pm$ 81	304 $\pm$ 23
<b>8-CPT</b>	43 $\pm$ 11	31 $\pm$ 1
<b>ZM-241,385</b>	619 $\pm$ 78	523 $\pm$ 13
<b>NECA</b>	616 $\pm$ 76	731 $\pm$ 94 <sup>a</sup>
<b>NECA-High</b>	4.1 $\pm$ 1.4	4 $\pm$ 1 <sup>a</sup>
<b>NECA-Low</b>	1273 $\pm$ 56	731 $\pm$ 94 <sup>a</sup>

a: D. Guo, Br J Pharmacol, 2014.<sup>22</sup>

The displacement of marker ligands DPCPX and ZM-241,385 binding from the  $hA_1AR$  and  $hA_{2A}AR$  by their competing ligands fitted well to either one-state or two-state ligand binding displacement models (Figure 4). The affinities found in MS binding displacement assays for the competing ligands CPA, 8-CPT, ZM-241,385, and NECA for the  $hA_1AR$  (Table 3) and UK-432,097, MSX-2, DPCPX, and NECA for the  $hA_{2A}AR$  (Table 4) were in good agreement to the radioligand binding assays. The two-state binding model fits observed for the agonists CPA and NECA on the  $hA_1AR$  were observed in radioligand binding assays as well, and the resulting high and low affinity values were in good agreement (Table 3).

**Table 4.** Affinity ( $K_i$  values) of UK-432,097, MSX-2, DPCPX, and NECA as determined in MS binding and radioligand binding displacement assays on  $hA_{2A}AR$ . Values are mean  $K_i$  in  $nM \pm SEM$  of at least three independent experiments performed in duplicate.

	$K_i \pm SEM$ (nM)	
	MS binding	Radioligand binding
<b>UK-432,097</b>	52 $\pm$ 1	22 $\pm$ 5 <sup>a</sup>
<b>MSX-2</b>	9.0 $\pm$ 0.3	5.7 $\pm$ 0.1
<b>DPCPX</b>	550 $\pm$ 141	667 $\pm$ 77
<b>NECA</b>	100 $\pm$ 12	64 $\pm$ 1 <sup>a</sup>

a: D. Guo, Br J Pharmacol, 2012.<sup>23</sup>



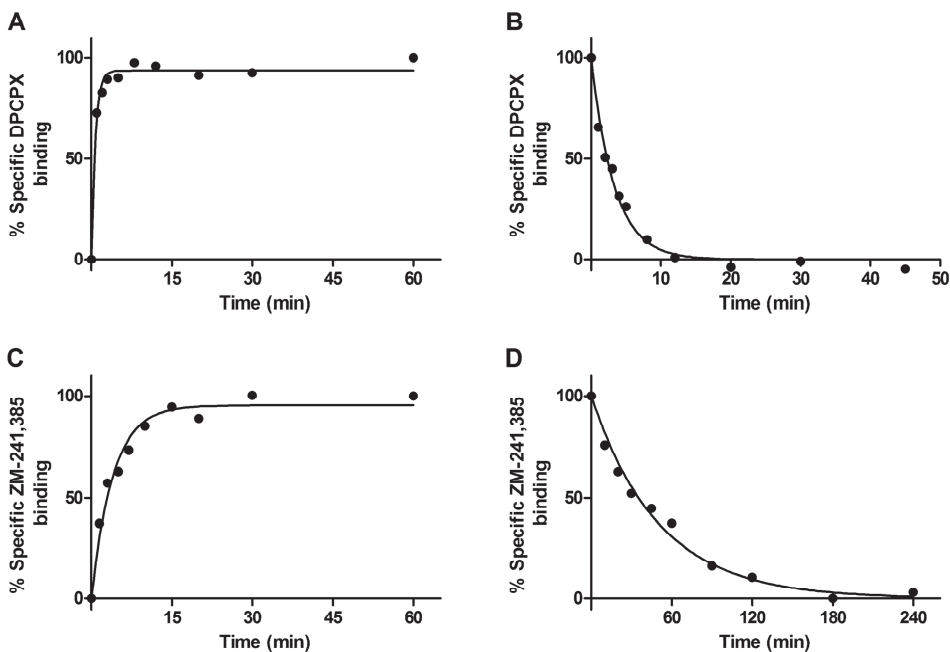


**Figure 5.** Association (**A, C**) and dissociation (**B, D**) of DPCPX on hA<sub>1</sub>AR (**A, B**) and ZM-241,385 on hA<sub>2A</sub>AR (**C, D**). Graphs show mean values of one representative MS binding association or dissociation experiment performed in duplicate.

The association and dissociation of marker ligands DPCPX and ZM-241,385 to the hA<sub>1</sub>AR and hA<sub>2A</sub>AR fitted well to one-phase association and dissociation models (Figure 5), and the resulting association and dissociation rates were in good agreement between MS binding and radioligand binding assays (Tables 5 and 6).

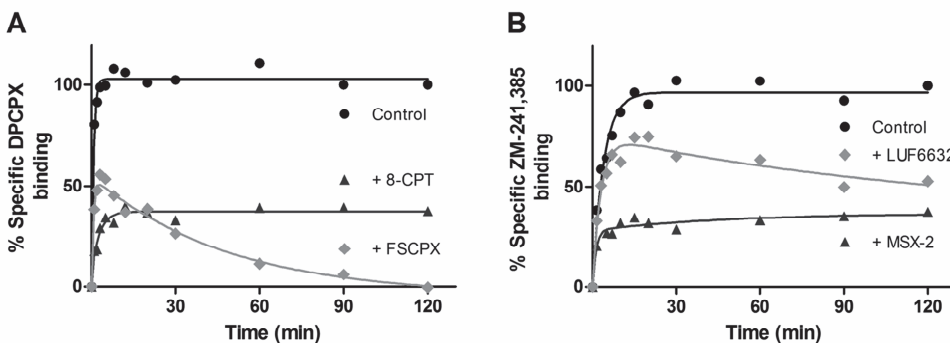


**Figure 6.** Competition association of DPCPX on hA<sub>1</sub>AR in the presence or absence of 250 nM 8-CPT and 250 nM FSCPX (**A**), and of ZM-241,385 on hA<sub>2A</sub>AR in the presence or absence of 90 nM MSX-2 and 15 nM LUF6632 (**B**). Graphs show mean values of one representative MS binding competition association experiment performed in duplicate.

**Table 5.** Association and dissociation rates of DPCPX, 8-CPT, and FSCPX determined in MS binding and radioligand binding assays on the hA<sub>1</sub>AR. MS binding (M/IS) values were obtained by analysis with compensation by internal standard, just as the MS binding values in Tables 2-4. MS binding (marker) values were obtained by analysis of marker chromatograms solely, without compensation by internal standard, and thus label-free. The kinetic values of DPCPX were determined by association and dissociation assays, while the kinetic values of 8-CPT and FSCPX were determined by competition association assays with 6 nM DPCPX as marker ligand. Values are mean  $k_{on}$  in M<sup>-1</sup> min<sup>-1</sup> ± SEM and mean  $k_{off}$  in min<sup>-1</sup> of at least three independent experiments performed in duplicate.

	$k_{on} \pm \text{SEM} (\text{M}^{-1} \text{min}^{-1})$			$k_{off} \pm \text{SEM} (\text{min}^{-1})$		
	MS binding (M/IS)	Radio-ligand binding	MS binding (marker)	MS binding (M/IS)	Radio-ligand binding	MS binding (marker)
<b>DPCPX</b>	2.0 ± 0.3 x10 <sup>8</sup>	1.4 ± 0.2 x10 <sup>8(a)</sup>	1.7 ± 0.4 x10 <sup>8</sup>	0.29 ± 0.02	0.25 ± 0.01 <sup>a</sup>	0.31 ± 0.02
<b>8-CPT</b>	5 ± 2 x10 <sup>7</sup>	6 ± 2 x10 <sup>7</sup>	3 ± 2 x10 <sup>7</sup>	1.4 ± 0.5	1.1 ± 0.3	1.2 ± 0.8
<b>FSCPX<sup>(b)</sup></b>	0.7 ± 0.2 x10 <sup>6</sup>	3.7 ± 1.0 x10 <sup>6(a)</sup>	0.7 ± 0.2 x10 <sup>6</sup>	0.004 ± 0.002	0.0010 ± 0.0002 <sup>a</sup>	0.006 ± 0.004

a: D. Guo, J Biomol Screen, 2013.<sup>26</sup>

b: Apparent kinetic values were calculated for covalently binding FSCPX

With the association and dissociation rates validated for the marker ligands, MS binding competition association assays were performed. The competition association curves in the presence of FSCPX (hA<sub>1</sub>AR) and LUF6632 (hA<sub>2A</sub>AR) yielded an “overshoot” shape typical for slowly dissociating ligands, while in the presence of 8-CPT (hA<sub>1</sub>AR) and MSX-2 (hA<sub>2A</sub>AR), the curves were typical for fast-dissociating ligands (Figure 6). FSCPX displaced the marker ligand DPCPX completely after 120 min. The association rates of 8-CPT and MSX-2 agreed well between MS binding and radioligand binding assays, but less so in case of FSCPX and LUF6632 (Tables 5 and 6). The dissociation rates of 8-CPT, MSX-2, and LUF6632 were in good agreement as well, but not the apparent dissociation rate of FSCPX.

**Table 6.** Association and dissociation rates of ZM-241,385, MSX-2, and LUF6632 determined in MS binding and radioligand binding assays on the hA<sub>2A</sub>AR. MS binding (M/IS) values were obtained by analysis with compensation by internal standard, just as the MS binding values in Tables 2-4. MS binding (marker) values were obtained by analysis of marker chromatograms solely, without compensation by internal standard, and thus label-free. The kinetic values of ZM-241,385 were determined by association and dissociation assays, while the kinetic values of MSX-2 and LUF6632 were determined by competition association assays with 3 nM ZM-241,385 as marker ligand. Values are mean  $k_{on}$  in  $M^{-1} \text{ min}^{-1} \pm \text{SEM}$  and mean  $k_{off}$  in  $\text{min}^{-1}$  of at least three independent experiments performed in duplicate.

	$k_{on} \pm \text{SEM} (M^{-1} \text{ min}^{-1})$			$k_{off} \pm \text{SEM} (\text{min}^{-1})$		
	MS binding (M/IS)	Radio-ligand binding	MS binding (marker)	MS binding (M/IS)	Radio-ligand binding	MS binding (marker)
<b>ZM-241,385</b>	$9.5 \pm 0.7 \times 10^7$	$13 \pm 6 \times 10^{7(a)}$	$9.8 \pm 2.0 \times 10^7$	$0.019 \pm 0.002$	$0.014 \pm 0.003^a$	$0.021 \pm 0.005$
<b>MSX-2</b>	$5.4 \pm 0.6 \times 10^6$	$2.4 \pm 0.2 \times 10^6$	$9.3 \pm 1.3 \times 10^6$	$0.027 \pm 0.005$	$0.026 \pm 0.004$	$0.063 \pm 0.022$
<b>LUF6632</b>	$0.7 \pm 0.1 \times 10^7$	$3.4 \pm 0.4 \times 10^{7(a)}$	$1.8 \pm 0.7 \times 10^7$	$0.0028 \pm 0.0001$	$0.0031 \pm 0.0002^a$	$0.030 \pm 0.011$

a: D. Guo, ChemMedChem, 2014.<sup>14</sup>

Linear regression performed on the correlation plots of MS binding data (based on M/IS detection) against radioligand binding data yielded the following coefficients of determination and equations:  $R^2 = 0.985$  and  $y = 1.04x - 0.199$  ( $K_i$  and  $K_D$ , Figure 7A),  $R^2 = 0.775$  and  $y = 0.738x + 2.09$  ( $k_{on}$ , Figure 7C), and  $R^2 = 0.968$  and  $y = 1.06x - 0.0550$  ( $k_{off}$ , Figure 7E). Similar correlation plots of MS binding data without IS compensation, solely based on marker peak area, against radioligand binding data yielded  $R^2 = 0.988$  and  $y = 1.05x - 0.299$  ( $K_i$  and  $K_D$ , Figure 7B),  $R^2 = 0.735$  and  $y = 0.767x + 1.82$  ( $k_{on}$ , Figure 7D), and  $R^2 = 0.940$  and  $y = 1.33x - 0.0168$  ( $k_{off}$ , Figure 7F).

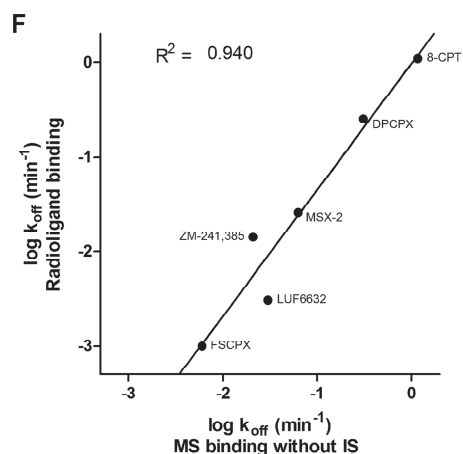
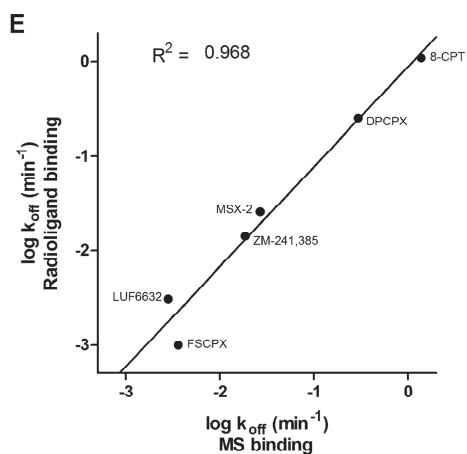
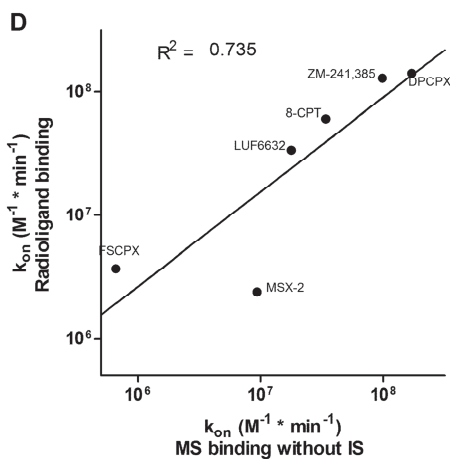
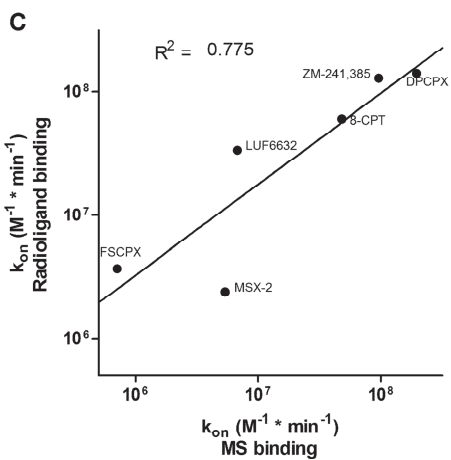
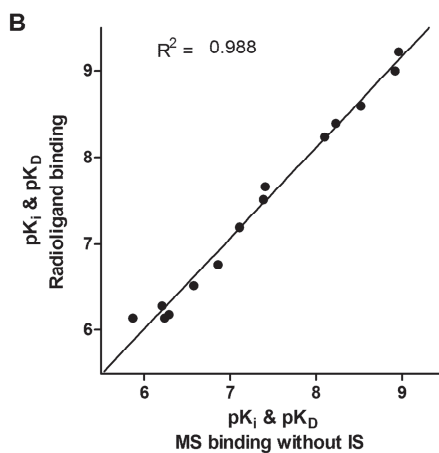
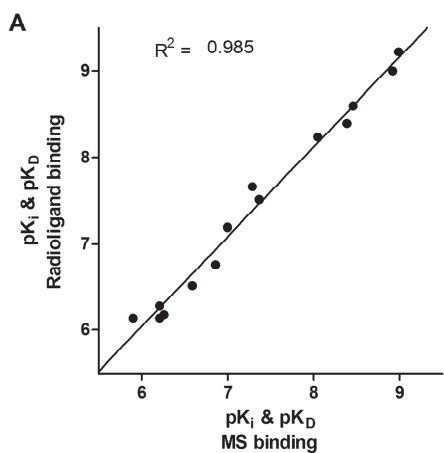


**Figure 7.** (Previous page). Correlation plots of results obtained by MS binding and radioligand binding assays on hA<sub>1</sub>AR and hA<sub>2A</sub>AR. Values of marker ligands DPCPX and ZM-241,385 were measured directly on their respective binding targets hA<sub>1</sub>AR and hA<sub>2A</sub>AR by saturation (**A**, **B**), association (**C**, **D**), and dissociation (**E**, **F**) assays, while values of the competing ligands were measured indirectly by displacement (**A**, **B**) and competition association assays (**C-F**). Affinity values in pK<sub>D</sub> and pK<sub>i</sub> (**A**, **B**), association rates in k<sub>on</sub> (**C**, **D**), and dissociation rates in log k<sub>off</sub> (**E**, **F**) were compared. Correlation plots **A**, **C**, and **E** show MS binding results standardized with deuterium-labeled internal standard, while **B**, **D**, and **F** show truly label-free MS binding results without internal standard. Data points represent mean values of at least three separate experiments performed in duplicate. R<sup>2</sup> values were calculated by linear regression performed on log-transformed values.

## Discussion

### Preparation of internal standards

Including an internal or external standard is good practice in mass spectrometry, to compensate for ion suppression by matrix effects from cell contents, sample evaporation, and instrumental drift.<sup>10</sup> We used the internal standard method as this is the most accurate manner to compensate for these sources of signal distortion and to increase the accuracy of MS methods. Preferably, the internal standard is a molecule with the same chemical properties as the molecule of interest but with a distinct mass. Hence, deuterated DPCPX (d4) and ZM-241,385 (d4) were synthesized to serve as internal standard for the MS binding assays on hA<sub>1</sub>AR and hA<sub>2A</sub>AR, respectively. The resulting mass difference between the parent compounds and their internal standards ensured minimal signal overlap by their isotope patterns. For the synthesis of [<sup>2</sup>H<sub>4</sub>]ZM-241,385 **5**, the pure isotopologue [<sup>2</sup>H<sub>4</sub>]tyrosine (SI 14) was commercially available as precursor for the [<sup>2</sup>H<sub>4</sub>]tyramine **4** building block. For the synthesis of [<sup>2</sup>H<sub>4</sub>]DPCPX **2**, the building block **1** was deuterated in-house by a rhodium-catalyzed reduction of two allylic double bonds in the presence of deuterium gas generated *in situ*. During this process, deuterium-hydrogen scrambling occurred which resulted in a mixture of isotopologues [<sup>2</sup>H<sub>0</sub>]DPCPX to [<sup>2</sup>H<sub>8</sub>]DPCPX in a Gaussian distribution as final product. This had no negative influence on the results of the MS Binding assays, since the masses of parent ions and fragments of the most abundant isotopologue [<sup>2</sup>H<sub>4</sub>]DPCPX **5** were selected for quantification.

## MS binding assays

Affinity, association, and dissociation rates measured directly for the marker ligands DPCPX on the hA<sub>1</sub>AR and ZM-241,385 on the hA<sub>2A</sub>AR were in good agreement to the values found in radioligand binding assays (Figures 3 and 5, Tables 2, 5, and 6). The good performance of the MS binding saturation, association, and dissociation assays in which solely the marker ligand and no competing ligand was present was a prerequisite to continue with the MS binding displacement and competition association assays.

To demonstrate the MS binding displacement assays, a combination of selective and nonselective agonists and antagonists were chosen as competing ligands. For the hA<sub>1</sub>AR these ligands were CPA, 8-CPT, ZM-241,385, and NECA, and for the hA<sub>2A</sub>AR they were UK-432,097, MSX-2, DPCPX, and NECA. The determined affinity values were in good agreement between MS binding and radioligand binding assays for all these competing ligands (Figure 4, Tables 3 and 4). Furthermore, the binding of agonists CPA and NECA to the hA<sub>1</sub>AR fitted to a pronounced two-phase displacement curve as was found before in radioligand binding assays.

Kinetic properties of ligands are of emerging interest and are thought to be important predictors of clinical performance.<sup>3,27</sup> Therefore, we developed and validated MS binding competition association assays by which kinetic properties of competing ligands can be analyzed by measuring the amount of bound marker ligand at different time points in the presence of one concentration of these competing ligands. A fast and a slowly dissociating competing ligand were chosen for each target. Fast- and slow-dissociating ligands yield distinct characteristic competition association graphs, without and with overshoot, respectively. For the hA<sub>1</sub>AR the ligands 8-CPT and FSCPX, and for hA<sub>2A</sub>AR MSX-2 and LUF6632 were tested. 8-CPT and MSX-2 dissociate fast from their targets. FSCPX is an irreversibly binding antagonist selective for the hA<sub>1</sub>R<sup>13, 28, 29</sup> and thus yields the characteristic overshoot graph for slowly dissociating ligands,<sup>26</sup> with the exception that it eventually displaces the marker ligand DPCPX completely (Figure 6A). LUF6632 was characterized earlier as a slowly dissociating ligand selective for the hA<sub>2A</sub>AR.<sup>14</sup>

Dissociation rates were in good agreement between the MS binding and radioligand binding competition association assays (Figure 7E, Tables 5 and 6), with the exception of the apparent dissociation rate of the irreversibly binding FSCPX (Table 5). Association rates found for the competing ligands in competition association assays varied more, especially

for the slowly or not at all dissociating ligands FSCPX and LUF6632 (Figure 7C, Tables 5 and 6). It has to be noted that as it binds irreversibly to the hA<sub>1</sub>AR, FSCPX does not actually dissociate from the target. However, fitting the FSCPX data into the competition association model still enables the calculation of apparent association and dissociation rates. Being apparent values, they may vary between studies which could be an explanation for the diverging kinetic rates of FSCPX found in MS binding and radioligand binding assays (Table 5).

Altogether, these results validate the use of MS binding assays to determine affinity values and dissociation rates by saturation, association, dissociation, and competition association assays. However, association rate determination was only accurate by direct measurement on the marker ligands.

### **Necessity of deuterium-labeled internal standard**

As mentioned above, including an internal or external standard is good practice in mass spectrometry. We used the internal standard method as this is the most accurate manner to compensate for sources of signal distortion. However, the use of a deuterium-labeled internal standard makes the MS binding assay a labeled assay, even if the marker ligand that binds to the target is itself unlabeled. For fast screening of new marker ligands, the use of an external standard or even no standard at all would be vastly advantageous, as the whole assay becomes an unlabeled assay. Moreover, to directly determine association and dissociation rates of nonlabeled ligands would be an improvement over the use of competition association assays. Therefore, we compared the performance of the MS binding assay with and without compensation by deuterium-labeled internal standard. Although in the latter case the resulting graphs of each separate experiment were somewhat less accurate,  $K_i$  and  $K_D$  values could still be determined without loss of accuracy (Figure 7B). The  $k_{off}$  values indirectly determined by the competition association assay correlated less well with radioligand binding assays, although retaining a good coefficient of determination (Figure 7F). The determination of  $k_{on}$  values correlated less well with radioligand binding assays irrespective of the use of an internal standard (Figures 7C and D). In contrast to this, the directly measured association and dissociation rates of marker ligands DPCPX and ZM-241,385 were still in good agreement with radioligand binding experiments (Tables 5 and 6).

## Conclusions

We developed and validated MS binding assays for the adenosine A<sub>1</sub> and A<sub>2A</sub> receptors. The results from ligand saturation, association, dissociation, and displacement assays were in good agreement with radioligand binding data. The results from competition association assays were in good agreement with radioligand binding data for dissociation rates but less so for association rates. Furthermore, we investigated the necessity to include deuterium-labeled internal standards in MS binding assays. Saturation, association, dissociation, and displacement assay results were still in good agreement with radioligand binding assays when the internal standard was not included. In competition association assays, the inclusion of an internal standard was beneficial for good correlation of dissociation rates with radioligand binding data. However, by excluding the use of internal standards in MS binding assays, it would be relatively simple to measure association and dissociation rates of a number of unlabeled ligands directly, without the need for competition association assays. We conclude that the use of deuterium-labeled internal standards is in this case unnecessary which makes the MS binding assay a truly unlabeled ligand binding assay. As this internal standard-free approach may be applied to other targets than the currently investigated adenosine A<sub>1</sub> and A<sub>2A</sub> receptors, we foresee the promising future application of MS binding to directly measure binding properties by saturation, association, and dissociation assays, without the use of any labeled internal standards.



## Supplemental information

Supplemental information includes full experimental procedures for synthesis of [<sup>2</sup>H<sub>4</sub>]DPCPX **2** and [<sup>2</sup>H<sub>4</sub>]ZM-241,385 **5**, including Schemes 3 and 4, and can be found with this article online at [dx.doi.org/10.1007/s11302-015-9477-0](https://doi.org/10.1007/s11302-015-9477-0)

## Acknowledgments

We kindly thank Dr. G. Höfner and Prof. K. T. Wanner (Ludwig Maximilians University, München, Germany) for their advice on MS binding assays and J. C. Schoeman (LACDR, Leiden University, The Netherlands) for his advice on triple quadrupole MS handling. MSX-2 and UK-432,097 were kind gifts from Prof. C. E. Müller (Bonn University, Germany) and Pfizer's Compound Transfer Program, respectively. This work was supported by the Netherlands Organization for Scientific Research - Chemical Sciences (Grant 714.011.001).

## References

1. Hulme EC and Trevethick MA, *Ligand binding assays at equilibrium: validation and interpretation*. Br J Pharmacol, 2010. 161(6): p. 1219-37.
2. Lohse MJ, Nuber S, and Hoffmann C, *Fluorescence/bioluminescence resonance energy transfer techniques to study G-protein-coupled receptor activation and signaling*. Pharmacol Rev, 2012. 64(2): p. 299-336.
3. Hoffmann C, Castro M, Rinken A, et al., *Ligand residence time at G-protein-coupled receptors-why we should take our time to study it*. Mol Pharmacol, 2015. 88(3): p. 552-60.
4. Grimm SH, Höfner G, and Wanner KT, *MS Binding assays for the three monoamine transporters using the triple reuptake inhibitor (1R,3S)-indatraline as native marker*. ChemMedChem, 2015. 10(6): p. 1027-39.
5. Hess M, Höfner G, and Wanner KT, *Development and validation of a rapid LC-ESI-MS/MS method for quantification of fluoxetine and its application to MS binding assays*. Anal Bioanal Chem, 2011. 400(10): p. 3505-15.
6. Fredholm BB, IJzerman AP, Jacobson KA, et al., *International Union of Basic and Clinical Pharmacology. LXXXI. Nomenclature and classification of adenosine receptors — an update*. Pharmacol Rev, 2011. 63(1): p. 1-34.
7. Chen JF, Eltzhösch HK, and Fredholm BB, *Adenosine receptors as drug targets — what are the challenges?* Nat Rev Drug Discovery, 2013. 12(4): p. 265-86.
8. Lohse MJ, Klotz KN, Lindenborn-Fotinos J, et al., *8-Cyclopentyl-1,3-dipropylxanthine (DPCPX) - a selective high affinity antagonist radioligand for A<sub>1</sub> adenosine receptors*. Naunyn Schmiedebergs Arch Pharmacol, 1987. 336(2): p. 204-10.
9. Alexander SPH and Millns PJ, *[<sup>3</sup>H]ZM241385 - an antagonist radioligand for adenosine A<sub>2A</sub> receptors in rat brain*. Eur J Pharmacol, 2001. 411(3): p. 205-10.
10. Mulvana DE, *Critical topics in ensuring data quality in bioanalytical LC-MS method development*. Bioanalysis, 2010. 2(6): p. 1051-72.
11. Botitsi HV, Garbis SD, Economou A, et al., *Current mass spectrometry strategies for the analysis of pesticides and their metabolites in food and water matrices*. Mass Spectrom Rev, 2011. 30(5): p. 907-39.

12. Müller CE, Maurinsh J, and Sauer R, *Binding of [<sup>3</sup>H]MSX-2 (3-(3-hydroxypropyl)-7-methyl-8-(m-methoxystyryl)-1-propargylxanthine) to rat striatal membranes—a new, selective antagonist radioligand for A<sub>2A</sub> adenosine receptors*. Eur J Pharm Sci, 2000. 10(4): p. 259-65.
13. Van Muijlwijk-Koezen JE, Timmerman H, Van der Sluis RP, et al., *Synthesis and use of FSCPX, an irreversible adenosine A<sub>1</sub> antagonist, as a 'receptor knock-down' tool*. Bioorg Med Chem Lett, 2001. 11(6): p. 815-8.
14. Guo D, Xia L, Van Veldhoven JP, et al., *Binding kinetics of ZM241385 derivatives at the human adenosine A<sub>2A</sub> receptor*. ChemMedChem, 2014. 9(4): p. 752-61.
15. Devi I and Bhuyan PJ, *An expedient method for the synthesis of 6-substituted uracils under microwave irradiation in a solvent-free medium*. Tetrahedron Letters, 2005. 46(34): p. 5727-29.
16. Soriano A, Ventura R, Molero A, et al., *Adenosine A<sub>2A</sub> receptor-antagonist/dopamine D<sub>2</sub> receptor-agonist bivalent ligands as pharmacological tools to detect A<sub>2A</sub>-D<sub>2</sub> receptor heteromers*. J Med Chem, 2009. 52(18): p. 5590-602.
17. Erickson RH, Hiner RN, Feeney SW, et al., *1,3,8-trisubstituted xanthines. Effects of substitution pattern upon adenosine receptor A<sub>1</sub>/A<sub>2</sub> affinity*. J Med Chem, 1991. 34(4): p. 1431-5.
18. Jörg M, Agostino M, Yuriev E, et al., *Synthesis, molecular structure, NMR spectroscopic and computational analysis of a selective adenosine A<sub>2A</sub> antagonist, ZM 241385*. Structural Chemistry, 2013. 24(4): p. 1241-51.
19. Jörg M, Shonberg J, Mak FS, et al., *Novel adenosine A<sub>2A</sub> receptor ligands: a synthetic, functional and computational investigation of selected literature adenosine A<sub>2A</sub> receptor antagonists for extending into extracellular space*. Bioorg Med Chem Lett, 2013. 23(11): p. 3427-33.
20. Ntai I, Phelan VV, and Bachmann BO, *Phosphonopeptide K-26 biosynthetic intermediates in Astrosporangium hypotensionis*. Chem Commun (Camb), 2006(43): p. 4518-20.
21. Smith PK, Krohn RI, Hermanson GT, et al., *Measurement of protein using bicinchoninic acid*. Anal Biochem, 1985. 150(1): p. 76-85.
22. Guo D, Venhorst SN, Massink A, et al., *Molecular mechanism of allosteric modulation at GPCRs: insight from a binding kinetics study at the human A<sub>1</sub> adenosine receptor*. Br J Pharmacol, 2014. 171(23): p. 5295-312.
23. Guo D, Mulder-Krieger T, P. IA, et al., *Functional efficacy of adenosine A<sub>2A</sub> receptor agonists is positively correlated to their receptor residence time*. Br J Pharmacol, 2012. 166(6): p. 1846-59.
24. Motulsky HJ and Mahan LC, *The kinetics of competitive radioligand binding predicted by the law of mass action*. Mol Pharmacol, 1984. 25(1): p. 1-9.
25. Adair GRA, Kapoor KK, Scolan ALB, et al., *Ruthenium catalysed reduction of alkenes using sodium borohydride*. Tetrahedron Letters, 2006. 47(50): p. 8943-4.
26. Guo D, Van Dorp EJ, Mulder-Krieger T, et al., *Dual-point competition association assay: a fast and high-throughput kinetic screening method for assessing ligand-receptor binding kinetics*. J Biomol Screen, 2013. 18(3): p. 309-20.
27. Guo D, Hillger JM, Ilzerman AP, et al., *Drug-target residence time—a case for G protein-coupled receptors*. Med Res Rev, 2014. 34(4): p. 856-92.
28. Scammells PJ, Baker SP, Belardinelli L, et al., *Substituted 1,3-dipropylxanthines as irreversible antagonists of A<sub>1</sub> adenosine receptors*. J Med Chem, 1994. 37(17): p. 2704-12.
29. Srinivas M, Shryock JC, Scammells PJ, et al., *A novel irreversible antagonist of the A<sub>1</sub>-adenosine receptor*. Mol Pharmacol, 1996. 50(1): p. 196-205.

# **Chapter 7**

## **Conclusions and future perspectives**

The main theme of this thesis, allosteric modulation effectuated through the sodium ion site of GPCRs, is inspired by the important role that this site appears to play in GPCR signaling. As sodium ions are abundant under physiological conditions they may affect GPCR signaling considerably. Receptor activation causes a substantial rearrangement of the sodium ion site, suggesting that it has an important role in this process.<sup>1</sup>

Chapter 2 reviews the current knowledge on allosteric modulation of amiloride and its derivatives binding to the sodium ion site of Class A GPCRs. Chapters 3 to 5 follow-up on the recent crystal structure of the adenosine  $A_{2A}$  receptor with a sodium ion bound.<sup>2</sup> Chapters 3 and 4 complement the crystal structure with additional results from combined biochemistry, biophysical, molecular dynamics, and mutational studies. Chapter 5 describes the synthesis of novel amiloride derivatives that bind in the sodium ion site but also protrude into the orthosteric binding site. In Chapters 3 to 5, radio-labeled ligands were used to quantify ligand binding to the receptor, and Chapter 6 describes an alternative approach towards ligand binding assays. Instead of using a radio-label, mass spectrometry was used to quantify the binding of an unlabeled ligand to the adenosine  $A_1$  and  $A_{2A}$  receptors.

## Conclusions

### **A versatile allosteric site and tool compounds to probe its properties**

Even though the sodium ion site is a well conserved allosteric site among Class A GPCRs, it is versatile in the ligands that it can bind and the resulting allosteric effects. Not only does it bind the sodium ion, but also the small molecule amiloride and its derivatives. Chapter 2 of this thesis reviews the variety of amiloride derivatives and the different allosteric effects that they can exert on Class A GPCRs. A general trend is the higher affinity for GPCRs of amilorides with lipophilic substituents over the parent amiloride. Amilorides have been found to allosterically modulate adenosine, adrenergic, dopamine, chemokine, muscarinic, serotonin and gonadotropin-releasing hormone receptors. Of these, the adenosine,  $\alpha$ -adrenergic, and dopamine receptors experience the highest degree of modulation by amiloride and analogues. Due to the fact that the sodium ion site is well conserved it is to be expected that amilorides can also bind and modulate other GPCRs not yet investigated for their sensitivity.

The allosteric effects triggered by amilorides binding to GPCRs can be divided in positive and negative allosteric modulation, and competitive and noncompetitive displacement of the orthosteric ligand. The type of allosteric effect depends on whether the orthosteric ligand is an agonist or an antagonist and on the specific GPCR type. Even for closely related sub-types of GPCRs the effects can be quite different. For most receptors amilorides act as negative allosteric modulators of both agonist and antagonist binding. However, for some receptors amilorides display probe dependency as they act as positive allosteric modulators of agonist binding but not of antagonist binding. Examples of this amiloride probe dependency have been found for the adenosine  $A_3$  and the  $\alpha_{2A}$ -adrenergic receptors. In the case of the  $\alpha_{2B}$ -adrenergic receptor differently substituted amiloride derivatives can even have either negative or positive allosteric effects on antagonist binding. The flexibility of such a conserved site to exert different allosteric effects by the binding of very similar molecules is intriguing and suggests a role for amino acids not directly involved in sodium ion binding.

## **A physiological role for allosteric modulation**

Allosteric modulation as a general concept has been found on many different targets, also beyond the GPCR superfamily. As a definition, allosteric sites are distinct from orthosteric sites where endogenous ligands bind. This implies that no (known) endogenous ligands bind to allosteric sites, and hence allosteric ligands are usually found in high-throughput screens of large collections of non-endogenous ligands.<sup>3</sup> This does not exclude that allosteric sites have no endogenous ligands binding to them, but in general these have not been found.<sup>4</sup> Without the need to accommodate the binding of endogenous ligands, allosteric sites have supposedly less evolutionary pressure to stay the same. This is an advantage for drug design for sub-types of GPCRs. The orthosteric site of receptor sub-types (for instance the adenosine A<sub>1</sub>, A<sub>2A</sub>, A<sub>2B</sub>, and A<sub>3</sub> receptors) endure evolutionary pressure to keep similar features, as they bind the same endogenous ligands, and this is a challenge when designing ligands selective for one sub-type. Allosteric sites which do not feel this evolutionary pressure can have more diverse features, making it easier to develop ligands that are sub-type selective.<sup>4,5</sup>

The allosteric sodium ion binding site is an exception to this rule. First of all, the sodium ion binds in this site, which may be defined as an endogenous ligand, for its abundant presence in the body. The sodium ion site is remarkably well conserved amongst Class A GPCRs, suggesting major evolutionary pressure to maintain its features.<sup>1</sup> Indeed, one of the conclusions of Chapter 3 of this thesis is that the physiological concentration of sodium ions is high enough to occupy the sodium ion site of 75 % of adenosine A<sub>2A</sub> receptors present in the body, substantially reducing their sensitivity to activation by endogenous adenosine. This points to a role of sodium ions as suppressors of in-vivo adenosine A<sub>2A</sub> receptor activation. Again, the high conservation of the sodium ion site amongst Class A GPCRs suggests that this is an important general mechanism for organisms to control GPCR activity. Indeed, the inhibitory effect of sodium ions at physiologically relevant concentrations has been found for many GPCRs. This also implies the importance to control sodium ion concentrations for in vitro ligand binding assays.

### **Sodium ions stabilize the adenosine A<sub>2A</sub> receptor in the inactive state**

Even without access to structural information, a few decades of studying the effects of sodium ions and amiloride on GPCRs established that they bind to an allosteric site, instead of the orthosteric site. The recent elucidation of GPCR crystal structures with a bound sodium ion revealed the molecular details of its binding in the allosteric sodium ion site. Previous crystal structures of GPCRs in the antagonist-bound state likely had a sodium ion bound in the sodium ion site, as usually a large concentration of sodium ions is added to stabilize the inactive state of the receptor, but the relatively small ion could not be detected due to the limited resolution of these structures.<sup>1</sup> The first crystal structure with sufficiently high resolution to reveal a bound sodium ion was of the adenosine A<sub>2A</sub> receptor.<sup>2</sup> The sodium ion was held by a ionic interaction with Asp52<sup>2,50</sup>, confirming previous results tying this residue to sodium ion effects,<sup>6</sup> and a hydrogen-bonding network of waters and amino acids forming the sodium ion site. One of the most eye-catching differences between the inactive sodium ion bound structure and the active structure was the occlusion of the sodium ion site in the active structure, which suggested that binding of a sodium ion to an agonist-bound receptor is impossible.

Chapter 3 follows up on this crystal structure studying in more detail the differences in allosteric effects exerted by sodium ions and amilorides binding in the sodium ion site. The allosteric effects of sodium ions, amiloride, and its analogue HMA on orthosteric ligand binding to the adenosine A<sub>2A</sub> receptor were evaluated by a combination of molecular dynamics, radioligand binding, and thermostability studies. It was concluded that an antagonist ([<sup>3</sup>H]ZM-241,385) and a sodium ion can bind to the receptor simultaneously, while the binding of an agonist ([<sup>3</sup>H]NECA) and a sodium ion excludes each other. The results indicated that binding of a sodium ion to the sodium ion site stabilizes the receptor in its inactive conformation, thereby prohibiting agonist binding, but facilitating antagonist binding. The stabilization of Trp246<sup>6,48</sup> by the sodium ion appeared to play an important role in maintaining the inactive conformation. This fits well with the previous identification of Trp246<sup>6,48</sup> as a “toggle switch” for receptor activation.<sup>7</sup>

In contrast to sodium ions, amiloride and HMA displaced both the agonist and antagonist, but they still displayed distinct allosteric effects between the two. Similar to sodium ions, the amilorides displaced agonist [<sup>3</sup>H]NECA competitively, while the amilorides and antagonist [<sup>3</sup>H]ZM-241,385 could bind simultaneously. Unlike sodium ions

however, the amilorides displaced the antagonist in a noncompetitive manner, likely by pushing Trp246<sup>6.48</sup> into a different rotameric position. This suggests that amiloride binding results in a delicate balance between improved stability of the inactive receptor conformation and an indirect, noncompetitive, interference with antagonist binding.

### **Mutations to further investigate the sodium ion site**

The presence or absence of a sodium ion in its binding site seems to dictate the conformation of the receptor in either its inactive or active states, respectively. Hence, Chapter 4 of this thesis focuses on the amino acids forming the sodium ion site and their purpose in receptor activation. Site-directed single point mutations into alanine of Asp52<sup>2.50</sup>, Ser91<sup>3.39</sup>, Trp246<sup>6.48</sup>, Asn280<sup>7.45</sup>, and Asn284<sup>7.49</sup> were evaluated for their effect on orthosteric ligand binding, allosteric modulation by sodium ions and amilorides, and receptor activation. Except for Asp52<sup>2.50</sup>, the mutation of these sodium ion site amino acids lowered the affinity of agonist [<sup>3</sup>H]NECA binding substantially, but did not affect antagonist [<sup>3</sup>H]ZM-241,385 binding as much. As Trp246<sup>6.48</sup> is the only residue interacting directly with an agonist binding in the orthosteric site, the residues Ser91<sup>3.39</sup>, Asn280<sup>7.45</sup>, and Asn284<sup>7.49</sup> must be important for maintaining a conformation of the receptor that is indirectly suitable for agonist binding.

All these sodium ion site mutations either abrogated or reduced the negative allosteric effect of sodium ions on agonist binding, but had mixed effects on amiloride and its derivative HMA. D52A<sup>2.50</sup> reduced their potency, confirming the docking pose of the amilorides in which their positively charged guanidinium moiety engages in an ionic bond with the negatively charged Asp52<sup>2.50</sup>, similar to the sodium ion. In contrast, W246A<sup>6.48</sup>, N280A<sup>7.45</sup>, and N284A<sup>7.49</sup> increased the potency of the amilorides, with a remarkably large effect of the Trp246<sup>6.48</sup> mutation. This indicates that these residues hinder the binding of amiloride and HMA into the sodium ion site.

Finally, mutation of the amino acids forming the sodium ion site substantially affected receptor activation. Mutations D52A<sup>2.50</sup> and N284A<sup>7.49</sup> completely abolished the receptor's ability to be activated, while mutations S91A<sup>3.39</sup> and N280A<sup>7.45</sup> induced constitutive activity of the receptor, and mutations S91A<sup>3.39</sup>, W246A<sup>6.48</sup>, and N280A<sup>7.45</sup> decreased the agonist activation response of the receptor. From this it can be concluded that besides their effect on sodium ion, amiloride, and orthosteric ligand binding, the amino acids forming the sodium ion site are involved in the activation mechanism of the adenosine A<sub>2A</sub> receptor.



In molecular dynamics simulations, D52A<sup>2.50</sup> caused the sodium ion to dissociate promptly towards a vestibule pocket, formed by Glu13<sup>1.39</sup> and His278<sup>7.43</sup>, suggesting a pathway for sodium ion entering the sodium ion site. Indeed these residues had been found to be important for allosteric modulation by sodium ions in a previous mutation study.<sup>8</sup> His278<sup>7.43</sup> is also important for agonist binding, as shown in the same study and in the agonist-bound crystal structure of the adenosine A<sub>2A</sub> receptor, suggesting a second site next to the sodium ion site where sodium ions can antagonize agonist binding.

### **Larger amiloride derivatives reach into the orthosteric binding site**

The abundance of different 5'-substituted amiloride analogues that can allosterically modulate the adenosine A<sub>2A</sub> receptor but also GPCRs in general, encourages further investigation of the possibilities for different moieties on this position. In Chapter 5, different phenethyl substitutions on the 5' position of amiloride were evaluated for their allosteric effect on binding of the antagonist [<sup>3</sup>H]ZM-241,385 to the wild-type and W246A<sup>6.48</sup> mutated adenosine A<sub>2A</sub> receptor. On the wild-type receptor, the 4-ethoxyphenethyl substituted amiloride yielded a higher potency than reference amiloride HMA, while methoxy and dioxolylphenethyl derivatives had potencies similar to HMA. Docking of these derivatives of amiloride in the sodium ion site suggested that their phenethyl moieties entered a hydrophobic pocket close to the sodium ion site, explaining the preference for lipophilic moieties on this position.

Just as for HMA, the novel phenethyl amiloride derivatives had a higher potency for the W246A<sup>6.48</sup> mutated receptor, confirming their binding in the sodium ion site. Indeed, docking of these amiloride phenethyl-derivatives revealed a steric clash with residue Trp246<sup>6.48</sup>, pushing it towards another rotameric position, just as observed for amiloride and HMA in Chapter 3. The bulkiest dioxolyl and ethoxyphenethyl derivatives benefited the most in their potency from the absence of the tryptophan, suggesting that bulkier 5' substituents increase the steric clash with Trp246<sup>6.48</sup>.

The docking modes of the amiloride derivatives predicted that their elongated phenethyl substituents protrude into the orthosteric site pocket and can engage in a direct competition with orthosteric ligands. This was supported by the observed effects of the amilorides on the dissociation kinetics of antagonist [<sup>3</sup>H]ZM-241,385 on the wild-type receptor. Whereas HMA accelerated antagonist dissociation the most, signifying a noncompetitive interaction, the phenethyl derivatives had less effect on antagonist

dissociation. The dioxolylphenethyl derivative did not affect the dissociation of the antagonist at all, signifying a completely competitive displacement of the antagonist.

### **An unlabeled ligand binding assay**

In Chapters 3 to 5 of this thesis radioligand binding assays were applied to quantify ligand binding to the adenosine A<sub>2A</sub> receptor. Although radioligands are recognized as robust and reliable tools in the measurement of ligand binding, they have their drawbacks in terms of safety, production costs, and waste disposal. Alternative ligand binding assays are therefore of interest. Such an alternative approach was sought in the quantification of the binding of unlabeled ligands to their targets by mass spectrometry, or MS binding. The ongoing development of mass spectrometers increases their sensitivity and has opened the possibility to accurately quantify the small amounts of ligands that are found in ligand binding assays, usually in the pM range. The group of Wanner has pioneered the MS binding assay for several targets, among which GPCRs.<sup>9</sup> In Chapter 6 of this thesis, we developed and validated the MS binding assays for additional GPCR targets, the adenosine A<sub>1</sub> and A<sub>2A</sub> receptors.

As unlabeled marker ligands for the MS binding assay DPCPX and ZM-241,385 were chosen, ligands with a high selectivity and affinity for the adenosine A<sub>1</sub> and A<sub>2A</sub> receptors, respectively. The application of marker ligands in MS binding is analogous to radioligands in radioligand binding, and the availability of radio-labeled versions of these ligands makes for a straightforward validation of the MS binding assay by radioligand binding assays. Although the ligand that is binding to the receptor itself is unlabeled, it is good practice in mass spectrometry to add a fixed concentration of internal standard to each injected sample to increase the accuracy of MS quantification. Preferably this is a deuterated version of the marker ligand, which has the same column retention time due to similar chemical properties, but can be discerned in MS by its different molecular weight. For this purpose, deuterium-labeled DPCPX and ZM-241,385 were synthesized. Subsequently, an LC-MS method to quantify pM concentrations of the marker ligands was developed, with their deuterium-labeled counterparts as internal standards.

With the MS quantification method developed, saturation, association, and dissociation MS binding assays were performed and validated against radioligand binding assays. Furthermore, displacement assays were performed and validated in which the

affinity of other ligands can be indirectly measured through their competition with the marker ligand. Finally, the MS binding assay was for the first time successfully applied to the competition association assay, in which the marker ligand competes with another ligand for association to the receptor. This allows for the determination of association and dissociation rates of the other ligand indirectly through fitting the association data of the marker ligand to the model of Motulsky and Mahan.<sup>10</sup>

The necessity to use an internal standard in the mass spectrometry quantification step was scrutinized. The internal standard is used to compensate for sources of signal distortion in MS quantification. Ligand binding assays typically use multiple measuring points to determine affinity and kinetic properties of ligands, and this already leads to a certain degree of compensation for deviations of individual points. This aspect of ligand binding assays could mean that compensation of MS quantification results by an internal standard does not add significantly to their accuracy. Indeed, similar  $K_i$ ,  $k_{on}$ , and  $k_{off}$  values were obtained from data that was either compensated by internal standard quantification and from data without this compensation, indicating that an internal standard is not strictly necessary in MS binding assays. Thus, the MS binding assay allows to measure affinity and kinetic ligand properties without the need to synthesize any labeled ligand.

## Future perspectives

### Protein structure elucidation and GPCRs

The field of GPCR structural biology has been greatly advanced by the elucidation of the X-ray crystal structures of 30 different types of GPCRs. As to the sodium ion site, the elucidation of sodium ion-bound GPCR structures has revealed the molecular details of sodium ion binding, adding importantly to the already existing body of pharmacological evidence of modulation of GPCRs by sodium ions. The availability of structural information inspires new pharmacological studies of the sodium ion site, as exemplified by Chapters 3 to 5 of this thesis.

Many GPCRs remain to be crystallized though, as the GPCR family consists of more than 800 different receptors. As GPCRs are membrane proteins, they are hydrophobic in nature and this is one of the challenges in growing crystals that are viable for X-ray diffraction. This has mainly to do with their stability when taken out of their natural membrane environment. Except for rhodopsin, GPCR crystal structures could only be solved with the help of different protein engineering methods, such as thermostabilizing point mutations, insertion of hydrophilic regions obtained from other proteins, and deletion of flexible loop and terminus regions.<sup>11</sup> Additionally, the resulting engineered GPCRs should reach sufficiently high expression levels to produce the large quantities of pure protein needed for the crystallization process. One approach to facilitate the elucidation of crystal structures of the remaining human GPCRs, is to systematically screen all of them for suitable engineered fusion constructs with sufficiently high expression levels.<sup>12</sup>

A limitation of X-ray crystallography is that it only catches a snapshot of the protein structure that is frozen in time. However, GPCRs are dynamic proteins with many different possible conformations. The comparison of antagonist (inactive) and agonist (active) bound structures may reveal the global movements required for receptor activation, but less stable intermediate conformations will be likely missed as the actual activation process is not followed. Techniques that allow following protein dynamics in time are in full development for GPCRs, for example solid- and solution-state nuclear magnetic resonance (NMR) and serial femtosecond crystallography (SFX).

NMR allows detecting the dynamics of isotopically labeled amino acids. The study of GPCRs by NMR has been primarily focused on GPCR regions due to protein size restrictions of this technique.<sup>13</sup> However, through isotope labeling of a limited number of amino acids spread over the receptor, the global dynamics of the receptor's backbone can be followed, as recently applied to the  $\beta_1$ -adrenergic receptor<sup>14</sup> and the adenosine  $A_{2A}$  receptor.<sup>15</sup> SFX enables to gather data from protein crystals by X-ray free electron laser (XFEL) without damaging the proteins, in contrast to X-ray crystallography.<sup>16</sup> This allows structural data to be obtained at room temperature, thus physiologically more relevant than X-ray crystallography, and from smaller crystals, simplifying the crystal growth step. Until now SFX has been used to obtain structural GPCR snapshots, for example for the serotonin 5-HT<sub>2B</sub> receptor,<sup>17</sup> but it holds the promise of time-resolved structural studies of GPCR activation, for example on the conformational changes of rhodopsin induced by light.<sup>18</sup>

### **Advances in molecular dynamics**

The availability of structural information opened the possibility to apply molecular dynamics to computationally simulate GPCR dynamics.<sup>19</sup> With the captured snapshot from a crystal structure as a starting point, molecular dynamics simulates 'in silico' the subsequent events on an atomic and femtosecond scale. This allows to follow various processes, such as structural rearrangements upon receptor activation,<sup>20</sup> ligand association,<sup>21</sup> and ligand dissociation.<sup>22</sup> As techniques to follow structural receptor dynamics in real-time are still nascent, molecular dynamics may provide a good alternative. Even if molecular dynamics is a powerful tool to understand receptor dynamics on a molecular scale, it remains a simulation depending on force-fields that only approximate actual atomic interactions. This makes it desirable to support conclusions drawn from 'in silico' molecular dynamics studies by 'wet lab' biochemical experiments, as demonstrated in Chapters 3 and 4 of this thesis.

One of the drawbacks of molecular dynamics is the vast amount of computational power needed to simulate complex systems such as GPCRs on an atomic scale.<sup>19</sup> Calculations to complete microsecond simulations typically take weeks or months, while conformational rearrangements upon GPCR activation may take milliseconds to complete.<sup>23,24</sup> Certain 'tricks' can be applied to increase calculation speeds and simulation lengths, such as reducing energy barriers and temperature accelerated molecular dynamics,<sup>25</sup> but these also reduce the accuracy of the simulation. However, the availability

of computing power keeps expanding exponentially, which continuously enables molecular dynamics to tackle more complex systems while decreasing calculation times and increasing simulation accuracy.

### **Bitopic ligands and their implications**

Next to crystal structures with a sodium ion bound, a few crystal structures with small molecule allosteric modulators bound have been elucidated to date, namely of the M2 muscarinic receptor and the metabotropic glutamate 1 and 5 receptors.<sup>26-28</sup> Most of GPCR crystal structures have been co-crystallized with high affinity orthosteric ligands, as these reinforce protein stability substantially.<sup>29</sup> The generally low affinity of allosteric modulators for GPCRs is a challenge for acquiring high resolution crystal structures with these co-crystallized. Amiloride and HMA are no exception with their affinities in the  $\mu\text{M}$  range. A crystal structure of the adenosine  $A_{2A}$  receptor with an amiloride derivative co-crystallized would add much information to the findings of Chapters 3 to 5 of this thesis, for instance the exact mechanism behind the observed probe dependency and the differences in competitive interaction with orthosteric ligands. The results of Chapter 5 imply the possibility to synthesize a bitopic ligand, which binds in both the allosteric sodium ion site and the orthosteric site of the adenosine  $A_{2A}$  receptor. The increase in possible interactions of such a bitopic ligand upon binding to the receptor would likely result in a higher affinity than of an 'ordinary' amiloride derivative, making it a viable option for co-crystallization with the adenosine  $A_{2A}$  receptor.

Another drawback of amiloride and HMA is their nonselectivity, as they do not only bind to many GPCRs but also to other proteins. This makes their application in cell-based assays complicated, as it would be hard to pin-point their effects to one target. However, cell-based assays are necessary to study the effects of amiloride binding on the receptor activation. The recent finding that HMA induces the same conformation of the adenosine  $A_{2A}$  receptor as a partial agonist emphasizes the value of such a study.<sup>15</sup> A bitopic ligand could offer a solution, as it may be more selective through interaction with less conserved residues in the orthosteric site. The same interactions with the orthosteric site will probably mean that they do not behave as 'classic' allosteric modulators, but it would still be interesting to study their effects on GPCR signaling in a more physiologically relevant system.

### **Mass spectrometry binding without internal standard**

The application of MS binding without the need for a deuterium-labeled internal standard in Chapter 6 of this thesis has interesting implications for its further development. However, the lack of an internal standard would require a careful control of factors that distort mass spectrometry read-outs, i.e. evaporation rates during the elution step, and drift and ion suppression during the quantification step. Evaporation rates may be reduced by improvements in the elution protocol, for example by incorporating an evaporation step and subsequent resuspension of the residue in fixed amounts of elution buffer. Improved drift suppression might be reached by ongoing improvements in mass spectrometry equipment. Regarding ion suppression, we observed in our work that variable ion suppression was mainly caused by the presence of changing concentrations of 'cold' ligand in the elution buffer. For displacement and competition association assays this situation is a given, but in saturation, association, and dissociation assays the 'cold' ligand is inherently absent, thereby removing a substantial source of ion suppression. Without the need to synthesize a deuterium labeled internal standard, the development of LC-MS quantification protocols for marker ligands would be relatively fast, and this would allow to directly determine the  $K_D$  value and  $k_{on}$  and  $k_{off}$  rate constants of a series of ligands.

### **Other mass spectrometry prospects in membrane protein research**

Mass spectrometry is also applied in other ways in membrane protein research. One example is endogenous or native mass spectrometry (nMS) which identifies different membrane protein-lipid or ligand complexes by their different sizes.<sup>30</sup> Differently to the MS binding assay, the protein-ligand complex is not denatured before the mass spectrometry detection step, so that the intact native membrane protein assembly can be probed. To keep the protein intact during the nMS analysis asks for a more complex approach than with MS binding, but has the possibility to yield valuable information about protein interactions, as endogenous protein ensembles with lipids, peptides, and drugs can be detected and identified by their differences in mass. This technique may therefore yield great opportunities to find new (endogenous) allosteric modulators of membrane proteins and GPCRs in particular.

## Final note

This thesis provides a detailed insight in the value of the allosteric sodium ion site for GPCR functioning. Inspired by a high resolution crystal structure of the adenosine  $A_{2A}$  receptor with a sodium ion bound, we explored different aspects of the sodium ion site. This resulted in insights into the probe dependency of sodium ions and amilorides, evidence for the crucial role of the amino acids of the sodium ion site in receptor signaling, and opportunities to design novel bitopic amiloride derivatives that bind in both the sodium ion site and the orthosteric site. Furthermore, an unlabeled ligand binding assay was developed for the adenosine  $A_1$  and  $A_{2A}$  receptors by means of mass spectrometry. This MS binding assay proves to be an excellent alternative for the conventional radioligand binding assay, without the need to synthesize any labeled ligand.



## References

1. Katritch V, Fenalti G, Abola EE, et al., *Allosteric sodium in class A GPCR signaling*. Trends Biochem Sci, 2014. 39(5): p. 233-44.
2. Liu W, Chun E, Thompson AA, et al., *Structural basis for allosteric regulation of GPCRs by sodium ions*. Science, 2012. 337(6091): p. 232-36.
3. Hardy JA and Wells JA, *Searching for new allosteric sites in enzymes*. Curr Opin Struct Biol, 2004. 14(6): p. 706-15.
4. May LT, Leach K, Sexton PM, et al., *Allosteric modulation of G protein-coupled receptors*. Annu Rev Pharmacol Toxicol, 2007. 47: p. 1-51.
5. Congreve M, Langmead CJ, Mason JS, et al., *Progress in structure based drug design for G protein-coupled receptors*. J Med Chem, 2011. 54(13): p. 4283-311.
6. Horstman DA, Brandon S, Wilson AL, et al., *An aspartate conserved among G-protein receptors confers allosteric regulation of  $\alpha_2$ -adrenergic receptors by sodium*. J Biol Chem, 1990. 265(35): p. 21590-5.
7. Nygaard R, Frimurer TM, Holst B, et al., *Ligand binding and micro-switches in 7TM receptor structures*. Trends Pharmacol Sci, 2009. 30(5): p. 249-59.
8. Gao ZG, Jiang Q, Jacobson KA, et al., *Site-directed mutagenesis studies of human  $A_{2A}$  adenosine receptors: involvement of Glu<sup>13</sup> and His<sup>278</sup> in ligand binding and sodium modulation*. Biochem Pharmacol, 2000. 60(5): p. 661-8.
9. Neiens P, Höfner G, and Wanner KT, *MS Binding Assays for  $D_1$  and  $D_5$  Dopamine Receptors*. ChemMedChem, 2015. 10(11): p. 1924-31.
10. Motulsky HJ and Mahan LC, *The kinetics of competitive radioligand binding predicted by the law of mass action*. Mol Pharmacol, 1984. 25(1): p. 1-9.
11. Tate CG and Schertler GFX, *Engineering G protein-coupled receptors to facilitate their structure determination*. Curr Opin Struct Biol, 2009. 19(4): p. 386-95.
12. Lv X, Liu J, Shi Q, et al., *In vitro expression and analysis of the 826 human G protein-coupled receptors*. Protein Cell, 2016. 7(5): p. 325-37.
13. Cohen LS, Fracchiolla KE, Becker J, et al., *GPCR structural characterization: Using fragments as building blocks to determine a complete structure*. Biopolymers, 2014. 102(3): p. 223-43.
14. Isogai S, Deupi X, Opitz C, et al., *Backbone NMR reveals allosteric signal transduction networks in the  $\beta_1$ -adrenergic receptor*. Nature, 2016. 530(7589): p. 237-41.
15. Ye L, Van Eps N, Zimmer M, et al., *Activation of the  $A_{2A}$  adenosine G-protein-coupled receptor by conformational selection*. Nature, 2016. 533(7602): p. 265-8.
16. Piscitelli CL, Kean J, De Graaf C, et al., *A molecular pharmacologist's guide to G protein-coupled receptor crystallography*. Mol Pharmacol, 2015. 88(3): p. 536-51.
17. Liu W, Wacker D, Gati C, et al., *Serial femtosecond crystallography of G protein-coupled receptors*. Science, 2013. 342(6165): p. 1521-4.
18. Deupi X, *Relevance of rhodopsin studies for GPCR activation*. Biochim Biophys Acta, 2014. 1837(5): p. 674-82.
19. Durrant JD and McCammon JA, *Molecular dynamics simulations and drug discovery*. BMC Biol, 2011. 9(71).
20. Dror RO, Arlow DH, Maragakis P, et al., *Activation mechanism of the  $\beta_2$ -adrenergic receptor*. Proc Natl Acad Sci U S A, 2011. 108(46): p. 18684-9.
21. Dror RO, Pan AC, Arlow DH, et al., *Pathway and mechanism of drug binding to G-protein-coupled receptors*. Proc Natl Acad Sci U S A, 2011. 108(32): p. 13118-23.
22. Guo D, Pan AC, Dror RO, et al., *Molecular basis of ligand dissociation from the adenosine  $A_{2A}$  receptor*. Mol Pharmacol, 2016. 89(5): p. 485-91.

23. Lohse MJ, Nuber S, and Hoffmann C, *Fluorescence/Bioluminescence Resonance Energy Transfer Techniques to Study G-Protein-Coupled Receptor Activation and Signaling*. 2012. 64(2): p. 299-336.
24. Henzler-Wildman K and Kern D, *Dynamic personalities of proteins*. Nature, 2007. 450(7172): p. 964-72.
25. Zamora RJ, Uberuaga BP, Perez D, et al., *The modern temperature-accelerated dynamics approach*. Annu Rev Chem Biomol Eng, 2016.
26. Kruse AC, Ring AM, Manglik A, et al., *Activation and allosteric modulation of a muscarinic acetylcholine receptor*. Nature, 2013. 504(7478): p. 101-6.
27. Wu H, Wang C, Gregory KJ, et al., *Structure of a class C GPCR metabotropic glutamate receptor 1 bound to an allosteric modulator*. Science, 2014. 344(6179): p. 58-64.
28. Doré AS, Okrasa K, Patel JC, et al., *Structure of class C GPCR metabotropic glutamate receptor 5 transmembrane domain*. Nature, 2014. 511(7511): p. 557-62.
29. Cooke RM, Brown AJH, Marshall FH, et al., *Structures of G protein-coupled receptors reveal new opportunities for drug discovery*. Drug Discov Today, 2015. 20(11): p. 1355-64.
30. Gault J, Donlan JAC, Liko I, et al., *High-resolution mass spectrometry of small molecules bound to membrane proteins*. Nat Methods, 2016. 13(4): p. 333-6.

# Summary

The study of allosteric modulation offers new insights in the activation mechanisms of G protein-coupled receptors (GPCRs). The sodium ion site is an allosteric site that is well conserved among Class A GPCRs. Even though it is well conserved, the allosteric sodium ion site is versatile in its allosteric effects and the size of ligands that can bind, from sodium ions to 5'-amino and 2-guanidino substituted amilorides (**Chapter 2**). The adenosine A<sub>2A</sub> receptor was the first GPCR to be crystallized with a sufficiently high resolution to reveal a sodium ion bound in the sodium ion site. In this thesis I applied the adenosine A<sub>2A</sub> receptor as a model GPCR for the study of allosteric modulation effected by the sodium ion site (**Chapters 3 – 5**), and together with the adenosine A<sub>1</sub> receptor for the development of a ligand binding assay based on mass spectrometry (**Chapter 6**).

The sodium ion site and the orthosteric site of the adenosine A<sub>2A</sub> receptor can be occupied simultaneously when an antagonist is bound in the orthosteric site, but not when an agonist is bound (**Chapter 3**). Sodium ions seem to stabilize the inactive conformation, thereby promoting antagonist binding, but excluding agonist binding at a physiologically relevant sodium ion concentration. By binding into the sodium ion site, amiloride analogues also exhibit distinct patterns of agonist and antagonist modulation.

Next to its effect on orthosteric ligand binding, the allosteric sodium ion site facilitates receptor signaling (**Chapter 4**). Mutation of the amino acids that form the sodium ion site influenced the affinity of ligands binding to it and to the orthosteric site, but also changed the capacity of the receptor as a whole to be activated by agonists. Mutation of the polar residues in the sodium ion pocket was shown to either abrogate (D52A<sup>2.50</sup> and N284A<sup>7.49</sup>) or reduce (S91A<sup>3.39</sup>, W246A<sup>6.48</sup>, and N280A<sup>7.45</sup>) the negative allosteric effect of sodium ions on agonist binding. Mutations D52A<sup>2.50</sup> and N284A<sup>7.49</sup> completely abolished receptor signaling, while mutations S91A<sup>3.39</sup> and N280A<sup>7.45</sup> elevated basal activity and mutations S91A<sup>3.39</sup>, W246A<sup>6.48</sup>, and N280A<sup>7.45</sup> decreased agonist-stimulated receptor signaling. In molecular dynamics simulations D52A<sup>2.50</sup> directly affected the mobility of sodium ions, which readily migrated to another pocket formed by Glu13<sup>1.39</sup> and His278<sup>7.43</sup>. The D52A<sup>2.50</sup> mutation also decreased the potency of amiloride with respect to orthosteric ligand

displacement, but did not change orthosteric ligand affinity. In contrast, W246A<sup>6.48</sup> increased some of the allosteric effects of sodium ions and amiloride, while orthosteric ligand binding was decreased.

Amiloride can be extended with substituents at the 5' position to produce amiloride derivatives with different allosteric properties and similar or even higher potencies than HMA at the wild-type adenosine A<sub>2A</sub> receptor (**Chapter 5**). The potency of a series of 5'-substituted amiloride derivatives was assessed by their ability to displace orthosteric radioligand [<sup>3</sup>H]ZM-241,385 from both the wild-type and sodium ion site W246A<sup>6.48</sup> mutant adenosine A<sub>2A</sub> receptors. Of this series, 4-ethoxyphenethyl-substituted amiloride 12l was found to be more potent than HMA. Similar to amiloride and HMA, the novel amiloride derivatives showed significantly higher potencies at the W246A<sup>6.48</sup> mutant adenosine A<sub>2A</sub> receptor, implying that Trp246<sup>6.48</sup> hinders the binding of these amiloride derivatives. HMA showed the largest allosteric effect on [<sup>3</sup>H]ZM-241,385 dissociation, whereas the most potent novel amilorides 12h, i, k, and l showed reduced or no effects on this dissociation process. This indicates that these novel amilorides engage in a more direct competition with the orthosteric ligand, and it can be hypothesized that they do so by intrusion into the orthosteric pocket. The striking differences in effect on the dissociation of [<sup>3</sup>H]ZM-241,385 between the wild-type and W246A<sup>6.48</sup> adenosine A<sub>2A</sub> receptors imply that Trp246<sup>6.48</sup> influences the nature of the allosteric interaction by amilorides.

Mass spectrometry is a valid alternative to radioligand detection for the quantification of ligand binding to the adenosine A<sub>1</sub> and A<sub>2A</sub> receptors (**Chapter 6**). Despite the robustness of radioligand binding assays, they carry inherent disadvantages in terms of safety precautions, expensive synthesis, special laboratory requirements, and waste disposal. Mass spectrometry is a method that can selectively detect ligands without the need of a label. The sensitivity of mass spectrometry equipment increases progressively, and currently it is possible to detect the low ligand quantities that are usually found in ligand binding assays. We developed a label-free mass spectrometry ligand binding (MS binding) assay for the adenosine A<sub>1</sub> and A<sub>2A</sub> receptors. Radioligand binding assays for both receptors are well established, and ample data is available to compare and evaluate the performance of an MS binding assay. To prove the feasibility of MS binding on the adenosine A<sub>1</sub> and A<sub>2A</sub> receptors we first developed a mass spectrometry detection method

for unlabeled DPCPX and ZM-241,385, which are ligands with high selectivity and affinity for the respective receptors. To serve as internal standards, both compounds were also deuterium-labeled. Subsequently, we investigated whether the two unlabeled compounds could substitute for their radiolabeled counterparts as marker ligands in binding experiments, including saturation, displacement, dissociation, and competition association assays. Furthermore, we investigated the accuracy of these assays if the use of internal standards was excluded. The results demonstrate the feasibility of the MS binding assay, even in the absence of a deuterium-labeled internal standard, and provide great promise for the further development of label-free assays based on mass spectrometry for other GPCRs.

**Chapter 7** concludes this thesis by reflecting on its contents and their place in the current state of GPCR research, and on the future perspectives that this field of research has to offer.



# Samenvatting

Onderzoek naar allosterische modulatie leidt tot nieuwe inzichten in het activatiemechanisme van aan G eiwitten gekoppelde receptoren ('G protein-coupled receptors', of afgekort GPCRs). Natriumionen binden aan een allosterische bindingsplaats die goed geconserveerd is binnen de klasse A van GPCRs. Desondanks laat deze bindingsplaats een grote verscheidenheid aan allosterische effecten en grootte van liganden die kunnen binden zien, van natriumionen tot 5'-amino en 2-guanidino gesubstitueerde amilorides (**Hoofdstuk 2**). De adenosine A<sub>2A</sub> receptor is de eerste GPCR waarvan een kristalstructuur opgehelderd werd met een voldoende hoge resolutie om een natriumion gebonden in de natriumion-bindingsplaats waar te kunnen nemen. In dit proefschrift wordt de adenosine A<sub>2A</sub> receptor gebruikt als voorbeeldreceptor om de allosterische effecten van de natriumion-bindingsplaats te onderzoeken (**Hoofdstukken 3 – 5**), en samen met de adenosine A<sub>1</sub> receptor om een methode te ontwikkelen waarmee ligandbinding aan de receptor gemeten kan worden met behulp van massaspectrometrie (**Hoofdstuk 6**).

De natriumion-bindingsplaats en de orthostere bindingsplaats van de adenosine A<sub>2A</sub> receptor kunnen tegelijkertijd bezet worden wanneer een antagonist in de orthostere plaats gebonden is, maar niet wanneer een agonist gebonden is (**Hoofdstuk 3**). Natriumionen lijken de inactieve toestand van de receptor te stabiliseren, waarmee de binding van antagonisten wordt bevorderd, terwijl de binding van agonisten grotendeels wordt verhinderd bij een fysiologische concentratie van natriumionen. Amiloride en derivaten hiervan laten bij binding in de natriumion-bindingsplaats eveneens verschillen zien in de allosterische modulatie van agonisten en antagonisten.

Naast de effecten op de binding van orthostere liganden, is de allosterische natriumion-bindingsplaats ook belangrijk voor de signaaltransductie door de receptor (**Hoofdstuk 4**). Door één voor één de aminozuren die de natriumion-bindingsplaats vormen te muteren, kon niet alleen de affiniteit van liganden die op die plaats binden beïnvloed worden, maar ook het vermogen van de hele receptor om door agonisten geactiveerd te worden. De vervanging van polaire aminozuren door alanine verhinderde de negatieve allosterische effecten van natriumionen op agonistbinding volledig (D52A<sup>2.50</sup> en N284A<sup>7.49</sup>) of gedeeltelijk (S91A<sup>3.39</sup>, W246A<sup>6.48</sup>, en N280A<sup>7.45</sup>). Mutaties D52A<sup>2.50</sup> en N284A<sup>7.49</sup> schakelden

receptoractivatie volledig uit, terwijl S91A<sup>3.39</sup> en N280A<sup>7.45</sup> de constitutieve activiteit van de receptor verhoogden, en S91A<sup>3.39</sup>, W246A<sup>6.48</sup>, en N280A<sup>7.45</sup> het vermogen van agonisten om de receptor te activeren verminderden. In simulaties die de receptordynamiek op atomair niveau volgen, had mutatie D52A<sup>2.50</sup> een direct effect op het in de kristalstructuur in de natriumion-bindingsplaats aanwezige natriumion, dat zich meteen naar een andere bindingsplaats bewoog, gevormd door de aminozuren Glu13<sup>1.39</sup> en His278<sup>7.43</sup>. Ook verlaagde D52A<sup>2.50</sup> de potentie van amiloride om orthostere liganden te verdringen, maar had deze mutant geen effect op de affiniteit van orthostere liganden. W246A<sup>6.48</sup> daarentegen vergrootte sommige allosterische effecten van natriumionen en amilorides, terwijl de affiniteit van orthostere liganden verminderde.

Door amiloride te substitueren op de 5' positie van het molecuul ontstaan amiloridederivaten met afwijkende allosterische eigenschappen en gelijke of zelfs hogere potentie dan referentiestof HMA op de wild-type adenosine A<sub>2A</sub> receptor (**Hoofdstuk 5**). De affiniteit van een serie van 5'-gesubstitueerde amiloridederivaten werd vastgesteld door hun verdringing van het orthostere radioligand [<sup>3</sup>H]ZM-241,385 van de wild-type en een in de natriumion-bindingsplaats gemuteerde W246A<sup>6.48</sup> adenosine A<sub>2A</sub> receptor te meten. Van deze serie was de 4-ethoxyphenethyl-gesubstitueerde amiloride 12l potenter dan HMA. Zoals eerder gezien voor amiloride en HMA, hadden de nieuwe amiloridederivaten een hogere affiniteit voor de W246A<sup>6.48</sup> gemuteerde receptor, wat aangeeft dat aminozuur Trp246<sup>6.48</sup> hun binding kan verhinderen. HMA had het grootste allosterische effect op de dissociatiesnelheid van [<sup>3</sup>H]ZM-241,385, terwijl de meest potente nieuwe amilorides 12h, i, k, en l een kleiner of zelfs geen effect op de dissociatie hadden. Dit geeft aan dat deze amilorides het orthostere ligand direct kunnen verdringen door de orthostere bindingsplaats binnen te dringen. Het grote verschil in het effect op de dissociatiesnelheid van [<sup>3</sup>H]ZM-241,385 tussen de wild-type en de W246A<sup>6.48</sup> gemuteerde receptor toont aan dat aminozuur Trp246<sup>6.48</sup> belangrijk is voor het soort allosterische interactie dat amilorides teweeg kunnen brengen.

Massaspectrometrie is een goed alternatief voor de detectie van radioliganden in de kwantificering van ligandbinding aan de adenosine A<sub>1</sub> en A<sub>2A</sub> receptoren (**Hoofdstuk 6**). Ondanks dat het meten van radioligandbinding een betrouwbare methode is, heeft het ook nadelen, zoals de te nemen veiligheidsmaatregelen, dure synthese, speciale laboratoriumvereisten, en afvalverwerking. Met massaspectrometrie kan de aanwezigheid



van liganden gemeten worden zonder ze te hoeven labelen met een radio-isotoop. De gevoeligheid van massaspectrometrie-apparatuur wordt beter en beter, en met de huidige stand van zaken kunnen de lage hoeveelheden van liganden die in bindingsexperimenten voorkomen gemeten worden. Dit hoofdstuk beschrijft de ontwikkeling van een label-loze massaspectrometrie-gebaseerde methode om ligandbinding te meten (MS-binding) voor de adenosine A<sub>1</sub> en A<sub>2A</sub> receptoren. Radioliganden worden veel gebruikt voor de meting van ligandbinding aan deze receptoren, waardoor er veel resultaten beschikbaar zijn om de MS-bindingsmethode mee te kunnen valideren. Eerst werd een methode ontwikkeld voor detectie met de massaspectrometer van ongelabeld DPCPX en ZM-241,385, liganden met een hoge selectiviteit en affiniteit voor respectievelijk de adenosine A<sub>1</sub> en A<sub>2A</sub> receptoren. Om als interne standaards in de massaspectrometrie-methode te dienen werden beide liganden ook gelabeld met deuterium. Vervolgens werd onderzocht of de twee ongelabelde liganden hun radio-gelabelde versies konden vervangen in verschillende bindingsexperimenten, zoals verzadigings-, verdringings-, dissociatie-, en competitie-associatie-experimenten. Verder werd onderzocht of het mogelijk was de interne standaard niet te gebruiken, zonder de betrouwbaarheid van de resultaten aan te tasten, met het doel de MS-bindingsmethode volledig ongelabeld te maken. De resultaten tonen aan dat de MS-bindingsmethode goed werkt, zelfs zonder het gebruik van een interne standaard, en dit is veelbelovend voor de verdere ontwikkeling van deze label-loze methode om ligandbinding te meten op andere GPCRs.

**Hoofdstuk 7** sluit dit proefschrift af met een beschouwing over de inhoud, hoe deze in de huidige stand van het GPCR-onderzoek past, en de vooruitzichten van dit onderzoeksveld.



# List of publications

Lenselink EB, Beuming T, Van Veen C, **Massink A**, Sherman W, Van Vlijmen HW, IJzerman AP (2016), *In search of novel ligands using a structure-based approach: a case study on the adenosine A<sub>2A</sub> receptor*, J Comput Aided Mol Des, Epub ahead of print.

**Massink A**, Louvel J, Adlere I, Van Veen C, Huisman BJH, Dijksteel GS, Guo D, Lenselink EB, Buckley BJ, Matthews H, Ranson M, Kelso M, IJzerman AP (2016), *5'-Substituted amiloride derivatives as allosteric modulators binding in the sodium ion pocket of the adenosine A<sub>2A</sub> receptor*, J Med Chem, 59(10): 4769-77.

**Massink A**, Holzheimer M, Hölscher A, Louvel J, Guo D, Spijksma G, Hankemeier T, IJzerman AP (2015), *Mass spectrometry-based ligand binding assays on adenosine A<sub>1</sub> and A<sub>2A</sub> receptors*, Purinergic Signal, 11(4): 581-94.

Romagnoli R, Baraldi PG, Lopez-Cara C, Cruz-Lopez O, Moorman AR, **Massink A**, IJzerman AP, Vincenzi F, Borea PA, Varani K (2015), *Synthesis and biological evaluation of a new series of 2-amino-3-aryl thiophene derivatives as agonist allosteric modulators of the A<sub>1</sub> adenosine receptor. A position-dependent effect study*, Eur J Med Chem, 101: 185-204.

**Massink A\***, Gutiérrez-de-Terán H\*, Lenselink EB, Ortiz Zacarías NV, Xia L, Heitman LH, Katritch V, Stevens RC, IJzerman AP (2015), *Sodium ion binding pocket mutations and adenosine A<sub>2A</sub> receptor function*, Mol Pharmacol, 87(2): 305-13.

Romagnoli R, Baraldi PG, IJzerman AP, **Massink A**, Cruz-Lopez O, Lopez-Cara LC, Saponaro G, Preti D, Aghazadeh Tabrizi M, Baraldi S, Moorman AR, Vincenzi F, Borea PA, Varani K (2014), *Synthesis and biological evaluation of novel allosteric enhancers of the A<sub>1</sub> adenosine receptor based on 2-amino-3-(4'-chlorobenzoyl)-4-substituted-5-arylethynyl thiophene*, J Med Chem, 57(18):7673-86.

Guo D, Venhorst SN, **Massink A**, Van Veldhoven JPD, Vauquelin G, IJzerman AP, Heitman LH (2014), *Molecular mechanism of allosteric modulation at G protein-coupled receptors: insight from a binding kinetics study at the human A<sub>1</sub> adenosine receptor*, Br J Pharmacol, 171(23): 5295-312.

Gutiérrez-de-Terán H\*, **Massink A\***, Rodríguez D, Liu W, Joseph JS, Katritch I, Heitman LH, Xia L, IJzerman AP, Cherezov V, Katritch V, Stevens RC (2013), *The role of a sodium ion binding site in the allosteric modulation of the A<sub>2A</sub> adenosine G protein-coupled receptor*, Structure, 21(12): 2175-85.

\*These authors contributed equally.

# Curriculum vitae

Arnault Massink was born on September 10th, 1982, in Paris, France. He graduated from the Gymnasium Haganum in The Hague in 2000 and studied Biology at Leiden University, starting in 2002. After obtaining his BSc degree he continued in 2009 to study Biology & Science Based Business at Leiden University and obtained his MSc degree *cum laude* in 2011. During his MSc education he performed a research internship at the Division of Medicinal Chemistry supervised by Dr. Laura Heitman, where he studied allosteric modulation and residence time of agonists on the adenosine A<sub>1</sub> receptor. Subsequently he performed a business internship at TNS NIPO, where he conducted quantitative market research in fast moving consumer goods.

After his graduation Arnault started his doctoral project in 2011 at the Division of Medicinal Chemistry, with Prof. Ad P. IJzerman as his promotor. His project was funded by an NWO TOP Grant “The crystal structure of the adenosine A<sub>2A</sub> receptor: the follow up” (Grant 714.011.001). During his PhD he investigated the allosteric sodium ion pocket of the adenosine A<sub>2A</sub> receptor and developed a mass spectrometry-based ligand binding assay for the adenosine A<sub>1</sub> and A<sub>2A</sub> receptors. He presented his research at various national and international symposia, such as the FIGON Dutch Medicine Days and the Gordon Conference on GPCR Dynamics and Function. Arnault is currently employed as a clinical research associate at Assign Clinical Research.



# Acknowledgements

I would like to thank the many people that supported me during my PhD. First of all, my promotor Prof. Ad IJzerman who guided me on my PhD path with his advice, suggestions, encouragement, inspiration, and his impeccable sense of humor. Dr. Laura Heitman, who supervised me in my research internship and inspired me to do a PhD with her great enthusiasm for science. All the other colleagues at the Division of Medicinal Chemistry, Andrea, Anna, Annelien, Bart, Dong, Elaine, Ellen, Elisabeth, Gerard, Hans, Henk, Ilze, Indira, Isaura, Jaco, Julia, Julien, Lance, Maarten, Maris, Miriam, Natalia, Rongfang, Shardul, Thea, Xue, and Zhiyi, for the coffee breaks, the pies, the discussions on science and matters not so much to do with science, the support in general, and the good times. My students Alex, Anna, Corine, Dave, Lance, Malene, Mira, Natalia, Noortje, and all the minor students, for their work and their contribution to the contents of my publications and thesis. My office mates in HB38, Andrea, Anna, Annelien, Bart, Brandon, Dora, Gerard, Hilde, Natalia, Rongfang, Shardul, and Willem, (plus the office mates in various other offices, Dong, Ellen, Henk, and Lance) for the nice and informal working environment. Hugo and Bart, experts in molecular dynamics and computational biology in general, without whose knowledge Chapters 3 and 4 would not have been possible. All my co-authors, for their work, suggestions, support, improvements, and all the other help in writing the chapters of my thesis. My girlfriend Julia, whom I met during my PhD and supported me from that moment on. My paranymphs Hans and Paul, for their support during my defense and for their friendship. All my friends, for the necessary relaxing outside of office hours. My parents, for giving the 'spark' of scientific curiosity. And of course all the people that I may have forgotten as acknowledgements can never be complete.